

CORONARY SPIRAL CT

Koen Nieman

Several chapters of this thesis are based on published papers, which are reproduced with permission of the co authors and the publishers. Copyright of these papers remains with the publishers. The printing of this thesis was supported by the department of Cardiology and Radiology of the Erasmus Medical Center, Rotterdam.

ISBN 90 9016844 3

Cover: K. Nieman / A.W. Zwamborn

Lay-out: A.W. Zwamborn

Printed by Ridderprint B.V. Ridderkerk

© 2003, K. Nieman

CORONARY SPIRAL CT

Coronaire Spiraal CT

PROEFSCHRIFT

ter verkrijging van de graad van doctor aan de
Erasmus Universiteit Rotterdam
op gezag van de
Rector Magnificus

Prof. dr. ir. J. H. van Bommel

en volgens besluit van het College voor Promoties.

De openbare verdediging zal plaatsvinden op
woensdag 4 juni 2003 om 09.45 uur

door

Koen Nieman
Geboren te Tilburg

PROMOTIECOMMISSIE

Promotor: Prof. dr. P.J. de Feijter

Overige leden: Prof. dr. P.W. Serruys
Prof. dr. M.L. Simoons
Prof. dr. T.A.W. van der Steen

Financial support by the Netherlands Heart Foundation (NHS) for the publication of this thesis is gratefully acknowledged.

Voor mijn ouders
Aan Nanae

Chapter 1	General Introduction and Outline of the Thesis	9
Part 2 Magnetic Resonance Imaging and EBCT		
Chapter 2	Non invasive Coronary Artery Imaging with Electron Beam Computed Tomography and Magnetic Resonance Imaging	15
Part 3 Imaging of the Coronary Lumen		
Chapter 3.1	Three dimensional Coronary Anatomy in Contrast Enhanced Multislice Computed Tomography	29
Chapter 3.2	Coronary Angiography with Multi slice Computed Tomography	39
Chapter 3.3	Usefulness of Multislice Computed Tomography for Detecting Obstructive Coronary Artery Disease	53
Chapter 3.4	Non invasive Coronary Angiography with Multislice Spiral Computed Tomography: Impact of Heart Rate	69
Chapter 3.5	CT of the Heart: Principles & Methods CT Angiography for the Detection of Coronary Artery Stenosis	81
Part 4 Imaging of the Coronary Wall		
Chapter 4.1	Non invasive Visualization of Atherosclerotic Plaques with Electron Beam and Multi slice Spiral Computed Tomography	103
Chapter 4.2	Computed Tomography for Acute Coronary Syndromes	113
Part 5 Imaging of Bypass Grafts, Stents and Function		
Chapter 5.1	CT Angiographic Evaluation of Post CABG Patients: Assessment of grafts and coronary arteries	129
Chapter 5.2	Non invasive Angiographical Evaluation of Coronary Stents with Multislice Spiral Computed Tomography	145
Chapter 5.3	Left Main Rapamycin Coated Stent: Invasive Versus Noninvasive Angiographic Follow up	155
Chapter 5.4	Four Dimensional Cardiac Imaging With Multislice Computed Tomography	159

Part 6 - Coronary Imaging with Next Generation Spiral CT

Chapter 6.1	Reliable Noninvasive Coronary Angiography With Fast Submillimeter Multislice Spiral Computed Tomography	163
Chapter 6.2	Computed Tomography Coronary Angiography	171
Chapter 7	Summary and Conclusions	195
	Samenvatting en Conclusies	201
	Dankwoord	205
	List of Publications	207
	Curriculum Vitae	211
	Color Section	215

1

General Introduction and Outline of the Thesis

Since the accidental angiogram of the right coronary artery by Sones in 1959, catheter based x ray angiography with selective contrast medium injection into the coronary artery has developed into a routine examination, and is still considered the gold standard for in vivo imaging of the coronary artery lumen. The invasive coronary assessment has been expanded by catheter based tools to determine the hemodynamical significance of obstructive disease, such as coronary flow velocity and pressure gradient measurement, and advanced cross sectional imaging techniques, such as intra coronary ultrasound and optical coherence tomography to evaluate the vessel wall morphology. Despite the high quality and diagnostic versatility, there are disadvantages to these catheter based imaging techniques. The examination requires puncture or dissection of a peripheral artery and advancement of catheters towards the heart, intubation of the coronary ostium by the catheter tip and injection of an iodine containing contrast medium into the coronary vasculature. This invasive procedure involves a certain morbidity, i.e. arterial bleeding, aneurysm or fistula formation, peripheral emboli and coronary dissection, as well as a small but not negligible mortality. Furthermore, cardiac catheterisation and the recovery period are generally not experienced as comfortable and require a short period of hospital admission. So despite the diagnostic superiority of conventional catheter based angiography, substantial effort has been invested in the development of noninvasive techniques for visualization of the coronary arteries. Several modalities, such as electron beam computed tomography (EBCT), magnetic resonance imaging (MRI) and most recently multislice spiral computed tomography (MSCT) have been investigated.

Non invasive assessment of the coronary arteries is not an easy task. The small and tortuous epicardial vessels follow multiple nonlinear courses around the heart and are in constant motion. Besides displacement due to cardiac contraction, the coronary arteries are also displaced by respiration. To visualize the coronary lumen, its characteristics need to be altered in such a way that it can be sufficiently discriminated from the vessel wall and surrounding tissues. For the purpose of stenosis quantification in vessels with a diameter as small as 2.3 mm, the spatial resolution would have to be less than 0.5 mm in all three dimensions. To differentiate plaque components, it may need to be better still. The acquisition or reconstruction of images needs to be synchronized to the cardiac cycle and to the respiration. Although the coronary arteries are never completely immobile, motion is limited during the mid to end diastolic phase.¹ For coronary visualization, the data acquisition or image reconstruction should be limited to this short period of relative immobility. Besides consistent ECG synchronization, the scan or reconstruction window needs to be as short as possible to reduce the occurrence of motion artifacts.

For complete coronary assessment, the entire coronary artery system needs to be covered within a practically feasible examination time. In the case of the computed tomography (CT) modalities, the entire heart needs to be covered within the time of a single breath hold to avoid multiple contrast injections. Ideally, a noninvasive technique should not be harmful and should be accessible to all patients.

The first computed tomography scanners were developed in the early 1970s, for which G. Hounsfield and A.M. Cormack received the Nobel Prize in 1979.² However, the low x tube rotation speed made these first scanners unsuitable for examination of the coronary arteries. Non mechanical electron beam CT (EBCT) was introduced in 1983.³ The scanner has a very short scan time, which is accomplished by replacement of the mechanically rotating x ray tube by an electron beam that is electromagnetically guided along a tungsten target ring within the gantry, allowing acquisition of a tomogram within 50 100 milliseconds. Several studies comparing contrast enhanced EBCT with conventional angiography have been published in the late 1990s.^{4 9}

In 1990 the first spiral or helical CT scanners were released, which allowed scanning of extended volumes within a shorter time. In 1998 the first multislice, or multidetector row spiral CT scanners were introduced that allowed acquisition of up to four slices simultaneously with an image acquisition time short enough to image the coronary arteries.^{10 14} The retrospectively reconstructed thin overlapping slices provides a high, and near isotropic image resolution. In 2002 a new generation of multislice spiral CT scanners, with a further increased rotation speed and thinner as well as an extended number of detector rows has been introduced, to improve the quality of spiral CT coronary angiography.^{15 17}

This dissertation describes the use and clinical potential of ECG gated multislice spiral computed tomography in patients with coronary artery disease. First the use of other non invasive cardiac imaging, i.e. the previously mentioned electron beam CT and magnetic resonance imaging is reviewed (chapter 2.1). Part 3 contains studies related to the characteristics of multislice spiral CT for the imaging of the heart and coronary arteries, and the diagnostic potential of ECG gated spiral CT coronary angiography to detect and visualize obstructive coronary artery disease in symptomatic patients, using conventional coronary angiography as the standard of reference. Part 4 is focussed on the feasibility and characteristics of coronary wall imaging by CT, including the assessment of non calcified atherosclerotic plaque material. The usefulness of contrast enhanced multislice spiral CT in symptomatic patients who previously underwent coronary artery bypass grafting and percutaneous coronary intervention with stent implantation is discussed in part 5. Finally, the first

results with the latest generation 16 slice computed tomography scanners and patient preparation with β receptor blockers are described in part 6, including a review and future outlook on the continuing development and clinical use of non invasive coronary angiography with spiral computed tomography.

REFERENCES

1. Wang Y, Watts R, Mitchell I, et al. Coronary MR angiography: selection of acquisition window of minimal cardiac motion with electrocardiography triggered navigator cardiac motion prescanning initial results. *Radiology* 2001;218:580 585.
2. Hounsfield GN. Computerized transverse axial scanning tomography: Part I, description of the system", *Br J Radiol* 1973;46:1016 1022.
3. Boyd DP, Lipton MJ. Cardiac Computed Tomography. *Proceedings of the IEEE* 1982;71:298 307.
4. Nakanishi T, Ito K, Imazu M, et al. Evaluation of coronary artery stenoses using electron beam CT and multiplanar reformation. *J Comput Assist Tomogr.* 1997;21:121 117.
5. Reddy G, Chernoff DM, Adams JR, et al. Coronary artery stenoses: assessment with contrast enhanced electron beam CT and axial reconstructions. *Radiology* 1998;208:167 172.
6. Schmermund A, Rensing BJ, Sheedy PF, et al. Intravenous electron beam computed tomographic coronary angiography for segmental analysis of coronary artery stenoses. *J Am Coll Cardiol.* 1998;31:1547 1554.
7. Rensing BJ, Bongaerts A, van Geuns RJ, et al. Intravenous coronary angiography by electron beam computed tomography: a clinical evaluation. *Circulation* 1998;98:2509 2512.
8. Achenbach S, Moshage W, Ropers D, et al. Value of electron beam computed tomography for the noninvasive detection of high grade coronary artery stenoses and occlusions. *N Engl J Med.* 1998;339:1964 1971.
9. Budoff MJ, Oudiz RJ, Zalace CP, et al. Intravenous three dimensional coronary angiography using contrast enhanced electron beam computed tomography. *Am J Cardiol.* 1999;83:840 845.
10. Nieman K, Oudkerk M, Rensing BJ, et al., Coronary angiography with multi slice computed tomography. *Lancet* 2001;357:599 603.
11. Achenbach S, Giesler T, Ropers D, et al. Detection of coronary artery stenoses by contrast enhanced, retrospectively electrocardiographically gated, multislice spiral computed tomography. *Circulation* 2001;103:2535 2538.
12. Knez A, Becker CR, Leber A, et al. Usefulness of multislice spiral computed tomography angiography for determination of coronary artery stenoses. *Am J Cardiol.* 2001;88:1191 1194.
13. Vogl TJ, Abolmaali ND, Diebold T, et al. Techniques for the detection of coronary atherosclerosis: multi detector row CT coronary angiography. *Radiology* 2002;223:212 220.

14. Kopp AF, Schroeder S, Kuettner A, et al. Non invasive coronary angiography with high resolution multidetector row computed tomography: results in 102 patients. *Eur Heart J.* 2002;23:1714 1725.
15. Flohr T, Stierstorfer K, Bruder H, et al. New Technical Developments in Multislice CT, Part 2: Sub Millimeter 16 Slice Scanning and Increased Gantry Rotation Speed for Cardiac Imaging. *RöFo, Fortschr Röntgenstr* 2002;174:1022 1027.
16. Nieman K, Cademartiri F, Lemos PA, et al. Reliable Noninvasive Coronary Angiography with Fast Submillimeter Multislice Spiral Computed Tomography. *Circulation* 2002;106:2051 2054.
17. Ropers D, Baum U, Pohle K, et al. Detection of coronary artery stenoses with thin slice multi detector row spiral computed tomography and multiplanar reconstruction. *Circulation* 2003; 107: 664 666.

Introduction

2

Non-invasive Coronary Artery Imaging with Electron Beam Computed Tomography and Magnetic Resonance Imaging

Pim J de Feyter
Koen Nieman
Peter MA van Ooijen
Matthijs Oudkerk

INTRODUCTION

Recent developments in hardware and software have increased the diagnostic capabilities of magnetic resonance imaging (MRI) and electron beam computed tomography (EBT) to visualise the cardiac anatomy, including the coronary arteries. Visualisation of the heart puts any diagnostic technique to the test, because the continuous cardiac motion distorts the image and high temporal resolution is required to “freeze” the heart to produce a sharp image.

In particular, non invasive visualisation of the coronary arteries is difficult because of the small size of the coronary arteries (2.5 mm in diameter), the complex, tortuous course making it often impossible to “catch” the coronary artery in one slice (tomogram), and the cardiac and respiratory motion causing loss of sharpness or motion artefacts.

In this article image acquisition and processing techniques of MRI and EBT will be presented. The clinical role of both techniques in cardiac imaging will be discussed, together with a brief introduction of the technical aspects.

MAGNETIC RESONANCE IMAGING: PHYSICS AND TECHNIQUE

MRI has excellent temporal and spatial resolution and is capable of visualising the cardiac anatomy. The advantages of MRI are its ability to acquire images non invasively, in the absence of ionising radiation, and in any tomographic plane without interference from surrounding bone or soft tissues. The basic concepts and clinical role of MRI can be found in excellent recent review articles.¹⁻⁵ In this paper we limit ourselves to a brief summary of MRI concepts.

MRI scanner

The MRI scanner consists of a magnet, gradient coils, and a body coil. The large magnet produces a strong homogeneous magnetic field, is cylindrical, and for imaging the patient is placed within the bore of the magnet. Gradient coils vary the strength of the magnetic field from one point to another and they determine the spatial information of the emitted MR signal necessary for the construction of the image. The bodycoil acts as an antenna, and transmits and receives radiofrequency (RF) waves.

Basic principles of MRI

Nuclei with an odd number of protons (such as hydrogen) possess a property called spin angular momentum—that is, the nucleus spins around its axis. Since the odd nuclei are positively charged, the spinning motion causes a magnetic momentum around it and acts as a small magnet. The strength of this magnetic moment is a property of the type of nucleus. Hydrogen nuclei possess a large magnetic moment, and are very abundant in the human body thereby making hydrogen the nucleus of choice for MRI. In the absence of an externally applied magnetic field (B_0) these individual magnetic moments have no preferred orientation, but when placed in

strong external magnetic field these magnetic moments align with the orientation of the external field. However, the spins do not exactly align but are at an angle to the external magnetic field (fig 1). This causes the spin to precess around the axis of the external magnetic field with a unique (resonant) frequency. The unique frequency of this precession is governed by the Larmor frequency equation $f = g \times M$, where f = frequency, g = gyromagnetic ratio (unique for each nucleus), and M = strength of magnetic field. The spins precess at random and give rise to a rather small secondary magnetic field (net tissue magnetisation, M) which at equilibrium is aligned longitudinally, along the axis of the main magnetic field (B_0) which is much larger, so that tissue magnetisation is “overruled” by the main magnetic field B_0 , making tissue magnetisation undetectable in the longitudinal axis. To “detect” this tissue magnetisation to produce an MR image it is necessary to disturb this equilibrium. An RF pulse emitted from the RF transmitter coil with a resonant frequency equal to the unique frequency of the precessing spins rotates the net longitudinal tissue magnetisation into the transverse plane (X Y plane) and synchronises the precession (fig 2). This allows the transverse magnetisation to be detected and measured. Termination of the RF pulse causes the perturbed nuclei to return (relax) to the original longitudinal alignment in the magnetic field and incoherent precession. As they relax a signal is emitted which is detected by the RF receiver. This is the MR signal from which the image is reconstructed. Different tissues relax at different rates, thus providing contrast between tissues. This signal needs to be processed to allow three dimensional location of the source (tissue protons) of the signal. A supplemental magnetic field gradient is applied (by the gradient coils) which causes a predictable variation of the magnetic field and thus a predictable resonant frequency of protons along an axis. This allows exact location of protons enabling precise image reconstruction.

CARDIAC MRI

MR coronary imaging: technique

Cardiac and respiratory motion are formidable problems making robust MR coronary angiography very difficult. Today conventional diagnostic coronary angiography is the undisputed standard of reference because a selective injection of contrast media reproduces in real time (no motion artefacts) the entire coronary artery (including collaterals), with an in plane resolution of 0.15 x 0.15 mm.

Coronary imaging with an image acquisition of 25 50 images per second (that is, 20 40 ms per acquisition), such as can be achieved with conventional diagnostic coronary angiography, would result in a nearly motion free image, but unfortunately such ultrafast MR acquisition techniques are not yet available. To circumvent these motion problems several other approaches must be used. To reduce cardiac motion disturbances one chooses a “quiet” window in the cardiac cycle during which the heart does not contract.

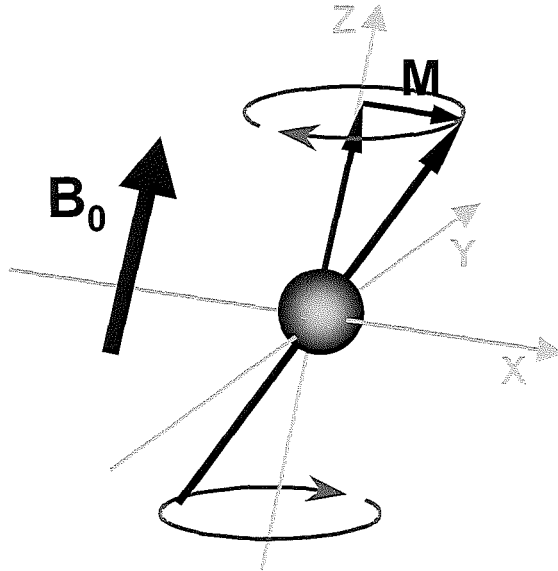


Figure 1. Spin angular momentum causing a magnetic dipole. B_0 , external magnetic field which causes spin to precess at an angle to B_0 . M , net tissue magnetisation aligned along Z axis.

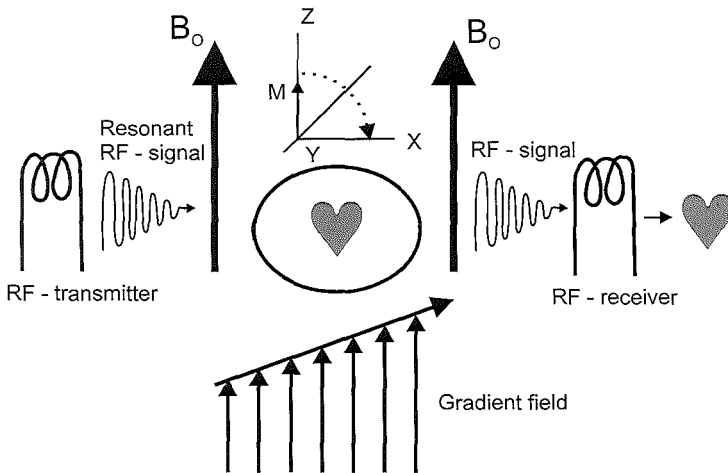


Figure 2. The patient (heart) is placed within a strong external magnetic field (B_0). The RF transmitter rotates the net tissue magnetisation in the transverse plane, and after termination, relaxation occurs which emits a signal detected by the RF receiver. The gradient coils produce a supplemental magnetic field gradient to allow precise location of the excited protons. The received signals have certain signal intensity (brightness) and location, both of which are processed to form the desired image.

This window is usually in mid and late diastole and lasts for about 100 ms to 150 ms. This window can be selected by triggering to the ECG signal so that the acquisition is performed in that predetermined window. This requires a stable heart rhythm and precludes patients with arrhythmias.

Respiratory motion artefacts can be reduced by using two acquisition approaches: (a) breathholding, and (b) respiratory gating. Breathholding for 20 seconds is possible in the majority of patients.

Respiratory gating techniques make use of a navigator technique, which monitors the movement of the diaphragm during respiration so that images are acquired only at the same predetermined diaphragm level. Potential navigator techniques allow longer acquisition times, during normal breathing, but irregularities in breathing pattern during long acquisition periods “shift” the diaphragm level, which may be (partly) overcome by adaptive windowing (to correct for diaphragm shift).

Another problem is the presence of epicardial fat, which produces a bright MR signal, which may interfere with the signal of blood within the coronary arteries. Fat saturation that is, a strong RF pulse that selectively saturates the magnetisation of fat bound hydrogen atoms, but not waterbound hydrogen atoms effectively suppresses this fat signal and is often used in MR coronary imaging.

MR coronary imaging to detect coronary stenosis

The detection of haemodynamically significant lesions with different MR techniques appears to be the “Holy Grail” of MR imaging (fig 3). So far, the results of detecting stenoses have been disappointing with sensitivities ranging from as low as 33% to as high as 90%^{1,2,6}. Overall the MR techniques are not robust enough to allow clinically reliable identification of a coronary lesion. The inability to reliably detect coronary stenosis is caused by: (1) the unacceptable quality of the images (mainly caused by problems of cardiac and respiratory motion) which makes interpretation unreliable or sometimes even impossible; (2) partial voluming of tortuous vessels; (3) intravoxel phase dispersion caused by complex or turbulent flow at coronary stenosis; (4) overlapping of adjacent anatomic structures, in particular the circumflex artery which is obscured by overlapping of the coronary sinus; (5) an inability to distinguish normal antegrade coronary flow from collateral filling of a vessel occurring beyond a severe stenosis or total occlusion; and (6) MR signal of the vessel wall or coronary plaque mimicking the blood signal of the vessel lumen.

Future of MR coronary imaging

There are three factors that must always be considered in MR coronary imaging: acquisition time, signal to noise ratio, and resolution. Improvement of one of the three is at the expense of one or both of the other two, and therefore MR imaging is about trying to find the optimal compromise.

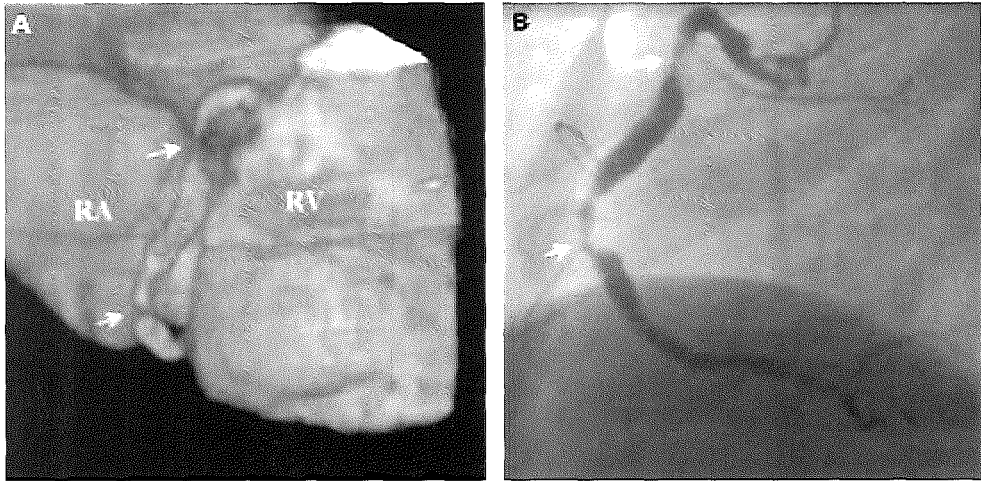


Figure 3. Visualisation of the right coronary artery by magnetic resonance (A) and by conventional (B) imaging. Two distinct stenoses are visible.

Table 1. Clinical role of MRI in cardiac disease

Established role: the evaluation of atria, ventricles, and pericardium

- congenital heart diseases
 - cardiac tumours (masses)
 - pericardial disease
 - left ventricular volume, mass
 - left ventricular function: wall thickness/systolic thickening
 - right ventricular function
-

Emerging role

- visualisation of coronary arteries
 - visualisation of bypass grafts
 - dobutamine stress MRI for coronary ischaemia to detect wall motion, abnormalities or myocardial contractile reserve
-

Potential role

- epicardial coronary flow velocity (rest/stress)
 - myocardial perfusion (rest/stress)
 - specific contrasts for myocardial necrosis or viable tissue
-

Ultrafast new MR scanners will allow: (a) shorter acquisition windows (less than 100 ms) which may dramatically reduce motion artefacts; and (b) three dimensional acquisition which offers the advantage of higher signal to noise ratio, and more isotropic pixel resolution. Small volume scan acquisition oriented along the coronaries, obtained during one breath hold, is feasible and appears promising⁷. The low contrast to noise ratio is expected to be improved by blood pool contrast media, so that the vessel lumen becomes more visible and protruding lesions can be distinguished. High gradient scanners are expected to improve the current spatial resolution of typical sequence of 1.5 x 1.5 x 3 mm to an in plane resolution of less than 1 mm. However, it may take several years before MR coronary angiography will evolve into a reliable clinical tool.

MR imaging to establish proximal course of coronary arteries

MR imaging is a reliable, patient friendly technique to assess the anomalous origin or proximal abnormal course of the right and left coronary arteries accurately⁸.

MR imaging of saphenous vein grafts

MR imaging of vein grafts is relatively easy because the grafts have a large diameter (4-8 mm) and are minimally affected by MR imaging of saphenous vein grafts MR imaging of vein grafts is relatively easy because the grafts have a large diameter (4-8 mm) and are minimally affected by cardiac and respiratory motion. The patency of grafts can be established by MR with a sensitivity of 85-90% and a specificity of 60-100%^{1,2}. However, these examinations only provide information on graft patency and no information about non occluding stenoses or graft patency of a sequential graft distal to a first coronary anastomosis, thus limiting the application in clinical practice.

MR imaging of right and left ventricle

Newer MR techniques (gradient echo imaging or echo planar imaging) allow acquisition of short axis (or long axis) slices within 50 ms with adequate image quality to assess quantitative evaluation of left ventricular function⁴.

The use of end diastolic and end systolic measurements allows calculation of stroke volume, ejection fraction, and ventricular mass. Wall motion abnormalities can be evaluated quantitatively by cine MR imaging (fig 4)⁹. Myocardial tagging allows for detection of very subtle wall motion abnormalities. MRI permits accurate delineation of epicardial and endocardial borders so that wall motion and systolic wall thickening can be analysed quantitatively. Stress MRI (using dobutamine) is emerging as a technique to detect coronary artery disease^{10,11}, and evaluation of myocardial contractile reserve by stress MRI appears useful for evaluating myocardial viability^{12,13}.

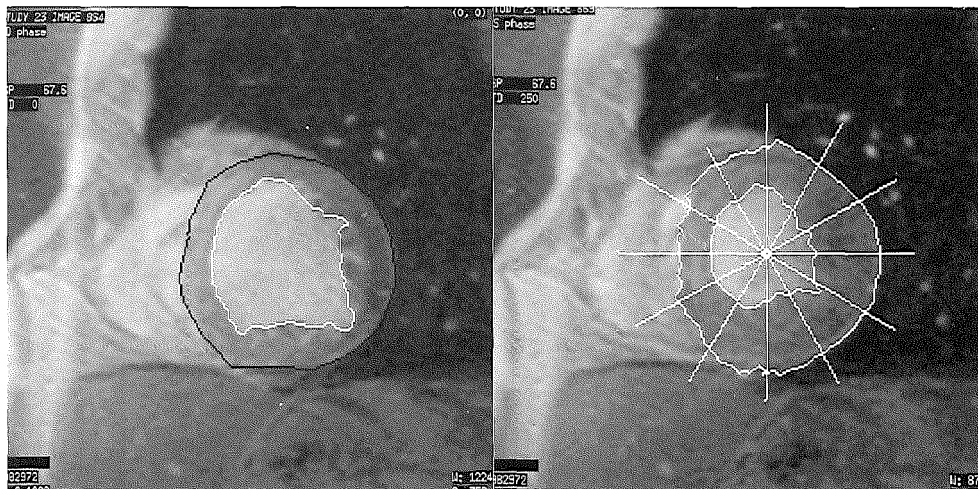


Figure 4. Diastolic (A) and systolic short axis view (B) of the left ventricle with contoured endocardial and epicardial borders. Plane B shows a segmentation pattern to assess the regional myocardial contractility. This case shows decreased contractility of the anterior septal wall in the systolic phase.

Myocardial perfusion imaging is emerging as a valuable tool to assess distribution of myocardial perfusion with high resolution^{14,15}. The anatomy and function of the right ventricle in particular is notoriously difficult to assess adequately. However, MR imaging allows evaluation of the right ventricle, which may prove to be useful to monitor congenital heart disease.

MR imaging of the cardiac anatomy

The presence of tumours or other masses involving the cardiac chambers, the pericardium, and extra cardiac structures can be reliably assessed with MRI¹⁶.

Limitations of MR imaging

Devices and metallic objects within the body may present a potential hazard for the patient. These objects may cause image artefacts, induce electric currents, cause excessive heating, or may move within the tissues. Patients with pacemakers and implantable defibrillators should not undergo MR imaging. Claustrophobia occurs in 2% of the patients, but the “open” configuration of new scanners will reduce this problem.

ELECTRON BEAM TOMOGRAPHY: PHYSICS AND TECHNIQUE

EBT is a tomographic x ray technique whereby only the structures in a selected slice (tomogram) of the patient are imaged sharply. The x ray photons passing through the body are differentially absorbed by the tissue, thus creating object contrast from which an image is reconstructed.

The EBT scanner is a dedicated ultrafast cardiac scanner, which is able to acquire tomograms within 100 ms¹⁷. This fast acquisition achieved because, unlike “conventional” computed tomographic (CT) scanners, there is no need to rotate the x ray source around the patient (which is energy and time consuming); rather the patient is positioned within a fixed source detector combination where x rays are produced with an electronically steered electron beam. The acquisition is obtained at predetermined relative motion free diastolic acquisition period, which is determined by high resolution ECG with triggering usually set at 80% of the RR interval. Breathholding necessary during acquisition of the tomograms to avoid respiratory motion artefacts. The tomogram thickness is set at 1.5 or 3 mm. Scanning is performed with the patient in supine position on the table. After each tomogram the table increment is set at 1.5 or 2 mm, resulting in contiguous non overlapping slices or slices with 1 mm overlap. One tomogram made during each RR interval. To completely cover the heart 40 to 60 transaxial tomograms are made during one breath hold. The data are obtained after injection of 150 ml contrast medium at 4 ml/s through an antecubital vein. The high contrast in plane resolution approximately 0.8 x 0.8 mm (6 line pairs/cm). The radiation exposure is estimated to be one third of that of a diagnostic coronary angiogram.

The image is constructed from many one dimensional projections, which are used to reconstruct a single slice of data (fig 5). A three dimensional data set is obtained by stacking many two dimensional tomograms from which three dimensional reconstructions are made usually using a surface shaded rendering or volume rendering technique.

EBT to assess coronary arteries

During contrast injection the mean CT density within the coronary arteries is about 165 200 Hounsfield units (HU) while the mean density of the myocardium (85 100 HU) and connective tissue (100 HU) is much lower, thus allowing visualisation of the contrast filled coronary lumen.

So far the results of healthy volunteers and approximately 300 patients have been published. In 75 80% of the cases the image quality is sufficient to allow reliable interpretation of the coronary arteries (fig 6)^{17 19}. The sensitivity to detect significant coronary stenosis ranges from 75 90% and the specificity from 80 94%. The diagnostic accuracy of EBT coronary angiography is highest in the left main artery and proximal and mid parts of the left anterior descending coronary artery, and moderate in proximal and mid parts of the right (RCA) and left circumflex (LCX) arteries. The distal coronary segments cannot be visualised.

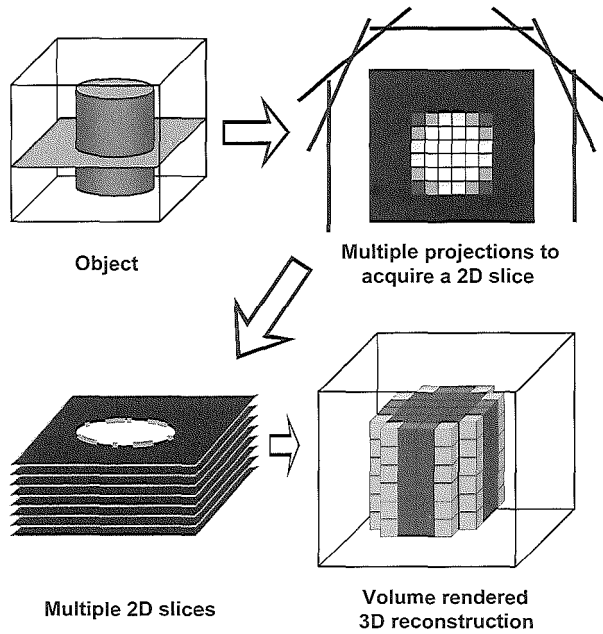


Figure 5. Schematic overview of EBT scanning to reconstruct a three dimensional image. 2D, two dimensional; 3D, 3 dimensional.

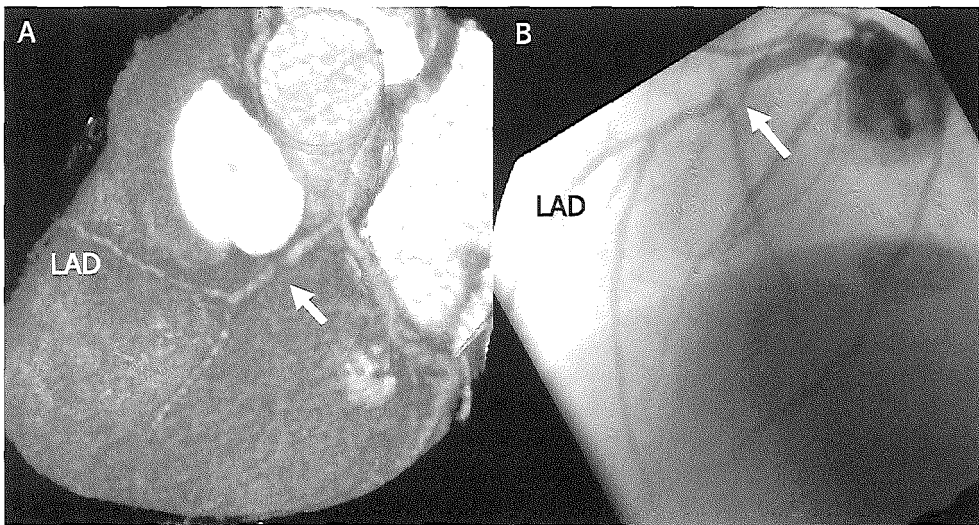


Figure 6. Electron beam CT coronary angiogram (A) and corresponding conventional angiogram (B), of a significantly stenosed (arrow) left anterior descending coronary artery (LAD).

Misdiagnosis is caused by cardiac motion artefacts (in particular of the RCA and LCX), inadvertent respiratory motion, overlapping anatomical structures, triggering problems due to irregular heart rhythm, and lumen interpretation problems in cases of severe overlying calcifications. Total coverage of the heart requires a rather long breath hold (for example, with a heart rate of 60 bpm and slice thickness of 3 mm, a 20 second breath hold covers 6 cm from base to apex) which is not always possible in patients.

EBT to assess bypass graft patency

Initially EBT was able to establish only the patency of coronary venous and arterial bypass graft patency by assessment of the individual transaxial angiograms. The diagnostic accuracy was high with a sensitivity of 95% and a specificity of 86.97%¹⁷. The recently introduced three dimensional rendering techniques were able to reconstruct the graft completely and thus allow assessment of non occluding obstructions (fig 7). The diagnostic accuracy to detect significant graft obstructions was high, with sensitivity ranging from 92.100% and specificity from 91.100%.

EBT for quantification of coronary calcification

To detect coronary calcium usually 20-30 contiguous, 3 mm EBT slices acquired at 100 ms are obtained. The tomograms, which are acquired during one breath hold, are triggered from an ECG at 80% of the RR interval to minimise cardiac motion. Coronary calcium in the wall has a high density relative to blood and thus is easily detected. The EBT scanner software allows the quantification of calcium area and density. CT attenuation of tissue is about ± 50 HU and arbitrarily a density of 130 HU and more are assumed to be calcium. The calcium scoring algorithm from Agatston is frequently used to calculate the amount of calcium²⁰. Calcium densities of 130-200 HU are assigned a score of 1, between 201-300 HU a score of 2, between 301-400 HU a score of 3, and > 401 HU a score of 4. These peak calcium density values are multiplied by the actual area (mm^2) of calcification per coronary tomographic segment to obtain the score. The score can be given per specific coronary artery or for the entire coronary system (the sum of the individual scores).

EBT is extremely sensitive in defining coronary vascular calcification, and the presence of coronary calcium is always indicative of coronary atherosclerosis²¹. The presence of calcification does not equate with the presence of a significant coronary stenosis, however, and the absence of calcification does not exclude a coronary lesion, including a vulnerable plaque, but the likelihood of the latter is low. There is a direct relation between the magnitude of the calcium score and the extent of the underlying coronary plaque burden and the presence of a severe coronary stenosis. However, site and extent of calcification do not equate with site specific stenosis, and a calcific plaque does not mean a stable plaque. There appears to be a relation between the presence of coronary calcification and the occurrence of adverse coronary events in asymptomatic individuals^{21,22}.

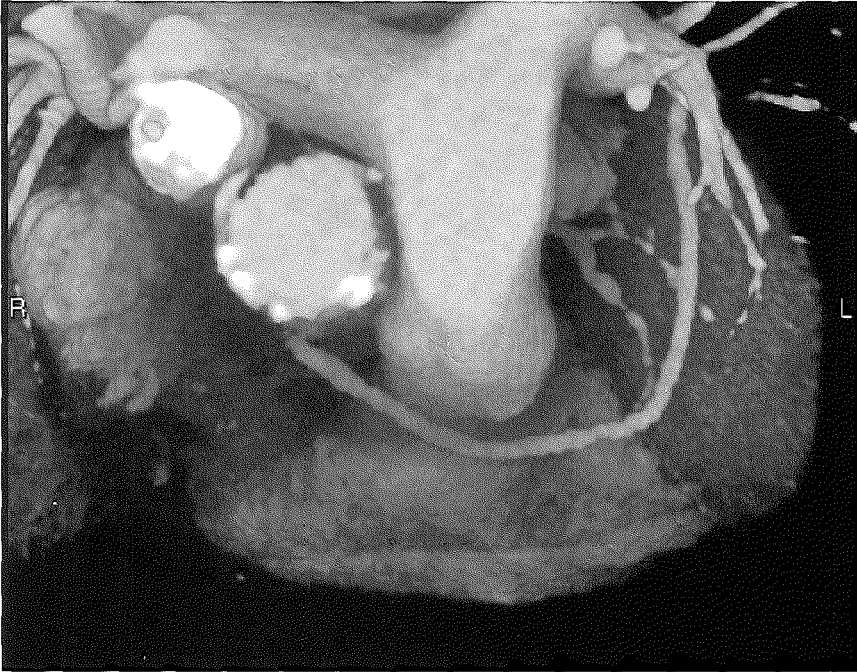


Figure 7. Visualisation of a sequential venous bypass graft without significant stenoses.

Table 2. Clinical role of EBT in cardiac disease

Established role

detection and quantification of coronary calcium

Emerging role

visualisation of coronary arteries
visualisation of bypass grafts

Under investigation

quantification of calcium in symptomatic patients and asymptomatic individuals

Potential role

left ventricle anatomy and function
right ventricle anatomy and function
myocardial perfusion

The place and role of EBT as a screening tool to predict coronary events, independent of the conventional risk factors such as hypertension, smoking, hypercholesterolaemia, diabetes, and family history, is controversial and requires more data before EBT can be recommended in low risk asymptomatic patients.

Future EBT coronary imaging

Although EBT has a high temporal (100 ms) and high in plane spatial resolution (0.8 mm x 0.8 mm), with image acquisition triggered to the ECG, its performance is not yet sufficiently robust for reliable coronary visualisation. Technical improvements may be expected, such as doubling the number of detector elements, so that the in plane resolution may improve from 6 line pairs/cm to 10 line pairs/cm or reducing the tomogram acquisition time from 100 ms to 50 ms. Coronary imaging with EBT is promising because calcium quantification provides information on the plaque burden of the coronary arteries, and contrast enhanced CT may reliably determine the severity of obstructive disease.

CONCLUSION

A major question, given the cost constraints for potential interested party, is which technique—MRI or EBT—should one purchase? This largely depends on the purpose for which the technique will be used. If one is interested in visualising coronary arteries or venous bypass grafts EBT seems more robust than MRI. Visualisation of the heart chambers and cardiac masses can be achieved equally effectively by both techniques. MRI is superior for studying left ventricular function and perfusion, and obviously flow can only be determined by MRI (although it is still in its early phase of development).

REFERENCES

1. van Geuns RJ, Wielopolski PA, de Bruin HG, et al. Basic principles of magnetic resonance imaging. *Prog Cardiovasc Dis* 1999;42:149 56.
2. van Geuns RJ, Wielopolski PA, de Bruin HG, et al. Magnetic resonance imaging of the coronary arteries: techniques and results. *Prog Cardiovasc Dis* 1999;42:157 66.
3. Brown MA, Semelka RC. MR imaging abbreviations, definitions, and descriptions: a review. *Radiology* 1999;213:647 62.
4. European Society of Cardiology/Association of European Paediatric Cardiologists. The clinical role of magnetic resonance in cardiovascular disease. Task Force of the European Society of Cardiology, in collaboration with the Association of European Paediatric Cardiologists. *Eur Heart J* 1998;19:19 39.
5. Wielopolski PA, van Geuns RJM, de Feyter PJ, et al. Review article: coronary arteries. *Eur Radiology* 2000;10:12 35.
6. Manning WJ, Li W, Edelman RR. A preliminary report comparing magnetic resonance coronary angiography with conventional angiography. *N Engl J Med* 1993;328:828 32.
7. Wielopolski PA, van Geuns RJ, de Feyter PJ, et al. Breath hold coronary MR angiography with volume targeted imaging. *Radiology* 1998;209:209 19.

8. Post JC, van Rossum AC, Bronzwaer JG, et al. Magnetic resonance angiography of anomalous coronary arteries. A new gold standard for delineating the proximal course? *Circulation* 1995;92:3163 71.
9. van der Geest RJ, Reiber JH. Quantification in cardiac MRI. *J Magn Reson Imaging* 1999;10:602 8.
10. van Rugge FP, van der Wall EE, Spanjersberg SJ, et al. Magnetic resonance imaging during dobutamine stress for detection and localization of coronary artery disease. Quantitative wall motion analysis using a modification of the centerline method. *Circulation* 1994;90:127 38.
11. Hundley WG, Hamilton CA, Thomas MS, et al. Utility of fast cine magnetic resonance imaging and display for the detection of myocardial ischemia in patients not well suited for second harmonic stress echocardiography *Circulation* 1999;100:1697 702.
12. Baer FM, Theissen P, Schneider CA, et al. Dobutamine magnetic resonance imaging predicts contractile recovery of chronically dysfunctional myocardium after successful revascularization. *J Am Coll Cardiol* 1998;31:1040 8.
13. Geskin G, Kramer CM, Rogers WJ, et al. Quantitative assessment of myocardial viability after infarction by dobutamine magnetic resonance tagging. *Circulation* 1998;98:217 23.
14. Saeed M, Wendland MF, Yu KK, et al. Identification of myocardial reperfusion with echo planar magnetic resonance imaging. Discrimination between occlusive and reperfused infarctions. *Circulation* 1994;90:1492 501.
15. Wu KC, Zerhouni EA, Judd RM, et al. Prognostic significance of microvascular obstruction by magnetic resonance imaging in patients with acute myocardial infarction. *Circulation* 1998;97:765 72.
16. Hoffmann U, Globits S, Frank H. Cardiac and paracardiac masses. Current opinion on diagnostic evaluation by magnetic resonance imaging. *Eur Heart J* 1998;19:553 63.
17. Rensing BJ, Bongaerts AH, van Geuns RJ, et al. Intravenous coronary angiography using electron beam computed tomography. *Prog Cardiovasc Dis* 1999;42:139 48.
18. Rensing BJ, Bongaerts A, van Geuns RJ, et al. Intravenous coronary angiography by electron beam computed tomography: a clinical evaluation. *Circulation* 1998;98:2509 12.
19. Moshage WE, Achenbach S, Seese B, et al. Coronary artery stenoses: three dimensional imaging with electrocardiographically triggered, contrast agent enhanced, electron beam CT. *Radiology* 1995;196:707 14.
20. Agatston AS, Janowitz WR, Hildner FJ, et al. Quantification of coronary artery calcium using ultrafast computed tomography. *J Am Coll Cardiol* 1990;15:827 32.
21. Wexler L, Brundage B, Crouse J, et al. Coronary artery calcification: pathophysiology, epidemiology, imaging methods, and clinical implications. A statement for health professionals from the American Heart Association writing group. *Circulation* 1996;94:1175 92.
22. Rumberger JA, Brundage BH, Rader DJ, et al. Electron beam computed tomographic coronary calcium scanning: a review and guidelines for use in asymptomatic persons. *Mayo Clin Proc* 1999;74:243 52.

3.1

Three-dimensional Coronary Anatomy in Contrast Enhanced Multislice Computed Tomography

Koen Nieman
Benno J Rensing
Arie Munne
Robert-Jan M van Geuns
Peter MT Pattynama
Pim J de Feyter

ABSTRACT

A number of three dimensional imaging modalities, such as MRI, EBT, ultrasound and multi slice CT have been introduced in cardiovascular medicine. One of the most recently developed techniques, multi slice CT coronary angiography, allows assessment of the small coronary vessels. The entire heart is scanned within a single breathhold and contrast enhanced images are reconstructed through retrospective ECG gating. Instead of the conventional 2D projection images, MSCT data can be displayed in a 3D volume rendered manner. We present an overview of the cardiac and coronary morphology as it is imaged with contrast enhanced MSCT. Further imaging characteristics of CT angiography will be discussed.

MSCT CORONARY ANGIOGRAPHY

Non invasive ECG gated angiography with multislice computed tomography (MSCT) is one of the most recent developments in the field of cardiac imaging. The revolutionary advancements in spiral CT technology have resulted in a high resolution 3D imaging modality that allows visualization of the coronary vessels and the detection of stenotic coronary artery disease.^{1,2} Rather than a projection image, like conventional selective X ray angiography, MSCT data can be reconstructed into a "true" 3D representation. Although dynamic volume rendered MSCT images can be created, it does not represent a specific cardiac contraction, like conventional high temporal resolution cine angiography, but rather a composition of 50 consecutive heart beats into a single cycle.³

The technique, which has been described extensively before, will be discussed briefly.^{4,5} The MSCT scanner is a spiral computed tomography scanner that acquires four channels, or four slices, of data simultaneously. After intravenous injection of a X ray contrast agent, the CT data are acquired continuously while recording the patient ECG, during a 30 40 seconds breathhold. ECG synchronous transverse slices are reconstructed with advanced spiral algorithms that improve the temporal resolution (125 250 ms). The 3D data set, that consists of around 200 overlapping slices (1.25 mm at an increment of 0.5 mm), can be further processed using 3D rendering software.

When the images are reconstructed during the middle to late diastolic phase, nearly motionless images can be obtained in patients with regular and relatively low heart rates.⁶ Compared to other non invasive imaging techniques the contrast to noise ratio is high, contrast enhanced blood, stents and calcifications appear white. Contrary to selective X ray coronary angiography, all blood containing cavities will become contrast enhanced. Depending on the contrast medium injection timing the venous system will be opacified as well. Motion artifacts present themselves as blurring and poorly defined edges. Beam hardening effects, displacement of CT signal, occur at the site of metal stents, surgical clips, calcifications and high concentrations of contrast, i.e. the superior caval vein and right atrium. This can degrade the image quality and prevent accurate assessment of specific vessel segments.

Table 1. MSCT coronary angiography protocol & scan characteristics

Data acquisition	Continuous overlapping spiral scan
Collimation protocol	4 slices of 1 mm
Contrast enhancement	IV X ray contrast medium, ± 15 18 s prior to scan
ECG synchronization	Retrospective gating
Temporal resolution	125 250 ms ^a
Eff. slice thickness	1.25 mm
In plane resolution	9 line pairs / cm
Through plane resolution	6 line pairs / cm

^aDepending on the heart rate

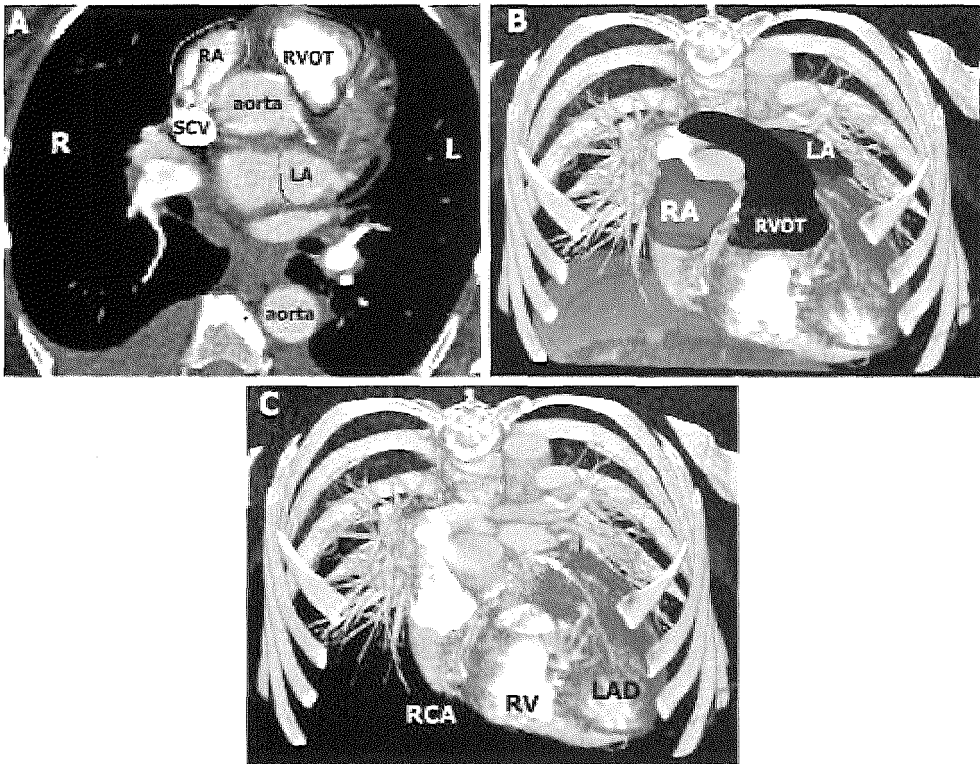


Figure 1. 3D volume rendering and manual segmentation of superimposing structures. Manual segmentation and removal of overlying structures: the right atrium (RA), right ventricle outflow tract (RVOT), the auricle of the left atrium (LA), and the diaphragm (A,B), thereby revealing the coronary arteries (C). SCV = superior caval vein.

IMAGE PREPARATION

The 3D CT data set can be evaluated using various post processing techniques. Multiplanar reconstructions allow visualization of any cross section through the volume. Oblique as well as curved cross sections can be created, which are particularly useful for assessment of specific coronary segments. Surface and volume rendered images offer a three dimensional representation of the heart and the epicardial vessels. Generally, superimposing structures need to be removed by means of manual segmentation for better visualization of the regions of interest (Fig. 1).

THE CORONARY ARTERIES

The coronary arteries are presented in a 3D fashion, which makes the images slightly difficult to interpret for most cardiologist used to X ray projection angiograms. Superimposing structures like the atria and appendages, pulmonary trunk and the cardiac veins can obscure the view and should preferably be removed.

The left coronary artery originates at the left sinus of Valsalva and soon after bifurcates into the left anterior descending (LAD, or anterior interventricular artery) and left circumflex coronary artery (LCX). The left coronary artery continues at the anterior side of the heart between the right and left ventricle. Several diagonal branches cross the left ventricular anterior wall (Fig. 3).

Although lesser in size, one or two branches can usually be observed penetrating the anterior part of the septum. The left circumflex artery, usually smaller in diameter compared to the LAD, encircles the mitral valve within the atrioventricular groove. The left atrial appendages usually need to be removed to expose the vessel's proximal course (Fig. 2). The obtuse marginal branches, occasionally of considerable size, supply the lateral ventricular wall (Fig. 3). Depending on the dominance of the left coronary system the circumflex coronary branch continues at the dorso posterior side. The right coronary artery (RCA) arises further caudal at the right aortic sinus. The RCA runs through the atrioventricular groove, encircling the tricuspid orifice, reciprocal to the LCX (Fig. 4). Small branches, to the right atrium, ventricle, conus or sinus node, are frequently observed. The RCA shows more displacement during the cardiac cycle compared to the left coronary artery.⁶ Particularly the middle segment of the RCA, which runs perpendicular to the transverse slices, is vulnerable to inadequate ECG gating. The distal segment runs between the dorso posterior side of the atrioventricular groove and the diaphragm. In 90% of the population, the posterior descending artery (PDA, or posterior interventricular artery) branches off from the RCA, and runs from the cardiac base to the apex, reciprocal to the LAD (Fig. 3). Depending on the dominance of the right coronary system the RCA produces a postero lateral branch, which crosses the posterior interventricular groove and continues on the left side to supply the dorsal left ventricular wall.

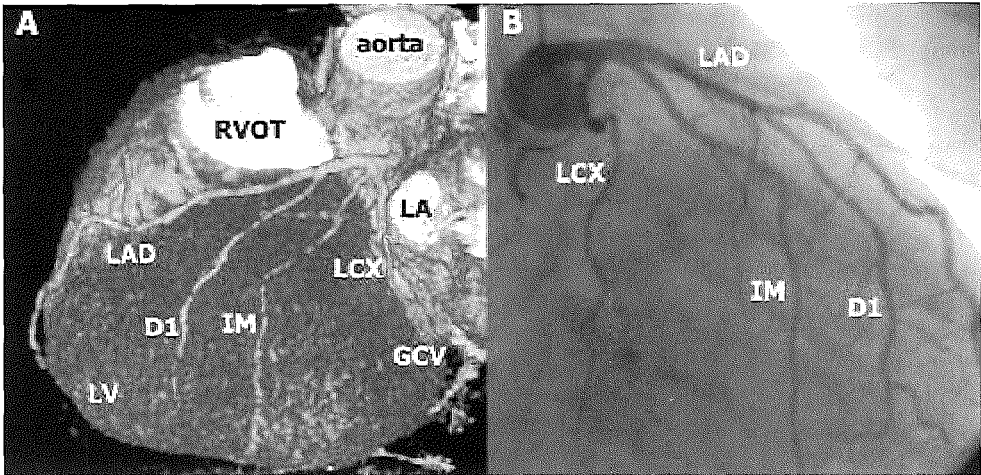


Figure 2. Left coronary artery MSCT angiogram (left anterior oblique view) and corresponding conventional angiogram (right anterior oblique view) of a normal left coronary artery. The right ventricle outflow tract (RVOT) and left atrium auricle (LA) have been removed. Besides the main stem, left anterior descending artery (LAD) and left circumflex artery (LCX) the intermediate (IM) and diagonal branch (D1) are also visible. LV = left ventricle, GCV = great cardiac vein.

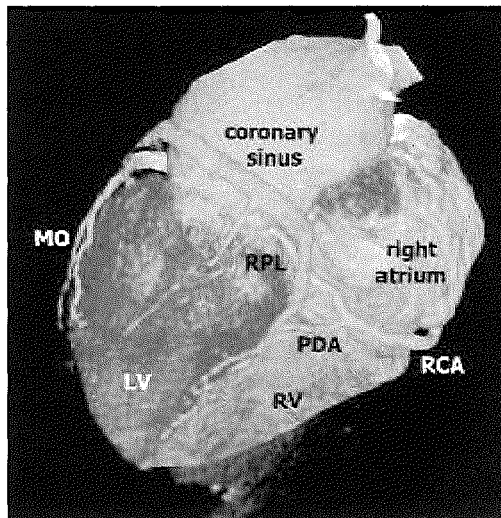


Figure 3. Diaphragmatic surface of the heart. MSCT image of the diaphragmatic surface of the heart. Following the atrioventricular groove the right coronary artery (RCA) bifurcates just proximal of the interventricular groove into a posterior descending artery (PDA) and posterolateral branch (RPL). The great cardiac vein runs parallel to the circumflex branch in the left atrioventricular groove and continues as the coronary sinus, which also collects blood from the (inter)ventricular groove. MO = marginal branch.

Anomalies of the coronary arteries are encountered in approximately 1% of all diagnostic angiograms.⁷ Most variations are of little clinical significance. However, some variation, in which a larger vessel runs between the aortic root and the pulmonary trunk can induce exercise related angina and can even be the cause of sudden death. In these cases assessment by MSCT or another 3D imaging technique can accurately depict coronary anatomy and its relation to the great vessels (Fig. 5).

High grade stenotic lesions in the coronary arteries can be detected with contrast enhanced MSCT (Fig. 6). Preliminary reports concerning the diagnostic accuracy of MSCT coronary angiography are promising. When the image quality is adequate for assessment, the sensitivity of MSCT to detect significant (>50%) stenoses in the proximal vessel segments ranged from 81% to 95%.^{3,8 10} Exclusion of lesions is possible in 80% to 97% of the vessel segments. So far, these results are comparable to the results achieved with electron beam CT: sensitivity 74% to 92% and specificity 79% to 94%.^{11 16}

THE CORONARY VENOUS SYSTEM

During conventional coronary angiography the venous system becomes visible only later after enhancement of the coronary arteries. Due to the duration of the CT data acquisition the arteries and their venous counterparts will be contrast enhanced in the same volume data set. The degree of enhancement depends on the timing of the contrast medium injection. More caudally situated veins, such as the coronary sinus, collect most contrast medium as the acquisition advances in a cranio caudal direction. Only when the timing of the scan is overdue or the Z axis starting point is selected inappropriately, will the great cardiac vein (GCV) at the proximity of the left coronary artery bifurcation become significantly enhanced.

Within the anterior interventricular groove the GCV runs, anti parallel to the LAD, from the apex towards the heart base. At the bifurcation of the left coronary artery the GCV makes a 90 degree turn and continues in the left atrioventricular groove (Fig. 7). Running parallel to the LCX, the GCV can obscure or the LCX and inhibit assessment of the smaller sized artery. After crossing the interventricular groove the great cardiac vein terminates at the coronary sinus, which connects to the dorso posterior side of the right atrium. Smaller veins return to the coronary sinus from the posterior interventricular groove and the right atrioventricular groove. Generally, with MSCT the diaphragmatic surface of the heart is dominated by the appearance of the venous rather than the arterial vessels (Fig. 3).

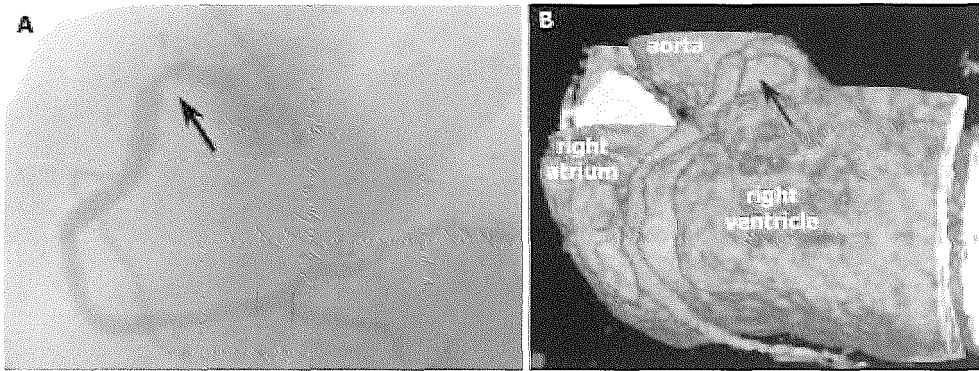


Figure 4. Right coronary artery. Conventional (A) and corresponding MSCT angiogram (B) of a right coronary artery, both left anterior oblique views. The top of the right atrium and the right ventricle have been removed to present the complete course of the RCA in the atrioventricular groove. The arrow indicates a mild stenosis in the proximal right coronary artery.

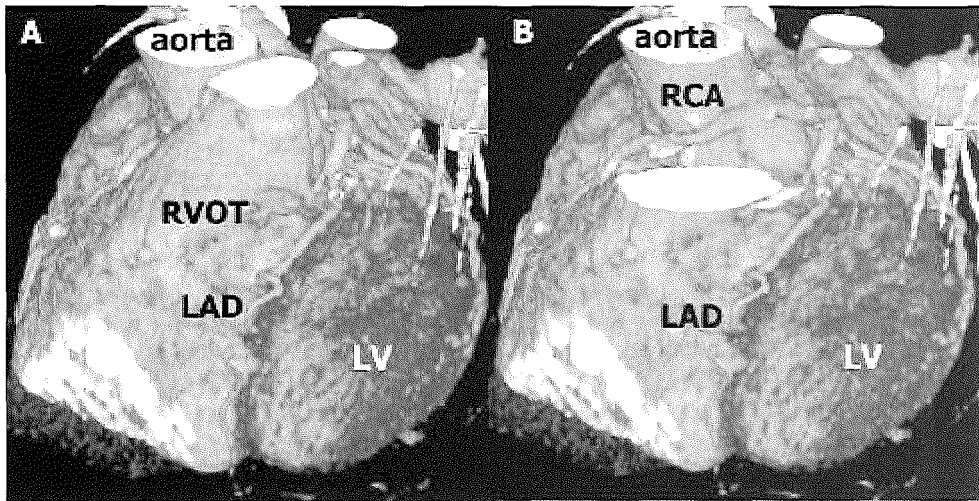


Figure 5. Anomalous coronary anatomy. MSCT angiogram of an anomalous right coronary artery (RCA), that originates from the left coronary sinus. The vessel's course between the aorta and pulmonary artery caused anginal symptoms in this patient.

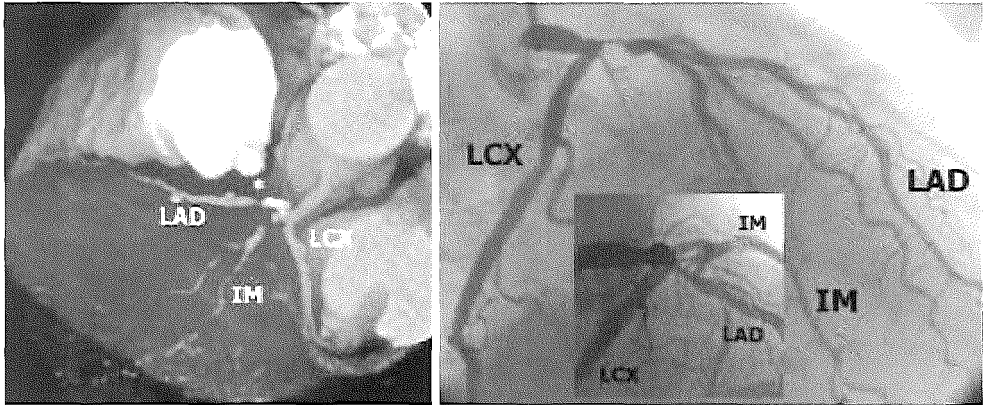


Figure 6. Coronary stenosis. The presence of significant stenoses (*) in the proximal left anterior descending artery (LAD) and intermediate branch (IM) could be confirmed by conventional angiography. On the MSCT scan, left cranial perspective, a calcium deposition seems to obscure the proximal part of the stenosis in the LAD. LCX = left circumflex artery.

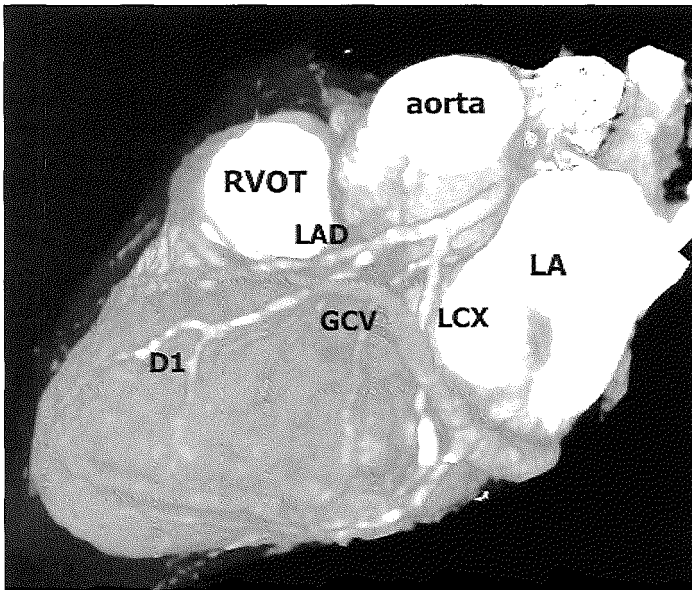


Figure 7. Great cardiac vein. The great cardiac vein can first be recognized at the anterior interventricular groove. Near the left coronary carina it makes a sharp turn and continues in the left atrioventricular groove. Also the arterial vessels can be appreciated in this image (left anterior oblique with cranial angulation).

FUTURE DEVELOPMENTS

Currently, MSCT scanners provide high quality cardiac images. Although rather robust images of the coronary artery are obtained frequently, MSCT coronary angiography is not sufficiently reliable to replace conventional coronary angiography, at this point. Future development will expectedly focus on higher rotation rates and expansion of the number of slices, which will improve both temporal and spatial resolution, decrease the total scan time and reduce motion artifacts.

MSCT angiography allows for non invasive imaging of the coronary arteries within a single breathhold. The examination can be performed within 15 minutes on an out patient basis. Because this technique lacks the potential complications and patient discomfort of conventional selective catheter based angiography, it might prove useful as a screening method for coronary artery disease in low risk individuals and as a diagnostic tool for follow up after surgical or angioplastic intervention.

CONCLUSION

Contrast enhanced MSCT allows high resolution, high contrast imaging of the heart and coronary vessels. These images are acquired non invasively and can be presented in a three dimensional fashion.

REFERENCES

1. Achenbach S, Ulzheimer S, Baum U, Kachelriess M, Ropers D, Giesler T, Bautz W, Daniel WG, Kalender WA, Moshage W: Noninvasive coronary angiography by retrospectively ECG gated multislice spiral CT. *Circulation* 2000;102:2823-2828
2. Nieman K, Oudkerk M, Rensing BJ, van Ooijen P, Munne A, van Geuns RJ, de Feyter PJ: Coronary angiography with multi slice computed tomography. *Lancet* 2001;357:599-603
3. Nieman K, van Ooijen P, Rensing B, Oudkerk M, de Feyter P. Four dimensional cardiac imaging with multi slice computed tomography. *Circulation* 2001, In press
4. Klingenberg K, Schaller S, Flohr T, Ohnesorge B, Kopp AF, Baum U: Subsecond multi slice computed tomography: basics and applications. *Eur J Radiol* 1999;31:110-124
5. Ohnesorge B, Flohr T, Becker C, Kopp AF, Schoepf UJ, Baum U, Knez A, Klingenberg K, Reiser MF: Cardiac imaging by means of electrocardiographically gated multisection spiral CT: initial experience. *Radiology* 2000;217:564-571
6. Wang Yi, Vidan Erez, Bergman GW: Cardiac motion of coronary arteries: variability in the rest period and implications for coronary MR angiography. *Radiology* 1999;213:751-758
7. Cieslinski G, Rapprich B, Kober G. Coronary anomalies: incidence and importance. *Clin Cardiol* 1993 Oct;16(10):711-5

8. Knez A, Becker C, Leber A, Becker A, Bruening R, Reiser M, Haberl R: non invasive angiography with multi detector helical computed tomography for evaluation of coronary artery disease. *J Am Coll Cardiol* 2000;2suppl.A:463
9. Kopp AF, Schroeder S, Kuettner A, Ohnesorge BM, Georg C, Claussen CD: Multidetector row CT for noninvasive coronary angiography: results in 102 patients. *RSNA Annual Meeting*, November 2000
10. Hong C, Becker CR, Knez A, Schoepf UO, Bruening RD, Reiser MF: Multislice CT coronary angiography for segmental analysis of coronary artery diseases. *RSNA Annual Meeting*, November 2000
11. Nakanishi T, Ito K, Imazu M, Yamakido M: Evaluation of coronary artery stenoses using electron beam ct and multiplanar reformation. *J Comput Assist Tomogr* 1997;21:121 127
12. Reddy PR, Chernoff DM, Adams JR, Higgins CB: Coronary artery stenoses: assessment with contrast enhanced electron beam CT and axial reconstructions. *Radiology* 1998;208:167 172
13. Schermund A, Rensing BJ, Sheedy PF, Bell MR, Rumberger JA: Intravenous electron beam CT coronary angiography for segmental analysis of significant coronary artery stenoses: feasibility and limitations. *J Am Coll Cardiol* 1998;31:1547 1554
14. Budoff MJ, Oudiz RJ, Zalace CP, Bakhsheshi H, Goldberg SL, French WJ, Rami TG, Brundage BH: Intravenous three dimensional coronary angiography using contrast enhanced electron beam computed tomography. *Am J Cardiol* 1999;83:840 845
15. Rensing BJ, Bongaerts A, van Geuns RJ, van Ooijen P, Oudkerk M, de Feyter PJ: Intravenous coronary angiography by electron beam computed tomography: a clinical evaluation. *Circulation* 1998;98:2509 2512
16. Achenbach S, Moshage W, Ropers D, Nossen J, Daniel WG: Value of electron beam computed tomography for the noninvasive detection of high grade coronary artery stenoses and occlusions. *N Engl J Med* 1998;31:1964 1971

3.2

Coronary Angiography with Multi-slice Computed Tomography

Koen Nieman
Matthijs Oudkerk
Benno J Rensing
Peter MA van Ooijen
Arie Munne
Robert-Jan M van Geuns
Pim J de Feyter

SUMMARY

Background:

A new generation of subsecond multi slice computed tomography (MSCT) scanners, which allow complete coronary coverage, are becoming widely available. We investigated the potential value of MSCT angiography in a range of coronary disorders.

Methods:

We studied 35 patients, including 11 who had undergone percutaneous transluminal coronary angioplasty and four who had had coronary artery bypass grafts, by both MSCT and conventional coronary angiography. After intravenous injection of a non ionic contrast medium with high iodine content, the entire heart was scanned within a single breath hold. The total examination time was no more than 20 min. The retrospective electrocardiographically gated reconstruction source images and three dimensional reconstructed volumes were analysed by two investigators, unaware of the results of conventional angiography.

Findings:

In the 31 patients without previous coronary surgery, 173 (73%) of the 237 proximal and middle coronary segments were assessable. In the assessable segments, 17 of 21 significant stenoses (>50% reduction of vessel diameter) were correctly diagnosed. The non assessable segments included four lesions. Misinterpretations were mainly the result of severe calcification of the vessel wall. Segments with implanted stents were poorly visualised, but stent patency could be assessed in all cases. Of the 17 segments of bypass grafts, 15 were assessable and four of five graft lesions were detected. Two cases of anomalous coronary anatomy could be visualised well.

Interpretation:

These preliminary data suggest that MSCT allows non invasive imaging of coronary artery stenoses and has potential to develop into a reliable clinical technique.

INTRODUCTION

Conventional X ray coronary angiography is the standard of reference for the assessment of coronary artery disease. It is an invasive and potentially harmful procedure with a small risk of serious events (arrhythmia, stroke, coronary artery dissection, death). Furthermore, the catheterisation procedure involves admission to hospital and discomfort for the patient. Therefore, conventional angiography should be undertaken only on strict clinical indications.

Magnetic resonance imaging and electron beam computed tomography have been investigated for noninvasive coronary imaging. However, both have significant limitations in reliable visualisation of the coronary arteries.¹⁻⁴ Multi slice computed tomography (MSCT) scanners have lately become widely available. These scanners have the potential to allow non invasive coronary angiography within a single breath hold by use of a rotation speed of 0.5 s and sophisticated algorithms for retrospective electrocardiographic (ECG) gating. We aimed in this study to assess the diagnostic potential of non invasive MSCT angiography for the assessment of coronary artery disease.

METHODS

35 patients (27 male, eight female; mean age 59 years [SD 11; range 28–77]) underwent both conventional and MSCT angiography of the coronary arteries or bypass grafts. 11 patients had previously undergone percutaneous transluminal coronary angioplasty with stent implantation, and four coronary artery bypass grafting. Two patients had a congenital coronary artery variant. Patients were included only if they had a regular heart rhythm and good pulmonary function. Exclusion criteria were: previous allergic reactions to iodine containing contrast media, severe renal failure, pregnancy, an unstable clinical condition, or circumstances of any kind that would not allow the patient to lie in a supine position. All patients scheduled for conventional coronary angiography at our centre were approached until the scanning slots allocated to the research project were filled. The study protocol was approved by the hospital's ethics committee and all patients gave informed consent.

A new generation of multi detector array CT scanners operate at an increased rotation rate (2 per s) and produce up to four slices simultaneously.⁵ These developments permit high speed scanning of large volumes with a high in plane resolution, as well as an improved Z axis resolution and a substantial improvement in the inter slice correlation.⁶ Partial scan reconstruction techniques, which apply a 90–180° reconstruction algorithm, improve the temporal resolution to 250 ms. These algorithms also reduce the effective slice thickness at an acceptable increase in noise and reduction in contrast.⁷ Recent modifications in the reconstruction software have further reduced the virtual temporal resolution at higher heart rates by combining the data from several heart cycles in one image, shortening the effective acquisition intervals to 125 ms. The in plane spatial resolution of the MSCT scanner is nine line pairs per cm.⁸ We used retrospective

gating, which allows post scan acquisition window selection and optimum gating.⁹ This approach improves the image quality and decreases the sensitivity to arrhythmia and ECG noise.

The patient was placed within the gantry of an MSCT scanner (Somatom plus 4 Volume Zoom, Siemens AG, Erlangen, Germany) in a supine position. Leads were attached for simultaneous ECG and image recording necessary for inter related image reconstruction. According to the expected location of the coronary arteries, obtained from the coronal scout view, the scan volume was defined, depending on the patient's ability to cooperate and characteristics (breath hold, heart rate) and the scan variables (pitch, slice thickness, scan time). For arterial grafts, the area to be covered was extended to the origin of the left internal mammary artery. Fixed scanning variables included the 0.5 s rotation time and a tube voltage of 140 kV. We used a protocol of four slices with a collimated slice thickness of 1 mm. The pitch (table feed per rotation divided by the single collimated slice thickness) was set at 1.5 for heart rates below 80 beats per min and 2.0 for faster heart rates. Depending on the selected pitch and volume to be covered, the total scan time was between 30 s and 40 s. After thorough instruction, most of the patients were able to suspend respiration for 40 s. To facilitate adequate breath holding, the patients were asked to hyperventilate before the start of the scan. Optimum contrast between blood and surrounding tissue was achieved by injection of 150 mL contrast agent with a high iodine content (350 g iodine per L; Iomeprol, Bracco Byk Gulden, Konstanz, Germany) into the antecubital vein at a rate of 3.5–4.0 mL/s. Scanning was started after 20 s. The radiation dose was estimated to be 4.9 mSv (ICRP 60, Monte Carlo, Aarhus University Hospital). The acquired CT and ECG data were sent to a separate workstation, and dedicated cardiac work in progress reconstruction software (Siemens Cardio Package, Siemens AG; and MatLab version 5.3, MathWorks Inc, Natick, MA, USA) was used to reconstruct the images. Transverse tomograms were reconstructed from the acquired CT data during a preselected interval of 125–250 ms, depending on the heart rate, within the cardiac cycle. To minimise motion artefacts, the reconstruction window was positioned in the mid to late diastolic phase at a fixed point before the next R wave. If ECG irregularities occur, the retrospective ECG gating can be corrected manually. Owing to the spiral motion of the detector row, the 4 x 1 mm collimation results in an effective slice thickness of 1.25 mm. Through reconstruction of overlapping slices at an increment of 0.8 mm, a stack of 130–150 slices is created. Further parameters include a 150 mm field of view and a 512x512 matrix, which results in an interpolated voxel size of 0.3 x 0.3 x 0.8 mm³.

The images were further processed on separate graphic workstations (Indigo 2 and O2, SGI, Mountain View, CA) by means of special software packages (Vitrea and Voxel View, Vital Images, Plymouth, MN, USA). To analyse the coronary arteries, several volume rendering techniques were used. Multiplanar reformatting allows the investigator to place and manoeuvre cross sectional image planes through a three dimensional volume. High level (>150 Hounsfield units) and narrow window

settings were used to discriminate between contrast-enhanced lumen and the vessel wall. Three dimensional volume rendering techniques with manual segmentation of overlying structures (Voxel View, Vital Images) were used to demonstrate the three dimensional course of the cardiac vessels around the heart. All scans were evaluated by consensus of two experienced investigators, who were unaware of the conventional angiographic results. If consensus could not be reached, a third investigator was consulted.

Cardiac catheterisation and contrast enhanced X ray coronary angiography were done according to standard techniques. Multiple views of the coronary arteries were obtained and stored on a CD ROM. The angiograms were evaluated by two cardiologists without knowledge of the MSCT angiographic findings. In cases of disagreement, a third cardiologist was consulted. Coronary artery segments were classified as significantly stenosed (diameter reduction $\geq 50\%$) or as normal or not significantly stenosed (diameter reduction $< 50\%$).

We investigated the proximal and middle segments of the coronary artery tree, which includes the proximal, middle, and distal segments of the right coronary artery, the left main artery, the proximal and middle segments of the left anterior descending artery, and the proximal and middle segments of the left circumflex artery, according to the guidelines of the American Heart Association.¹⁰ Thus, eight segments per patient were available for assessment. After localisation, the respective segments were first semiquantitatively classified as assessable or not. Segments with stents were excluded. Results from the two angiographic techniques were compared, with conventional angiography serving as the standard of reference.

RESULTS

The median time between conventional and MSCT angiography was 9 days (range 0–39). During the MSCT investigations, no severe complications occurred. Two patients developed an allergic skin reaction, one within 1 h and the other 48 h after injection of the contrast agent. Average investigation time, including preparation and scanning, was less than 20 min. Reconstruction of the images took about 45 min, preparation of the three dimensional volumes up to 1 h, and each evaluation around 15 min.

Among the 31 patients without previous coronary surgery, the conventional coronary angiogram showed disease of one vessel in eight patients, two vessels in four, three vessels in three, and four vessels in one (including the left main artery). 15 patients showed no significant lesions. 248 artery segments were available for analysis. After exclusion of 11 stented segments, 73% (173 of 237 segments) were assessable by MSCT (table 1). The reasons why segments could not be assessed are given in table 2.

The non assessable segments included three lesion containing segments of right coronary artery and one of the left main artery.

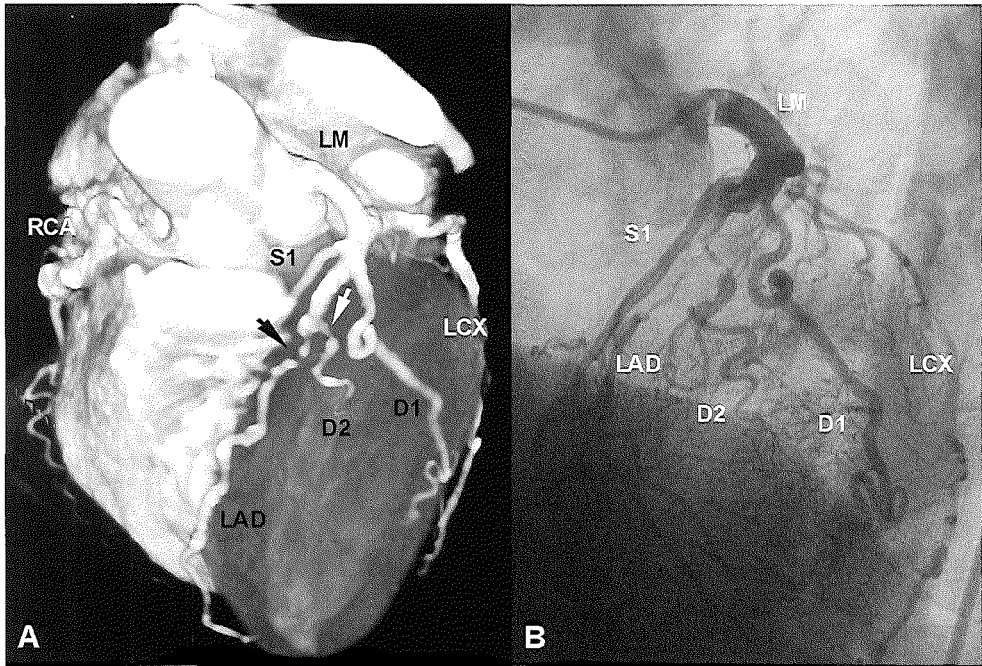


Figure 1. Left anterior oblique projection with cranial angulation by MSCT coronary angiography (A) and conventional coronary angiography (B). Occlusion (black arrow) of the left anterior descending artery (LAD) with collateral filling of the distal LAD as well as a severe stenosis (white arrow) of the second diagonal branch (D2), were detected with both modalities. The septal branch (S1) and the first diagonal artery (D1) are well visualised. The proximal left circumflex artery (LCX) appears severely calcified on the MSCT angiogram. LM=left main coronary artery.

(A full color version of this illustration can be found in the color section)

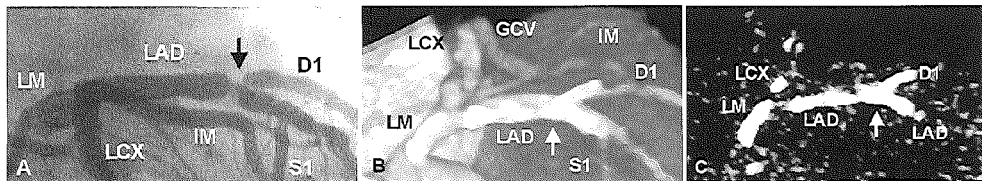


Figure 2. Conventional and MSCT angiography of left anterior descending artery (LAD).

A: Conventional X ray coronary angiogram shows a stenosis (black arrow) in LAD proximal to the first diagonal artery (D1).

B: Owing to extensive calcification, the stenosis is obscured (white arrow) on the MSCT angiogram.

C: High density threshold MSCT representation of the LAD, which exclusively shows the calcifications in the vessel wall. LM=left main coronary artery; LCX=left circumflex artery; S1=first septal branch; GCV=great cardiac vein.

Table 1: Number of assessable segments in 31 patients

Segment	Number assessable/total
Right coronary artery	
Proximal	26/29 (90%)
Middle	18/30 (60%)
Distal	20/31 (65%)
Left main artery	
29/30 (97%)	
Left anterior descending artery	
Proximal	28/30 (93%)
Middle	20/26 (77%)
Left circumflex artery	
Proximal	21/30 (70%)
Middle	11/31 (35%)
Total	173/237 (73%)
11 segments with an implanted stent were excluded.	

Table 2: Reasons for non assessability of vessel segments

	Left main	Left anterior descending	Left circumflex	Right coronary	Total
Cardiac motion/arrhythmia	0	0	2	14	16
Extensive calcifications	1	6	5	3	15
Small vessel (<1.5 mm)	0	0	12	0	12
Adjacent contrast filled structures*	0	1	6	3	10
Non cardiac motion (breathing)	0	0	2	5	7
Poor opacification	0	1	2	1	4

*Veins or ventricle.

17 (81%) of 21 significant lesions were correctly detected, and 148 (97%) of 152 normal or non significantly diseased segments were correctly diagnosed by MSCT (figure 1, table 3). Arterial calcification (figure 2), as well as blending with overlying vessels, led to the four falsepositive and four false negative interpretations (table 3). Of the 11 patients with intracoronary stents, six were scanned within 2 weeks of the procedure and five were scanned when they presented with recurrent symptoms. All stents could be localised and related to the vessel in which they were positioned. Beam hardening and partial volume artefacts hampered visualisation of the lumen within the stent.

Nevertheless, the vessel segment distal to the stent could be recognised in all cases, indicating stent patency, confirmed by conventional angiography.

Four patients (three men, one woman) had previously undergone coronary artery bypass grafting. The average time between surgery and the MSCT scan was 9 years (range 4–13). All patients underwent conventional coronary angiography because of recurrent symptoms. The group consisted of three arterial (five anastomoses) and three venous grafts (with 12 distal anastomoses). The investigators were familiar with the surgeon's operative report but unaware of the results of conventional angiography. Image quality was adequate for assessment in 15 of 17 available conduits. Two arterial conduits could not be assessed owing to the small vessel size and artefacts caused by metal clips.

No stenoses were observed by either MSCT or conventional angiography in the arterial conduits. In the venous grafts, two stenoses and two completely occluded conduits were correctly diagnosed by MSCT (figure 3). One vessel apparently occluded on MSCT was patent on conventional angiography. Two patients presented with anomalous anatomy of the coronary vessels. In both cases the coronary anatomy could be presented in a readily interpretable threedimensional image (figure 4).

DISCUSSION

We found that significant stenoses (>50% reduction in diameter) in the proximal and middle coronary arteries could be detected by MSCT coronary angiography. Segments of the left main and left anterior descending arteries were visualised in most cases (90%), and six of eight stenoses were correctly detected. Visualisation of the right coronary artery is more sensitive to motion artefacts, which resulted in a lower proportion of interpretable segments (71%). Nevertheless, all seven lesions were correctly diagnosed. The left circumflex artery was the most difficult to examine. This artery is small in many people, and it easily blends with adjacent contrast filled structures such as the great cardiac vein and the left atrium. Only 51% of the circumflex segments were assessable, and two of four stenoses were detected.

In the presence of intracoronary stents, high density artefacts, combined with partial volume effects, prevent adequate assessment of the small vessel lumen within the struts of the stent. However, patency can be assessed if enhancement by contrast medium is observed in the vessel segment distal to the stent. In larger diameter vessels, such as the carotid arteries, the in stent lumen can be assessed quite well.¹¹ Assessability of the stented segments is expected to increase with the improvement of spatial resolution and the use of less radio opaque alloys for stents. Coronary artery bypass grafts, because of their size and relative immobility, can be reliably imaged. In patients with an anomalous origin or course of the coronary arteries, MSCT displays, in contrast to conventional angiography, a three dimensional map of the coronary anatomy, which allows easy identification of a high risk course of a coronary artery between the pulmonary artery and the aorta (figure 4).

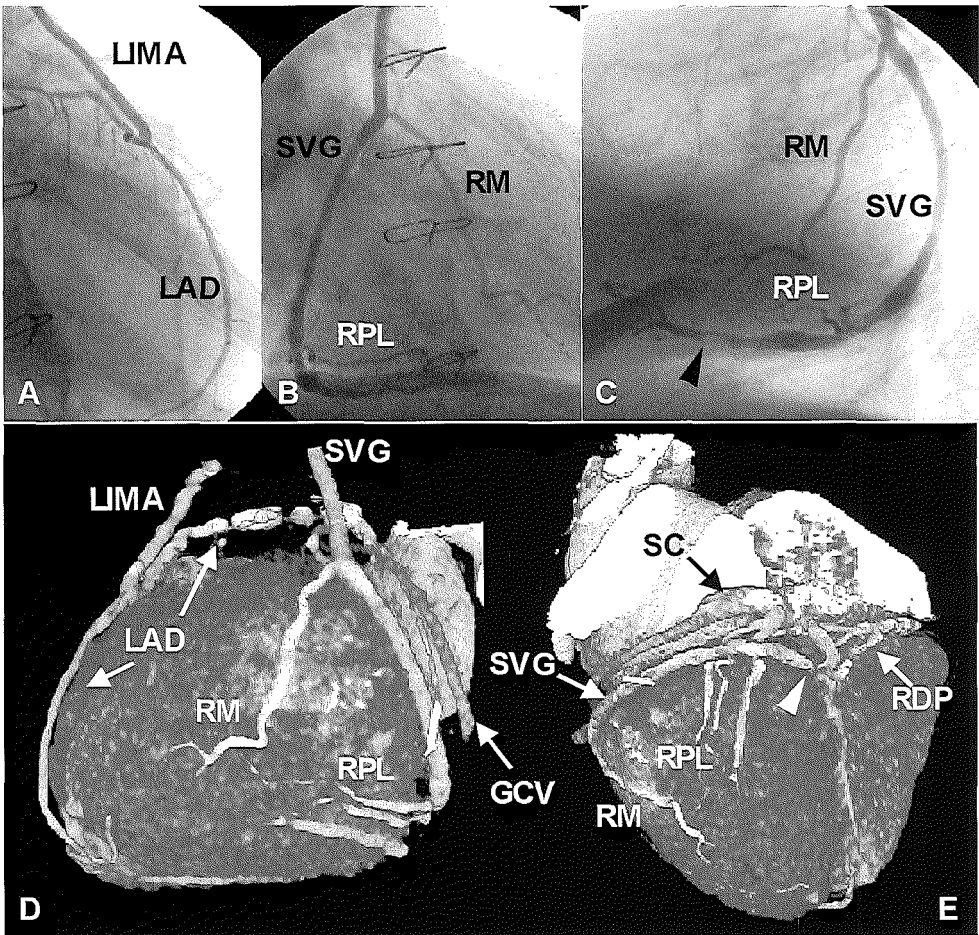


Figure 3. Conventional coronary angiography (A, B, C) and MSCT angiography (D, E) of a patient with previous coronary artery bypass grafting. Left internal mammary artery (LIMA) is anastomosed to the left anterior descending artery (LAD). A saphenous vein graft (SVG) jumps via the marginal branch (RM) to the posterolateral branch (RPL) and the right descending posterior branch (RDP). The last segment shows a significant lesion (arrow head). SC=coronary sinus; GCV=great cardiac vein.

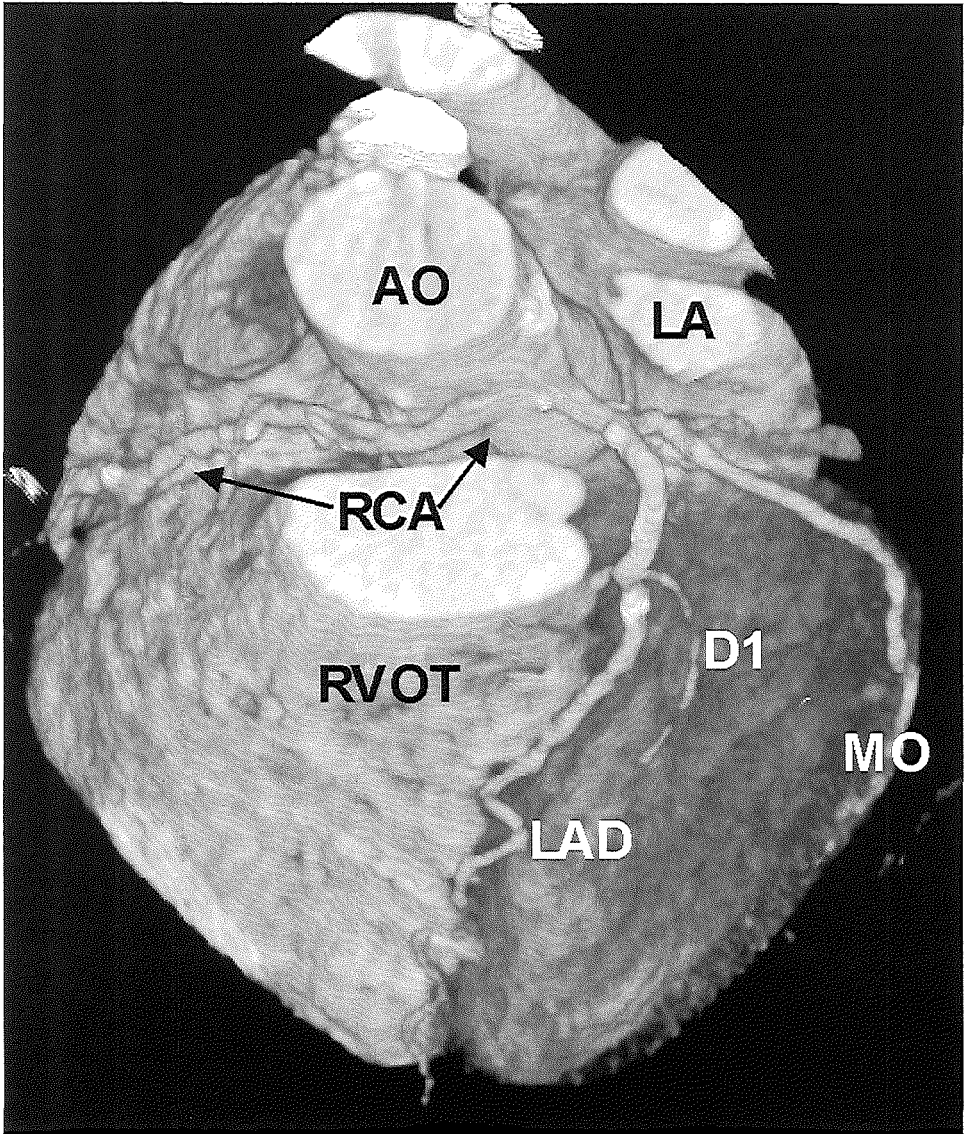


Figure 4. Three dimensional reconstruction (cranio left anterior view) of an MSCT scan of a coronary anomaly.

Aberrant right coronary artery (RCA) originates from left aortic sinus near left main coronary artery and runs between aorta (AO) and pulmonary artery, which has been removed, to right atrioventricular groove. This notorious anomaly can lead to myocardial infarction and sudden death. RVOT=right ventricle outflow tract; LA=left atrium; LAD=left anterior descending artery; D1=first diagonal artery; MO=marginal branch. (A full color version of this illustration can be found in the color section)

Despite these satisfying initial results, some technical limitations remain. Although manual repositioning of the R wave indicators during retrograde gating improves the synchronisation of acquisition intervals between consecutive heartbeats, cardiac motion artefacts cannot be entirely prevented. For instance, the middle segment of the right coronary artery, which is mobile during the cardiac cycle, runs perpendicular to the transverse slices. Consequently, this vessel is more vulnerable to arrhythmia and inaccurate triggering, which results in discontinuity between the consecutive slices. Movement of the patient, such as breathing, also causes motion artefacts, which can be reduced by thorough instruction before scanning.

The presence of extensive calcifications can complicate correct assessment of the lumen of the coronary arteries. The high contrast calcium depositions cannot be sufficiently isolated from the contrast enhanced vessel lumen and may result in non assessable segments or misinterpretation. Nevertheless, severe calcification of the coronary arteries is related to coronary artery disease, and its detection will contribute to clinical decision making.¹²

Magnetic resonance coronary angiography can visualise the coronary anatomy and detect stenotic lesions in the proximal segments of the coronary arteries.¹³⁻¹⁸ However, the diagnostic accuracy varies substantially between studies.^{1,19} The advantages of magnetic resonance angiography are the absence of ionising radiation and iodine contrast agents and the opportunity to combine the assessment of the coronary arteries with the examination of other features related to ischaemic heart disease, such as ventricular function, myocardial perfusion, and coronary flow.²⁰ However, this technique is still hampered by poor spatial resolution, long scan times, image degeneration by metal objects (stents, sternal wires), and contraindications to magnetic resonance imaging.

The electron beam CT scanner is a non mechanical sequential CT scanner, in which the electron beam that produces the X rays rotates around the patient. Because there are no mechanically rotating components, the temporal resolution (100 ms) is high. However, the inplane spatial resolution is slightly lower than in MSCT.⁸ Electron beam CT is prospectively gated. When a 1.5 mm slice thickness protocol is applied, it can cover 6 cm in 40 heart beats, which allows only scanning of the proximal and middle segments of the coronary arteries of a normal sized heart.^{2,3} The entire heart can be covered with a 3 mm protocol at the cost of a reduction in Z axis resolution.

The non invasive modalities still fall short of the diagnostic superiority of conventional coronary angiography, but these new techniques are only in the early stages of development. Further technical refinement of the individual modalities and introduction of computer systems that allow significantly faster data processing will accelerate the clinical implementation of non invasive coronary angiography.

Besides being a non invasive alternative, MSCT and electron beam CT offer additional information about the spatial orientation of vessels and are able to identify and quantify calcium deposition within the vessel wall.

Those with a (shared) subscription to *the Lancet*, can view several movies of rotating volume rendered coronary angiograms at the following website: <http://www.thelancet.com>

REFERENCES

- 1 Wielopolski PA, van Geuns RJ, de Feyter PJ, Oudkerk M. Coronary arteries. *Eur Radiol* 2000; 10: 12–35.
- 2 Rensing BJ, Bongaerts A, van Geuns RJ, et al. Intravenous coronary angiography by electron beam computed tomography: a clinical evaluation. *Circulation* 1998; 98: 2509–12.
- 3 Achenbach S, Moshage W, Ropers D, Nossen J, Daniel WG. Value of electron beam computed tomography for the noninvasive detection of high grade coronary artery stenoses and occlusions. *N Engl J Med* 1998; 339: 1964–71.
- 4 de Feyter PJ, Nieman K, van Ooijen P, Oudkerk M. Non invasive coronary artery imaging with electron beam computed tomography and magnetic resonance imaging. *Heart* 2000; 84: 442–48.
- 5 Klingenbeck Regn K, Schaller S, Flohr T, Ohnesorge B, Kopp AF, Baum U. Subsecond multi slice computed tomography: basics and applications. *Eur J Radiol* 1999; 31: 110–24.
- 6 Hu H, He HD, Foley WD, Fox SH. Four multidetector row helical CT: image quality and volume coverage speed. *Radiology* 2000; 215: 55–62.
- 7 Kachelreiss M, Kalender WA. Electrocardiogram correlated image reconstruction from subsecond spiral computed tomography scans of the heart. *Med Phys* 1998; 25: 2417–31.
- 8 Becker CR, Knez A, Leber A, et al. Erste Erfahrungen mit der Mehrzeilen detektorspiral CT in der Diagnostik der Arteriosklerose der Koronargefasse. *Radiologe* 2000; 40: 118–22.
- 9 Ohnesorge B, Flohr T, Becker C, et al. Cardiac imaging by means of electrocardiographically gated multisection spiral CT: initial experience. *Radiology* 2000; 217: 564–71.
- 10 Austen WG, Edwards JE, Frye RL, et al. A reporting system on patients evaluated for coronary artery disease. *Circulation* 1975; 51: 5–40.
- 11 Leclerc X, Gauvrit JY, Pruvo JP. Usefulness of CT angiography with volume rendering after carotid angioplasty and stenting. *Am J Roentgenol* 2000; 174: 820–22.
- 12 Bielak LF, Rumberger JA, Sheedy PF II, Schwartz RS, Peyser PA. Probabilistic model for prediction of angiographically defined obstructive coronary artery disease using electron beam computed tomography calcium score strata. *Circulation* 2000; 102: 380–85.
- 13 Post JC, van Rossum AC, Hofman MB, Valk J, Visser CA. Three dimensional respiratory gated MR angiography of coronary arteries: comparison with conventional coronary angiography. *Am J Roentgenol* 1996; 166: 1399–404.
- 14 Pennell DJ, Bogren HG, Keegan J, Firmin DN, Underwood SR. Assessment of coronary artery stenosis by magnetic resonance imaging. *Heart* 1996; 75: 127–33.
- 15 Huber A, Nikolaou K, Gonschior P, Knez A, Stehling M, Reiser M. Navigator echo based respiratory gating for three dimensional MR coronary angiography: results from healthy volunteers and patients with proximal coronary artery stenoses. *Am J Roentgenol* 1999; 173: 95–101.

- 16 Sandstede JJ, Pabst T, Beer M, Geis N, Kenn W, Neubauer S, Hahn D. Three dimensional MR coronary angiography using the navigator technique compared with conventional coronary angiography. *Am J Roentgenol* 1999; 172: 135–39.
- 17 Kessler W, Achenbach S, Moshage W, et al. Usefulness of respiratory gated magnetic resonance coronary angiography in assessing narrowings (\geq or =50%) in diameter in native coronary arteries and in aortocoronary bypass conduits. *Am J Cardiol* 1997; 80: 989–93.
- 18 van Geuns RJM, de Bruin HG, Wielopolski PA, et al. MRI of the coronary arteries: clinical results from three dimensional evaluation of a respiratory technique. *Heart* 1999; 82: 515–19.
- 19 van Geuns RJM, Wielopolski PA, de Bruin HG, et al. MR coronary angiography with breath hold targeted volumes: preliminary clinical results. *Radiology* 2000; 217: 270–77.
- 20 Pattynama PM, De Roos A, Van der Wall EE, Van Voorthuisen AE. Evaluation of cardiac function with magnetic resonance imaging. *Am Heart J* 1994; 128: 595–607.

3.3

Usefulness of Multislice Computed Tomography for Detecting Obstructive Coronary Artery Disease

Koen Nieman
Benno J Rensing
Robert-Jan M van Geuns
Arie Munne
Jurgen MR Ligthart
Peter MT Pattynama
Gabriel P Krestin
Patrick W Serruys
Pim J de Feyter

ABSTRACT

The latest generation of multislice spiral computed tomography (MSCT) scanners is capable of noninvasive coronary angiography. We evaluated its diagnostic accuracy to detect stenotic coronary artery disease (CAD). In 53 patients with suspected CAD, contrast enhanced MSCT and conventional angiography were performed. The CT data were acquired within a single breathhold, and isocardiophasic slices were reconstructed by means of retrospective electrocardiographic gating. Coronary segments of ≥ 2 mm in diameter, measured by quantitative angiography, were evaluated. In 70% of the 358 available segments, image quality was regarded as adequate for assessment. The overall sensitivity, specificity, and positive and negative predictive values to detect $\geq 50\%$ stenotic lesions in the assessable segments were 82% (42 of 51 lesions), 93% (285 of 307 nonstenotic segments), and 66% and 97%, respectively, regarding conventional quantitative angiography as the gold standard. Proximal segments were assessable in 92%, and distal segments and side branches in 71% and 50%, respectively. Including the undetected lesions in nonassessable segments, overall sensitivity decreased to 61% but remained 82% for lesions in proximal coronary segments. MSCT correctly predicted absent, single, or multiple lesions in 55% of patients. Thus, despite potentially high image quality, current MSCT protocols offer only reasonable diagnostic accuracy in an unselected patient group with a high prevalence of CAD.

INTRODUCTION

Over the past decades, the feasibility of noninvasive coronary imaging has been explored using different modalities, such as magnetic resonance imaging and electron beam computed tomography.^{1,2} Despite encouraging initial results, neither technique is yet considered suitable for routine clinical use. Recent developments in multislice spiral computed tomography (MSCT) have expanded the potential of intravenously contrast enhanced spiral computer tomographic coronary angiography. At an increased gantry rotation rate, up to 4 slices can be acquired. The improved temporal and spatial resolutions have created the opportunity to acquire high quality images of the entire heart within 1 single breathhold.^{3,4} We evaluated the diagnostic accuracy of retrospective, electrocardiographically synchronized MSCT angiography to detect coronary artery disease (CAD) of therapeutically relevant arteries in 53 patients using the conventional x ray angiogram as the gold standard.

METHODS

Study group

MSCT angiography was performed in 53 patients, who were referred for angiographic evaluation of suspected CAD. Patient characteristics are listed in Table 1. Patients who previously underwent angioplasty with stent implantation or coronary bypass surgery were excluded. Further exclusion criteria were irregular heart rates, previous allergic reaction to iodine contrast media, renal insufficiency (serum creatinine >100 mmol/L), pregnancy, respiratory impairment, unstable clinical status, or marked heart failure. The median interval between the catheterization procedure and MSCT angiography was 10 days. A total of 19 patients were included in a preliminary report.⁵ The study was approved by the local ethical committee and informed consent was obtained from all patients.

MSCT scan protocol

The MSCT scans were obtained during breathhold, preceded by a short session of instructed hyperventilation (Somatom Plus 4 VolumeZoom, Siemens, Forchheim, Germany). First, a fast localization scan was performed to determine the boundaries of the heart. For contrast enhanced angiographic acquisition, a fixed delay of 18 seconds was used between start of the contrast injection (Iomeprol, Bracco Byk Gulden, Konstanz, Germany) and onset of the scan. A collimation protocol of 4 1.0 mm slices was used at a table increment of 1.5 mm/rotation for heart rates <80 beats/min, or 2.0 mm/rotation for heart rates \geq 80 beats/min, to assure gapless data reconstruction and to limit oversampling. Depending on the dimensions of the heart, the scan time varied between 30 and 45 seconds (Table 2).

Retrospective electrocardiographically gated image reconstruction

From the MSCT data and the recorded electrocardiogram, an overlapping stack of isocardiophasic transverse slices (1.25 mm, increment of 0.5 to 0.8 mm) were reconstructed using a 180° rotation partial scan algorithm.³ For heart rates <65 beats/min, a single segment reconstruction algorithm is applied to reconstruct slices during a 250 ms interval within each separate RR interval. For heart rates \geq 65 beats/min, a 2 segment algorithm combines isocardiophasic data from 2 consecutive RR intervals. The effective reconstruction interval, which varies from 125 to 250 ms, depends on a complex relation between the gantry rotation speed, patient heart rate, and table feed, which are described elsewhere.⁴ At least 3 data sets were created with a reconstruction window positioned within the diastolic phase starting at 300, 400, and 500 ms before the following R wave. Other window positions were reconstructed if satisfactory results were not achieved. One data set with the least motion artifacts, typically reconstructed at approximately 400 ms before the next R wave or more toward 300 ms at higher heart rates, was selected for further analysis (Table 2).

TABLE 1. Patient Characteristics (n = 53)

General Characteristics

Age (yrs) (range)	56 ± 10 (28 – 79)
Men/women	40/13
Average heart rate (beats/min)	68 ± 12
No. of arteries with ≥50% stenoses in ≥2.0 mm segments	
0	14 (26%)
1	23 (43%)
>1	16 (30%)
Obstructive lesions	
50% – 90% stenosis	56 (81%)
100% occlusions	13 (19%)

TABLE 2. Scan Parameters

Tube current (mA)	300
Tube voltage (kV)	120
Collimation	4 X 1 mm
Table feed per gantry rotation (pitch)	1.5*
Scan time (s)	30–45
Contrast agent: iomeprol (350 mg [iodine]·ml ⁻¹)	150 ml at 4 ml·s ⁻¹
Synchronization to the electrocardiogram	Retrospectively
Effective slice thickness (mm)	1.25
Reconstruction increment (mm)	0.5 or 0.8
Field of view (mm)	130 – 180
Matrix	512 x 512
Z axis coverage (mm)	90 – 135
In plane resolution (line pairs·cm ⁻¹)	8
Through plane resolution (line pairs·cm ⁻¹)	6

* For HR >80 pitch = 2.0

Data processing

A stack of approximately 200 images was transferred to off line graphic workstations for further postprocessing (O2 & Indigo 2, SGI, Mountain View, California). Depending on the coronary morphology and quality of the data set, several postprocessing techniques were applied to assess the coronary arteries (Vitrea & VoxelView, Vital images Inc., Plymouth, Minnesota). The axial source images and multiplanar reconstruction, which allows positioning of 2 dimensional cross sectional image planes through the volume data set and interactive tracking of the vessels, were used for detecting stenotic lesions. In addition, other techniques such as 3 dimensional volume rendering and maximum intensity projections were applied to present an overview of the coronary status.

Data analysis

All coronary artery segments were assessed by 2 investigators who were blinded to conventional coronary angiographic results (Table 2).⁶ According to the image quality, each vessel segment was classified as either assessable or not. The assessed by 2 investigators who were blinded to conventional coronary angiographic results (Table 2). According to the image quality, each vessel segment was classified as either assessable or not. The assessable segments were screened for the presence of significant narrowing (>50% lumen diameter reduction) or complete occlusion. In case of disagreement, a final decision was reached by consensus. Because smaller segments are generally not considered for revascularization, only vessel segments with a diameter of ≥ 2.0 mm, as measured by quantitative coronary angiography, were included for analysis.

Conventional coronary angiography

Cardiac catheterization and selective x ray coronary angiography were performed according to standard techniques. From 2 orthogonal projections, quantitative coronary angiography of all coronary branches and side branches was performed to identify the segments with a diameter of ≥ 2.0 mm. The angiograms were screened for stenotic lesions using quantitative coronary angiography in 2 orthogonal projections to confirm significance: $\geq 50\%$ vessel lumen diameter reduction. An average value determined the severity of the stenotic lesions.

TABLE 3 Diagnostic Accuracy of Multislice Spiral Computed Tomographic Angiography Stratified According to Coronary Branch*

		Coronary
Branches		All
Segments		1–16
Assessability	Available segments	513
	Assessable segments	358 (70%)
Causes for nonassessability	Cardiac motion	51 (33%)
	Calcium deposits	30 (19%)
	Other cause	43 (28%)
	Unspecified	31 (20%)
Coronary narrowings †	Total	51 (18)
	Complete occlusions	12 (1)
	Partial stenoses ≥50%	39 (17)
Diagnostic accuracy	Sensitivity	82% (71%–91%)
	Specificity	93% (91%–94%)
	PPV	66% (57%–72%)
	NPV	97% (95%–98%)
	Sensitivity, all available segments ‡	61% (51%–69%)
Causes for misinterpretation	Total	31
	Calcium deposits	16
	Cardiac motion	10
	Other cause	5

*Significant stenosis: ≥50% lumen diameter reduction; minimal vessel lumen diameter 2.0 mm.

†Number of lesions in the nonassessable segments in parentheses.

‡Sensitivity for all ≥2.0 mm segments. Undetected lesions in nonassessable segments were regarded as false negative scores.

to Detect Significant Coronary Stenoses in the Assessable Coronary Segments,

Arteries			
Right 1-4, 16	LM 5	LAD 6-10	LC 11-15
156	53	175	129
104 (67%)	52 (98%)	134 (77%)	68 (53%)
28 (54%)	—	8 (20%)	15 (25%)
7 (13%)	1 (100%)	15 (37%)	7 (11%)
13 (25%)	—	11 (27%)	19 (31%)
4 (8%)	—	7 (17%)	20 (33%)
18 (7)	3	21 (6)	9 (5)
8	—	3 (1)	1
10 (7)	3	18 (5)	8 (5)
94% (75%–100%)	100%	86% (66%–96%)	44% (17%–67%)
94% (90%–95%)	100%	88% (84%–90%)	95% (91%–98%)
77% (61%–82%)	100%	56% (43%–63%)	57% (22%–87%)
99% (95%–100%)	100%	97% (93%–99%)	92% (98%–95%)
68% (51%–79%)	100%	67% (49%–81%)	29% (11%–44%)
6	0	17	8
2		9	5
4		5	1
0		3	2

LAD = left anterior descending coronary artery; LC = left circumflex coronary artery; LM = left main coronary artery; NPV = negative predictive value; PPV = positive predictive value.

Usefulness of MSCT detection of coronary obstruction

TABLE 4. Diagnostic Accuracy of MSCT Detect Significant Coronary Stenoses in

Branches Segments		All 1–16
Assessability	Available segments	513
	Assessable segments	358 (70%)
Causes for nonassessability	Cardiac motion	51 (33%)
	Calcium deposits	30 (19%)
	Other cause	43 (28%)
	Unspecified	31 (20%)
Coronary narrowings †	Total	51 (18)
	Complete occlusions	12 (1)
	Partial stenoses ≥50%	39 (17)
Diagnostic accuracy	Sensitivity	82% (71%–91%)
	Specificity	93% (91%–94%)
	PPV	66% (57%–72%)
	NPV	97% (95%–98%)
	Sensitivity, all available segments ‡	61% (51%–69%)
Causes for misinterpretation	Total	31
	Calcium deposits	16
	Cardiac motion	10
	Other cause	5

*Significant stenosis; ≥50% lumen diameter reduction; minimal vessel lumen diameter 2.0 mm.

†Number of lesions in the non assessable segments between brackets.

‡Sensitivity for all ≥2.0 mm segments. Undetected lesions in nonassessable segments were regarded as false negative scores.

Assessable Coronary Segments, Stratified as Proximal, Middle, Distal, or Side Branch Segments*

Proximal Right 1, LM 5, LAD 6	Middle Right 2, LAD 7, LC 11	Distal right 3, LAD 8, LC 13	Side Branches PDA, D9, D10, RM12, RM14, PL15/16
155	134	118	106
142 (92%)	89 (66%)	75 (64%)	52 (49%)
4 (31%)	20 (44%)	19 (44%)	8 (15%)
8 (62%)	14 (31%)	4 (9%)	4 (7%)
1 (8%)	5 (11%)	16 (37%)	21 (39%)
—	6 (13%)	4 (9%)	21 (39%)
25 (3)	13 (8)	7 (2)	6 (5)
5 (1)	5	2	—
20 (2)	8 (8)	5 (2)	6 (5)
92%(77%–99%)	85%(57%–97%)	71%(33%–94%)	50%(15%–84%)
96%(93%–97%)	90%(85%–92%)	94%(90%–97%)	89%(85%–94%)
82% 69%–88%)	58%(39%–67%)	56%(26%–73%)	38%(11%–63%)
98%(95%–100%)	97%(92%–100%)	97%(93%–99%)	93%(88%–98%)
82%(67%–91%)	52%(33%–69%)	56%(25%–80%)	27%(8%–52%)
7	10	6	8
3	3	3	7
4	4	2	—
—	3	1	1

D = diagonal branch; PDA = posterior descending coronary artery;
PL = posterolateral branch; RM = marginal branch.

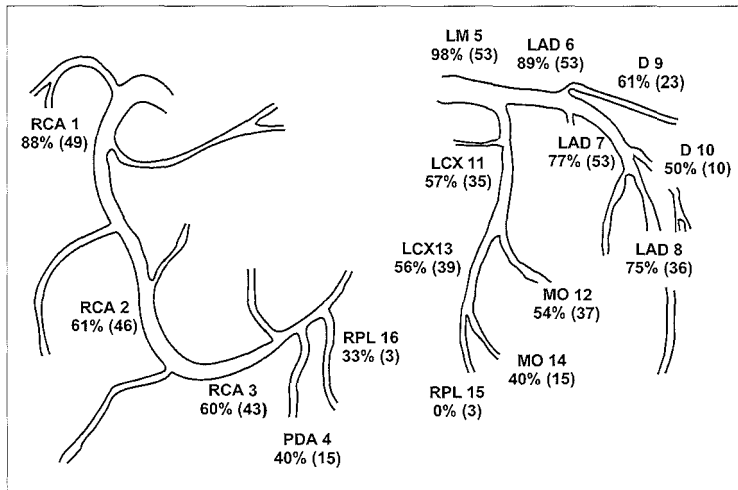


FIGURE 1. Assessable segments as a percentage of the available therapeutically relevant (diameter ≥ 2 mm) segments (*in parentheses*). D=diagonal; LAD=left anterior descending; LCX= left circumflex; LM=left main; MO=marginal; PDA=posterior descending coronary artery; RCA=right coronary artery; RPL= posterolateral branch.

TABLE 5. Diagnostic Accuracy Per Patients of MSCT*

Lesions	Assessable Segments		All Segments†	
	Accuracy‡	Predictive Value§	Accuracy‡	Predictive Value§
All	36/53 (68%)	36/53 (68%)	29/53 (55%)	29/53 (55%)
No lesions	15/20 (75%)	15/19 (79%)	9/14 (64%)	9/19 (47%)
Single lesion	12/24 (50%)	12/15 (80%)	9/23 (39%)	9/15 (60%)
Multiple lesions	9/9 (100%)	9/19 (47%)	11/16 (69%)	11/19 (58%)

*Figures are only according to the number of affected segments. Mismatching between individual lesions and locations was neglected.

†All ≥ 2 mm segments. Lesions in nonassessable segments as false negative scores.

‡Correct MSCT classification divided by number of patients (by conv. angiography).

§Correct MSCT classification divided by number of diagnoses (by MSCT).

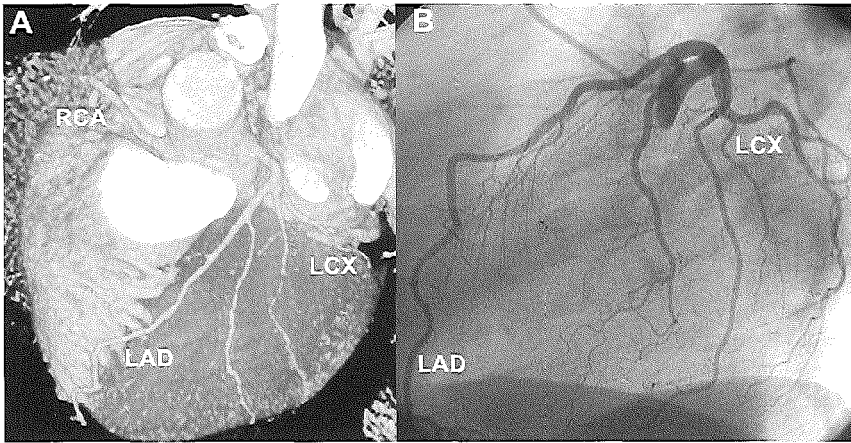


FIGURE 2. Volume rendered multislice CT (A) and conventional coronary angiogram (B). The left anterior descending coronary artery (LAD), including the proximal, intermediate, and diagonal side branches, and the small circumflex artery (LCX) can be assessed. Also, the proximal right coronary artery (RCA) can be observed. Interruptions are introduced by the volumerendering technique in the small distal intermediate branch.

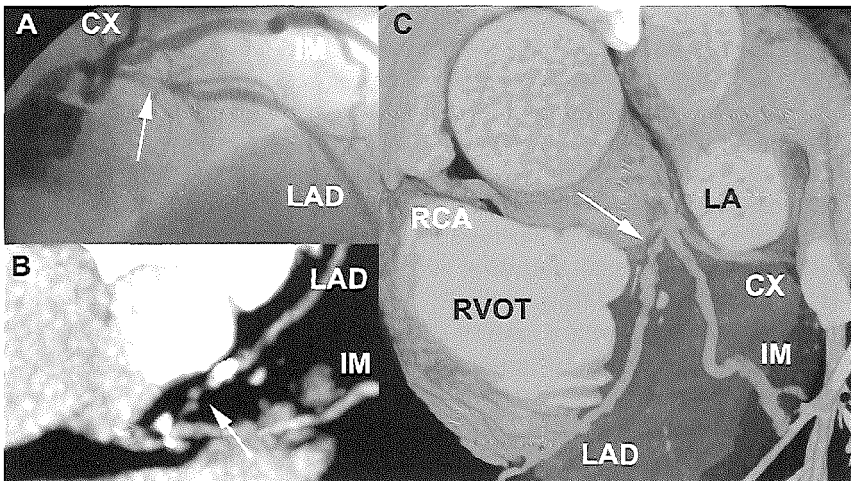


FIGURE 3. Stenotic lesion in the proximal part of the left anterior descending artery (LAD). (A), corresponding conventional angiogram (B), thin slab multiplanar reconstruct angiogram, and (C), volume rendered MSCT coronary angiogram. The proximal left anterior descending coronary artery (LAD) is significantly obstructed: 70% lumen diameter reduction, reference diameter 2.78 mm (arrow). The lesion is accompanied by discrete calcium deposits. CX= circumflex branch; IM=intermediate branch; LA=left atrium; RVOT=right ventricular outflow tract; other abbreviation as in Figures 1 and 2.

Statistical analysis

Continuous variables were expressed as means \pm SD. The diagnostic accuracy was expressed as sensitivity, specificity, negative predictive value, and positive predictive value. The descriptive statistics were stratified according to coronary segment: right vessel branch, left main artery, left anterior descending artery, and left circumflex coronary artery; proximal (right 1, left main, left anterior descending 6), middle (right 2, left anterior descending 7, left circumflex 11), distal (right 3, left anterior descending 8, left circumflex 13) or side branches, and individual patients. Precision of the diagnostic parameters was expressed using 95% confidence interval. Conventional (quantitative) coronary angiography was regarded as the standard of reference. Concordance between observers for the detection of stenotic lesions was calculated and expressed by the κ value.

RESULTS

Except for 2 cases of a mild allergic skin reaction to the contrast medium, no adverse events were encountered. The average scan time was 37 ± 4 seconds, and the entire examination was generally completed within 20 minutes. Depending on the data quality and complexity of the coronary status, postprocessing and assessment required 10 to 30 minutes. After exclusion of all segments that were either anatomically absent, too small (<2.0 mm vessel diameter), or not enhanced due to complete occlusion of a more proximal segment, 513 segments were available for assessment (Table 3). Of these coronary artery segments, 70% (358 of 513) were assessable (Figure 1). The left main coronary artery was assessable in all but 1 case of severe calcium deposition. Assessability of the left anterior descending coronary artery (77%) was frequently reduced by excessive calcium deposits (37%), whereas the right coronary artery proved most vulnerable to residual motion. Multiple factors, such as breathing artifacts, blending with adjacent structures and low overall contrast, in addition to motion artifacts, were responsible for nonassessability of the left circumflex coronary artery (Table 3). The overall sensitivity and specificity to detect significant stenoses in the assessable ≥ 2 mm segments was 82% and 93%, respectively. The positive and negative predictive values were 66% and 97%, respectively. All 3 stenoses in the left main coronary artery were detected. The sensitivity to detect lesions in the assessable right and left anterior descending coronary artery segments (94% and 86%) was better than it was for the left circumflex branches (44%) (Figures 2 and 3).

By including stenoses in the nonassessable vessels, overall sensitivity decreased to 61%. Both calcium deposits and residual motion were responsible for misinterpretations (Table 3). Proximal segments were more frequently assessable than distal segments, and a significantly higher sensitivity to detect stenoses was achieved. Only half of the side branches could be evaluated (Table 4 and Figure 4).

Inter and intraobserver variabilities were reasonable with k values of 0.65 and 0.66, respectively. Seventyfour percent of the patients with ≥ 1 obstructed segment and 64% of the those without lesions were correctly identified by MSCT (Table 5).

DISCUSSION

Advanced therapeutic options and improved patient survival have created a need for earlier and repeat coronary visualization in more and older patients. Despite the diagnostic superiority of selective x ray coronary angiography, safety and budgetary concerns have promoted the development of noninvasive alternatives. In a preliminary study, we evaluated the feasibility of MSCT coronary angiography and described a variety of clinical cases, including patients with bypass grafts and intracoronary stents.⁵ The size and homogeneity of the current study group allows analysis of the technique's diagnostic accuracy, which shows a fairly good sensitivity to detect obstructive disease. Despite a substantial number of falsepositive results, most significant stenoses (82%) were detected in the assessable segments. The large number of nonassessable vessel segments remain a source of concern. However, the good specificity suggests that this technique may be particularly suitable for exclusion of stenosis in patients with a low likelihood of extensive CAD, such as young patients with atypical chest pain. Even with a less than optimal image quality, total occlusions remain detectable. Only 1 occluded, but collaterally filled, left anterior descending coronary artery was considered nonassessable due to severe calcium deposits, and was therefore not diagnosed. The higher prevalence of occlusions in the right coronary artery may be responsible for a high sensitivity despite the motion artifacts that are more frequently observed in the right coronary artery (Figure 4). Our group consisted of patients with few physical complaints, a stable clinical condition, and a high prevalence of lesions. A patient selection bias can therefore be expected.

Our study confirms a previous report by Achenbach et al,⁷ who assessed 68% of ≥ 2 mm diameter vessels in 64 patients and reported a sensitivity and specificity of 91% and 84% to detect $>70\%$ stenosis, and 85% and 76% to detect $>50\%$ lesions, respectively. Including the lesions in nonassessable vessels, sensitivity decreased to 58%. Other investigators⁸ reported similar results at recent scientific meetings. According to a number of studies that used electron beam computed tomography, 75% to 90% of the proximal and middle coronary segments were assessable. The sensitivity and specificity to detect $>50\%$ lesions in these assessable segments ranged from 74% to 92% and 79% to 94%, respectively.⁹⁻¹⁴ Currently, noninvasive screening for obstructive CAD is routinely performed using exercise electrocardiography, planar scintigraphy, single proton emission computed tomography, and stress echocardiography. In a review by Lee and Boucher,¹⁵ averaged sensitivities of 68%, 79%, 88%, and 76%, respectively, to detect CAD in stable angina pectoris were reported. Although these figures still appear favorable compared with the current performance of MSCT, these modalities provide functional data on the presence and severity of CAD, but lack site specific anatomic information.

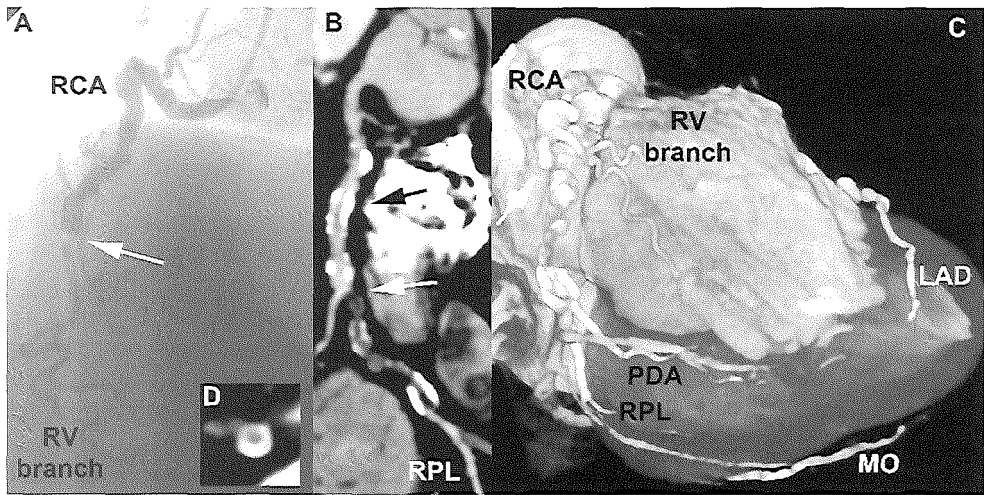


FIGURE 4. Occlusion of distal right coronary artery. (A) conventional angiogram and (B, C and D) MSCT angiogram of a severely calcified right coronary artery (RCA). Although the lumen of the proximal and middle segment cannot be accurately assessed due to severe calcifications, occlusion at the level of the acute marginal branch is evident, both on the curved multiplanar reconstruction (B) and volume rendered image (C). The posterior descending artery (PDA) and posterior lateral branch (RPL) are filled by collateral vessels. The distal left anterior descending coronary artery (LAD) and a marginal branch (MO) from the left circumflex artery can be observed curving around the apex.

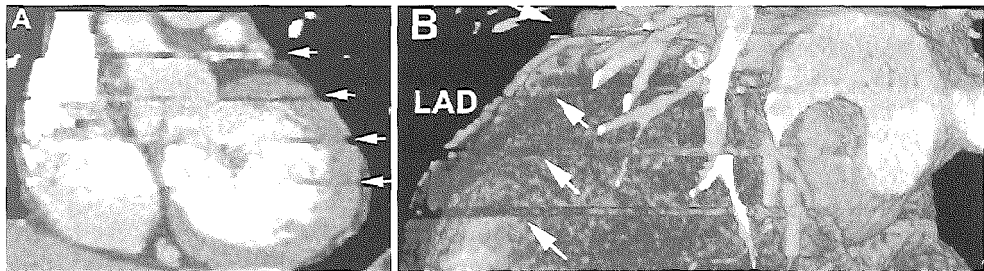


FIGURE 5. Gating artifacts due to arrhythmia. Due to multiple extrasystolic contractions, a number of slices were reconstructed during a different cardiac phase (A). The appearance of several obstructions in the left anterior descending coronary artery (LAD) is created in 3 dimensional volume-rendered representation (B).

Technical limitations

The presence of extensive calcium deposits in the vessel wall, combined with volume averaging, creates artifacts that hamper assessment and cause misinterpretations. Partial volume effects will most likely decrease in the future by improvement of the spatial resolution, but at this moment, patients with extensive coronary wall calcifications, who can be identified by a nonenhanced calcium scan, are best excluded from computed tomographic angiography.

The current temporal resolution, between 125 and 250 ms, is adequate at low heart rates. To improve the temporal resolution at higher heart rates, multisegment reconstruction algorithms should be applied. Because the benefit strongly varies throughout the acquisition depending on the momentary heart rate, significant improvement in resolution cannot be guaranteed and comes at the expense of increased radiation exposure. At an increasing number of centers, the scan quality is improved by administering short acting β receptor blocking agents.¹⁶ Other currently limiting factors are irregular heart rhythms such as atrial fibrillation and recurrent premature extrasystolic contractions (Figure 5). The currently required 40 second breath hold is too long in a nonselective patient group. The next generation of MSCT scanners has been heralded at recent scientific meetings. Extending the current performance capacities, these scanners will be equipped with a larger number of thinner detector rows and rotate at an additionally increased speed. Several manufacturers are introducing prospectively triggered tube current modulation to reduce radiation exposure, currently estimated to be around 6 mSv (Siemens, Forchheim, Germany). Aided by advanced interactive and high speed postprocessing applications, noninvasive assessment of CAD is expected in the near future.

REFERENCES

1. Wielopolski PA, van Geuns RJ, de Feyter PJ, Oudkerk M. Coronary arteries. *Eur Radiol* 2000;10:12–35.
2. Rensing BJ, Bongaerts AH, van Geuns RJ, van Ooijen PM, Oudkerk M, deFeyter PJ. Intravenous coronary angiography using electron beam computed tomography. *Prog Cardiovasc Dis* 1999;42:139–148.
3. Ohnesorge B, Flohr T, Becker C, Kopp AF, Schoepf UJ, Baum U, Knez A, Klingenberg Regn K, Reiser MF. Cardiac imaging by means of electrocardiographically gated multisection spiral CT: initial experience. *Radiology* 2000;217: 564–571.
4. Ohnesorge B, Flohr T, Becker C, Knez A, Schoepf UF, Klingenberg Regn K, Bruening R, Reiser MF. Technical aspects and applications of fast multislice cardiac CT. In: Reiser MF, Takahashi M, Modic M, Bruening R, eds. *Medical Radiology—Diagnostic Imaging and Radiation Oncology*. Berlin, Germany: Springer, 2000:121–130.
5. Nieman K, Oudkerk M, Rensing BJ, van Ooijen PMA, Munne A, van Geuns RJM, de Feyter PJ. Coronary angiography with multi slice computed tomography. *Lancet* 2001;357:599–603.

6. Austen WG, Edwards JE, Frye RL, Gensini GG, Gott VL, Griffith LS, McGoon DC, Murphy ML, Roe BB. A reporting system on patients evaluated for coronary artery disease. Report of the Ad Hoc Committee for Grading of Coronary Artery Disease, Council on Cardiovascular Surgery, American Heart Association. *Circulation* 1975;51:5–40.
7. Achenbach S, Giesler T, Ropers D, Ulzheimer S, Derlien H, Schulte C, Wenkel E, Moshage W, Bautz W, Danier WG, Kalender WA, Baum U. Detection of coronary artery stenoses by contrast enhanced, retrospectively electrocardiographically gated, multislice spiral computed tomography. *Circulation* 2001;103: 2535–2538.
8. Knez A, Becker C, Leber A, Becker A, Bruening R, Reiser M. Non invasive angiography with multi detector helical computed tomography for evaluation of coronary artery disease (abstr). *J Am Coll Cardiol* 2000;2(suppl A):463.
9. Achenbach S, Moshage W, Ropers D, Nossen J, Daniel WG. Value of electron beam computed tomography for the noninvasive detection of high grade coronary artery stenoses and occlusions. *N Engl J Med* 1998;339:1964–1971.
10. Nakanishi T, Ito K, Imazu M, Yamakido M. Evaluation of coronary artery stenoses using electron beam CT and multiplanar reformation. *J Comput Assist Tomogr* 1997;21:121–127.
11. Reddy PR, Chernoff DM, Adams JR, Higgins CB. Coronary artery stenoses: assessment with contrast enhanced electron beam CT and axial reconstructions. *Radiology* 1998;208:167–172.
12. Schermund A, Rensing BJ, Sheedy PF, Bell MR, Rumberger JA. Intravenous electron beam CT coronary angiography for segmental analysis of significant coronary artery stenoses: feasibility and limitations. *J Am Coll Cardiol* 1998;31: 1547–1554.
13. Rensing BJ, Bongaerts A, van Geuns RJ, van Ooijen P, Oudkerk M, de Feyter PJ. Intravenous coronary angiography by electron beam computed tomography: a clinical evaluation. *Circulation* 1998;98:2509–2512.
14. Budoff MJ, Oudiz RJ, Zalace CP, Bakhsheshi H, Goldberg SL, French WJ, Rami TG, Brundage BH. Intravenous three dimensional coronary angiography using contrast enhanced electron beam computed tomography. *Am J Cardiol* 1999;83:840–845.
15. Lee TH, Boucher CA. Noninvasive tests in patients with stable coronary artery disease. *N Engl J Med* 2001;344:1840–1845.
16. Becker CR, Ohnesorge BM, Schoepf UJ, Reiser MF. Current development of cardiac imaging with multidetector row CT. *Eur J Radiol* 2000;36:97–103.

3.4

Non-invasive Coronary Angiography with Multislice Spiral Computed Tomography: Impact of Heart Rate

Koen Nieman
Benno J Rensing
Robert Jan M van Geuns
Jeroen Vos
Peter M T Pattynama
Gabriel P Krestin
Patrick W Serruys
Pim J de Feyter

ABSTRACT

Objective:

To evaluate the impact of heart rate on the diagnostic accuracy of coronary angiography by multislice spiral computed tomography (MSCT).

Design:

Prospective observational study.

Patients:

78 patients who underwent both conventional and MSCT coronary angiography for suspicion of de novo coronary artery disease (n=53) or recurrent coronary artery disease after percutaneous intervention (n=25).

Setting:

Tertiary referral centre.

Methods:

Intravenously contrast enhanced MSCT coronary angiography was done during a single breath hold, and ECG synchronised images were reconstructed retrospectively. All coronary segments of ≥ 2.0 mm without stents were evaluated by two investigators and compared with quantitative coronary angiography. Patients were classified according to the average heart rate (mean (SD)) into three equally sized groups: group 1, 55.8 (4.1) beats/min; group 2, 66.6 (2.8) beats/min; group 3, 81.7 (8.8) beats/min.

Results:

Image quality was sufficient for analysis in 78% of the coronary segments in patients in group 1, 73% in group 2, and 54% in group 3 ($p < 0.01$). The sensitivity and specificity for detecting significant stenoses ($\geq 50\%$ lumen reduction) in these assessable segments were: 97% (95% confidence interval (CI) 84% to 100%) and 96% in group 1; 74% (52% to 89%) and 94% in group 2; and 67% (33% to 90%) and 94% in group 3 ($p < 0.05$). Accounting for all segments of ≥ 2.0 mm, including lesions in non assessable segments as false negatives, the sensitivity decreased to 82% (28/34 lesions, 95% CI 69% to 91%), 61% (14/23 lesions, 42% to 77%), and 32% (6/19 lesions, 15% to 50%), respectively ($p < 0.01$).

Conclusions:

MSCT allows reliable coronary angiography in patients with low heart rates.

INTRODUCTION

Contrast enhanced multislice spiral computed tomography (MSCT) is a promising non invasive technique for the detection, visualisation, and characterisation of stenotic coronary artery disease.¹⁻⁴ However, MSCT has relatively poor temporal resolution compared with other methods of non invasive coronary imaging such as electron beam computed tomography (EBCT) and magnetic resonance imaging.⁵⁻⁷ Therefore MSCT remains sensitive to cardiac motion artefacts.^{1,2,8}

We investigated the impact of average heart rate during acquisition of the MSCT angiograms on the accuracy of the technique for detecting stenotic coronary artery disease.

METHODS

Population

MSCT angiography was undertaken in 78 patients (mean (SD) age 56.9 (10.1) years; 57 men, 21 women). They were suspected of having coronary artery disease (n = 53) or presented with recurrent symptoms after percutaneous coronary interventions (n = 25) (table 1). Exclusion criteria were: not being in sinus rhythm, having an allergy to iodine containing contrast media, renal failure (serum creatinine > 100 µmol/l), pregnancy, respiratory impairment, or pronounced cardiac failure.

The study was approved by the local ethics committee, and informed consent was obtained from all patients.

Data acquisition

Contrast enhanced MSCT examinations were done in the supine position during a single breath hold (Somatom Plus 4 VolumeZoom, Siemens AG, Forchheim, Germany). A fixed delay of 20 seconds was instituted between the start of the intravenous contrast injection (150 ml of Iomeprol (350 mgI/ ml), given at a rate of 3.5–4.0 ml/s) and the onset of the scan. An ECG was recorded during the continuous CT data acquisition. A 4 x 1.0 mm scan protocol was applied at a table increment of 1.5 mm per gantry rotation (rotation time 500 ms) for heart rates of < 80 beats/min. At faster heart rates (≥80 beats/min) the table feed could be increased to 2.0 mm per rotation. A tube voltage of 120 kV and a current of 300 mA were typically applied. Depending on the cardiac dimensions and table feed, the scan time varied between 25–45 seconds.

Image reconstruction

After acquisition of the raw spiral CT data, retrospective ECG synchronised slices were reconstructed. A detailed description of ECG gated image reconstruction can be found elsewhere.⁹ In summary, a single slice can be reconstructed from the CT data from a 180° x ray tube rotation, acquired in 250 ms at a rotation time of 500 ms.

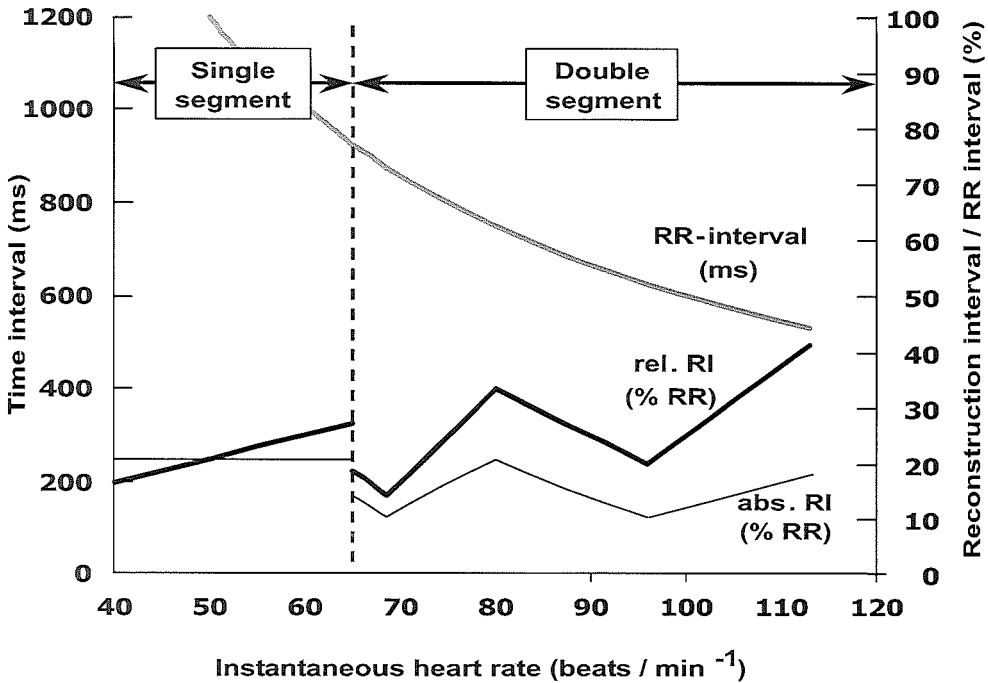


Figure 1. Heart rate dependency of the temporal resolution. Isocardiophasic transverse slices are reconstructed according to the recorded ECG using a 180° rotation partial scan algorithm. For heart rates up to 65 beats/min a single segment reconstruction algorithm is applied to reconstruct slices during a 250 ms reconstruction window (abs. RI) within each separate cardiac cycle. To improve the effective temporal resolution and reduce motion artefacts, a double segment reconstruction algorithm—which combines isocardiophasic data from two consecutive RR intervals—is applied at heart rates over 65 beats/min. The effective reconstruction interval per cardiac cycle depends on a complex relation between the gantry rotation time and the duration of the cardiac cycle. At a given rotation speed it varies between 125 ms at favourable and 250 ms at unfavourable heart rates. The relative reconstruction interval (rel. RI)—that is, the ratio between the absolute reconstruction interval and the total R to R wave interval (%)—progressively increases at higher heart rates (Siemens Somatom Plus 4 VolumeZoom with a rotation time of 500 ms).

When the heart rate is above 65 beats/min, data from consecutive cycles are combined, which improves the effective temporal resolution.

Depending on the instantaneous heart rate, the slice reconstruction time varies between 125–250 ms (fig 1). Because data were acquired continuously, the reconstruction window can be positioned at any point within the cardiac cycle. Routinely, at least three datasets with reconstruction windows starting at 300 ms, 400 ms, and 500 ms before the onset of the next R wave were reconstructed.

Other window positions within the diastolic phase were reconstructed if no satisfactory result was achieved. In a side by side comparison of the axial slices, the dataset with least motion artefacts was then selected for further analysis.

Typically a dataset at around 400 ms reconstruction showed the best result, but at higher heart rates the most optimal window was positioned closer towards 300 ms before the next R wave. Besides retrospective ECG gating, spiral scanning also allows selection of an image reconstruction increment (0.5 mm) below the effective slice thickness (1.25 mm). As a result of the overlapping slice reconstruction, near isotropic voxel dimensions are created (0.3 x 0.3 x 0.5 mm).

Image processing

The image datasets were processed on a separate workstation and analysed using multiplanar reconstruction, thin slab maximum intensity projections, and volume rendering, in addition to the axial source images. Blinded for the conventional coronary angiography findings, two investigators assessed each coronary artery segment (according to the American Heart Association guidelines) and a final decision was reached by consensus.¹⁰ Depending on the image quality, each vessel segment was classified as either assessable or not. Because of metal artefacts, coronary segments containing stents were excluded from assessment. Vessel segments with a diameter of ≥ 2.0 mm, according to quantitative coronary angiography, were screened for the presence of $\geq 50\%$ lumen diameter reduction and compared with the results of the conventional angiographic examination.

Statistical analysis

Continuous variables are expressed as mean (SD). Descriptive statistics, sensitivity, specificity, negative predictive value, and positive predictive value, using a 95% confidence interval (CI), were stratified according to average heart rate in three equally sized groups. A χ^2 test was used to compare dichotomous variables. The diagnostic value was given for assessable segments, all segments of ≥ 2.0 mm, and per patient. For analyses that include both assessable and non assessable segments, the undetected lesions were classified as false negative results. Conventional (quantitative) coronary angiography was regarded as the gold standard.

RESULTS

The mean (SD) data acquisition time was 36.9 (3.8) seconds. Overall, 505 (68%) of 741 coronary segments could be assessed. In patients with a lower average heart rate, more segments of > 2.0 mm were assessable (fig 2).

In all, 48 of 57 significant stenoses (84%) and 424 of 448 normal and non significantly narrowed segments (98%) were correctly identified in the assessable segments (fig 3). The positive and negative predictive value were 67% and 98%, respectively. Including stenotic lesions in non assessable segments, the overall sensitivity decreased to 64% (48 of 76 lesions).

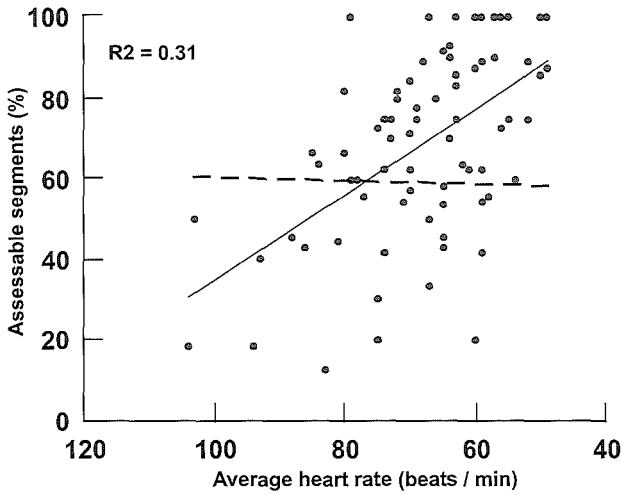


Figure 2. Heart rate dependency of coronary segment assessability. At lower heart rates >2.0 mm segments per patient are assessable. The interrupted trend line represents the number of segments of > 2.0 mm diameter, as a ratio of 16 potentially available segments, which is independent of the patient's heart rate.

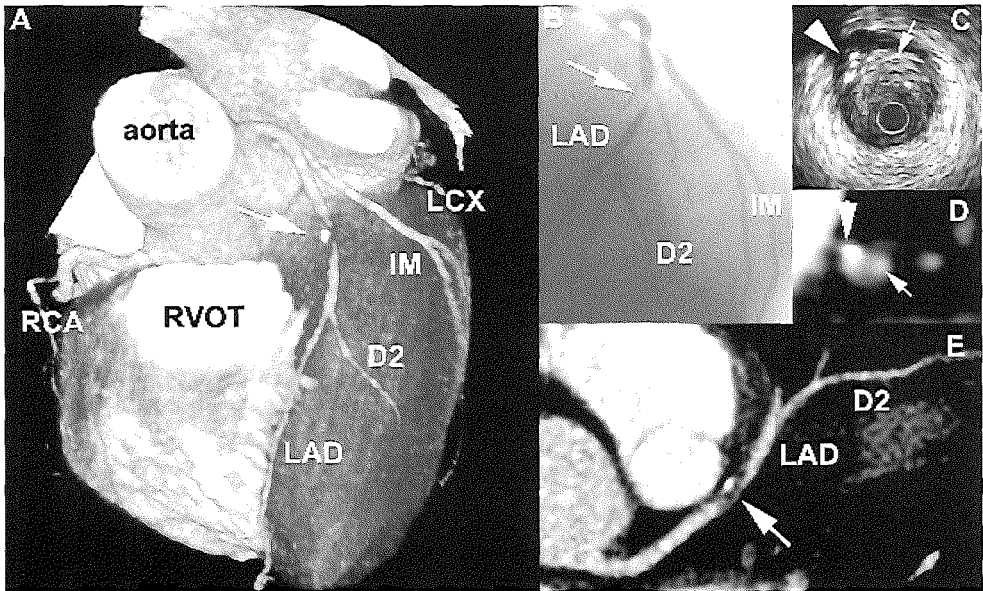


Figure 3. Multislice computed tomography (MSCT) angiogram of an obstructed left anterior coronary artery (LAD) and a heart rate of 49 beats/min. A significant stenosis (arrow) can be observed in the LAD. The three dimensional volume rendered overview (A) shows the lesion just distal to a small diagonal branch, which is confirmed by conventional angiography (B). The cross sectional (D) and longitudinal reconstructions (E) show a partially calcified lesion, which is confirmed by intracoronary ultrasound (C). D2, second diagonal branch; IM, intermediate branch; LCX, left circumflex coronary artery; RCA, right coronary artery. RVOT, right ventricular outflow tract.

Misinterpretations, both false positive and negative, were caused by calcification and motion artefacts.

The total group of 78 patients was divided into three groups of 26 patients according to their heart rate ranking from low to high. The quality of the MSCT images of patients in group 1, with the lowest heart rate (mean (SD) 55.8 (4.1) beats/min, range 49–62), was sufficient for analysis in 78% of the coronary segments. For patients in group 2 (66.6 (2.8) beats/min, range 63–72) and group 3 (81.7 (8.8) beats/min, range 73–104), 73% and 54% of the segments, respectively, were assessable ($p < 0.01$). The sensitivity and specificity for detecting significant stenoses in the assessable segments were 97% (28/29) and 96%, 74% (14/19) and 94%, and 67% (6/9) and 94%, for groups 1, 2, and 3, respectively ($p < 0.05$). Accounting for all segments of ≥ 2.0 mm, including lesions in non assessable segments as false negatives, the sensitivity decreased to 82% (28/34), 61% (14/23), and 32% (6/19), respectively ($p < 0.01$).

Complete and accurate results were achieved more often in patients in group 1 (73%) than in those in group 2 (54%) or group 3 (42%). Only at high heart rates (group 3) significantly more right coronary artery segments were classified as non assessable in comparison with left anterior descending coronary artery segments—58% and 35%, respectively ($p < 0.01$). These findings are amplified in table 1 and illustrated by representative cases in fig 4. The interobserver and intraobserver variability (the latter based on 19 randomly selected patients) for detecting stenosis were reasonably good, with κ values of 0.69 and 0.64, respectively.

From the recorded ECGs of 10 randomly selected patients we calculated the averaged relative heart rate variation during the scan. Initially, a brief deceleration can be observed; after approximately 20 seconds, however, the heart rate progressively increases (fig 5).

DISCUSSION

Residual cardiac motion artefacts remain a major cause of image degradation in MSCT coronary angiography.^{2, 3, 8} The right coronary artery appears particularly vulnerable because of its extensive motion radius and short motion free period.¹¹ In a recently published study, an inverse relation between heart rate and the image quality of MSCT coronary angiography was reported.¹² However, that study did not investigate the consequences for diagnostic accuracy because there was no comparison with a gold standard (conventional angiography).

MSCT image reconstruction takes place during the diastolic phase when motion is relatively sparse.¹¹ The length of this motion free period is inversely related to the heart rate. Conversely, there is a direct relation between the length of the reconstruction interval—that is, the temporal resolution—and the occurrence of cardiac motion artefacts. The temporal resolution depends on the gantry rotation time, which, owing to mechanical constraints, is currently limited to a maximum of 500 ms.

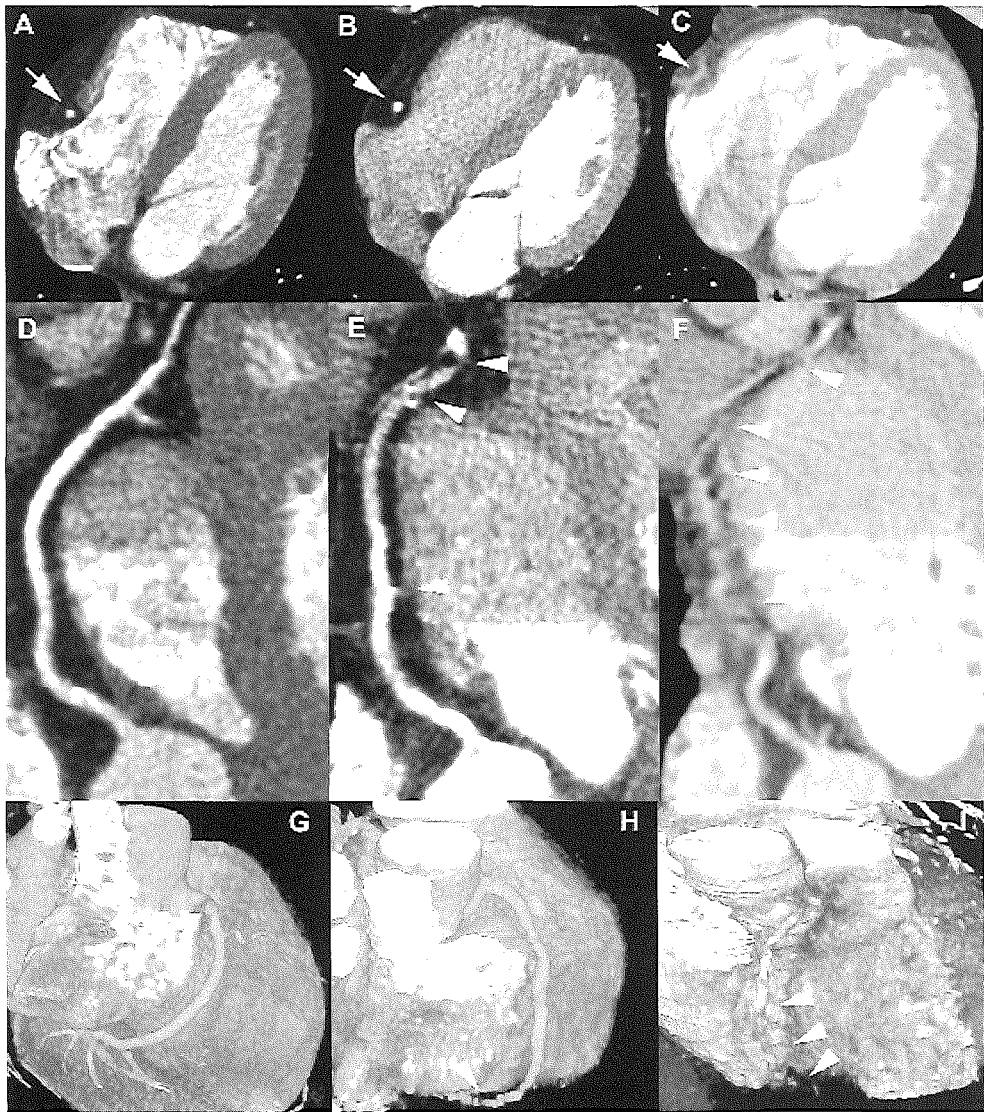


Figure 4. Multislice computed tomography (MSCT) angiograms at different heart rates. The axial source images (A,B,C), curved multiplanar reconstructions (D,E,F), and volume rendered reconstructions (G,H,I) of a normal right coronary artery (RCA, arrows) in patients with an average heart rate of 49 beats/min (A,D,G), 64 beats/min (B,E,H), and 81 beats/min (C,F,I), respectively, are shown. Motion artefacts (arrowheads) hinder assessment of the distal RCA in the second case and nearly the entire RCA in the third. RV, right ventricle.

Table 1: Baseline characteristics, assessability, and diagnostic accuracy of multislice computed tomographic (MSCT) angiography in detecting >50% coronary artery stenoses.

		Groups			
		All (n=78)	Group 1 (n=26)	Group 2 (n=26)	Group 3 (n =26)
Baseline characteristics					
Heart rate (beats/min)	Mean (SD)	68.0 (12.1)	55.8 (4.1)	66.6 (2.8)	81.7 (8.8)
	Range	49 to 103	49 to 62	63 to 72	73 to 104
Age (mean (SD))		56.9 (10.1)	58.3 (9.7)	58.9 (9.7)	53.4 (10.2)
Sex (male/female)		57/21	18/8	23/3	16/10
>50% stenotic lesions*		57 (76)	29 (34)	19 (23)	9 (19)
Stents		31	9	15	7
Assessability					
Relevant segments†		741	244	251	246
Assessable segments‡		505 (68%)	191 (78%)	182 (73%)	132 (54%)
Causes of non assessability‡	Cardiac motion	73 (10%)	10 (4%)	15 (6%)	48 (20%)
	Calcifications	40 (5%)	17 (7%)	15 (6%)	8 (3%)
	Other causes ¶	35 (5%)	5 (2%)	4 (2%)	26 (11%)
	Non specific	88 (12%)	21 (9%)	35 (14%)	32 (13%)
Diagnostic accuracy (95% CI)					
Assessable coronary segments	Sensitivity	84% (74% to 92%)	97% (84% to 100%)	74% (52% to 89%)	67% (33% to 90%)
	Specificity	95% (93% to 96%)	96% (94% to 97%)	94% (91% to 96%)	94% (91% to 95%)
	PPV	67% (58% to 73%)	82% (71% to 85%)	58% (41% to 70%)	43% (21% to 58%)
	NPV	98% (97% to 99%)	99% (97% to 100%)	97% (94% to 99%)	97% (95% to 99%)
Sensitivity , all aviable segments (95% CI)§		63% (54% to 71%)	82% (69% to 91%)	61% (42% to 77%)	32% (15% to 50%)
Accuracy per patient level**					
Causes of misinterpretation	Total	33	7	15	11
	Calcification	17	5	8	4
	Cardiac motion	11	–	5	6
	Other causes	5	2	2	1

*The number of lesions including non assessable segments given in brackets.

†All >2.0 mm segments, but excluding segments containing stents.

‡Percentages of the (relevant) >2.0 mm segments given in brackets.

¶Other causes include: respiratory motion, blending with adjacent contrast filled structures (vein, right ventricle), artefacts from pacemaker wire.

§Sensitivity including undetected lesions in non assessable segments as false negative.

**Percentage of patients with completely true positive or true negative diagnoses, including undetected lesions in non assessable segments as false negative.

CI, confidence interval.

PPV, positive predictive value.

NPV, negative predictive value.

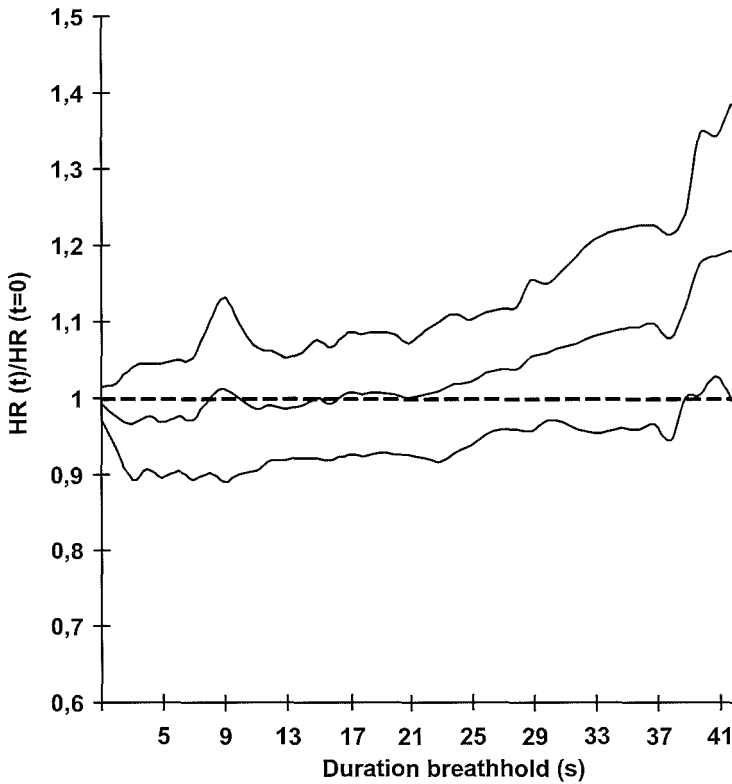


Figure 5. Heart rate variation during breath holding. Averaged relative heart rate (SD) of 10 randomly selected cases is shown. After an initial deceleration caused by a Valsalva induced vagal response, the heart rate progressively increases after approximately 20 seconds.

Thus, by using a standard 180° rotation reconstruction algorithm, the temporal resolution is 250 ms. For comparison, EBCT has a temporal resolution of 100 ms and most magnetic resonance coronary angiography sequences use acquisition windows of between 100–150 ms.^{6,7} At low heart rates a sufficiently long motion free window is usually available during the mid diastolic phase. Because this window narrows at higher heart rates, an algorithm has been developed that combines data from consecutive heart cycles and thereby potentially reduces the reconstruction time per cycle down to 125 ms.

Optimal performance with this bisegmental algorithm can only be achieved at certain favourable heart rates. Furthermore, this potential reduction of motion artefacts comes at the price of a higher radiation exposure because the algorithm requires a relatively low table speed.

Besides motion artefacts, other factors such as the presence of high density material (stents or coronary calcifications), adjacent contrast filled cavities and

veins, and incomplete breath holding complicate the assessment of the coronary arteries. Extensive calcium deposition causes high density artefacts that prevent proper luminal assessment. In our group with the lowest heart rates, calcifications were the most common cause of assessment limitation and lesion misinterpretation. Patients with advanced coronary atherosclerosis do not currently benefit from MSCT angiography, and nonenhanced computed tomography, which detects extensive calcium deposition, can be helpful in identifying these patients. Despite the optimisation of the temporal resolution at higher heart rates, we have shown that the assessability and diagnostic accuracy are significantly higher at lower heart rates, and deteriorate at higher heart rates. A temporary reduction in heart rate by giving short acting oral or intravenous β receptor blocking agents before the data acquisition can be expected to improve image quality. A reduction in the total scan time, either by faster gantry rotation or by more slices, will reduce the heart rate acceleration towards the end of the breath hold. A short scan time will also be beneficial in respect of venous contrast enhancement and patient motion.

REFERENCES

- 1 Nieman K, Oudkerk M, Rensing BJ, et al. Coronary angiography with multi slice computed tomography. *Lancet* 2001;357:599–603.
- 2 Achenbach S, Giesler T, Ropers D, et al. Detection of coronary artery stenoses by contrast enhanced, retrospectively electrocardiographically gated, multislice spiral computed tomography. *Circulation* 2001;103:2535–8.
- 3 Knez A, Becker C, Leber A, et al. Non invasive angiography with multi detector helical computed tomography for evaluation of coronary artery disease [abstract]. *J Am Coll Cardiol* 2000;101(suppl A):463.
- 4 Schroeder S, Kopp AF, Baumbach A, et al. Noninvasive detection and evaluation of atherosclerotic coronary plaques with multislice computed tomography. *J Am Coll Cardiol* 2001;37:1430–5.
- 5 Ohnesorge B, Flohr T, Becker C, et al. Cardiac imaging by means of electrocardiographically gated multisection spiral CT: initial experience. *Radiology* 2000;217:564–71.
- 6 Wielopolski PA, van Geuns RJ, de Feyter PJ, et al. Coronary arteries. *Eur Radiol* 2000;10:12–35.
- 7 Rensing BJ, Bongaerts A, van Geuns RJ, et al. Intravenous coronary angiography by electron beam computed tomography: a clinical evaluation. *Circulation*. 1998;98:2509–12.
- 8 Achenbach S, Ulzheimer S, Baum U, et al. Noninvasive coronary angiography by retrospectively ECG gated multislice CT. *Circulation* 2000;102:2823–8.
- 9 Ohnesorge B, Flohr T, Becker C, et al. Technical aspects and applications of fast multislice cardiac CT. In: Reiser MF, Takahashi M, Modic M, et al, eds. *Medical radiology – diagnostic imaging and radiation oncology*. Berlin: Springer, 2001:121–30.
- 10 Austen WG, Edwards JE, Frye RL, et al. A reporting system on patients evaluated for coronary artery disease. Report of the ad hoc committee for grading of coronary artery disease, Council on Cardiovascular Surgery, American Heart Association. *Circulation* 1975;51:5–40.

- 11 Wang Y, Vidan E, Bergman GW. Cardiac motion of coronary arteries: variability in the rest period and implications for coronary MR angiography. *Radiology* 1999;213:751-8
- 12 Hong C, Becker CR, Huber A. ECG gated reconstructed multi detector row CT coronary angiography: effect of varying trigger delay on image quality. *Radiology* 2001;220:712-17.

3.5

CT Angiography for the Detection of Coronary Artery Stenosis

Koen Nieman
Filippo Cademartiri
Peter MT Pattynama
Pim J de Feyter

To be published in: UJ Schoepl (Ed.).
CT of the heart: principles and methods.
Humana Press, USA.

INTRODUCTION

In the past decade we have witnessed the development of non invasive coronary imaging using different imaging modalities. Computed tomography (CT) and magnetic resonance imaging (MRI) modalities have been applied for the quantification of coronary calcium, detection of coronary and bypass graft occlusion and most recently the characterization of non calcified plaque material. However, the decisive application of non invasive coronary CT or MRI, which determines whether it will find widespread clinical application, will be the detection of coronary stenosis. The first comparative study between MRI and conventional coronary angiography was published in 1993¹, and numerous studies followed using various data acquisition techniques.² Since 1997 a number of studies have compared ECG triggered electron beam computed tomography (EBCT) and conventional coronary angiography, also with promising results.³⁻⁹ In 1999 four slice multislice spiral computed tomography (MSCT) was introduced and the first comparative publications appeared in 2001.¹⁰⁻¹⁶ In 2002 the first results were published using 16 slice MSCT scanners with a sub millimeter slice thickness and rotation time of less than a half second.¹⁷ In this chapter we will discuss the practical considerations, diagnostic value and remaining limitations of MSCT coronary imaging for the detection of coronary stenosis. The clinical utility and future developments will be discussed, as well as a comparison with other non invasive imaging techniques.

IMAGING REQUIREMENTS OF NON-INVASIVE CORONARY ANGIOGRAPHY

Catheter-based selective X-ray coronary angiography

Conventional X ray coronary angiography with selective contrast enhancement of the coronary arteries remains the gold standard for the in vivo detection and quantification of coronary artery stenosis. Multiple high contrast projections with a 0.1 x 0.1 mm image resolution are acquired each heart cycle. Besides accurate quantitative assessment, the dynamic injection of contrast provides functional flow information. Catheter based angiography can be complemented with advanced coronary imaging techniques, such as intra coronary ultrasound (ICUS) or optical coherence tomography (OCT), and flow or pressure measurements to determine the functional severity of a coronary obstruction. Competing with a technique of such quality and versatility seems impossible. However, there are also a number of practical disadvantages to catheter based coronary imaging. Additionally to the considerable costs, this invasive procedure involves a certain amount of patient discomfort and a small but not negligible risk of morbidity and mortality. Therefore conventional coronary angiography is applied with a degree of reservation, when adequate supportive evidence has been obtained, such as by exercise testing, and when either percutaneous intervention or bypass surgery are anticipated.

Requirements for non-invasive coronary angiography

In order to visualize the coronary arteries and find coronary artery disease at an earlier stage, and to follow up patients with known disease, a non invasive, and preferably less costly imaging technique would be desirable. To ensure sufficient image quality, non invasive techniques require a high spatial resolution to image small coronary arteries, high temporal resolution to acquire motion free images, adequate contrast to distinguish the coronary lumen from the vessel wall, and particularly in the case of computed tomography a short scan time to acquire all data within the duration of a comfortable breath hold. Finally, to maintain the advantage of a lower health risk, the non invasive method should minimize the use of radiation and contrast media, which particularly applies to computed tomography.

Besides attempting to approximate the diagnostic quality of conventional angiography, computed tomography and magnetic resonance imaging provide additional information regarding the cardiac and three dimensional coronary anatomy and the composition of the vessel wall.

ACQUISITION, RECONSTRUCTION, POST-PROCESSING AND EVALUATION

Data acquisition and image reconstruction

A detailed description of the general data acquisition and image reconstruction considerations for MSCT coronary angiography can be found in the previous chapters. For the assessment of the coronary arteries the highest image quality is required. This means the fastest X source rotation speed and thinnest detector collimation possible, while still allowing complete scanning of the entire heart within a single breath hold. Images are routinely reconstructed during the diastolic cardiac phase to minimize motion artefacts, and out of a number of reconstructions at a slightly varying reconstruction window position the most optimal data set is used for image analysis. Particularly at higher heart rates, different vessel segments are most optimally visualized during different phases.

Post-processing and data analysis

The coronary lumen can be assessed using different post processing techniques (figure 1). Generally, maximum intensity projections (MIP) of thin slabs, or multiplanar reformations (MPR), oriented parallel to the coronary of interest, are used in addition to the axial source images. MIP provides smooth high contrast images, and has the advantage that longer sections of a vessel can be visualized in the same plane. However, when calcifications or stents are present, the coronary lumen becomes obscured by these high attenuating structures, in which case MPR or the axial source images are more suitable. For presentation purposes and three dimensional orientation of the referring physician, advanced post processing techniques are available such as curved MPR, volume rendering and virtual angiосcopy.

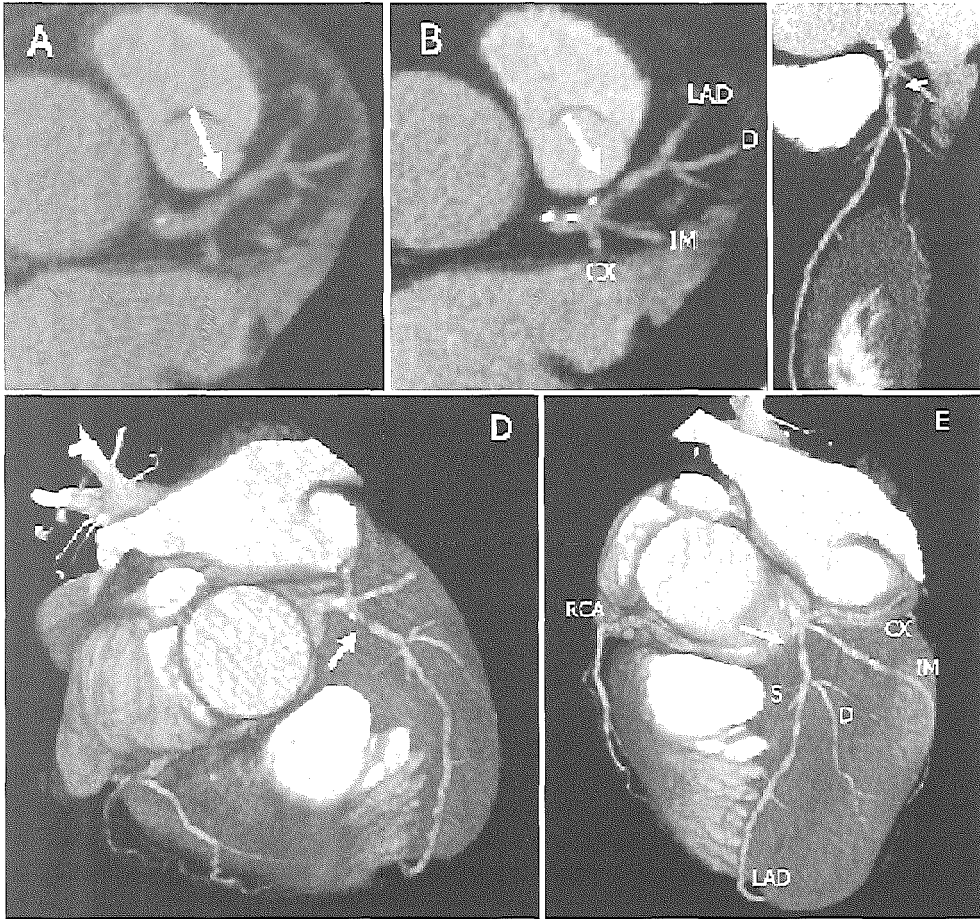


Figure 1. Post processing techniques. A stenotic lesion (arrow) in the proximal left anterior descending coronary artery (LAD), displayed using multi planar reformation (A), thin slab maximum intensity projection (B), curved maximum intensity projection (C), and volume rendering (D and E). Right coronary artery (RCA), diagonal (D), intermediate (IM), circumflex (CX) and septal branch (S).

DIAGNOSTIC PERFORMANCE OF FOUR-SLICE MSCT

MSCT compared to conventional coronary angiography

The first multislice spiral computed tomography scanners (MSCT), introduced in 1999 and equipped with four parallel detector arrays, were the first mechanical CT scanners that allowed assessment of the coronary artery lumen. The first studies that compared MSCT coronary angiography and the gold standard of conventional X ray coronary angiography were published in early 2001, with promising results (table 1). The studies were performed with comparable techniques but varied in study design. The patient population varied between 31 and 102, and consisted of patients suspected of obstructive coronary artery disease and an indication for conventional coronary angiography. Therefore, the average number of diseased vessels varied between 0.9 and 1.5 per patient. Most studies considered a lumen diameter reduction of 50% as significant^{10 14,16}, while others used a 70% cut off point.^{11,15} In two studies the main coronary branches: left main (LM), left anterior descending (LAD), left circumflex (LCX) and right coronary artery (RCA) were evaluated as a whole, including all >2.0 mm branches^{11,15}, while the other studies assessed a predefined number of proximal, middle and distal coronary segments, according to the ACC/AHA guidelines, regardless of the vessel diameter.^{10,12 14} One study considered all coronary segments, including side branches, with a minimal diameter of 2.0 mm.¹⁶ All studies were performed by single centers, and all but one were based on a consensus reading by two blinded observers. The first three studies did not use additional beta receptor blocking medication to reduce the patient's heart rate during the data acquisition.

Image interpretability

The percentage of coronary arteries or coronary segments with a subjectively adequate image quality varied between 6% and 32% in the different studies. Reasons for non assessability mainly related to motion artifacts caused by residual cardiac motion, severe coronary calcification and voluntary patient movement, but also include the inability to discriminate the coronary artery lumen from adjacent contrast enhanced structures, technical scanner failure and insufficient scan range (figure 2). With four slice MSCT scanners the entire heart can be covered within the duration of a long breath hold of 35 45s. However, a scan time of up to 40 seconds proves too long in a substantial number of patients. Other incidental causes for reduced interpretability are beam hardening artefacts from the high concentration of contrast medium in the superior caval vein or pacemaker wires. While MSCT in patients with arrhythmia is generally discouraged because of the end diastolic volume variation, occasional premature contractions occur in many patients and can adversely affect the assessment.

Table 1. Diagnostic performance of multislice spiral CT to detect coronary stenosis, using conventional coronary angiography as the standard of reference.

	β	N	Assess.	D	Prev	Excl	Se	Sp	PPV	NPV	Se ^a	
Nieman [10]	4	31	Segment	50%	0.9	27%	81%	97%	81%	97%	68%	
Achenbach [11]	4	64	Branch	50%	1.1	32%	85%	76%	56%	93%	55%	
				70%	0.9	32%	91%	84%	59%	98%	58%	
Knez [12]	4	43	Segment	50%	1.2	6%	78%	98%	84%	96%	51%	
Vogl [13]	4	+	64	Segment	50%	NR	28%	75%	99%	92%	98%	NR
Kopp [14] ^b	4		102	Segment	50%	1.5	15%	86%	96%	76%	98%	86%
							93%	97%	81%	99%	93%	
Giesler [15] ^c	4	+	100	Branch	70%	1.0	29%	91%	89%	66%	98%	49%
Nieman [16] ^c	4		78	Segment	50%	0.9	32%	84%	95%	67%	98%	63%
Nieman [17]	16	+	58	Branch	50%	1.1	0	95%	86%	80%	97%	95%
Ropers [18]	16	+	77	Branch	50%	1.0	12	93%	81%	92%	85%	73%

Use of betablockers (β); method of assessment (assess.); Diameter reduction considered significantly stenosed (D); Number of stenotic vessel per patient (Prev.); Percentage of excluded segments/branches (Excl); Sensitivity (Se), specificity (Sp), positive (PPV) and negative predictive value (NPV) regarding the assessable segments/branches; Sensitivity including missed lesions in non assessable segments/branches (Se^a).

^b Results by two observers, without consensus reading.

^c Studies include patients from earlier publications.

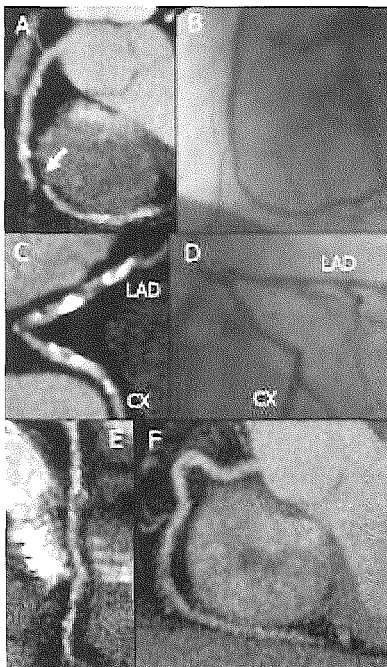


Figure 2. Image artefacts. The accuracy of MSCT can be affected by a number of artefacts. Consecutive slabs are reconstructed during different cardiac phases in the occurrence of irregular heart beats, which results in stair step artefacts or in complete discontinuity of the artery (arrow), as in this case (A & B). The presence of extensive calcification of the left anterior descending (LAD) and circumflex coronary artery (CX) limits the assessability due to partial volume artefacts and beam hardening (C & D). At faster heart rates image degrading motion artefacts occur (E). Particularly in overweight patients the attenuation by the surrounding tissue, such as the liver, can decrease the signal to noise ratio. In this case the distal RCA, which runs at the same level as the liver, is poorly assessable (F).

All studies show that the left main coronary artery can nearly always be evaluated. Of the remaining main branches the left anterior descending coronary artery (LAD) is least affected by motion artefacts. The most important cause for non assessability in case of the LAD is the presence of extensive calcifications. The right coronary artery (RCA), which has a large motion radius and short motion sparse period during the diastole, is branch that is most affected by motion artefacts caused by residual cardiac motion during the image reconstruction interval. The left circumflex coronary artery (LCX) also suffers from motion artefacts. Occasionally it can be difficult to distinguish the small LCX from the adjacent contrast enhanced cardiac vein. The fact that proximal vessels are better visualized than more distal branches is only partially related to diameter size. Both the middle segment of the RCA as well as the LCX have a larger motion radius compared to the proximal segments. The more distal branches and side branches are most difficult to visualize. In a study that compared the assessability of the different coronary segments with a minimal diameter of 2.0 mm, the proximal RCA was evaluable in 88%, compared to 61% of the middle and 60% of the distal segments. While assessment of the proximal LAD was possible in 89%, compared to 77% of the middle and 75% of the distal segments. In this study the proximal and the middle segments of the LCX were equally difficult to evaluate, 57% and 56%, respectively.¹⁹

Detection of coronary obstruction

When considering only the coronary arteries or segments that were imaged with sufficient image quality, the sensitivity of 4 slice MSCT to detect significant coronary obstruction, defined as (50% lumen diameter reduction, ranges between 75% and 95%, and the specificity between 76% and 99%.^{10 16} As can be expected the sensitivity and specificity are inversely correlated, as well as the number of excluded segments and the diagnostic performance in the assessable segments. The positive and negative predictive value ranged between 56% and 99%, and 93% and 99%, respectively. Compared to >50% lesions, Achenbach et al found a higher diagnostic performance for the detection of lesions with a lumen diameter reduction of at least 70%.¹¹ The results show that exclusion of disease in a normal vessel is less challenging than the classification of a diseased vessel as significantly stenosed or not, particularly in the presence of extensive calcification. The apparent size of the calcium deposits causes overestimation of the total plaque size, which results in false positive assessments. According to some investigators, MSCT coronary angiography may be most valuable as a tool to exclude significant lesions in patients with a relatively low pre test likelihood for the presence of stenoses, and not for the staging of patients with very high likelihood and expectedly advanced coronary artery degeneration. Figures 3 8 are examples of MSCT imaging of coronary obstruction with corresponding conventional X ray angiograms.

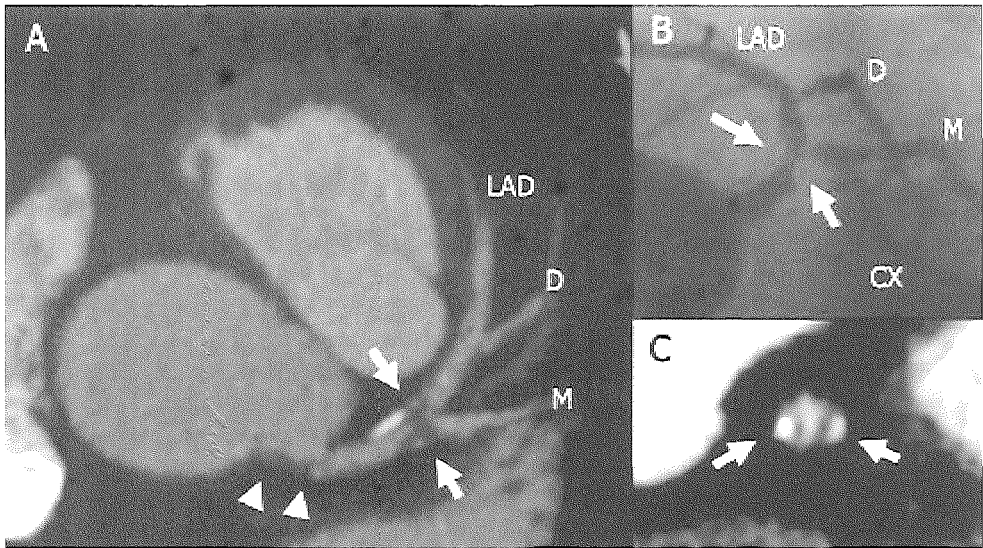


Figure 3. Lesions in the left main bifurcation. A significant lesion (arrow), consisting of two partially calcified plaques is situated at the distal part of the left main coronary artery, obstructing both the left anterior descending (LAD) as well as the left circumflex branch (CX) (A). The cross section of the vessel confirms the distinct configuration of the lesions (C). Additionally, more non calcified plaque material (arrow head) can be observed in the proximal part of the left main artery (arrow heads) (A). Diagonal (D) and marginal (M) branch.
(A full color version of this illustration can be found in the color section)

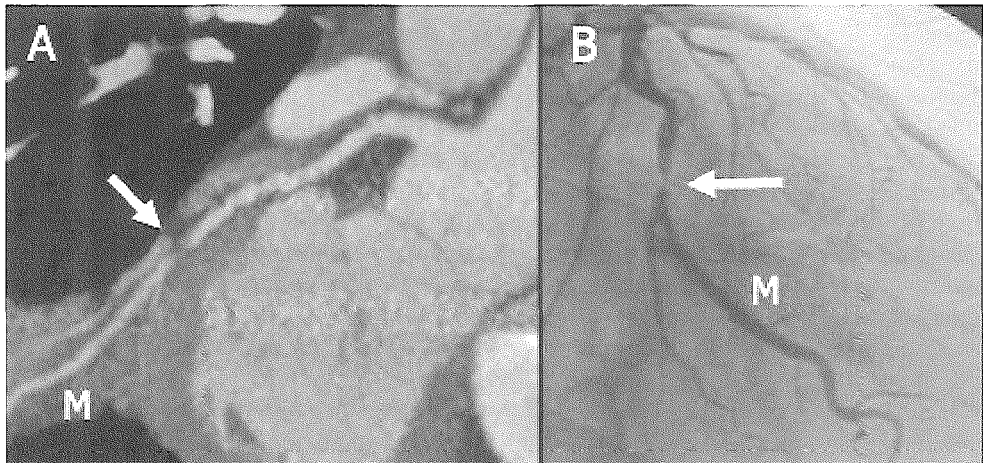


Figure 4. Significant lesion in the left circumflex coronary artery. A significant lesion (arrow) was found in the mid segment of the left circumflex branch, just proximal of the bifurcation of a major marginal branch (M), both by MSCT (A) and conventional angiography (B).

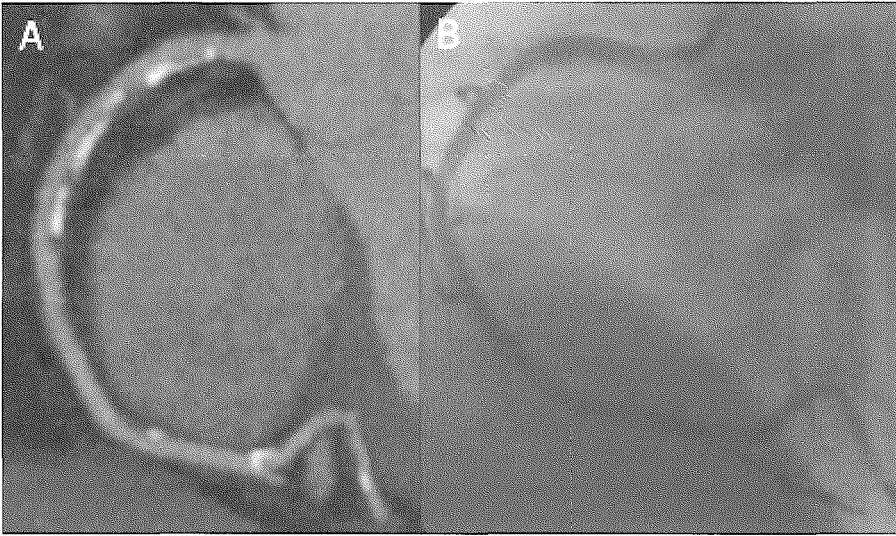


Figure 5. Diffuse coronary artery disease. This right coronary artery shows extensive atherosclerotic degeneration, with calcified and non calcified plaque material along the entire length of the proximal inner curve, and separate lesions more distally (A). Although the MSCT shows no severe stenosis, the absence of significant lesions was more straightforward on the conventional angiogram.

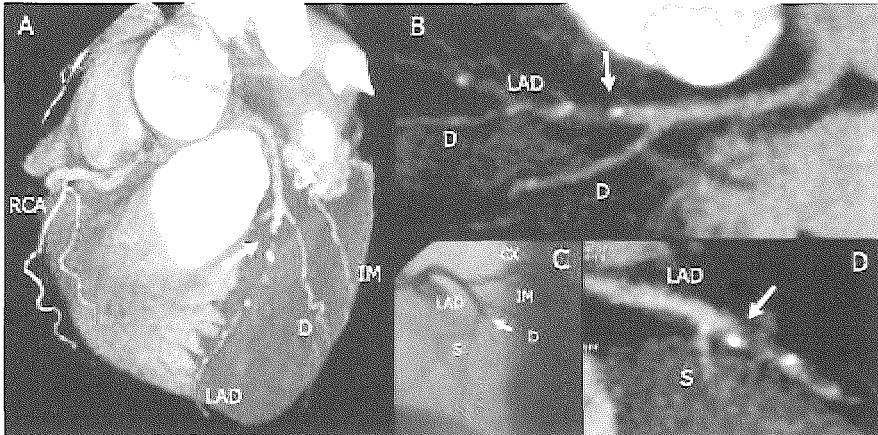


Figure 6. Occlusion of the left anterior descending coronary artery. Three dimensional reconstruction (A) and curved multiplanar reconstruction (B) of a CT coronary angiogram showing an occluded (arrow) left anterior descending coronary artery (LAD) (B), which was confirmed by conventional by conventional coronary angiography (C). A sagittal cross section shows in detail the different plaque components, both calcified and non calcified, as well as some residual contrast enhancement within the obstructed segment (D). Right coronary artery (RCA), diagonal (D), intermediate (IM) and circumflex branch (CX).

(A full color version of this illustration can be found in the color section)

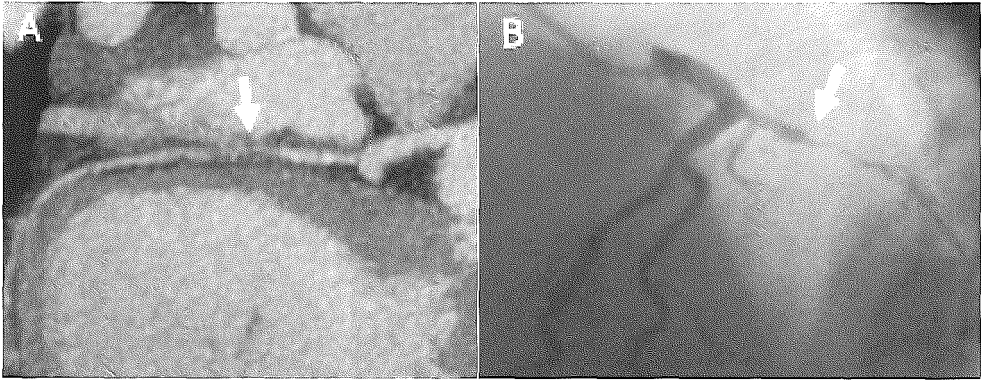


Figure 7. Occlusion of the left circumflex coronary artery. Curved maximum intensity projection (MIP) of a predominantly non calcified occlusion (arrow) of the left circumflex branch (A), confirmed by conventional coronary angiography (B). the distal segment is filled by collaterally by the left anterior descending coronary artery.

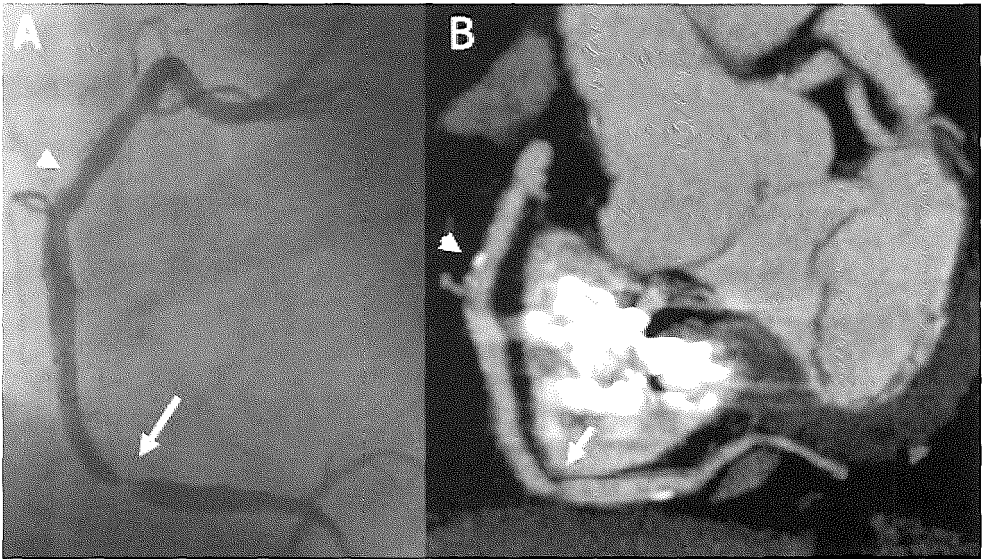


Figure 8. Stenosis of the distal right coronary artery. Using thin slab maximum intensity projection (MIP), a stenotic lesion (arrow) is demonstrated in the distal right coronary artery (A). Also minor wall irregularities, caused by small calcified lesions (arrow heads), can be observed, and were confirmed by conventional angiography (B).
(A full color version of this illustration can be found in the color section)

In a study comparing the diagnostic accuracy of MSCT in relation to the proximity of the coronary segment, a sensitivity and specificity of 92% and 96% were found in the largest proximal segments (RCA1, LM, LAD6), 85% and 90% for the middle segments (RCA2, LAD7, LCX11), 71% and 94% for the distal segments (RCA3, LAD8, LCX13) and 50% and 89% for the side branches.¹⁹ In the study by Kopp et al, the sensitivity to detect stenotic lesions significantly increased, to 97%/99%, by selectively assessing the proximal and middle coronary segments.¹⁴

The segments and vessels that were excluded from analysis because of inadequate image quality contained a substantial number of undetected lesions. If these lesions in non evaluable vessels are included in the analysis, as false negative interpretations, the sensitivity is much lower in most studies, between 49% and 93%.^{10 16}

SIXTEEN-SLICE CORONARY ANGIOGRAPHY

To date two studies has been published comparing MSCT and conventional coronary angiography using 16 slice MSCT.^{17,18} The advantages offered by this new technique are a faster rotation time of 0.42 s, an extended number of thinner detector rows (0.75 mm), and shorter total scan time of approximately 20 seconds. For the ECG gated protocol, the 12 central detector rows were applied. To optimise the image quality, consistent heart rate control was incorporated into both protocol. In the study by Nieman et al, patients with a pre scan heart rate over 65 beats per minute were given an oral dose of 100 mg metoprolol one hour prior to the examination, decreasing the average heart to 57 b.p.m.. Ropers et al, used 50 mg of atenolol to decrease the heart rates of all patients with >60 b.p.m., down to an average heart rate of 62 b.p.m. Only 7% and 12% of the coronary branches contained sections with a poor image quality. Compared to the other branches the right coronary artery was still most vulnerable to image quality degradation. Nieman et al, irrespectively of the image quality, evaluated all branches with a minimal luminal diameter of 2.0 mm, and found a sensitivity and specificity of 95% and 86% to detect significantly stenosed branches. The positive and negative predictive value were 80% and 97%.¹⁷ All four missed lesions were located in the LCX and marginal branches, no lesions were missed in the left main, left anterior descending or right coronary artery. The twenty overestimations included seven lesions with a sub significant (40 49%) diameter reduction, according to quantitative coronary angiography. Including only the evaluable (88%) vessels (minimal diameter 1.5 mm), Ropers et al found a sensitivity and specificity of 92% and 93% to detect significant stenoses. Without exclusion of non evaluable lesions the sensitivity was 73%.¹⁸

PATIENT-BASED ASSESSMENT

Understanding that different methods of data analysis and presentation were used is important to compare the results of the previously mentioned studies. For instance, by using an evaluation based on the individual coronary segments, the relative and absolute number of non diseased segments is much larger, compared to the number of non diseased branches in case of a main branch based analysis. One of the consequences is that for the segment based studies, the specificity is often better compared to the branch based studies. Perhaps a more comparable indicator towards the clinical applicability of MSCT coronary angiography is the diagnostic accuracy based on the individual patients. Using 4 slice MSCT Giesler et al showed that in 39 out of 100 patients (39%) all vessels could be evaluated.¹⁵ In the study by Knez et al, the accuracy to detect no, single, double or triple vessel disease was 74% (32/43 patients) after exclusion of the non assessable segments.¹² Nieman et al, reported a 56% (45/78 patients) accuracy to distinguish no, single or multi vessel disease, without the exclusion of non assessable segments.¹⁶ A high heart rate affects also the diagnostic accuracy per patient in a negative way.¹⁶ By 16 slice MSCT, Nieman et al reported a patient based accuracy to distinguish no, single or multi vessel disease of 78% (table 2).¹⁷ In this study the number of diseased vessels was overestimated in a number of patients, but none with significant coronary stenoses were falsely evaluated as normal, without exclusion of non assessable segments. Ropers et al, correctly assessed 85% as having one or more lesions.¹⁸

CONSIDERATIONS AND LIMITATIONS

Temporal resolution and the heart rate

The coronary arteries are in constant motion and therefore an infinitely short acquisition or reconstruction time is required to acquire completely motionless images. Angiography studies have shown that during diastole a brief moment of near immobility occurs.²⁰ The moment and duration of this window of imaging opportunity varies per person and per vessel, but always shortens at higher heart rates. Generally, the right coronary artery moves at a wider radius and has a shorter motion sparse period compared to the left coronary artery. The right coronary artery is therefore most vulnerable to motion artefacts caused by cardiac motion (Figure 2).

The temporal resolution of 4 slice MSCT scanners is 250 ms at low heart rates. At a heart rate of 50 b.p.m. the duration of the heart cycle measures 1200 ms, of which 21% is required for the reconstruction of a set of axial slices. At a heart rate of 80 b.p.m. ratio is 33% and at 120 b.p.m. the ratio is 50%, thereby increasing the occurrence of motion artifacts. Considering the fact that the shortening of the diastolic phase at higher heart rates is more substantial than the shortening of the systolic phase, the negative effect of a fast heart rate on the image quality is even more profound.

Table 2. Patient based diagnostic performance of MSCT coronary angiography

	4 slice MSCT [19] Segment based (N=53)		16 slice MSCT [17] Vessel based (N=58)	
	Accuracy	Predictive value	Accuracy	Predictive value
No lesions	9/14 (64%)	9/19 (47%)	7/7 (100%)	7/8 (88%)
Single lesion/vessel	9/23 (39%)	9/15 (60%)	12/16 (75%)	12/20 (60%)
Multiple lesions/vessel	11/16 (69%)	11/19 (58%)	26/35 (74%)	26/30 (87%)
Overall	29/53 (55%)	29/53 (55%)	45/58 (78%)	45/58 (78%)

At higher heart rates multi segment reconstruction algorithms can improve the effective temporal resolution by combining data from consecutive heart cycles. However, this reduction is highly dependent on the actual heart rate, and does not always result in an improvement of image quality. Using a bi segmental reconstruction algorithm at a rotation time of 500 ms, a heart rate of 68 b.p.m. results in an effective temporal resolution of 125 ms, while at 80 b.p.m. the non complementary configuration of the X ray source and detector array allows no reduction at all, maintaining a 250 ms effective temporal resolution. Up to approximately 75 b.p.m. the relative temporal resolution, the ratio of the image reconstruction interval to the RR interval, is less than 30%. The use of more than two segments for reconstruction of a set of slices, which potentially reduces the duration of the image reconstruction interval per cycle to less than 100 ms, requires a very slow table propagation, resulting in an increased radiation exposure to the patient.

Motion artefacts

Motion artefacts are probably the most important limitation of MSCT coronary angiography and lead to substantial numbers of non assessable investigations. The high number of non assessable vessels reduces the clinical applicability of the technique. Two studies evaluated the diagnostic accuracy of MSCT in relation to the heart rate of the patient. Giesler et al, divided 100 patients into four groups and showed in patients with a heart rate below 60 b.p.m. motion artefacts occurred in only 8% of the coronary arteries, compared to 18% at a heart rate between 61 and 70 b.p.m., 41% at a heart rate between 71 and 80 b.p.m., and 22% at a heart rate of more than 80 b.p.m.. The respective percentage of non assessable vessels: 22%, 23%, 50% and 24%, resulted in a degrading overall sensitivity to detect >70% coronary diameter narrowing: 67%, 55%, 35% and 22%, for the respective heart rate groups.¹⁵ In a study by Nieman et al, 78 patients were equally divided into 3 groups according to the average heart rate during MSCT coronary angiography. In the low heart rate group (56(4 b.p.m.), intermediate heart rate group (67(3 b.p.m.), and high heart rate group (82(9 b.p.m.), the number of assessable segments were 78%, 73% and 54%,

resulting in an overall sensitivity to detect >50% luminal stenosis of 82%, 61% and 32%, respectively. The accuracy of MSCT to classify patients as having no, single or multivessel disease, without exclusion of non assessable segment, was 73%, 54% and 42%, for each respective group.¹⁶ Based on these and other experiences, many centers have introduced the administration of anti chronotropic medication, such as beta blockers, particularly in patients with higher heart rates, to reduce the occurrence of motion artefacts, and improve the accuracy of MSCT coronary angiography.

State of the art scanners now have a rotation time below 500 ms, and combined with sufficient heart rate control, the reliability of MSCT has substantially improved (table 1). It needs to be established up till what heart rate these faster scanners can acquire motion sparse images, but it seems unlikely that a rotation time of 400 ms or more provides sufficient image quality in the majority of patients with a heart rate over 80 b.p.m., when the coronary arteries are concerned.

Respiration and the scan time

Respiratory motion is suppressed during scanning by maintaining an inspiratory breath hold. Using four slice scanners the relatively long scan time of 35-45 seconds, that is required to scan the entire heart at a thin collimation, can be too long in a substantial number of patients. In addition to respiratory motion artefacts, the long breath hold increases the patient's heart rate, resulting in an increased occurrence of cardiac motion artifacts. The new generation MSCT scanners are equipped with up to 16 slices and have a faster rotation, which results in a total scan time below 20s. A breath hold of 20s can be performed by most patients, and does not result in a significant acceleration of the heart rate.

Arrhythmia

Inappropriate ECG synchronization results in inter slice discontinuity (Figure 2). Contrary to prospectively ECG triggered modalities, such as electron beam computed tomography and most magnetic resonance imaging sequences, ECG gated spiral CT image reconstruction allows for retrospective editing of the ECG. This can be useful to correct for inappropriate interpretation of the ECG by the reconstruction algorithm and provides an opportunity to manually insert R wave indicators in case of ECG noise. Patients with continuous arrhythmia, editing of the ECG will suffice. For instance, during atrial fibrillation, the end diastolic volume constantly varies because of the alternating filling time. Thereby, the heart will be displaced and have a different shape and position at each consecutive heart cycle and acquisition. Apart from cardiac motion artefacts, this results in severe, and non correctable inter slice discontinuity and non interpretable results. On the other hand, non sinus rhythm, delayed conduction or otherwise unusual configuration of the ECG is no contra indication for MSCT, as long as the RR interval variation is within an acceptable range.

Stents and surgical material

Material with strong X ray attenuating characteristics, such as metal and calcium, cause beam hardening and partial volume artefacts. Because stents are positioned within the coronary, adjacent to the lumen, assessment of the lumen diameter is impaired. In patients who underwent bypass grafting, sternal wires and vascular clips can cause streak artefacts that hamper proper assessment of the bypass grafts as well as coronary arteries. Both patient groups will be discussed in more detail in following chapters. Occasionally, pacemaker wires in the right heart can cause identical artefacts obscuring the right coronary artery. In case of bi ventricular pacing systems, with wires positioned in the cardiac veins, assessment of the left circumflex and the left anterior descending coronary arteries are severely hampered.

Calcifications

Calcium deposits also cause a strong attenuation of the X ray and are the most frequent cause of high density artefacts, such as partial voluming and beam hardening artefacts. Partial volume artefacts are directly, but not solely related to the size of the voxel, or three dimensional image elements. The direct result is that calcified plaque material appears larger than it actually is, thereby increasing the apparent severity of the lumen narrowing and complicating accurate assessment (Figure 2). By experience most reviewers will take the overestimation into account when assessing the lumen diameter of a calcified lesion. Nevertheless, an accurate (semi)quantitative assessment of coronary arteries with extensive coronary calcification remains less reliable, and patients with suspected or known advanced coronary artery disease are therefore not the most suitable candidates for CT coronary angiography.

All studies comparing MSCT and conventional coronary angiography report that extensive calcification of the coronary arteries prevented assessment of a substantial number of segments and resulted in a number of false positive or false negative interpretations of significant stenoses.^{10 19} In order to avoid contrast enhanced CT angiography in these individuals, some proposed to perform a low dose non enhanced scan in all patients prior to angiography to determine the amount of calcium in the coronary arteries, and exclude unsuitable candidates.

EBCT AND MR CORONARY ANGIOGRAPHY

Electron beam computed tomography

In 1997 the first studies comparing electron beam computed tomography (EBCT) with conventional angiography were published. All but one study were performed using an 1.0 mm overlapping 3.0 mm slice thickness.^{3 5,7 9} In one study a non overlapping 1.5 mm detector collimation was applied.⁶ The non mechanical EBCT is a sequential CT scanner.

Prospectively triggered by the patient's electrocardiogram (ECG) a single slice is acquired, after which the table advanced to the next slice position. The acquisition is performed during the diastolic phase and the exact timing of the electron generation is based on the preceding heart cycles. Due to the lack of mechanically rotating elements, the slice acquisition time is very short: 100 ms. The one slice sequential scan design requires a long scan time, and breath hold, to cover the entire heart. To increase the scan coverage atropine can be injected to increase the heart rate, and consequently the number of slices that can be acquired within a certain breath hold time.⁶

Table 3. Diagnostic performance of electron beam CT to detect coronary stenosis, using conventional coronary angiography as the standard of reference

	A	N	Assess.	D	Prev	Excl.	Se	Sp	PPV	NPV	Sea	
Nakanishi [3]	3.0	37	Vessel	50%	0.8		74%	94%	68%	93%	74%	
Reddy [4]	3.0	23	Vessel	50%	1.3	10%	88%	78%	65%	94%	77%	
Schmermund [5]	3.0	+	28	Segment	50%	1.1	28%	82%	88%	57%	96%	70%
Rensing [6]	1.5	+	37	Segment	50%	1.1	81%	77%	94%	73%	95%	63%
Achenbach [7]	3.0		125	Vessel	70%	0.8	25%	92%	94%	78%	98%	70%
Budoff [8]	3.0		52	Vessel	50%	≥1.1	11%	78%	91%	78%	91%	NR
Achenbach [9]	3.0		36	Vessel	75%	≥1.0	20%	92 %	94%	85%	92%	NR

Use of atropine (A); method of assessment (Assess.); Diameter reduction considered significantly stenosed (D); Number of stenotic vessel per patient (Prev.); Percentage of excluded segments/branches (Excl.); Sensitivity (Se), specificity (Sp), positive (PPV) and negative predictive value (NPV) regarding the assessable segments/branches; Sensitivity including missed lesions in non assessable segments/branches (Sea). Not reported (NR).

Comparative studies against conventional angiography

Table 3 lists the results from the comparative publications between contrast enhanced EBCT and conventional coronary angiography for the purpose of the detection of significant coronary artery obstruction. The study populations ranged from 23 to 125 patients. The use of atropine to increase the number of acquisitions per breath hold was reported in two studies.^{6,7} At low heart rates, breath hold durations of >50s were reported. In one study no segments were excluded³, in the others between 10% and 28% of the segments and vessels were excluded due to impaired image quality. Similar to MSCT non interpretability was caused by motion artefacts and extensive calcification. Considering the assessable segments and vessels, the sensitivity to detect significant luminal narrowing ranged from 74% to 92%. The specificity ranged from 63% to 94%. The positive and negative predictive value ranged from 57% to 85% and 91% and 98%, respectively. If lesions in non assessable vessels were included as false negative results the overall sensitivity decreased to 63% and 77%, although these figures were only reported in five studies. Contrary to the MSCT studies, the many of the EBCT studies were limited to the proximal and middle coronary segments.^{6,7}

Future developments

A recently introduced generation of EBCT scanners acquires two slices simultaneously, and is capable of scanning several times during one heart cycle, which increases the radiation exposure, but allows for retrospective selection of the dataset at the most optimal phase. The slice acquisition time has been decreased to 50 ms which will further improve the image quality with regard to motion artefacts. Whether the use of thinner slices and faster scan times has a negative effect on the contrast to noise is currently unknown. Future studies will need to determine the incremental diagnostic value of this new EBCT technology.

Magnetic Resonance Imaging

Due to the lack of X radiation and use of less harmful and optional contrast media, magnetic resonance imaging is an attractive modality for non invasive imaging, including coronary angiography. Various scanning techniques and data acquisition sequences have been explored, and compared to conventional coronary angiography. The first experiences in 1993 were very promising, reporting a sensitivity and sensitivity to detect significant coronary stenosis of 90% and 92% in 39 patients.¹ Currently respiratory gated volumetric acquisitions of the entire heart are acquired, or smaller targeted volumes are acquired during single breath hold acquisitions. Intravenous injection of contrast media can be applied but is not mandatory to image the coronary artery lumen. Many comparative studies using different two and three dimensional techniques have been published with widely varying results.² Between 4% and 48% of the vessels and segments needed to be excluded because of insufficient image quality. The sensitivity and specificity to detect significant coronary obstruction ranges from 38% to 93% and 54% to 97%, respectively.² A recent multicenter trial using a respiratory gated free breathing scan protocol and a study population of 109 patients has been published by Kim et al in 2001.²¹ The investigators reported a sensitivity of 93% and specificity of 42% to detect significant lesions in the assessable (84%) proximal and middle coronary segments. The overall sensitivity, including lesions in non assessable segments, was not reported.

Despite it's benign nature MR coronary angiography is complicated by a relatively low three dimensional image resolution of rarely less than 1 mm³, long scanning time and inconsistent image quality. Compared to CT, the acquisition of the coronary MR is time consuming and requires dedicated scanners and image sequences as well as experienced operators.

DISCUSSION

Multi slice spiral CT is currently the most accurate non invasive angiographical modality for the detection of coronary stenosis. Despite the use of radiation and contrast media, MSCT coronary angiography is a relatively safe and simple procedure. All data can be acquired within 20 seconds, often providing predictable image quality, depending on the heart rate and the coronary calcium status of the patient. The contrast to noise ratio is high and the three dimensional resolution of the current generation scanners is less than 0.3 mm^3 . This high spatial resolution allows imaging of small branches, often neglected in the MR and EBCT studies.

Clinical implementation of MSCT coronary angiography

MSCT coronary angiography will, however, not within the foreseeable future replace coronary angiography as the reference coronary imaging tool. Conventional angiography is being performed without severe complications in the vast majority of patients. Conventional angiography consistently provides high quality data, with an excellent spatial resolution that allows quantitative assessment of the severity of the stenotic lesion. Apart from motion artefacts, image noise or calcium related artefacts, with a slice thickness between 0.5 and 1.0 MSCT can not be expected to provide comparable quantitative assessments. Conventional angiography can also be complemented by functional flow assessment and advanced plaque imaging techniques. Finally, conventional angiography can immediately be followed by a percutaneous interventional procedure to treat the obstructive problem. In patients with a modest heart rate MSCT could, however, provide a useful and reliable alternative to diagnostic catheter based angiography for the initial detection and localization of coronary stenoses. Additionally, because of its non invasive nature, MSCT coronary angiography can be introduced into the diagnostic work up of patients with anginal complaints at an earlier stage, when catheter based angiography is not yet indicated. Potential applications are the exclusion of an acute coronary obstruction in patients with atypical chest pain at the emergency ward, coronary artery stenosis in patients who need major (non cardiac) surgery, or obstructive disease in patients with inconclusive stress test. MSCT may also be valuable when repeated angiographic follow up is indicated, or after percutaneous coronary intervention or coronary artery bypass surgery (table 4).

Additional value of MSCT coronary angiography

Besides being a non invasive alternative to conventional coronary angiography, MSCT provides additional and possible valuable information with respect to the coronary artery wall, that is not provided by standard X ray coronary angiography (Figures 1, 3, and 5). Non stenotic atherosclerotic material is visualized well and the value of plaque characterizing by MSCT is currently being investigated and will be discussed in the following chapters.²² Furthermore, MSCT presents a three dimensional depiction of the coronary arteries, which can be useful when a coronary anomaly is suspected.²³

Table 4: Potential applications of CT coronary angiography

Early detection of stenoses in non symptomatics

Exclusion of coronary disease:

high risk patients

prior to major (non cardiac) surgery

Detection and/or exclusion of stenoses:

Atypical (unstable) chest pain

Non conclusive stress tests

Substitution for diagnostic X ray coronary angiography:

Prior to percutaneous coronary intervention

High risk patients: aortic disease

Adjuvant to coronary angiography:

Plaque characterization

Complicated coronary intubation

Follow up:

Percutaneous coronary intervention

Bypass surgery

Diseased vessels can easily be related to an infarcted, or perfusion depleted myocardial segment. Besides the coronary arteries, the MSCT scan includes high quality volumetric information of the entire heart and lower lungs, resulting in (accidental) early detection of abnormalities, including pericardial disease, intra cardiac thrombi, morphologic valvular disease (calcifications, thickening), lung tumours, etc. Finally, the raw MSCT data can be used for reconstruction of different cardiac phases, to evaluate the ventricular performance: ventricular cavity volumes, ejection fraction and regional myocardial wall thickening.²⁴

Further improvement

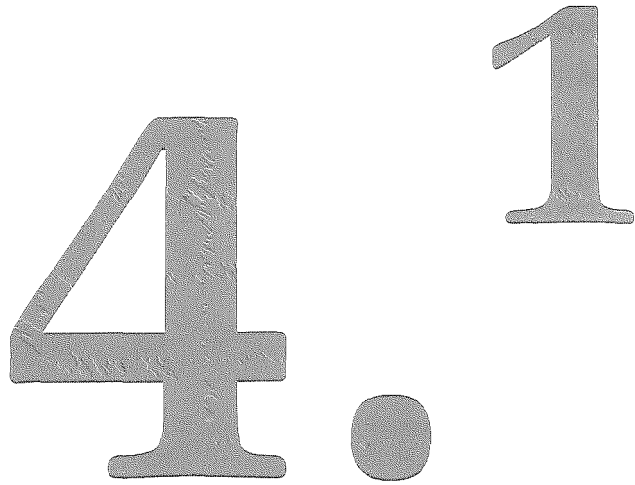
To further improve the quality and quantitative potential of MSCT coronary angiography, the fundamental characteristics, such as the spatial and temporal resolution need to be further optimised. Evaluation of three dimensional MSCT angiograms may become more efficient, and better reproducible with dedicated

post processing tools. More sophisticated tools that combine an accurate reproducible assessment with presentable overviews are currently being developed, and will improve the clinical implementation of MSCT coronary angiography as a non invasive tool to localize obstructive coronary artery disease.

REFERENCES

1. Manning WJ, Li W, Edelman RR, et al. A preliminary report comparing magnetic resonance coronary angiography with conventional angiography. *N Engl J Med.* 1993;328 832.
2. Fayad ZA, Fuster V, Nikolaou K, et al. Computed tomography and magnetic resonance imaging for noninvasive coronary angiography and plaque imaging. Current and potential future concepts. *Circulation* 2002 106:2026 2034.
3. Nakanishi T, Ito K, Imazu M, et al. Evaluation of coronary artery stenoses using electron beam CT and multiplanar reformation. *J Comput Assist Tomogr.* 1997;21:121 127.
4. Reddy G, Chernoff DM, Adams JR, et al. Coronary artery stenoses: assessment with contrast enhanced electron beam CT and axial reconstructions. *Radiology* 1998;208:167 172.
5. Schmermund A, Rensing BJ, Sheedy PF, et al. Intravenous electron beam computed tomographic coronary angiography for segmental analysis of coronary artery stenoses. *J Am Coll Cardiol.* 1998;31:1547 1554.
6. Rensing BJ, Bongaerts A, van Geuns RJ, et al. Intravenous coronary angiography by electron beam computed tomography: a clinical evaluation. *Circulation* 1998;98:2509 2512.
7. Achenbach S, Moshage W, Ropers D, et al. Value of electron beam computed tomography for the noninvasive detection of high grade coronary artery stenoses and occlusions. *N Engl J Med.* 1998;339:1964 1971.
8. Budoff MJ, Oudiz RJ, Zalace CP, et al. Intravenous three dimensional coronary angiography using contrast enhanced electron beam computed tomography. *Am J Cardiol.* 1999;83:840 845.
9. Achenbach S, Ropers D, Regenfus M, et al. Contrast enhanced electron beam computed tomography to analyse the coronary arteries in patients after acute myocardial infarction. *Heart.* 2000;84:489 493.
10. Nieman K, Oudkerk M, Rensing BJ, et al., Coronary angiography with multi slice computed tomography. *Lancet* 2001;357:599 603.
11. Achenbach S, Giesler T, Ropers D, et al. Detection of coronary artery stenoses by contrast enhanced, retrospectively electrocardiographically gated, multislice spiral computed tomography. *Circulation* 2001;103:2535 2538.
12. Knez A, Becker CR, Leber A, et al. Usefulness of multislice spiral computed tomography angiography for determination of coronary artery stenoses. *Am J Cardiol.* 2001;88:1191 1194.
13. Vogl TJ, Abolmaali ND, Diebold T, et al. Techniques for the detection of coronary atherosclerosis: multi detector row CT coronary angiography. *Radiology* 2002;223:212 220.
14. Kopp AF, Schröder S, Köttnner A, et al. Non invasive coronary angiography with high resolution multidetector row computed tomography: results in 102 patients. *Eur Hear J.* 2002;23:1714 1725.

15. Giesler T, Baum U, Ropers D, et al. Noninvasive visualization of coronary arteries using contrast enhanced multidetector CT: influence of heart rate on image quality and stenosis detection. *Am J Roentgenol.* 2002;179:911 916.
16. Nieman K, Rensing BJ, van Geuns RJ, et al. Non invasive coronary angiography with multislice spiral computed tomography: impact of heart rate. *Heart.* 2002;88:470 474.
17. Nieman K, Cademartiri F, Lemos PA, et al. Reliable noninvasive coronary angiography with fast submillimeter multislice spiral computed tomography. *Circulation* 2002;106:2051 2054.
18. Ropers D, Baum U, Pohle K, et al. Detection of coronary artery stenoses with thin slice multi detector row spiral computed tomography and multiplanar reconstruction. *Circulation* 2003 (in press).
19. Nieman K, Rensing BJ, van Geuns RJM, Munne A, Ligthart JMR, Pattynama PMT, Krestin GP, Serruys PW, de Feyter PJ. Usefulness of multislice computed tomography for detecting obstructive coronary artery disease. *Am J Cardiol.* 2002;89:913 918.
20. Wang Y, Watts R, Mitchell I, et al. Coronary MR angiography: selection of acquisition window of minimal cardiac motion with electrocardiography triggered navigator cardiac motion prescanning initial results. *Radiology* 2001;218:580 585.
21. Kim WY, Daniel PG, Stuber M, et al. Coronary magnetic resonance angiography for the detection of coronary stenoses. *N Engl J Med.* 2001;345:1863 1869.
22. Schroeder S, Kopp AF, Baumbach A, et al. Noninvasive detection and evaluation of atherosclerotic coronary plaques with multislice computed tomography. *J Am Coll Cardiol.* 2001;37:1430 1435.
23. Ropers D, Gehling G, Pohle K, et al. Anomalous course of the left main or left anterior descending coronary artery originating from the right sinus of Valsalva. Identification of four common variations by electron beam tomography. *Circulation* 2002;105:e42 e43.
24. Dirksen MS, Bax JJ, de Roos A, Jukema JW, van der geest RJ, Geleijns K, Boersma E, van der Wall EE, Lamb HJ. Usefulness of dynamic multislice computed tomography and left ventricular function in unstable angina pectoris and comparison with echocardiography. *Am J Cardiol.* 2002;90:1157 1160.



**Non-invasive Visualization of
Atherosclerotic Plaques
with Electron Beam and Multi-slice
Spiral Computed Tomography**

Koen Nieman
Aad van der Lugt
Peter MT Pattynama
Pim J de Feyter

SUMMARY

As an alternative to intra coronary modalities, electron beam (EBCT) and multislice spiral computed tomography (MSCT) are able to non invasively image the coronary arteries. In addition to stenosis detection, MSCT has the ability to visualize atherosclerotic plaques, and by distinguishing different tissue components it may hold promise as a non invasive technique for the identification of vulnerable plaques.

INTRODUCTION

Currently, catheter based imaging modalities provide the most complete insight into the morphological, hemodynamical and histopathological characteristics of atherosclerotic lesions in the in vivo coronary arteries. However, atherosclerosis is a dynamic process and plaque size and contents have been described to change, sometimes over very short intervals. The advantages of non invasive imaging techniques are the opportunity to detect lesions earlier, possibly before symptoms occur, and to monitor the progression or stabilization of coronary plaques over time.

Non-invasive coronary angiography

State of the art computed tomography (CT) scanners are now being used for non invasive coronary angiography and have the potential to visualize and assess the contents of atherosclerotic lesions. Contrary to conventional angiography, which visualizes an entire coronary artery in a fraction of a second, acquisition of a complete CT angiogram requires a sequence of heart cycles. To ensure isocardiographically consistent data, the acquisition needs to be synchronized to the patient's heart cycle. Generally, the data acquisition is restricted to the diastolic cardiac phase, when coronary displacement is minimal. Furthermore, the length of the interval within each heart rate needs to be minimized to prevent motion artefacts. For assessment of the coronary lumen, an iodine containing contrast medium is intravenously injected, and the data is acquired during the first pass contrast plateau. To prevent respiratory motion artefacts the scan is performed during a single inspiratory breath hold. The spatial resolution of the different CT scanners varies, but ranges up to 0.6 mm for the in plane and up to 0.8 mm for the through plane spatial resolution.

Electron beam computed tomography

Due to the lack of mechanically rotating parts, the electron beam CT (EBCT) scanner can acquire data very fast, the scan time per slice is 100 ms and may decrease to 50 ms in the future.¹ The acquisition of consecutive axial slices is prospectively triggered by the ECG, and executed during the late diastolic phase. By pharmacologically increasing the heart rate (atropine i.v.) up to 60 slices of 1.5 or 3.0 mm can be acquired within a 40 second breath hold.

Multislice spiral computed tomography

The currently available generation of multislice spiral CT scanners, which are produced by a number of manufacturers, acquire four 1.0 millimetre slices at a rotation time of 500 ms. The CT data and ECG are acquired continuously during a single breath hold and retrospectively reconstructed according to the recorded ECG.² A stack of over 200 overlapping 1.25 mm slices are reconstructed at a retrospectively selectable cardiac phase. To compensate for the relatively lower temporal resolution (<250 ms) optimal image quality requires a low heart rate, which can be induced by administration of beta receptor blocking medication prior to the scan. The upcoming generation of MSCT scanners acquire between 8 and 16 sub millimetre slices at a further increased rotation speed. The continuous data acquisition of MSCT results in a higher radiation exposure, in comparison to EBCT.

CT CORONARY ANGIOGRAPHY

Both EBCT and MSCT have been used to visualize the coronary lumen in order to detect obstructive coronary artery disease. If adequate image quality is achieved both CT modalities yield a good diagnostic accuracy for the detection of significantly stenotic lesions (figure 1).³⁻¹¹ The poorer spatial resolution and modest longitudinal scan range limit the performance of EBCT angiography. While MSCT angiography is more often hindered by motion artefacts, particularly in patients with high heart rates. In general CT angiography is hindered by high density material, such as calcifications or stents, in the proximity of the coronary artery.

CORONARY CALCIUM QUANTIFICATION

The use of EBCT to detect and quantify coronary calcium deposits started in the early nineties. Computed tomography is very sensitive to the detection of calcifications and no injection of contrast media is required. The correlation between sequential EBCT and MSCT calcium score seems to be good.¹²⁻¹⁴ For the purpose of screening asymptomatic patients prospectively ECG triggered acquisition of sequential slices is preferred to minimize the radiation exposure. The reproducibility of the MSCT based calcium score can be improved by acquiring spiral data for retrospectively ECG gated reconstruction, but at the cost of a significantly increased radiation dose. Currently, most available data have been acquired with EBCT and the semi quantitative Agatston score.¹⁵ The detection and quantification of coronary calcium have been applied for the exclusion of coronary artery disease in patients presenting with acute angina at the emergency ward, and the detection of coronary stenosis in symptomatic patients.¹⁶⁻¹⁹ Most patients with symptomatic obstructive coronary disease have a positive calcium score, however, the specificity of calcium scoring for this purpose is poor in comparison to other non invasive tests.

Table 1. Characteristics of currently used EBCT (Imatron C 150) and MSCT (4 slice generation) coronary angiography protocols

	Electron Beam CT	Multislice Spiral CT
Acquisition mode	Consecutive	Spiral
Cardiac synchronisation	Prospective triggering	Retrospective gating
Detector collimation	1.5 or 3.0 mm (2.0mm overlap)	4 x 1.0 mm
Acquisition optimisation	Atropine i.v. (↑Z coverage)	Betablocker p.o./i.v. (↓ motion artefacts)
Temporal resolution	100 ms	250 ms
In plane resolution	6 line pairs/cm	8 9 line pairs/cm
Slice thickness	1.5 or 3.0 mm	1.25 mm

* Heart rate = 70 min⁻¹

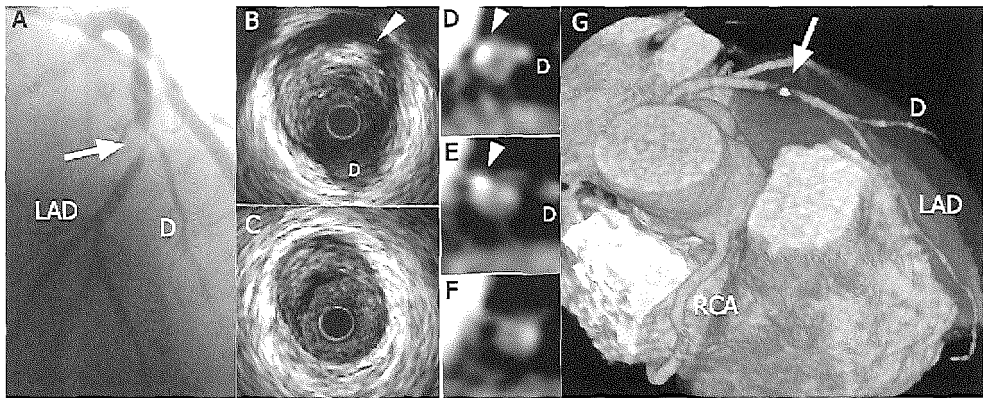


Figure 1. Comparable plaque features with intracoronary ultrasound and multislice spiral CT. Conventional selective coronary angiogram (Fig. A) of the left coronary artery showing a significant lesion (arrow) at the level of the bifurcation of the left anterior descending coronary artery (LAD and the first diagonal branch (D)). Intra coronary ultrasound (Figs. B and C) shows a plaque that is partially calcified (arrow head). Multi planar reconstructions (Figs. D, E and F) of the LAD show cross sectional views of the LAD that correspond with the ultrasound findings. A three dimensional reconstruction of the MSCT angiogram (Fig. G) shows the partially calcified stenotic lesion (arrow). Right coronary artery (RCA). The CT data were acquired with a Somatom VolumeZoom (Siemens, Germany), rotation time 500 ms, detector collimation: 4 x 1.0 mm).

Most patients with an acute myocardial infarction have a positive calcium score.²⁰ The presence and amount of coronary calcium is correlated to the occurrence of adverse coronary events.²¹⁻²³ Whether the presence of calcium in a plaque determines plaque stability or instability remains a matter of debate. The amount of calcium is, however, correlated to the total atherosclerotic plaque burden, and consequently the likelihood of one or more vulnerable plaques being present somewhere in the coronary artery system. While the presence of calcium may not indicate vulnerability of a particular plaque, it could be useful to detect vulnerable patients.²⁴ The predictive value of calcium screening in asymptomatic individuals, incremental to the traditional risk factors, and in comparison to other non invasive tests, remains to be determined.²⁵

ASSESSMENT OF ATHEROSCLEROTIC PLAQUES

Histopathologic studies have shown that plaques with an increased likelihood of rupture have distinct features, which are different from plaques that are considered stable. A positively remodelled eccentric atherosclerotic lesion, containing a large necrotic lipid core, covered by a thin fibrous cap, is considered more prone to rupture. Plaques containing no or only a small lipid core covered by a thick fibrous cap are regarded as more stable. Based on the tissue specific X ray attenuation characteristics, computed tomography is able to distinguish fat tissue, fibrous tissue, contrast medium and calcium or bone. Theoretically, computed tomography should be able to differentiate plaques that are calcified, predominantly fibrous or plaques that contain a large lipid pool.

Plaque imaging in the carotid arteries

In larger and less mobile vessels, such as the aorta and carotid arteries, plaque components are more easily recognized. Already in 1984 it was demonstrated that thin section (1.5 mm) CT of the neck was able to detect intimal disease in the carotid bifurcation. Differentiation of atheroma from thrombus was not possible because both were hypodense with respect to the arterial wall and the contrast filled lumen. Calcifications in the wall of the artery were frequently seen.^{26,27}

Estes et al and Oliver et al. studied patients, scheduled for carotid endarterectomy, with CT Angiography. Axial 3 mm slices of the bifurcation were compared with histologic sections of the surgical specimen.^{28,29} Hyperdense structures corresponded with calcifications, hypodense regions with lipid or hemorrhage, and isodense regions with fibrosis (figure 2 and 3). Fibrous tissue had higher Hounsfield Units (HU) than lipid (90 (24 HU versus 39 (12 HU).²⁹ MSCT allows evaluation of the carotid bifurcation with thinner slices (0.5-1.0 mm) than single slice spiral CT, and multiplanar reconstruction of the disease vessel.

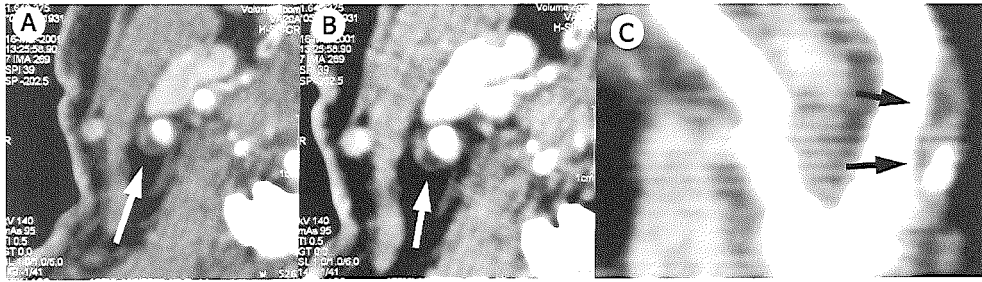


Figure 2. Axial and sagittally reconstructed images of a carotid bifurcation with eccentric atherosclerotic thickening of the wall. Panel A with window level setting of 500/150 revealed a contrast enhanced lumen and thickening of the wall. Panel B with window level setting of 250/70 allows the evaluation of different plaque components. A hypodense region (lipid core) covered by an isodense cap (fibrous cap) is clearly visualised in axial and sagittal plane (Panel C).

(A full color version of this illustration can be found in the color section)

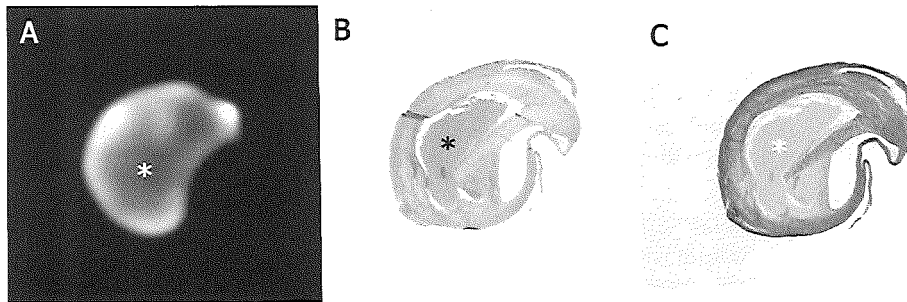


Figure 3. Thin section CT of a surgical specimen obtained during carotid endarterectomy with corresponding histological sections (haematoxylin eosin and Elastic van Gieson staining). CT imaging reveals a central hypodense core (*) which corresponds with the lipid core in the histological sections.

(A full color version of this illustration can be found in the color section)

Imaging of coronary plaques

Visualization of atherosclerotic plaque material in the coronary arteries is even more challenging due to the small size of the plaques and continuous displacement of the vessels. Schroeder et al compared contrast enhanced MSCT images of plaques in the proximal coronary arteries with intra coronary ultrasound. The echogenicity of the dominant plaque components were compared to the average CT attenuation values, or Hounsfield units (HU), within the plaque.³⁰ Obviously, plaques containing calcium have high HU values and were readily identified.

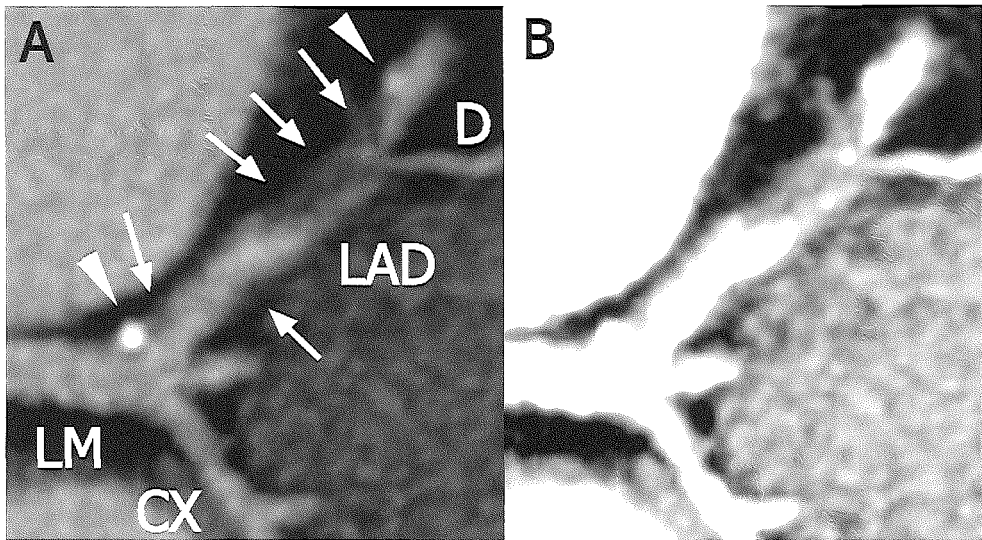


Figure 4. Coronary artery plaque imaging. A MSCT coronary angiogram displaying the left coronary trifurcation. At the proximal left anterior descending coronary artery (LAD) a partly calcified plaque can be observed. Non calcified plaque material can be found along the LAD. Proximal to the origin of the first septal and diagonal branches (D) a atherosclerotic lesion, largely consisting of non calcified tissue, obstructs the vessel lumen. The CT density varied between 30 and 50 HU. The CT data were acquired with a Somatom Sensation 16 (Siemens, Germany), rotation time 420 ms, detector collimation: 12 x 0.75 mm).

Plaques with low HU values (14 (26 HU) correlated well with those with low echogenicity on ICUS (figure 1 and 4). Lesions with slightly higher values (91(21 HU) correlated well to plaques with intermediate echogenicity. The four slice scanner that was used in this study has a good in plane, but relatively modest through plane resolution (1.25 mm effective slice thickness). Phantom studies and histopathological comparisons of ex vivo examinations with improved scanning equipment shows promising results.^{31,32}

Future outlook

Until recently, in vivo evaluations were limited to rough estimations regarding the predominant plaque content. The upcoming generation of scanners will be equipped with an extended number of sub millimetre slices. This improvement of spatial resolution will reduce partial volume effects and allow for differentiation of smaller parts. The increased rotation rate will improve the temporal resolution of the scanner and reduce blurring due to residual cardiac motion.

Magnetic resonance imaging allows high in plane resolution imaging of coronary plaques with possible better tissue differentiation compared to MSCT. Multiple acquisitions and data averaging are required for a single image and the slice thickness generally between 3 and 5 millimetres may be responsible for partial voluming of different components. The assessment is usually limited to short vessel segments to maintain acceptable scan times. MRI does, however, not require X radiation or injection of iodine containing contrast media, which makes it a more ideal method for serial assessments. A strategy of site specific interrogation with MRI, of lesions that were previously detected on a MSCT roadmap, has been suggested.

The technical developments in both magnetic resonance imaging and computed tomography will determine the clinical applicability of non invasive coronary plaque characterization.

REFERENCES

1. Electron Beam Computed Tomography. In: Seeram E (Ed.). *Computed Tomography: Physical Principles, Clinical Applications, and Quality Control*. Philadelphia, USA: W.B. Saunders Company, 2001; 154-164.
2. Ohnesorge B, Flohr T, Becker C, et al. Technical Aspects and Applications of Fast Multislice Cardiac CT. In: Reiser MF, Takahashi M, Modic M, Bruening R (Eds). *Medical radiology Diagnostic Imaging and Radiation Oncology*. Berlin, Germany: Springer; 2001; 121-30.
3. Reddy G, Chernoff DM, Adams JR, Higgins CB. Coronary artery stenoses: assessment with contrast enhanced electron beam CT and axial reconstructions. *Radiology*. 1998; 208:167-172.
4. Schmermund A, Rensing BJ, Sheedy PF, Bell MR, Rumberger JA. Intravenous electron beam computed tomographic coronary angiography for segmental analysis of coronary artery stenoses. *J Am Coll Cardiol*. 1998; 31:1547-1554.
5. Rensing BJ, Bongaerts A, van Geuns RJ, van Ooijen P, Oudkerk M, de Feyter PJ. Intravenous coronary angiography by electron beam computed tomography: a clinical evaluation. *Circulation*. 1998; 98:2509-2512.
6. Achenbach S, Moshage W, Ropers D, Nossen J, Daniel W. Value of electron beam computed tomography for the detection of high grade coronary artery stenoses and occlusions. *N Engl J Med*. 1998; 339:1964-1971.
7. Budoff MJ, Oudiz RJ, Zalace CP, Bakhsheshi H, Goldberg SL, French WJ, Rami TG, Brundage BH. Intravenous three dimensional coronary angiography using contrast enhanced electron beam computed tomography. *Am J Cardiol*. 1999; 83:840-845.
8. Nieman K, Oudkerk M, Rensing BJ, van Ooijen P, Munne A, van Geuns RJ, de Feyter PJ. Coronary angiography with multi slice computed tomography. *Lancet* 2001; 357:599-603.
9. Achenbach S, Giesler T, Ropers D, Ulzheimer S, Derlien H, Schulte C, Wenkel E, Moshage W, Bautz W, Daniel WG, Kalender WA, Baum U. Detection of coronary artery stenoses by contrast enhanced, retrospectively electrocardiographically gated, multislice spiral computed tomography. *Circulation* 2001; 103:2535-8.

10. Knez A, Becker CR, Leber A, Ohnesorge B, Becker A, White C, Haberl R, Reiser MF, Steinbeck G. Usefulness of multislice spiral computed tomography angiography for determination of coronary artery stenoses. *Am J Cardiol.* 2001 Nov 15;88(10):1191 4.
11. Vogl TJ, Abolmaali ND, Diebold T, Engelmann K, Ay M, Dogan S, Wimmer Greinecker G, Moritz A, Herzog C. Techniques for the Detection of Coronary Atherosclerosis: Multi detector Row CT Coronary Angiography. *Radiology* 2002; 223: 212 220.
12. Becker CR, Kleffel T, Crispin A, Knez A, Young J, Schoepf UJ, Haberl R, Reiser MF. Coronary artery calcium measurement: agreement of multirow detector and electron beam CT. *AJR Am J Roentgenol.* 2001 May;176(5):1295 8.
13. Horiguchi J, Nakanishi T, Ito K. Quantification of coronary artery calcium using multidetector CT and a retrospective ECG gating reconstruction algorithm. *AJR Am J Roentgenol.* 2001 Dec;177(6):1429 35.
14. Carr JJ, Crouse JR 3rd, Goff DC Jr, D'Agostino RB Jr, Peterson NP, Burke GL. Evaluation of subsecond gated helical CT for quantification of coronary artery calcium and comparison with electron beam CT. *AJR Am J Roentgenol.* 2000 Apr;174(4):915 21.
15. Agatston AS, Janowitz WR, Hildner FJ, Zusmer NR, Viamonte M, Detrano R. Quantification of coronary artery calcium using ultrafast computed tomography. *J Am Coll Card* 1990;15:827 32.
16. McLaughlin VV, Balogh T, Rich S. Utility of electron beam computed tomography to stratify patients presenting to the emergency room with chest pain. *Am J Cardiol.* 1999 Aug 1;84(3):327 8, A8.
17. Haberl R, Becker A, Leber A, Knez A, Becker C, Lang C, Bruning R, Reiser M, Steinbeck G. Correlation of coronary calcification and angiographically documented stenoses in patients with suspected coronary artery disease: results of 1,764 patients. *J Am Coll Cardiol.* 2001 Feb;37(2):451 7.
18. Kennedy J, Shavelle R, Wang S, Budoff M, Detrano RC. Coronary calcium and standard risk factors in symptomatic patients referred for coronary angiography. *Am Heart J.* 1998 Apr;135(4):696 702
19. Budoff MJ, Georgiou D, Brody A, Agatston AS, Kennedy J, Wolfkiel C, Stanford W, Shields P, Lewis RJ, Janowitz WR, Rich S, Brundage BH. Ultrafast computed tomography as a diagnostic modality in the detection of coronary artery disease: a multicenter study. *Circulation.* 1996 Mar 1;93(5):898 904.
20. Raggi P, Callister TQ, Cooil B, He ZX, Lippolis NJ, Russo DJ, Zelinger A, Mahmorian JJ. Identification of patients at increased risk of first unheralded acute myocardial infarction by electron beam computed tomography. *Circulation.* 2000;101:850 5.
21. Detrano RC, Wong ND, Doherty TM, Shavelle RM, Tang W, Ginzton LE, Budoff, MJ, Narahara KA. Coronary calcium does not accurately predict near term future coronary events in high risk adults. *Circulation.* 1999 May 25;99(20):2633 8.
22. Arad Y, Spadaro LA, Goodman K, Newstein D, Guerci AD. Prediction of coronary events with electron beam computed tomography. *J Am Coll Cardiol.* 2000 Oct;36(4):1253 60.
23. Raggi P, Cooil B, Callister TQ. Use of electron beam tomography data to develop models for prediction of hard coronary events. *Am Heart J.* 2001 Mar;141(3):375 82.
24. Greenland P, Smith Jr SC Jr, Grundy SM. Improving coronary heart disease risk assessment in asymptomatic people: role of traditional risk factors and noninvasive cardiovascular tests. *Jul;38(1):105 10. Circulation* 2001 Oct 9;104(15):1863 7.

25. Robert A. O'Rourke, Bruce H. Brundage, Victor F. Froelicher, Philip Greenland, Scott M. Grundy, Rory Hachamovitch, Gerald M. Pohost, Leslee J. Shaw, William S. Weintraub, William L. Winters, Jr, James S. Forrester, Pamela S. Douglas, David P. Faxon, John D. Fisher, Gabriel Gregoratos, Judith S. Hochman, Adolph M. Hutter, Jr, Sanjiv Kaul, Robert A. O'Rourke, William S. Weintraub, William L. Winters, Jr, and Michael J. Wolk. American College of Cardiology/American Heart Association Expert Consensus Document on Electron Beam Computed Tomography for the Diagnosis and Prognosis of Coronary Artery Disease: Committee Members. *Circulation* 102: 126-140.
26. Heinz ER, Pizer SM, Fuchs H, Fram EK, Burger P, Drayer BP, Osborne DR. Examination of the extracranial carotid bifurcation by thin section dynamic CT: direct visualization of intimal atheroma in man (Part 1). *AJNR Am J Neuroradiol* 1984;5(4):355-9.
27. Heinz ER, Fuchs J, Osborne D, Drayer B, Yeates A, Fuchs H, Pizer S. Examination of the extracranial carotid bifurcation by thin section dynamic CT: direct visualization of intimal atheroma in man (Part 2). *AJNR Am J Neuroradiol* 1984;5(4):361-6.
28. Oliver TB, Lammie GA, Wright AR, Wardlaw J, Patel SG, Peek R, Ruckley CV, Collie DA. Atherosclerotic plaque at the carotid bifurcation: CT angiographic appearance with histopathologic correlation. *AJNR Am J Neuroradiol* 1999;20(5):897-901.
29. Estes JM, Quist WC, Lo Gerfo FW, Costello P. Noninvasive characterization of plaque morphology using helical computed tomography. *J Cardiovasc Surg (Torino)* 1998;39(5):527-34.
30. Schroeder S, Kopp AF, Baumbach A, Meisner C, Kuettner A, Georg C, Ohnesorge B, Herdeg C, Claussen CD, Karsch KR. Noninvasive Detection and Evaluation of Atherosclerotic Coronary Plaques With Multislice Computed Tomography. *J Am Coll Cardiol* 2001; 37: 1430-1435.
31. Ohnesorge BM, Flohr TG, Schroeder S, Kopp AF, Becker CR, Klingenberg K. Evaluation of Atherosclerotic Coronary Plaques with ECG gated Multislice Spiral CT: A Phantom Study with Submillimeter Slice width and Initial Clinical Experience. *Radiology* 2001; 221 (Suppl.): 503.
32. Nikolaou K, Becker CR, Babaryka G, Mulders M, Loehrs U, Reiser MF. High resolution Magnetic Resonance and Multi slice CT Imaging of Coronary Artery Plaques in Human ex Vivo Coronary Arteries. *Radiology* 2001; 221 (Suppl.): 503.

4.2

Computed Tomography for Acute Coronary Syndromes

Pim J de Feyter
Koen Nieman

Theroux A (Ed.). Acute Coronary Syndrome
A Companion to Braunwald's Heart Disease
WB Saunders, New York, USA (in press)

INTRODUCTION

Coronary artery wall and lumen imaging poses the greatest challenge to any diagnostic technique, because the coronary arteries are small and tortuous and course in complex multiple planes around the heart, while cardiac contraction and respiration cause motion artifacts.

Therefore, coronary imaging requires high spatial resolution and high speed acquisition techniques. In the mid 1980s high speed scanning, the Electron Beam Computed Tomography (EBCT) was introduced. This scanner was capable of acquiring tomograms in as little as 50 ms and 100 ms. The high spatial resolution and high speed acquisition allowed detection and quantification of coronary calcification and in a substantial number of patients sufficient quality imaging of the contrast enhanced coronary arteries was achieved.

More recently, another high spatial resolution and fast acquisition technique has been introduced: multi slice computed tomography (MS CT). This technique is also able to detect and quantify coronary calcifications and to visualize coronary arteries.

Both non invasive coronary imaging techniques are gradually emerging as new diagnostic tools into the cardiology department and the usefulness of both techniques in the diagnosis and management of coronary artery disease, and in particular acute coronary syndromes, is just beginning to evolve.

CT TECHNOLOGY

The electron beam CT scanner is a non mechanical sequential scanner. After each acquisition, a 216° electron beam sweep that requires only 100 ms, the table is advanced 1.5 or 2.0 mm to the next slice position. By use of prospective ECG triggering single slices are acquired at every second heart beat to allow for the table translations. A greater number of slices can be acquired at higher heart rates, which can be promoted by administration of a small dose of atropine prior to the test. Generally, a Z range of 7-10 cm can be covered during a 35-45s breathhold. Two angiographic protocols are being used: a consecutive 1.5 mm slice protocol or an overlapping 31.0 mm slice protocol, with a table increment of 2.0 mm.

Multislice Spiral Computed Tomography

The multislice CT scanner is a mechanical spiral scanner. Contrary to sequential scanners, the table moves continuously while spiral CT data from up to four detector rows are acquired simultaneously. Most scanners use a 4 x 1 mm collimation protocol at a table increment of 1.5 mm per gantry rotation, which results in a Z coverage of around 12 cm per breathhold. Retrospectively, the data is matched to the recorded ECG and an overlapping set 1.25 mm slices can be reconstructed at any given cardiac phase. A consequence of continuous scanning is an increased exposure to radiation.

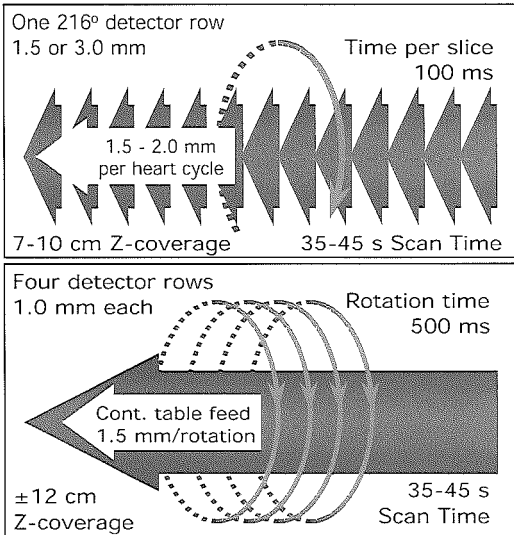


Figure 1. EBCT schema. The EBCT scanner is a non mechanical scanner without a rotating X ray tube. Instead, an electron beam is directed by deflection coils along a 210° tungsten ring. A complete sweep can be performed within 100 ms or less. After collision with the target rings roentgen rays are produced. The roentgen rays are collimated and a narrow fan beam is directed through the patient. Attenuation projections are collected by a stationary 216° detector ring at the opposite side. The electron gun is triggered by the patient's electrocardiogram. According to a number of preceding heart beats the moment of data acquisition is determined, at for instance 70 % of the RR interval, at which time the electron gun is activated and CT data are acquired. After the acquisition the table is advanced to the next slice position.

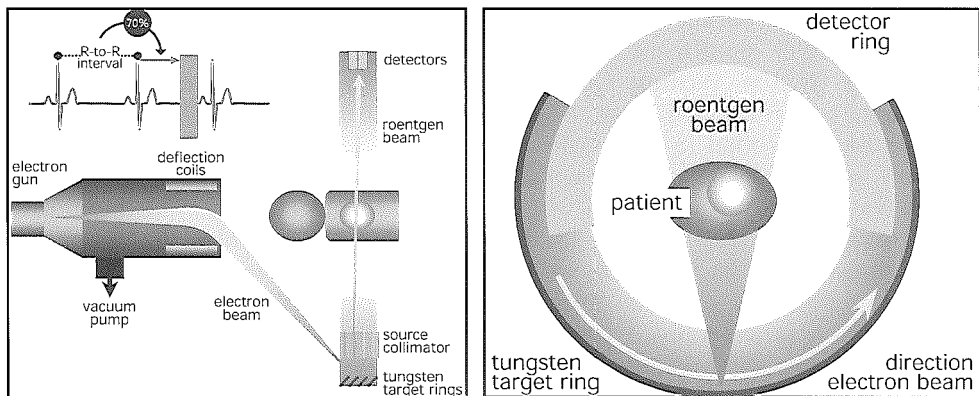


Figure 2. Sequential vs. spiral. The electron beam CT scanner acquires one slice at every second heart beat. Depending on the collimation protocol and the heart rate a Z range of 7-10 cm can be covered within the time of a breathhold. The multislice spiral CT scanner continuously acquires data from 4 detector rows at a table increment of 3 mm per second, resulting in a Z coverage of about 12 cm in a breathhold. From 250 ms of spiral data 1.25 mm slices can be reconstructed after the acquisition at any moment within the cardiac phase.

At an X ray tube rotation time of 500 ms images can be created using advanced reconstruction algorithms requiring 250ms of data, or less. This relatively lower temporal resolution can be compensated by use of beta receptor blocking medication prior to the examination.

CORONARY CALCIUM

Quantification of coronary calcification

EBCT is a safe and sensitive tool to detect and quantify coronary artery calcification. The epicardial arteries can readily be identified because the density of coronary blood is higher than that of the surrounding peri arterial fat. Coronary wall calcium is easily identified because the density of calcium is much higher than that of peri arterial fat and coronary blood (fig. 3 and 4).

Histological studies have shown that a tissue density of ≥ 130 HU is highly correlated with calcified coronary plaques.¹ A calcium scoring system has been devised based on the density of the calcific plaque and the area of calcium deposits: the Agatston score.² The threshold for a calcific lesion is set at a density of 130 HU for an area of ≥ 1 mm². The Agatston score was calculated by multiplying the area of each calcific lesion by a density measure defined by the peak density number of the lesion. The density measure is 1 for a peak density of 130-199 HU, 2 for 200-299 HU, 3 for 300-399 HU and 4 for ≥ 400 HU. The total calcium score was determined by adding up all lesion scores.

Coronary calcium to predict obstructive coronary artery disease

The diagnostic accuracy of the presence of coronary calcium detected with EBCT to predict significant obstructive coronary artery disease was recently established by the Writing Group, appointed by the American College of Cardiology and American Heart Association.³ In a meta analysis a total of 3683 patients were enrolled in 16 studies. The prevalence of coronary artery disease was on average 60 %. The weighted average sensitivity, specificity and predictive accuracy was 80.4 %, 40 % and 59 % respectively. The individual study sensitivity values ranged from 68 % to 100 %, whereas the specificity values ranged from 21 % to 100 %. The wide variation in outcomes reflects the differences in study patients, minimum area of calcified tissue required for a calcific lesion (area's ranged from 0.5 mm² to 2.0 mm²), number of acquired tomograms and slice thickness (3mm to 6 mm).

Coronary calcium to predict coronary death or non-fatal MI in asymptomatic high risk individuals

Coronary calcification is a specific component of coronary atherosclerosis. Individual patients exhibit a wide spectrum of coronary lesions, varying from early non calcified lesions to far advanced complicated calcific lesions. The presence or absence of coronary calcium does not reliably distinguish between the presence or absence of a stable or vulnerable plaque.

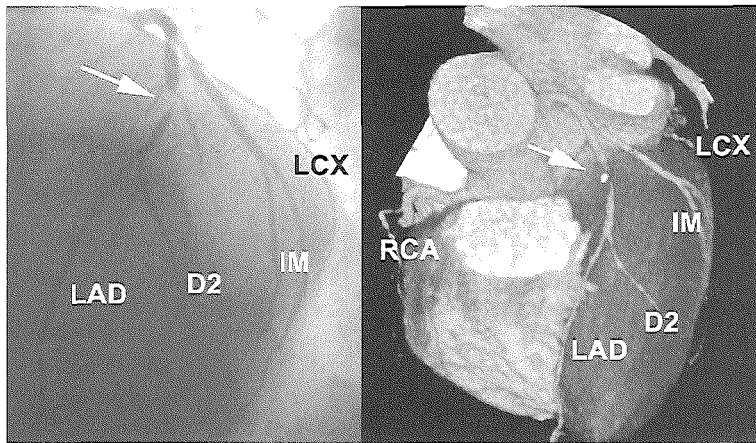


Figure 3. Conventional and multislice spiral CT (MSCT) coronary angiogram (3D volume rendered) of a patient with a stenotic coronary lesion in the mid left anterior descending branch (LAD), just distal from the small first diagonal branch. Also the calcified contents of the plaque are visualized on the MSCT angiogram. The left circumflex coronary artery (LCX), right coronary artery (RCA), second diagonal branch (D2) and intermediate branch (IM) can also be appreciated.

The presence and extent of coronary calcium appears closely related to the overall atherosclerotic plaque burden. A large amount of calcium increases the likelihood of the presence of a vulnerable plaque, but does not specifically identify a vulnerable plaque. On the other hand, absence of calcium does not exclude atherosclerotic disease, including a vulnerable plaque, but its presence is very unlikely.⁴

The presence and extent of coronary calcium may have predictive value for subsequent coronary events in a symptomatic individuals.^{5,9} Data of three long term follow up studies have been published (Table 1).^{5,7,9} All three studies investigated high risk a symptomatic populations. It is important to note that first, the predictive value of a calcium score is only relevant if this adds incremental predictive value to traditional risk factors. And, second, calcium deposition increases with age and is sex related, these scores should be adjusted for age as well as for sex, to provide optimal predictive value.

Detrano et al demonstrated that assessment of calcium score was not an accurate predictor of death or non fatal myocardial infarction.⁵ Furthermore the calcium score did not add incremental information to traditional risk factors. However a calcium score > 44 HU was associated with a 2.3 higher likelihood to suffer a non fatal myocardial infarction or death than study subjects with lower scores. When they divided their population into tertiles according to the height of the calcium scores, it appeared that the highest tertile was associated with the highest event rate.

Arad et al demonstrated in their study that a coronary calcium score ≥ 160 HU was associated with an odds ratio of 22.2 of risk of death or non fatal myocardial infarction compared to individuals with lower score.⁷ The calcium scores remained independently associated with outcome after adjustments for self reported risk factors.

Finally Raggi et al showed that, if age and sex were taken into account in dividing individuals into percentiles, the age and sex specific percentile coronary score not only provided the best predictive model for predicting death and non fatal myocardial infarction but also provided incremental prognostic value to traditional risk factors for coronary artery disease.⁹

A calcium score of 0 was associated with a 0.12 % risk per year of death and non fatal MI and this was 3.0 % risk per year if calcium was present.

In an earlier study Raggi et al, reporting about 632 individuals followed for 32 ± 7 months, it appeared that both the height of the absolute calcium score and the calcium score divided into quartiles were closely related to the annualized event rate (table 2).⁸ Thus, although the data are conflicting about the precise predictive value of coronary calcium scoring, it may be concluded that overall the presence of calcium is associated with a higher risk of adverse coronary events (table 3).

Coronary calcium to predict coronary death and non-fatal MI in symptomatic patients after coronary angiography

Coronary lumen stenosis and coronary calcium are different manifestations of coronary atherosclerosis. Both coronary angiography and coronary calcium assessment provide an estimate of the total coronary plaque burden, but both techniques underestimate the extent and severity of the total plaque burden when compared to histology.⁴

Extent and severity of coronary artery disease as assessed by coronary angiography has been shown to provide predictive value for coronary death and non fatal myocardial infarction. Coronary calcium may have additional predictive value in patients who underwent coronary angiography. Two studies have addressed this issue (table 4).^{10,11} Detrano et al demonstrated that the risk of coronary death or non fatal myocardial significantly increased with the calcium load.¹⁰ Patients with a calcium score above median (is >75 HU) had a six times higher event rate than those with lower scores. If patients were divided into quartiles according to ascending order of calcium amount it was shown that an event occurred in 1 patient in the first quartile, 2 events in the second quartile, 8 in the third quartile and 10 events in the fourth quartile. The calcium score predicted hard events just as well as the number of angiographically diseased coronary arteries; however logistic regression showed that calcium amount independently contributed toward the probability of subsequent coronary events.

Table 1. Risk stratification in a symptomatic individuals

Author	Nr. of patients	Risk	Follow up (months)	Mean age	% male	Endpoints		Agatson score*
						death	non fatal MI	
Detrano [5]	1196	High	41 ±5	66 ±8	89	17	29	> 0 HU
Arad [7]	1172	High ¹	43 (38-47)	53 ±11	71	3	15	> 160 HU
Raggi [9]	676	High ²	32 ±7	52 ±12	51	9	21	> 0 HU

* score according to Agatson

¹ self referred

² referred by primary care physician

Table 2. Calcium score and annualized event rate

Absolute Ca score (NP)	Annualized event rate %	Quartile CS %	Annualized event rate %	Odds ratio
0 (292)	11	1	2	10
1-99 (219)	21	2	2	1.0 (0.1, 16.1)
100-400 (74)	41	3	14	6.2 (0.7, 52.1)
> 400 (28)	48	4	45	21.5 (2.8, 162.4)

(from Raggi, Circulation 2000; 101: 850)

Table 3. Predictive value of calcium score

Relative risk of	Detrano	Arad	Raggi	
Death, non fatal MI, compared to lower Ca scores	>44 HU 2.3	>160 HU 22.2	0 HU 0.12 %*	>0 HU 3.0 %*

* risk per year

Keelan et al showed that patients with a calcium score ≥ 100 HU had a relative risk of 3.2 (95 % CI : 1.17 – 8.71) of death or non fatal myocardial infarction than those with a lower score.¹¹

Multivariate analysis including traditional risk factors, previous coronary event history, angiographic findings and calcium score showed that only age and coronary artery calcification extent were independent predictors of hard events with a relative risk ratio of 1.72 (95 % CI 1.02, 2.91) and 1.88 (95 % CI 1.02, 3.48) respectively suggesting that calcium extent adds significant prognostic information.

Coronary calcification in acute coronary syndromes

Histopathologic and intra coronary ultrasound studies have shown that early, non obstructive atherosclerotic lesions which contain a large lipid pool and carry a high risk of rupturing, are not calcified and may not be detected by EBCT.¹ Although calcific lesions are thought to be stable they are an estimate of the total atherosclerotic plaque burden and thus associated with a higher likelihood of vulnerable plaques. Thus a positive or negative calcium scan does not exclude the presence or absence of a vulnerable plaque and calcium is neither a marker for stable or unstable plaque.

Schmermund et al reported on the value of EBCT detected coronary calcium in acute coronary syndromes.¹² One hundred eighteen patients, 57 ± 11 years of age with previous myocardial infarction (n = 101) or unstable angina (n = 17) were investigated. One hundred five (95 %) of 110 patients with significant obstructive disease and one of the 8 patients (13 %) without significant obstructive disease had a positive calcium scan. A negative calcium scan was present in 5 patients (5 %) with and 7 (87 %) patients without significant obstructive disease. These patients were younger and were active smokers. Raggi et al⁸ confirmed these findings in 172 patients with an acute myocardial infarction. Ninety six percent of these patients showed coronary calcium, and the extent of calcium was higher than expected with regard to age and sex. These studies confirm the notion that the vast majority of patients with an acute coronary syndrome have a positive calcium scan and that absence of coronary calcium does not exclude the presence of a vulnerable plaque, however the likelihood of the presence of a vulnerable plaque is low.

CT-scanner used in Emergency Department

Three studies have evaluated the merits of CT scanning in screening patients admitted to an emergency department who have new recent onset chest pain, with non specific ECG findings and no enzyme rise and no history of coronary artery disease.^{13 15}

Laudon et al compared EBCT scan findings with cardiac evaluation findings including treadmill stress testing, radio nuclide testing, dobutamine echo stress testing and coronary angiography in 100 patients presenting at the emergency department.¹³

Table 4. Coronary calcification to predict coronary death or non fatal myocardial infarction in patients after coronary angiography

Author	Nr. of patients	Age yrs	Males %	Follow up period	Death/non fatal MI
Detrano (1996)	422	55 ±12	57	30 ±13 months	13/8
Keelan (2001)	288	56 ±11	77	Mean 6.9 yrs	22

Table 5. Predictive value calcium scan of cardiac death and non fatal MI for patients presenting at emergency department

Calcium scan	event rate* 30 days (P)	event rate** 50 ±10 months (P)
Negative	0 % (48)	0 % (76)
Positive	4.4 % (86)	15.6 % (116)

* McLaughlin, Am J Cardiol 1999; 84: 327

** Georgiou, JACC 2001; 38: 105

Because the prevalence of coronary calcium greatly increases with age they studied men (54 %) between 30 and 55 years of age and women (46 %) between 40 and 65 years. The scan was positive if there was a Calcium score of >0. The sensitivity of the positive calcium scan was 100 % (95 % CI : 77 % to 100 %) and the specificity was 63 % (95 % CI : 54 % to 75 %). Resulting in a negative predictive value of 100 % (95 % CI to 100 %).

McLaughlin et al studied 134 patients, 53 patients, 53 ±2 years of age, 63 % women, who presented with chest pain at the emergency room.¹⁴ A calcium score of > 1 was considered a positive test. The patients were followed for 30 days and the occurrence of sudden death, non fatal myocardial infarction percutaneous coronary angioplasty of bypass surgery was recorded. A positive scan was found in 86 patients and in this group 7 coronary events (8 %) including 4 non fatal MIs, 2 bypass surgery and 1 angioplasty, occurred.

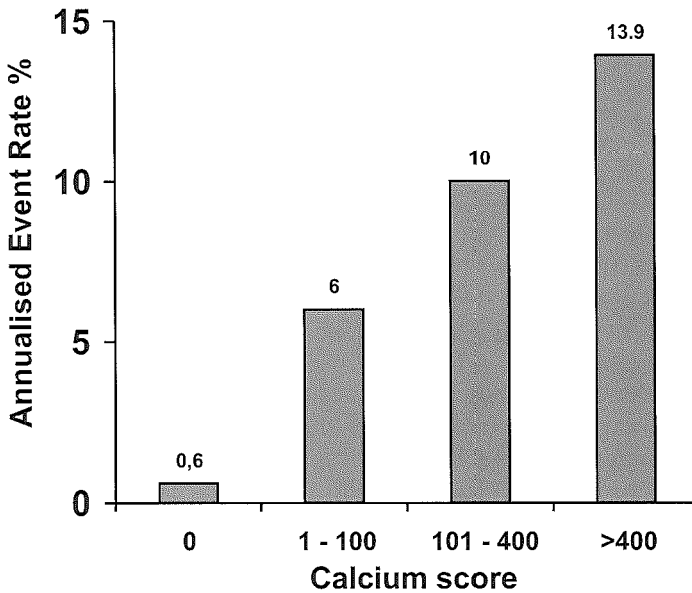


Figure 5. Annualized rates of cardio vascular events: death, MI, CAGB, PTCA, hospitalization for angina and ischemic stroke (from Georgiou et al, J Am Coll Cardiol 2001; 38 : 105)

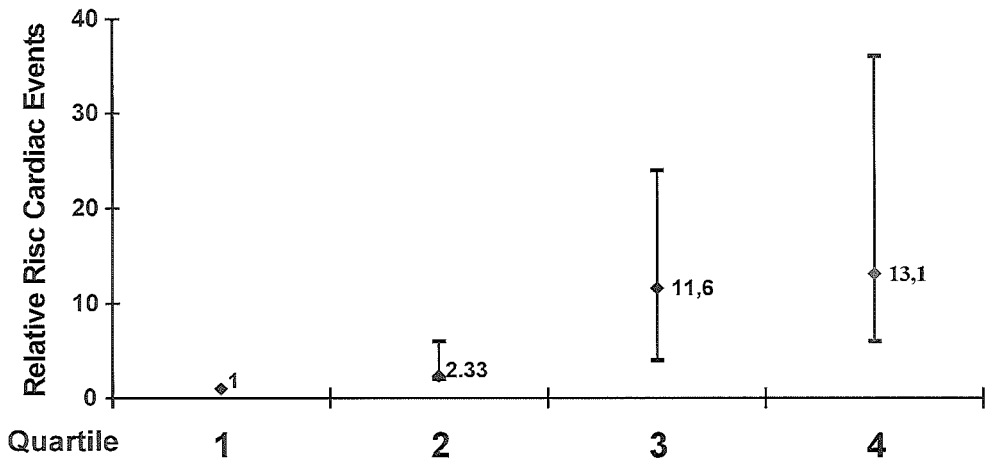


Figure 6. Relative risk for cardiac vascular events using age en gender – adjusted quartiles. Confidence intervals (95 %) are presented for each quartile (from Georgiou et al, J Am Coll Cardiol 2001; 38 : 105)

A negative scan was seen in 46 patients (36 %) and no events occurred in this group (table 5). Thus the negative predictive value of 100 % suggested that patients with a negative calcium scan can be safely discharged.

Georgiou et al conducted a prospective observational study of 192 patients admitted to the emergency department for chest pain syndromes.¹⁵ The mean age was 53 ± 9 years, 46 % were women. They followed these patients for a mean of 50 ± 10 months. Hard events occurred in 30 patients: cardiac death (11) and non fatal MI (19) and an additional soft events occurred in another 28 patients: CAGB 9, PTCA 4, hospitalization for angina 11 and ischemic stroke 4.

Patients with a negative test were event free and in those with a positive test the hard adverse event rate was 15.6 % (table 5). It appeared that higher calcium scores were associated with a higher annualized event rate (fig. 5). Adjustment for age and gender further risk stratified patients showing that relative risk's for total cardiovascular events increased in the third and fourth quartiles (fig. 6). Multivariate analyses showed that calcium score and age and gender adjusted risk profiles were stronger independent predictors than the traditional risk factors and age.

It should be mentioned that all 3 studies investigated relatively small number of patients and that they studied relatively young patients because the higher prevalence of calcium in elderly patients would lead to a low specificity of the calcium scan test, making it less clinically useful.

It may be concluded that in middle aged patients admitted with chest pain to an emergency department who have a negative calcium scan can be safely discharged obviating the need for further provocative testing. However, a positive calcium scan test is essentially useless and further testing is required in these patients.

CT CORONARY ANGIOGRAPHY

EBCT and MS CT have emerged as two non invasive diagnostic tools which are able to visualize the proximal and mid segments of the coronary tree and which may detect significant obstructive coronary artery disease (fig. 3). The diagnostic value of both techniques is presented in table 6 and 7.^{16 24} It should be noted that the diagnostic power of these techniques has been evaluated in elective symptomatic patients, but has not specifically been evaluated in patients with acute coronary syndromes, but there is no reason to believe that this would be different in patients with acute coronary syndromes. Obviously the above preliminary results are, in this stage of technical development, not sufficient to replace conventional diagnostic angiography. Significant hurdles to be taken are current limitations in spatial and temporal resolution, whereas calcification of the coronary wall seriously may hinder assessment of the coronary lumen so that underlying obstructive disease will be unnoticed.

Table 6. EBCT coronary angiography: accuracy to detect >50% stenoses

Authors	Patients (n)	Assessable (%)	Sensitivity (%)	Specificity (%)
Nakanishi et al	37	NR	74	91
Reddy et al	23	90	88	79
Schermund et al	28	88	83	91
Rensing et al	37	81	77	94
Achenbach et al	125	75	92	94
Budoff et al	52	90	78	91
Overall ^a	302	81	84	92

NR: not reported

Assessable: image quality adequate for classification

^a Corrected for patient numbers

Table 7. MSCT coronary angiography: accuracy to detect significant 50% stenoses

Authors	Patients (n)	Assessable (%)	Sensitivity (%)	Specificity (%)
Knez et al	49	86	90	NR
Kopp et al	102	NR	91	87
Sakuma et al	12	NR	74 ^a	96 ^a
Hong et al	25	NR	95	80
Nieman et al	31	73	81	97
Achenbach et al	64	68	91 ^a	84 ^a
Overall ^b	283		89	87

NR: not reported

Assessable: image quality adequate for classification

^a High grade (>75% diameter reduction) stenoses

^b Corrected for patient numbers

CT PLAQUE IMAGING

Rupture of a vulnerable plaque with superimposed coronary thrombosis is the most frequently occurring pathological event that causes an acute coronary event. The risk of plaque disruption depends on plaque composition and plaque containing a large lipid pool are more prone to disruption than fibrous or calcific plaques.

Non invasive assessment of plaque components would be a desirable step forward in the risk stratification of patients with known or suspected coronary artery disease. MS CT does allow identification of plaque components into soft, intermediate and calcific based on the differences of tissue in attenuation of the X ray resulting in differences in density expressed in Hounsfield Units. This method is much alike the coronary ultra sound identification of plaques into soft, fibrous and calcific based on the echogenicity of the plaque. Schroeder et al investigated 34 plaques in 15 patients.²³ Intra coronary Ultrasound classified these plaques into soft, intermediate and calcific. Using MS CT, soft plaques had a density of 14 ± 26 HU, intermediate plaques 91 ± 21 HU and calcific plaques 419 ± 194 HU. It is of note that the identification of plaque components is rather crude and should require confirmation with histological studies. However, these first results demonstrated that MS CT was able to identify soft rupture prone lesions and this technique may be used in the future as an risk stratification tool.

References

1. Rumberger, J.A., et al., Coronary artery calcium area by electron beam computed tomography and coronary atherosclerotic plaque area. A histopathologic correlative study. *Circulation*, 1995. 92(8): p. 2157-62.
2. Agatston, A.S., et al., Quantification of coronary artery calcium using ultrafast computed tomography. *J Am Coll Cardiol*, 1990. 15(4): p. 827-32.
3. O'Rourke, R.A., et al., American College of Cardiology/American Heart Association Expert Consensus Document on electron beam computed tomography for the diagnosis and prognosis of coronary artery disease. *J Am Coll Cardiol*, 2000. 36(1): p. 326-40.
4. Wexler, L., et al., Coronary artery calcification: pathophysiology, epidemiology, imaging methods, and clinical implications. A statement for health professionals from the American Heart Association. Writing Group. *Circulation*, 1996. 94(5): p. 1175-92.
5. Detrano, R.C., et al., Coronary calcium does not accurately predict near term future coronary events in high risk adults. *Circulation*, 1999. 99(20): p. 2633-8.
6. Arad, Y., et al., Predictive value of electron beam computed tomography of the coronary arteries. 19 month follow up of 1173 asymptomatic subjects. *Circulation*, 1996. 93(11): p. 1951-3.
7. Arad, Y., et al., Prediction of coronary events with electron beam computed tomography. *J Am Coll Cardiol*, 2000. 36(4): p. 1253-60.
8. Raggi, P., et al., Identification of patients at increased risk of first unheralded acute myocardial infarction by electron beam computed tomography. *Circulation*, 2000. 101(8): p. 850-5.

9. Raggi, P., B. Cooil, and T.Q. Callister, Use of electron beam tomography data to develop models for prediction of hard coronary events. *Am Heart J*, 2001. 141(3): p. 375 82.
10. Detrano, R., et al., Prognostic value of coronary calcification and angiographic stenose in patients undergoing coronary angiography. *J Am Coll Cardiol*, 1996. 27(2): p. 285 90.
11. Keelan, P.C., et al., Long term prognostic value of coronary calcification detected by electron beam computed tomography in patients undergoing coronary angiography. *Circulation*, 2001. 104(4): p. 412 7.
12. Schmermund, A., et al., Coronary artery calcium in acute coronary syndromes: a comparative study of electron beam computed tomography, coronary angiography, and intracoronary ultrasound in survivors of acute myocardial infarction and unstable angina. *Circulation*, 1997. 96(5): p. 1461 9.
13. Laudon, D.A., et al., Use of electron beam computed tomography in the evaluation of chest pain patients in the emergency department. *Ann Emerg Med*, 1999. 33(1): p. 15 21.
14. McLaughlin, V.V., T. Balogh, and S. Rich, Utility of electron beam computed tomography to stratify patients presenting to the emergency room with chest pain. *Am J Cardiol*, 1999. 84(3): p. 327 8, A8.
15. Georgiou, D., et al., Screening patients with chest pain in the emergency department using electron beam tomography: a follow up study. *J Am Coll Cardiol*, 2001. 38(1): p. 105 10.
16. Reddy, G.P., et al., Coronary artery stenoses: assessment with contrast enhanced electron beam CT and axial reconstructions. *Radiology*, 1998. 208(1): p. 167 72.
17. Schmermund, A., et al., Intravenous electron beam computed tomographic coronary angiography for segmental analysis of coronary artery stenoses. *J Am Coll Cardiol*, 1998. 31(7): p. 1547 54.
18. Rensing, B.J., et al., Intravenous coronary angiography by electron beam computed tomography: a clinical evaluation. *Circulation*, 1998. 98(23): p. 2509 12.
19. Achenbach, S., et al., Value of electron beam computed tomography for the noninvasive detection of high grade coronary artery stenoses and occlusions. *N Engl J Med*, 1998. 339(27): p. 1964 71.
20. Budoff, M.J., et al., Intravenous three dimensional coronary angiography using contrast enhanced electron beam computed tomography. *Am J Cardiol*, 1999. 83(6): p. 840 5.
21. Nieman, K., et al., Coronary angiography with multi slice computed tomography. *Lancet*, 2001. 357: p. 599 603.
22. Achenbach, S., et al., Detection of coronary artery stenoses by contrast enhanced, retrospectively electrocardiographically gated, multislice spiral computed tomography. *Circulation*, 2001. 103(21): p. 2535 8.
23. Schroeder, S., et al., Noninvasive detection and evaluation of atherosclerotic coronary plaques with multislice computed tomography. *J Am Coll Cardiol*, 2001. 37(5): p. 1430 5.

5.1

CT Angiographic Evaluation of Post-CABG Patients: Assessment of Grafts and Coronary Arteries

Koen Nieman
Peter MT Pattynama
Benno J Rensing
Robert-Jan M van Geuns
Pim J de Feyter

ABSTRACT

Purpose:

To evaluate the accuracy of ECG gated multidetector row CT (MDCT) in the detection of obstruction of both bypass grafts and coronary arteries in symptomatic post CABG patients.

Material and methods:

ECG gated, contrast enhanced MDCT angiography was performed in 24 post bypass surgery patients. All graft and coronary segments (≥ 2 mm diameter) were evaluated by two independent and blinded observers for the presence of occlusion and stenosis (50 99% lumen reduction). Conventional angiography was regarded as the standard of reference. Descriptive parameters were calculated and the results for arterial grafts, venous grafts and coronary arteries, and for high and low heart rates were compared using a two sided Fisher's exact test.

Results:

Observer 1 and 2 found all (60/60) and 95.0% (57/60) of the venous graft segments assessable, with an overall detection of all 17 occlusions and 3 (50.0%) and 5 (83.3%) out of 6 stenoses, respectively. Of the 26 arterial graft segments, observer 1 and 2 found 73.1% (19) and 57.7% (15) assessable. In the assessable segments, 4/4 and 2/3 stenoses and occlusions were detected, while 1 and 2 obstructions were located in non assessable segments, respectively. Of the 211 ≥ 2.0 mm coronary segments, 69.2% (146) and 66.4% (140) were assessable, in which detection of 50 100% obstruction yielded a sensitivity of 89.9% (71/79) and 79.4% (54/68) and specificity of 74.6% (50/67) and 72.2% (52/72), for each observer. Contrary to the assessment of the venous and arterial grafts, diagnostic performance of MSCT with respect to the coronary arteries was significantly better in patients with low heart rates ($P < 0.01$).

Conclusion:

MDCT allows non invasive angiographic evaluation of both coronary arteries and bypass grafts in post CABG patients. In venous grafts MDCT is more effective compared to arterial grafts and diffusely diseased coronary arteries.

INTRODUCTION

In the United States an estimated 571,000 coronary bypass operations were performed in 1999. In 24% of these patients angina recurs within a year, and in more than 40% within 6 years.¹ A total of 25% of grafts are found to be occluded within 5 years after surgery.² Symptoms recur because of progression of disease in the coronary arteries and de novo disease in the venous bypass grafts, whereas arterial grafts generally remain free of disease. Earlier studies have demonstrated that non invasive techniques such as magnetic resonance imaging (MRI) and computed tomography (CT) can evaluate the patency of grafts. However, a clinically useful imaging technique should not only be able to detect graft disease, but also progression of disease in the coronary arteries. Thus, the purpose of our study was to evaluate the accuracy of ECG gated multidetector row CT (MDCT) in the detection of obstruction of both bypass grafts and coronary arteries in symptomatic post CABG patients.

MATERIALS AND METHODS

Population

Twenty four patients, who were referred to our center for conventional angiographic evaluation because of recurrent symptoms after coronary artery bypass grafting (CABG), were included. 7 patients had only venous grafts, 4 only arterial grafts, and 13 both venous and arterial grafts. Of the 23 venous grafts, 17 had 2 or more sequential anastomoses. Of the 17 patients with an arterial graft, 4 had more sequential anastomoses. One patient had a right left internal mammary arteries (IMA) T graft with 5 distal anastomosis. Further patient characteristics are summarized in table 1. Patients with irregular heart rates, allergy to iodine containing contrast media, renal failure (serum creatinine $>100 \text{ mmol.l}^{-1}$), significant respiratory or cardiac failure were excluded. The time interval between the MDCT scan and the surgical procedure was 9.6 ± 5.2 years. Two patients underwent redo CABG. The median time interval between the respective angiographic procedures was 11 days. The study was approved by the institutional ethical committee and informed consent was obtained from all patients.

MSCT data acquisition and image reconstruction

The patients were examined with a multidetector row computed tomography scanner that acquires four channels of data at an X ray tube rotation time of 500 ms (Somatom Plus 4 VolumeZoom, Siemens AG, Forchheim, Germany).³ After attachment of the leads for electrocardiogram (ECG) recording, patients were examined in a supine position while breath holding. To facilitate the relatively long breath hold (35-45 s), a short session of instructed hyperventilation was performed prior to the scan. First a fast localization scan was performed to determine the scan range, and identify the metal indicators at the site of the proximal venous graft anastomosis.

Table 1. Patient Characteristics

General characteristics	N=24
Age (range)	63.7±10.2 (36 80)
Gender (male/female)	20 / 4
MSCT CABG interval (years)	9.6±5.2
Average heart rate (min 1)	64.2±13.0 (48 88)
Bypass graft status	
Only venous grafts	7 patients
Only arterial grafts	4 patients
Venous and arterial grafts	13 patients
Venous grafts	23, 60 segments
Arterial grafts	18, 26 segments
Venous graft occlusion (100%)	17 segments
Venous graft stenosis (50 99%)	6 segments
Arterial graft occlusion (100%)	5 segments
Arterial graft stenosis (50 99%)	1 segments
Coronary obstruction (50 100%)	102 segments

Table 2. Scan Parameters

Parameter	
Collimation (number x diameter (mm) of detectors)	4 x 1
Table feed per gantry rotation (pitch)	1.5*
Tube output: voltage (kV), mAs	120, 300
Scan time (s)	35 45
Contrast agent: iomeprol (350 mg iodine per ml)	150 ml at 4 ml.s ⁻¹
ECG synchronization	Retrospective gating
Effective slice thickness (mm)	1.25
Reconstruction increment (mm)	0.5
Field of View (mm)	130 180
Matrix	512 x 512
In plane resolution (line pairs.cm ⁻¹)	8
Through plane resolution (line pairs.cm ⁻¹)	6

* For HR>80 pitch = 2.0

The scan range included the entire course of the venous graft, but not the most proximal part of the internal mammary artery (IMA) grafts, to maintain a manageable breath hold period. A fixed delay of 20 s was applied between intra venous injection of contrast medium (Iomeprol 350 mgI/ml, Bracco Byk Gulden, Konstanz, Germany) and onset of the data acquisition. The radiation exposure depends on the individual scan parameters and varies between 5 and 10 mSv. The average heart rate was $63.7 \pm 10.2 \text{ min}^{-1}$, and no additional beta receptor blocking medication was administered prior to the examination. Further scan parameters are summarized in table 2.

The details of ECG gated image reconstruction have been described previously.⁴ In summary, isocardiophasic axial slices are reconstructed from MDCT data that is acquired during a 180° X ray tube rotation, using a partial scan reconstruction algorithm. At a rotation time of 500 ms the length of the image reconstruction window (IRW) is therefore 250 ms. At heart rates beyond 65/min a potential reduction of the effective IRW down to 125 ms is achieved by combining data from consecutive RR intervals, provided that the table speed is sufficiently low in order to sample each position on the longitudinal axis at least twice.⁴ Because data are acquired continuously, images can be reconstructed at any time point within the cardiac cycle. To obtain nearly motion free results the IRW is positioned within the mid to late diastolic phase. Initially, three data sets, with an IRW starting at 300 ms, 400 ms and 500 ms before the following R wave, were compared. If none of these showed adequate image quality, alternative IRW positions were explored. For low heart rates, the most optimal IRW position was 400 ms, at higher heart rates 350 ms or 300 ms before the next R wave yielded the best results. The axial slices with an effective slice thickness of 1.25 mm were reconstructed at an overlapping interval of 0.5 mm, by which the inter slice correlation is improved. From the recorded ECG trace the average heart rate during the scan was calculated. All scans were performed without complications. Generally the examination, including patient preparation and image reconstruction, required between 10 and 30 minutes.

Image processing and data analysis

A stack of approximately 250 overlapping transverse slices were further processed and analyzed on a separate workstations (O2 & Indigo 2, SGI, Mountain View, CA, USA), with case dependent application of post processing techniques (Vitrea & VoxelView, Vital images Inc., Plymouth, MN, USA). Thin slab maximum intensity projections (MIP) allow assessment of extended lengths of the vessels at once. In the presence of calcium or metal, MIP results in assessment limiting overprojection, and double oblique multi planar reconstructions are then more suitable. Volume rendered reconstructions were used for three dimensional orientation and global presentation of results. Finally, findings were confirmed on the axial source images.

All coronary artery segments (according to AHA/ACC Guidelines) and bypass graft segments, regarding consecutive graft anastomosis as separate segments,

were independently evaluated by two investigators, who were aware of the initial CABG procedure, but blinded towards the current angiographic results.⁵ According to the image quality, each coronary or graft segment was classified as either interpretable, or not. The venous graft segments were first screened for the presence of totally occluded segments. In the remaining segments, those that were considered patent by each observer, the image quality was then re evaluated and interpretable segments were screened for the presence of stenotic lesions: luminal narrowing of 50-99% of the lumen diameter. The arterial grafts were assessed similarly, but because of their relatively small diameter size, no distinction between total occlusion or significant narrowing was made.

Based on conventional quantitative coronary angiography, only coronary segments with a minimal reference diameter of 2.0 mm were included for analysis. The presence or absence of calcium was noted for each coronary segment. After evaluation of the interpretability of the MDCT data, all assessable segments were screened for the presence of significant stenosis, including total occlusion.

Conventional coronary angiography

Arterial catheterization and selective X ray angiography of the coronary arteries and bypass grafts were performed according to standard techniques. Using CAAS software (Pie Medical, Maastricht, The Netherlands), quantitative coronary angiography (QCA), which involves catheter derived image calibration and automated vessel contour detection, of two orthogonal projections of the coronary arteries was performed to identify segments with a ≥ 2.0 mm diameter. The angiographic films were screened by an experienced intervention cardiologist for stenotic lesions (50-99% diameter reduction) or occlusions in the bypass grafts and coronary arteries. The diameter stenosis was determined by the averaged luminal narrowing from two orthogonal projections.

Statistical analysis

The descriptive statistics were stratified for coronary artery segments, venous bypass graft segments and arterial graft segments. Each graft, and each consecutive anastomosis in case of sequential grafts, was regarded as a separate graft segment. Conventional QCA was regarded as the standard of reference. The diagnostic parameters in patients with a low (≥ 65 min⁻¹) or faster average heart rate (< 65 min⁻¹) during the data acquisition, were compared, based on the results of observer 1. Continuous variables were expressed as means and standard deviations. The diagnostic results by each of two observers to detect lesions in the assessable segments were expressed as sensitivity, specificity, negative predictive value (PV) and positive PV. The overall sensitivity, which regards lesions in non interpretable segments as false negatives assessments, was calculated in addition. Concordance between observers for the detection of obstructive lesions were calculated and expressed by the κ value.

Precision of the diagnostic parameters and inter observer variability were expressed using a 95% confidence interval. Results between arterial grafts, venous grafts and coronary arteries, and low and high heart rate patients, were compared using a two sided Fisher's exact test.

RESULTS

Venous bypass grafts

Of the 60 venous segments, patency could be assessed in 100.0% (60) and 95.0% (57) by observer 1 and 2 and both detected all 17 occlusions (100.0%). Specificity 97.7% (42/43) and 97.5% (39/40), positive predictive value (PPV) 94.4% (17/18), negative predictive value (NPV) 100.0% (42/42 and 39/39) for observers 1 and 2 respectively (table 3, figures 1-4). Of the segments that were considered patent, observer 1 could assess 90.5% (38/42) for the presence of non complete stenoses, and correctly detected 3 out of 5 stenoses (60.0%), while another one was situated in a non assessable segment. The specificity, PPV and NPV were 87.9% (29/33), 42.9% (3/7) and 93.5% (29/31), respectively.

Observer 2 could assess 94.9% (37/39) of the apparently patent segments and detected 5 out of 6 stenoses (83.3%). The specificity, PPV and NPV were 90.3% (28/31) and 62.5% (5/8), 96.6% (28/29).

Inter observer variability with respect to the detection of venous graft disease was good: $\kappa = 0.74$ (95% CI: 0.52–0.96), particularly for occlusions: $\kappa = 0.91$ (95% CI: 0.63–1.00).

Arterial bypass grafts

Observer 1 could assess 73.1% (19/26) of the arterial graft segments, detected all 4 occlusions (100.0%) in the assessable segments, One non complete stenosis in a non assessable segment was missed. Specificity, PPV and NPV were 93.3% (14/15), 80.0% (4/5) and 100.0% (14/14), respectively (table 4).

Observer 2 found 57.7% (15/26) of the arterial segments assessable, correctly detected one occlusion and the only stenosis (66.7%), but missed 3 occlusions, of which 2 were in non assessable segments. Specificity, PPV and NPV were 83.3% (10/12), 50.0% (2/2) and 90.9% (10/11).

Coronary arteries

Based on the conventional angiogram an average of 8.8 ± 1.7 coronary segments with a minimal diameter of 2.0 mm were available per patient. Observer 1 and 2 found 69.2% (146/211) and 66.4% (140/211) of these segments interpretable. In the assessable segments significant obstruction, including complete occlusions, was detected with a sensitivity of 89.9% (71/79) and 79.4% (54/68), specificity of 74.6% (50/67) and 72.2% (52/72), PPV of 80.7% (71/88) and 73.0% (54/74), and NPV of 86.2% (50/58) and 78.8% (52/66), respectively (table 5, figure 3). The inter observer variability was reasonably good: $\kappa = 0.68$ (95% CI: 0.50–0.86).

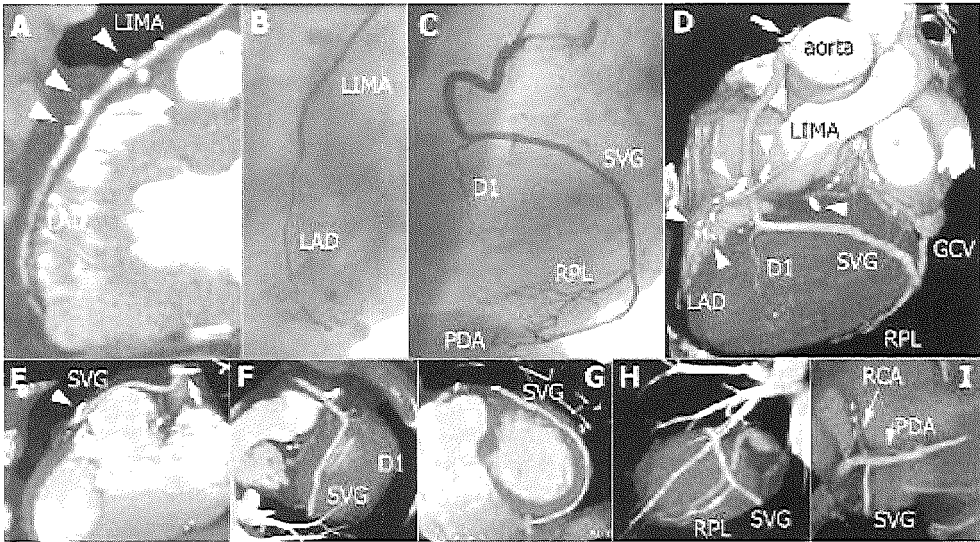


Figure 1. Arterial and venous bypass grafts. Contrast enhanced MDCT angiography: maximum intensity projections (A,E I) and 3D volume rendering (D), and corresponding conventional angiography (B,C) in a patient with a left internal mammary artery graft (LIMA) connected to the left anterior descending coronary artery (LAD) (A,B). Additionally, a venous graft (SVG) runs from the aorta (C,D,E) to the diagonal branch (D1) (C,D,F), with consecutive jumps to the posterolateral branch (RPL) (C,D,H) and posterior descending coronary artery (PDA) (C,I). Surgical clips (arrowheads) and a bypass indicator (arrow) appear as bright structures (A,D,E). Great cardiac vein (GCV).
(A full color version of this illustration can be found in the color section)

Unfortunately, 22.5% (23/102) and 33.3% (34/102) of the significantly obstructed segments were missed due to degraded image quality. Calcifications, which were the cause of many non interpretable segments, were present in 69.5% of the ≥ 2.0 mm coronary segments.

A significantly larger percentage of the venous grafts could be evaluated compared to the arterial grafts and coronary arteries ($P < 0.001$) for both observers. The overall sensitivity to detect $\geq 50\%$ lesions showed a similar trend, but only reached significance for observer 2 ($P < 0.01$), and not observer 1 ($P = 0.26$).

Influence of the heart rate

Motion artefacts, caused by residual cardiac motion, were a major contributor to the non interpretability of the MDCT images. In the patient group with a heart rate below 65 beats per minute, the coronary arteries were better interpretable ($P < 0.001$), and showed a higher sensitivity ($P < 0.01$) compared to the group with a higher heart rate. For the arterial grafts there was a trend towards better interpretability in the lower heart rate group ($P = 0.06$). The venous grafts were well assessable regardless of the heart rate (table 6).

Table 3. Diagnostic Accuracy of MDCT Angiography to Detect Venous Graft Disease in the Assessable Segments

Graft Occlusion (100%)	Observer 1	Observer 2
Assessable (%)	60/60 (100.0)	57/60 (95.0)
Sensitivity (%, CI)	17/17 (100.0, 83.4 100.0)	17/17 (100.0, 83.4 100.0)
Specificity (%, CI)	42/43 (97.7, 91.1 100.0)	39/40 (97.5, 90.5 100.0)
Positive PV (%, CI)	17/18 (94.4, 78.8 100.0)	17/18 (94.4, 78.8 100.0)
Negative PV (%, CI)	42/42 (100.0, 93.3 100.0)	39/39 (100.0, 92.8 100.0)
Lesions in non assessable segments	0	0
Overall Sensitivity* (%, CI)	17/17 (100.0, 83.4 100)	17/17 (100.0, 83.4 100)
Graft Stenosis (50 99%)	Observer 1	Observer 2
Assessable (%)	38/42 (90.5)	37/39 (94.9)
Sensitivity (%, CI)	3/5 (60.0, 18.4 92.0)	5/6 (83.3, 40.8 99.1)
Specificity (%, CI)	29/33 (87.9, 81.6 92.7)	28/31 (90.3, 82.1 93.4)
Positive PV (%, CI)	3/7 (42.9, 13.1 65.7)	5/8 (62.5, 30.6 74.3)
Negative PV (%, CI)	29/31 (93.5, 86.8 98.7)	28/29 (96.6, 87.7 100.0)
Lesions in non assessable segments (%)	1 (16.7%)	0
Overall Sensitivity* (%, CI)	3/6 (50.0, 15.0 83.2)	5/6 (83.3, 40.8 99.1)

* Sensitivity, regarding lesions in segments non assessable by MDCT as false negative.
Predictive value (PV); 95% Confidence interval (CI)

Table 4. Diagnostic Accuracy of MDCT Angiography to Detect Arterial Graft Disease in the Assessable Segments

Obstructions (50 100%)	Observer 1	Observer 2
Assessable (%)	19/26 (73.1)	15/26 (57.7)
Sensitivity (%, CI)	4/4 (100.0, 46.2 100.0)	2/3 (66.7, 13.6 98.2)
Specificity (%, CI)	14/15 (93.3, 79.0 100.0)	10/12 (83.3, 70.1 91.2)
Positive PV (%, CI)	4/5 (80.0, 37.0 100.0)	2/2 (50.0, 10.2 73.6)
Negative PV (%, CI)	14/14 (100.0, 84.6 100.0)	10/11 (90.9, 76.4 100.0)
Lesions in non assessable segments (%)	1 (20.0)	2 (40.0)
Overall Sensitivity* (%, CI)	4/5 (80.0, 35.2 98.2)	2/5 (40.0, 7.9 71.3)

* Sensitivity, regarding lesions in segments non assessable by MDCT as false negative. Predictive value (PV); 95% Confidence interval (CI)

Table 5. Diagnostic Accuracy of MDCT Angiography to Detect Coronary Artery Disease in the Assessable Segments

Obstructions (50 100%)	Observer 1	Observer 2
Assessable (%)	146/211 (69.2)	140/211 (66.4)
Sensitivity (%, CI)	71/79 (89.9, 83.0 94.7)	54/68 (79.4, 70.7 86.5)
Specificity (%, CI)	50/67 (74.6, 66.5 80.3)	52/72 (72.2, 64.0 78.9)
Positive PV (%, CI)	71/88 (80.7, 74.5 85.0)	54/74 (73.0, 65.0 79.4)
Negative PV (%, CI)	50/58 (86.2, 76.8 92.8)	52/66 (78.8, 69.8 86.0)
Lesions in non assessable segments (%)	23 (22.5)	34 (33.3)
Overall Sensitivity* (%, CI)	71/102 (69.6, 63.3 75.0)	54/102 (52.9, 46.3 58.8)

* Sensitivity, regarding lesions in segments non assessable by MDCT as false negative. Predictive value (PV); 95% Confidence interval (CI)

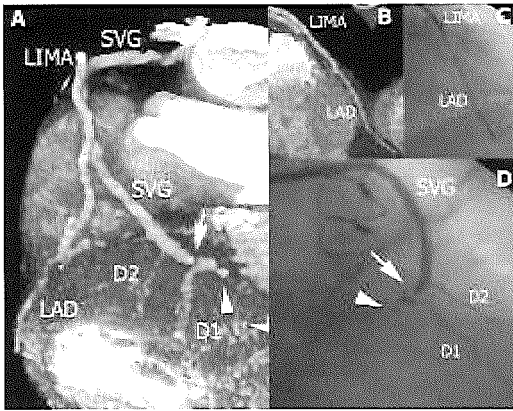


Figure 2. Venous graft disease. Contrast enhanced MDCT angiography: 3D volume rendering (A) and curved multiplanar reconstruction (B), and corresponding conventional angiography (C,D) with an arterial and venous bypass graft. The non diseased left internal mammary artery graft (LIMA) is anastomosed to the left anterior descending coronary artery (LAD) (A,B,C). A venous graft (SVG) originates from the aorta and is anastomosed to the second diagonal branch (D2). The following graft segment between the second and first diagonal branch (D1) shows a significant stenosis (arrow). Distal to the first diagonal branch the venous graft is completely occluded (arrow head) (A), which could be confirmed on the conventional angiogram (D: 20° left anterior oblique, 30° caudal angulation).

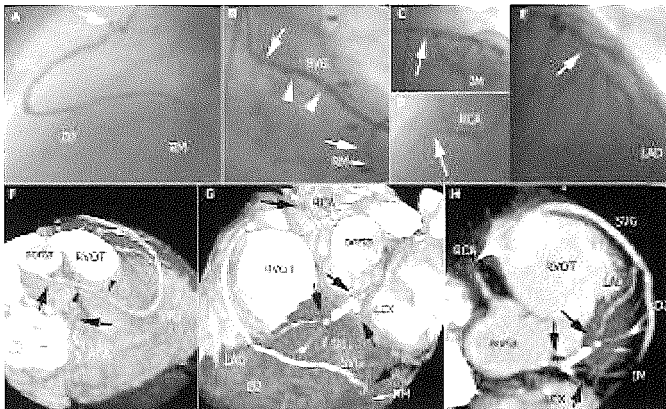


Figure 3. Venous graft and native coronary artery disease. Contrast enhanced MSCT angiography: 3D volume rendering (F,G) and maximum intensity projection (H), and conventional angiography in a patient after bypass surgery. At the proximal anastomosis of the venous graft (SVG) near the aorta a significant lesion was detected (arrow), as well as two low grade lesions (arrowheads) further down the first segment (A (90° LAO, B: 30° RAO),F). After a non stenosed second segment, between the second diagonal branch (D2) and the marginal branch (RM) (A,G), the final segment between the marginal branch and the posterior lateral branch was found to be occluded (A,B,G). Assessment of the native coronary system revealed that both the proximal right (RCA) and the left circumflex coronary artery (LCX) were occluded (C (right anterior oblique projection) D,G,H). The left main is borderline significantly stenosed (arrow), and an additional lesion was found in the distal left anterior descending coronary artery (LAD) (arrow) (C,E (0° LAO, 30° cranial angulation),G). The mid segment of the left anterior descending coronary artery (LAD) was regarded non assessable due to extensive calcium deposits (G,H). Right ventricular outflow tract (RVOT).

(A full color version of this illustration can be found in the color section)

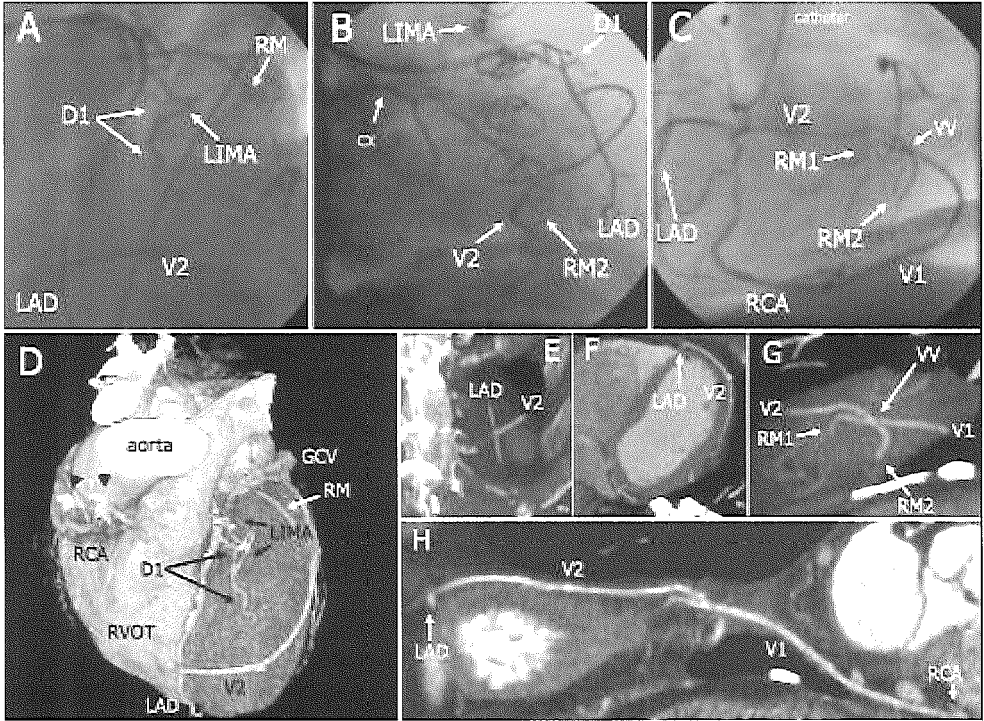


Figure 4. Redo CABG. Contrast enhanced MDCT: 3D volume rendering (D), maximum intensity projection (E G) and curved multiplanar reconstruction (H)), and conventional coronary angiogram (45° left lateral oblique (LAO), with cranial angulation and left main contrast injection of contrast (A), 30° right anterior oblique (RAO) with caudal angulation with LM injection (B) and 90° LAO view with RCA injection (C), after a complex redo CABG procedure. The initial bypass procedure consisted of a left internal mammary artery graft (LIMA) via the diagonal branch (D1) to the left anterior descending coronary artery (LAD), of which the last segment was occluded (A,D). Selective angiography of the LIMA was could not be performed. Of the sequential venous graft (V1) to the distal right coronary artery (RCA) and marginal branch (RM1) the proximal segment was occluded, leaving only the conduit between the RCA and the RM1 patent (C,G,H). One year after the initial procedure an additional venous graft (V2) was placed from the aorta to the LAD, the remaining segment of the first venous graft segment between the RM1 and the RCA (VV), and finally a marginal side branch (RM2) (A H). Within one year the patient returned with anginal complaints, and occlusion of the first segment of V2 between the aorta and the LAD was detected (A F,H). The metal artifacts (arrowheads), caused by the metal indicators, at the aortic root reveal the original proximal anastomoses of the occluded grafts (D).

DISCUSSION

Symptomatic post bypass surgery patients often pose a challenging diagnostic problem to the angiographer. The calcified, tortuous and diffusely diseased coronary arteries and degenerated bypass grafts complicate precise delineation of the culprit lesions. High quality angiograms and thorough knowledge of the coronary anatomy are required to adequately determine revascularization options. To perform this angiographic evaluation in a non invasive fashion is even more challenging. Non invasive imaging techniques are hampered by specific limitations.

Even though the scan range was not extended to cover the entire course of the proximal IMA grafts, in which no obstructions were found by conventional angiography, the scan still required a long breath hold that could not be performed by a number of patients. Voluntary and cardiac motion were the major cause for non assessability and misinterpretation. Extensive calcification of the coronary arteries and degenerated grafts, as well as the vascular clips in the proximity of arterial grafts (figure 1), are the cause of beam hardening and partial volume artifacts that hinder assessment by suggesting or obscuring obstruction.

Despite these technical limitations, our study shows that MDCT angiography allows very accurate assessment of graft patency, and in addition provides relevant information concerning the presence of significant obstructive disease in the bypass grafts and progression of disease of the native coronary arteries. The diagnostic accuracy exceeds that of conventional and single detector row helical CT.^{6,7} EBCT evaluation of grafts was initially performed on individual tomograms and later by three dimensional reconstructions, with good sensitivity (80% 100%) and specificity (82% 100%) to detect graft occlusion.^{8 12} In cases of adequate image quality (84%) Achenbach et al were able to detect significantly stenosed, but patent, grafts as well.¹¹ Additionally, EBCT flow studies have been performed to determine graft patency.^{13 15} Our study confirms the results by Ropers et al, who used MDCT to examine 65 patients and 182 grafts, and reported a sensitivity and specificity 97% and 98%, to detect graft occlusion, and 75% (12/16) and 92% (56/61) to detect significant stenosis in grafts of adequate image quality (62%).¹⁶ In this study, however, the coronary arteries were not included in the evaluation.

Non invasive follow up of a patient that underwent CABG cannot be restricted to visualization of the bypass grafts alone, and should include visualization of the coronary arteries. A number of promising studies concerning the use of MDCT for non invasive coronary angiography have been published. It appeared that the diagnostic accuracy was reasonable but complete assessment can be hindered by calcium deposits in the vessel wall and motion artifacts, particularly in patients with high heart rates.^{17 20} Assessment of the native vessels in patients who underwent bypass surgery is more challenging compared to those who present with an earlier stage of atherosclerotic disease.

Table 6. Influence of the Heart Rate on the Diagnostic Accuracy of MDCT Angiograph to Detect Obstructive Disease in the Assessable Segments (observer 1)

		HR < 65 min ⁻¹ (N=11)	HR (65 min ⁻¹ (N=13)	P value (Fisher's test)
	Average HR ±SD (min ⁻¹)	52.1 ±4.9	74.4 ±7.5	
	HR range (min ⁻¹)	48 60	66 88	
Venous graft occlusion	Assessability (%)	33/33 (100.0)	27/27 (100.0)	
	Sensitivity (%)	8/8 (100.0)	9/9 (100.0)	
	Specificity (%)	24/25 (96.0)	18/18 (100.0)	NS
	Overall sensitivity* (%)	8/8 (100.0)	9/9 (100.0)	
Venous graft stenosis	Assessability (%)	23/24 (95.8)	15/18 (83.3)	NS
	Sensitivity (%)	2/2 (100.0)	1/3 (33.3)	NS
	Specificity (%)	18/21 (85.7)	11/12 (91.7)	NS
	Overall sensitivity* (%)	2/3 (66.7)	1/3 (33.3)	NS
Arterial graft stenosis	Assessability (%)	8/8 (100.0)	11/18 (61.1)	0.06
	Sensitivity (%)	1/1 (100.0)	3/3 (100.0)	
	Specificity (%)	7/7 (100.0)	7/8 (87.5)	NS
	Overall sensitivity* (%)	1/1 (100.0)	3/4 (75.0)	NS
Coronary stenosis or occlusion	Assessability (%)	87/97 (89.7)	59/114 (51.8)	<0.001
	Sensitivity (%)	41/45 (91.1)	30/34 (88.2)	NS
	Specificity (%)	34/42 (81.0)	16/25 (64.0)	NS
	Overall sensitivity* (%)	41/50 (82.0)	30/52 (57.7)	<0.01

HR = heart rate; * Sensitivity, regarding lesions in non assessable segments as false negative.

Advanced atherosclerotic degeneration results in small diffusely narrowed vessels with an abundant presence of calcifications in the arterial wall, which complicates proper assessment of the vessel lumen. The high number of obstructions, and the fact that a bypass graft anastomosis is obviously suggestive for the presence of a stenotic lesion in the proximal part of a coronary artery, the moderate assessability is only partly reflected in the diagnostic results.

Image degradation due to residual cardiac motion occurs predominantly in patients with faster heart rates. In the near future, faster rotation of the X ray tube will increase the temporal resolution of the scanner. Until substantially faster scanners become available, motion artifacts can be reduced by administration of beta receptor blocking medication prior to the scan to reduce the heart rate. The introduction of sub millimeter detector rows is expected to improve the assessment of severely calcified coronary segments, as well as small distal branches.

REFERENCES

1. Cameron A, Davis KB, Rogers WJ. Recurrence of angina after coronary artery bypass surgery: predictors and progression (CASS Registry). *J Am Coll Cardiol* 1995; 26:895 899.
2. Fitzgibbon GM, Kafka HP, Leach AJ, Keon WJ, Hooper GD, Burton JR. Coronary bypass graft fate and patient outcome: angiographic follow up of 5,065 grafts related to survival and reoperation in 1,388 patients during 25 years. *J Am Coll Cardiol* 1996; 28:616 626.
3. Ohnesorge B, Flohr T, Becker C, et al. Cardiac imaging by means of electrocardiographically gated multisection spiral CT: initial experience. *Radiology* 2000; 217:564 571.
4. Ohnesorge B, Flohr T, Becker C, et al. Technical aspects and applications of fast multislice cardiac CT. In: Reiser MF, Takahashi M, Modic M, Bruening R (Eds). *Medical radiology diagnostic imaging and radiation oncology*. Berlin, Germany: Springer 2001;121 130.
5. Austen WG, Edwards JE, Frye RL, et al., A reporting system on patients evaluated for coronary artery disease. Report of the Ad Hoc Committee for Grading of Coronary Artery Disease, Council on Cardiovascular Surgery, American Heart Association. *Circulation* 1975; 51:5 40.
6. Engelmann MG, von Smekal A, Knez A, et al. Accuracy of spiral computed tomography for identifying arterial and venous coronary graft patency. *Am J Cardiol* 1997; 80:569 574.
7. Tello R, Costello P, Ecker C, Hartnell G. Spiral CT evaluation of coronary artery bypass graft patency. *J Comput Assist Tomogr* 1993; 17:253 259.
8. Stanford W, Brundage BH, MacMillan R, et al. Sensitivity and specificity of assessing coronary bypass graft patency with ultrafast computed tomography: results of a multicenter study. *J Am Coll Cardiol* 1988; 12:1 7.
9. Bateman TM, Gray RJ, Whiting JS, Matloff JM, Berman DS, Forrester JS. Cine computed tomographic evaluation of aortocoronary bypass graft patency. *J Am Coll Cardiol* 1986; 8:693 698.

10. Bateman TM, Gray RJ, Whiting JS, et al. Prospective evaluation of ultrafast cardiac computed tomography for determination of coronary bypass graft patency. *Circulation* 1987; 75:1018 1024.
11. Achenbach S, Moshage W, Ropers D, Nossen J, Bachmann K. Noninvasive, three dimensional visualization of coronary artery bypass grafts by electron beam tomography. *Am J Cardiol* 1997; 79:856 861.
12. Ha JW, Cho SY, Shim WH, et al. Noninvasive evaluation of coronary artery bypass graft patency using three dimensional angiography obtained with contrast enhanced electron beam CT. *AJR Am J Roentgenol* 1999; 172:1055 1059.
13. Lu B, Dai RP, Zhuang N, Budoff MJ. Noninvasive assessment of coronary artery bypass graft patency and flow characteristics by electron beam tomography. *J Invasive Cardiol* 2002; 14:19 24.
14. Muhlberger V, Knapp E, zur Nedden D. Predictive value of computed tomographic determination of the patency rate of aortocoronary venous bypasses in relation to angiographic results. *Eur Heart J*. 1990 May; 11:380 388.
15. Ueyama K, Ohashi H, Tsutsumi Y, Kawai T, Ueda T, Ohnaka M. Evaluation of coronary artery bypass grafts using helical scan computed tomography. *Catheter Cardiovasc Interv*. 1999; 46:322 326.
16. Ropers D, Ulzheimer S, Wenkel E, et al. Investigation of aortocoronary artery bypass grafts by multislice computed tomography with electrocardiographic gated image reconstruction. *Am J Card* 2001; 88:792 795.
17. Achenbach S, Giesler T, Ropers D, et al. Detection of coronary artery stenoses by contrast enhanced, retrospectively electrocardiographically gated, multislice spiral computed tomography. *Circulation* 2001; 103:2535 2538.
18. Knez A, Becker CR, Leber A, et al. Usefulness of multislice spiral computed tomography angiography for determination of coronary artery stenoses. *Am J Cardiol* 2001; 88:1191 1194.
19. Nieman K, Rensing BJ, van Geuns RJ, et al. Usefulness of multislice computed tomography for detecting obstructive coronary artery disease. *Am J Cardiol*. 2002; 89:913 918.
20. Vogl TJ, Abolmaali ND, Diebold T, et al. Techniques for the detection of coronary atherosclerosis: multi detector row CT coronary angiography. *Radiology* 2002; 223:212 220.

5.2

Non-invasive Angiographical Evaluation of Coronary Stents with Multislice Spiral Computed Tomography

Koen Nieman
Filippo Cademartiri
Rolf Raaijmakers
Peter MT Pattynama
Pim J de Feyter

Herz 2003 (in press)

SUMMARY

The numbers of patients with obstructive coronary artery disease, who undergo coronary angioplasty with implantation of stents, is ever increasing. As an alternative to catheter based angiography, ECG gated multislice spiral CT allows non invasive imaging of the coronary arteries. However, coronary stents have been notoriously difficult to assess by CT. In vitro experiments were performed, using varying detector collimations, contrast concentrations, stent positions and stent diameter sizes, to evaluate the feasibility and image characteristics of stents. The stent related high density artefacts expand the apparent size of the stent struts. This blooming effect is a fairly constant phenomenon, and therefore relatively less evident in larger diameter stents. The in vivo images show the same artefacts, but assessment is further complicated by motion, lower contrast to noise and vessel wall calcifications. The clinical value of CT after percutaneous coronary intervention currently remains largely limited to the detection of stent occlusion, and the progression of coronary artery disease in the remaining non stented segments. Subtle in stent abnormalities can not be reliably imaged. Some relief will be offered by improvements in scanner technology, but more effective would be the use of less radiopaque stent material.

INTRODUCTION

Over the last decade the management of refractory angina has changed dramatically with the introduction of percutaneous coronary angioplasty. More than 1 million percutaneous coronary interventions are performed each year, and the majority of these procedures involve the placement of one or more stents. Unfortunately, angioplasty is not permanently curative and most patients will eventually develop recurrent symptoms at some time after the procedure. Until the introduction of the coated stents, neointimal hyperplasia caused clinically significant re stenosis at least 20%.^{2,4} Although the occurrence of re stenosis may be significantly reduced by these drug eluting stents, progression of atherosclerotic degeneration in the remaining vessels is not affected.

Multislice spiral computed tomography (MSCT) allows contrast enhanced angiography of the coronary arteries. The diagnostic accuracy of this non invasive technique to detect coronary stenoses is good, particularly in the absence of extensive vascular calcification and in patients with low heart rates.^{1,3,5,7} Patients who undergo percutaneous coronary intervention (PCI) with stent placement, are likely to develop recurrent anginal complaints in the period after the procedure and will often need repeated angiographic evaluation of the coronary arteries. In the event of in stent re stenosis or newly developed coronary obstruction, therapeutic options remain available, even in case of a compromising physical condition of the patient: advanced age, cardiac or non cardiac co morbidity. A non invasive technique to visualize the coronary arteries in this patient group would be highly desirable.

Potential clinical indications for angiography could include suspected early (thrombotic) occlusion of stents after the procedure, or later for the detection of in stent restenosis and progression of coronary artery disease in the non stented vessel segment.

Coronary stents

Stents are small expandable devices that are delivered through small catheters, and either directly, or after balloon dilatation, expanded in coronary artery. The purpose of the stent is to maintain the lumen diameter after dilatation, or to restore the endothelial integrity after a dissection. The devices are expected to sustain considerable inward radial force, while maintain longitudinal flexibility. Over the years the designs of stents have evolved and the currently used types are laser cut stainless steel meshes that are well expandable, strong, flexible, and well visualized on conventional angiography. Recent developments in stent design include stents coated with pharmaceuticals to prevent restenosis, biodegradable stents, non metallic and/or MR compatible stents.

In vitro imaging of coronary stents

To study the image characteristics of stents we expanded several types of stainless steel stents (by a number of manufacturers), with a 3.0 or 4.0 mm diameter, in silicon tubes with a corresponding diameter. The tubes were filled with a diluted contrast medium and scanned with two different detector collimations: 4×1.0 mm and 2×0.5 mm. The stents were positioned both in a longitudinal (parallel to the scan direction) and transverse position (perpendicular to the scan direction). The stationary stents were scanned without the use of an ECG synchronized protocol.

The experiments showed that, despite the lack of cardiac motion, and the use of very thin slices, high density artefacts cause the stent struts to appear much larger than they actually are (Figure 1). The density of the stents is inhomogeneous and depends on the distribution of the thin struts throughout the 3D image matrix, but the maximum values range from 600 to more than 1500 Hounsfield units (HU). The partial volume artefacts and beam hardening result in a higher average CT density value within the in stent lumen. While there remains a small (1 mm) region of artifact free lumen in the central in stent lumen of the 4.0 mm stents, there is density elevation throughout the 3.0 mm stents, an observation that was consistent for all types of stents we evaluated (Figure 2). The contrast medium concentration, within the clinically used range, did not significantly influence this phenomenon (Figure 3). The three dimensional reconstructions of the larger stents show distinct patterns, unique to the stent type (Figure 4). The appearance depends on the stent design, but also displays the interaction of the strut configuration, the pathway of the X ray beam and spatial resolution of the scanner. This is illustrated in figure 5, which shows the 3D representation of a stent scanned in two different directions. These experiments show that even under in vivo conditions, without cardiac motion or surrounding tissues and using thin detector collimation (0.5 mm), the imaging of particularly small stents is difficult.

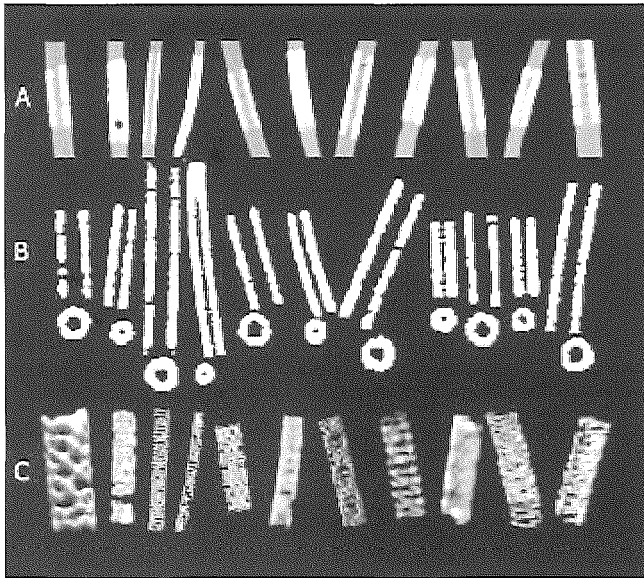


Figure 1. In vitro imaging of coronary stents. The first series (sliding window settings) show longitudinal 2D cross sections of the stents and the contrast enhanced lumen within the stents (A). The second series shows the long and short axis view of the stents with a zero window and level setting depending on the maximum stent density value (B). The 4.0 mm stents have a 1.2 mm lumen, unaffected by partial volume effects. The smaller, 3.0 mm, stents show a near occluded lumen, indicating increased density values throughout the in stent lumen. The last series shows the 3D appearance of the stents (C). The second stent contains an air bubble. The imaged stents are, from left to right: Seaqueance 4.0 and 3.0 mm (Nycomed Amersham, Paris, France), Multilink RX Tristar 4.0 and 3.0 mm (Guidant ACS, Temecula, USA), Synthesis Star 4.0 and 3.0 mm (CardioVascular Dynamics, Irvine, USA), Crossflex LC 4.0 mm (Cordis, Miami, USA), Multilink RX Penta 4.0 mm (Guidant ACS), Crossflex 4.0 mm (Cordis), Multilink RX Tetra 3.0 mm (Guidant), Multilink Duet 4.0 mm (Guidant).

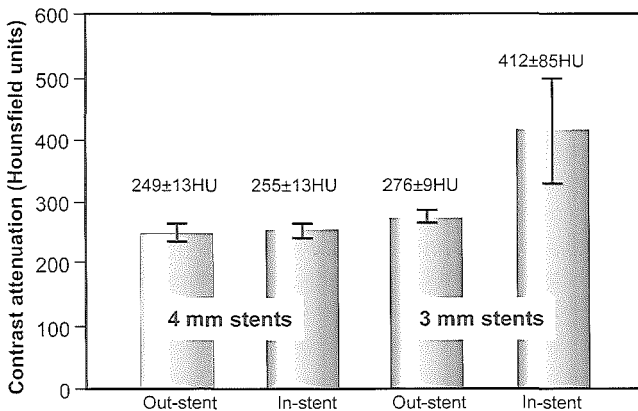


Figure 2. The in stent density value (Hounsfield Units (HU)) in 4.0 mm stents is approximately equal to that outside of the stent. In 3.0 mm stents, partial volume effects cause elevation of the density values throughout the in stent lumen.

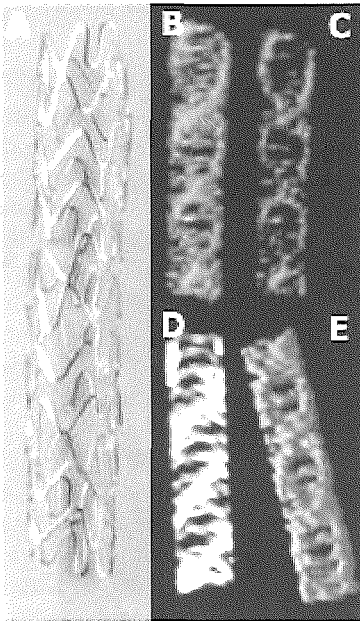


Figure 4. MSCT appearance of a 4.0 mm Crossflex LC stent (Cordis, Miami, Florida). The strut design of the stent is too detailed to be represented well by MSCT. However, due to locally increased densities of struts and metal, the appearance of a double helix is created on the 3D images.

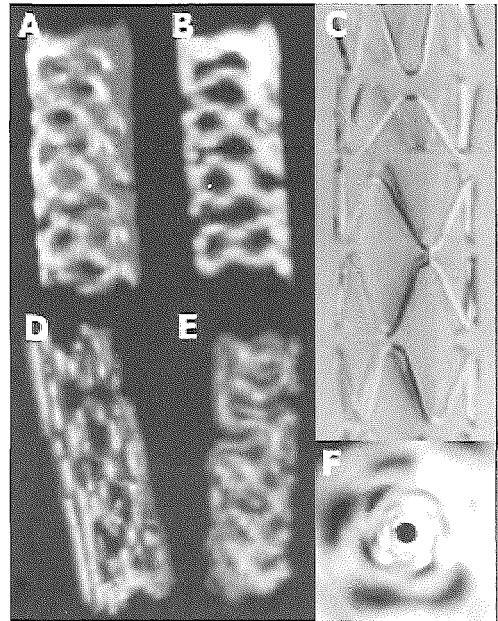


Figure 5. MSCT appearance of a 4.0 mm Seaquence stent (Nycomed Amersham, Paris, France) (C). The three dimensional images show the enlarged stent struts compared to the actual stent dimensions (A,B,C). Panel D and E show the changing appearance when scanned either in a transverse or longitudinal position. Panel F shows an endoscopic view of the stent.

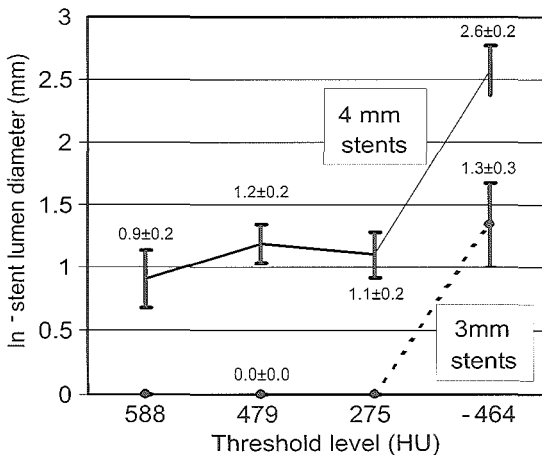


Figure 3. For three clinically relevant concentrations of contrast medium: 588 Hounsfield Units (HU), 479 HU, 275 HU, no significant differences between the measured artifact free areas (mm²) were measured. Without contrast medium (464 HU), the artifact free lumen is substantially larger.

In vivo coronary stent imaging

In the presence of stents, the standard contrast enhanced ECG gated MSCT protocol is used with a 4 x 1.0 mm, and more recently 12 x 0.75 mm detector collimation.^{5,6} The density of stents is higher than any other material in or around the heart, including the contrast enhanced lumen, which is why these devices are easily recognized on both non enhanced and contrast enhanced CT images (Figure 6). In vivo imaging of stents is complicated by the same image degrading artefacts as those that were encountered in the in vitro experiments (Figure 7 and table 1). In non coronary vessels with a larger diameter, beam hardening and partial volume effects are present, but limited to the proximity of the stent wall (Figure 8 and 9). In the coronary arteries, the artefacts are of the same magnitude, but because of the small diameter, there is only little artefact free lumen left that can be assessed reliably. Apart from the small vessel and stent size, partial volume effects and beam hardening artefacts, there are additional complications. The tissues surrounding the heart cause X ray scattering, and a reduction of the contrast to noise. Finally residual cardiac motion is one of the major causes of non assessability in multislice spiral CT coronary angiography, particularly in patients with high heart rates. The use of betablockers, in order to reduce the heart rate, and prevent the occurrence of residual motion artefacts, significantly improve the interpretability of MSCT coronary angiography.

Coronary stent imaging in clinical practice

Despite these limitations, MSCT may still be useful in patients who underwent coronary stenting. Stents with thinner struts cause less artefacts, and are therefore better assessable (Figure 6). Occlusion, or the presence of a severe stenosis, is generally detectable by CT (Figure 10). However, non significantly stenotic neo intimal hyperplasia, stent malapposition, tissue prolaps, and other subtle irregularities in the proximity of the stent wall, are usually lost in the metal artefacts. Examination of small stents in distal branches and patients with a fast heart rate, rarely provide satisfactory results. Finally, patients who underwent angioplasty are at risk for recurrent symptoms due to progression of obstructive disease in the native, non stented, coronary vessels, which can be detected by MSCT.

Requirements for reliable coronary stent imaging

To better image the coronary arteries, MSCT scanners need thinner detectors to reduce partial volume effects. Sixteen slice MSCT scanners are equipped with an extended number of thinner slices, rotate at a higher speed, and show significant improvement of the image quality and diagnostic accuracy to detect stenotic coronary artery disease.⁵ Recent experience with this new technology also suggests improved assessability of coronary stents (Figures 10 and 11). Some correction of the high density artefacts could be provided by development of more dedicated filtering of the data.

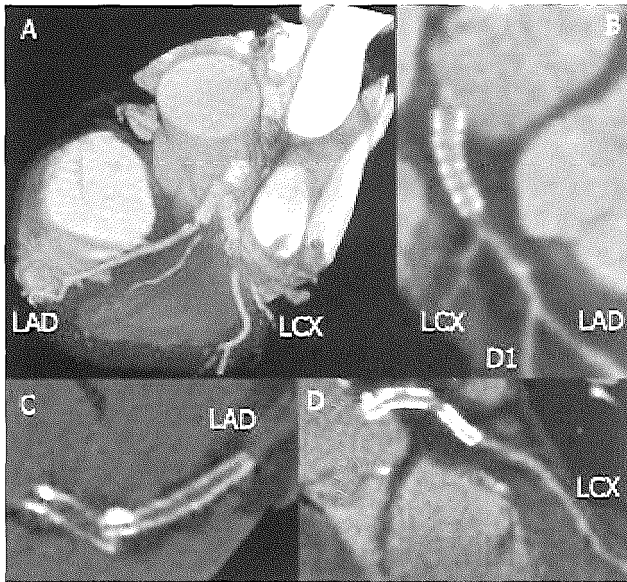


Figure 6. Three stents in the left main coronary artery (LM), left anterior descending coronary artery (LAD) and left circumflex coronary artery (LCX) (A). A patent low density stent in the LM (B). Non enhanced scan of two stents in the LM and LCX (C). A patent 4.0 mm diameter stent in the LM and a less assessable 3.0 mm stent in the LCX (D). Diagonal branch (D1).

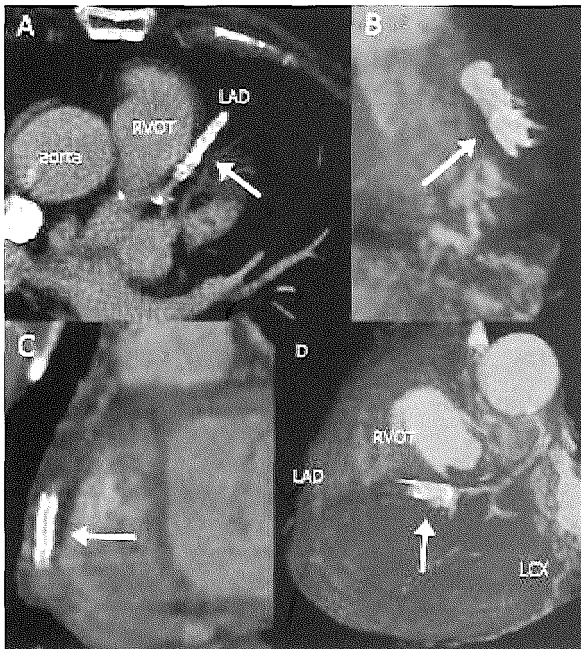


Figure 7. Complicated imaging of coronary stents. High density stent in a calcified left anterior descending coronary artery (LAD) (A). Motion and a high density stent in the right coronary artery (RCA) (B). A high density stent in the mid RCA. A high density stent and motion in the LAD (D). Left circumflex coronary artery (LCX), right ventricular outflow tract (RVOT).

Table 1. Limitations in coronary stent imaging

Characteristic	Complication
High density stent material (steel)	High density artefacts, or blooming
Small stent / vessel size and limited spatial resolution	Small artefact free lumen
Spiral scan mode	Wide based SSP, increased partial voluming
Heterogeneous X ray spectrum	Beam hardening artefacts
Residual cardiac motion	Motion artefacts
Location within the chest	Increased image noise

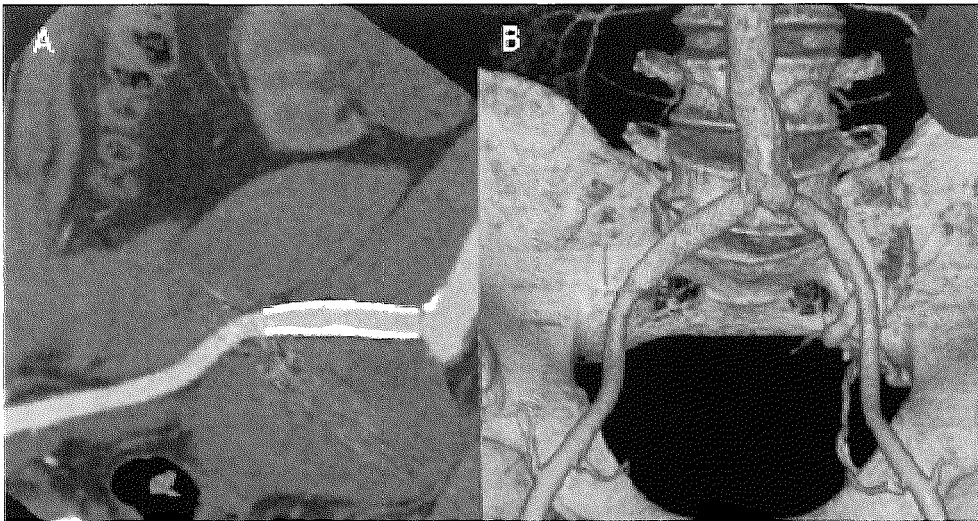


Figure 8. Curved multi planar reconstruction (A) and 3D volume rendered reconstruction (B) of a stent in the proximal right iliac artery.

But perhaps the most straightforward way to improve stent imaging, is to implant stents without metal artefacts, in the first place. Current stents consist of thinner struts, but use of low density non metallic material would even be more efficient. Additionally, the development of temporary biodegradable stents also reserve the option of non invasive follow up by MSCT coronary angiography.

Figure 9. Curved reconstruction and cross section (inset) of a carotid stent with non stenotic neo intimal hyperplasia.

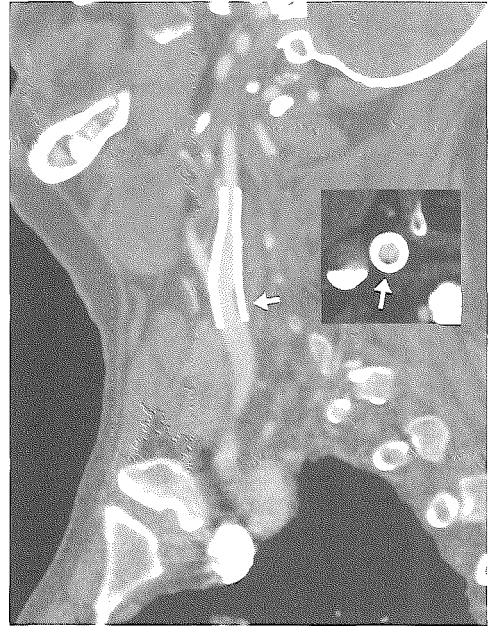


Figure 10. Two small (3.0 mm diameter) stents in the proximal right (A), and proximal left anterior descending coronary artery in a axial (B) and longitudinally reconstructed cross section (C). In both stents the stent struts can be distinguished.

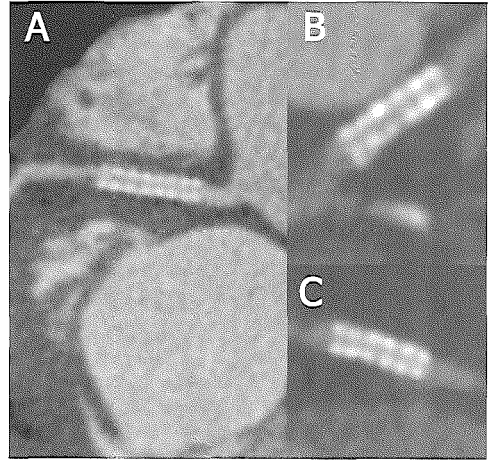
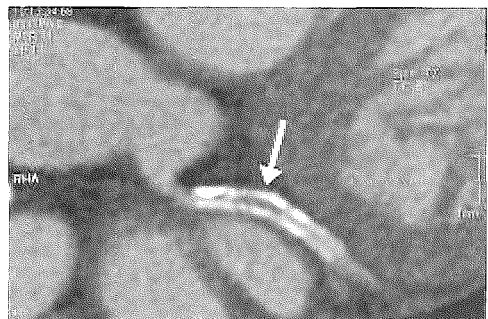


Figure 11. In stent occlusion (arrow) of a device in the proximal left circumflex coronary artery. The distal vessel segment is most likely contrast enhanced by collateral filling.



CONCLUSIONS

In the recent year considerable progress has been made in non invasive imaging of the coronary arteries. Although advancements in scanner technology will expectedly improve the assessment of coronary arteries with stents, the role of MSCT after percutaneous coronary intervention is for the time being limited to exclusion of complete stent obstruction and evaluation of coronary artery disease in the remaining non stented segments.

REFERENCES

1. Achenbach S, Giesler T, Ropers D, Ropers D, Ulzheimer S, Derlien H, Schulte C, Wenkel E, Moshage W, Bautz W, Daniel WG, Kalender WA, Baum U. Detection of coronary artery stenoses by contrast enhanced, retrospectively electrocardiographically gated, multislice spiral computed tomography. *Circulation* 2001;103:2535 8.
2. Kiemeneij F, Serruys PW, Macaya C, Rutsch W, Heyndrickx G, Albertsson P, Fajadet J, Legrand V, Materne P, Belardi J, Sigwart U, Colombo A, Goy JJ, Disco CM, Morel MA. Continued benefit of coronary stenting versus balloon angioplasty: five year clinical follow up of Benestent I trial. *J Am Coll Cardiol*. 2001;37:1598 603.
3. Knez A, Becker CR, Leber A, Ohnesorge B, Becker A, White C, Haberl R, Reiser M. Usefulness of multislice spiral computed tomography angiography for determination of coronary artery stenoses. *Am J Cardiol*. 2001;88:1191 4.
4. Morice MC, Serruys PW, Sousa JE, Fajadet J, Ban Hayashi E, Perin M, Colombo A, Schuler G, Barragan P, Guagliumi G, Molnar F, Falotico R. A randomized comparison of a sirolimus eluting stent with a standard stent for coronary revascularization. *N Engl J Med*. 2002;346:1773 80.
5. Nieman K, Cademartiri F, Lemos P, Raaijmakers R, Pattynama P, de Feyter P. Reliable non invasive coronary angiography using sub millimetre multislice spiral CT. *Circulation* 2002 (in press).
6. Nieman K, Rensing BJ, van Geuns RJM, Vos J, Pattynama PMT, Krestin GP, Serruys PW, de Feyter PJ. Non invasive coronary angiography with multislice spiral CT: Impact of Heart rate. *Heart* 2002;88:470 4 (in press).
7. Vogl TJ, Abolmaali ND, Diebold T, Engelmann K, Ay M, Dogan S, Wimmer Greinecker G, Moritz A, Herzog C. Techniques for the detection of coronary atherosclerosis: multi detector row CT coronary angiography. *Radiology* 2002;223:212 220.

5.3

Left Main Rapamycin-Coated Stent: Invasive Versus Noninvasive Angiographic Follow-Up

Koen Nieman
Jurgen MR Ligthart
Patrick W Serruys
Pim J de Feyter

A 47 year old man with a history of recurrent coronary interventions underwent percutaneous coronary intervention (PCI) of the left main coronary artery with implantation of a rapamycin coated stent (BX Velocity 4.0x18 mm). At 6 month follow up, with no physical complaints, he underwent conventional and multislice spiral computed tomography (MSCT) coronary angiography.

Intravenously contrast enhanced MSCT (Siemens Somatom Plus 4 Volume Zoom, Siemens AG) showed a wellpositioned stent in the left main coronary artery with no indication of lumen diameter reduction or neointimal hyperplasia (Figure 1). By means of virtual coronary angiography, a 3 dimensional reconstructed internal view is provided (Movie I). An animated movie of the volume rendered data offers an external overview of the coronary anatomy and the stent (VoxelView, Vital Images) (Figure 1C, Movie II).

These findings were confirmed by conventional catheterbased coronary angiography and intracoronary ultrasound (CVIS Atlantis 40 Mhz 3F catheter, Boston Scientific) (Figures 2 and 3).

This case illustrates the feasibility of noninvasive angiographic follow up after PCI. In our experience, however, these results could only be obtained in larger diameter stents.

With a (shared) subscription to *Circulation*, a virtual endoscopic passage through the stent, a complete intra coronary ultrasound pull back acquisition can be viewed at the following web page: <http://www.circulationaha.org>

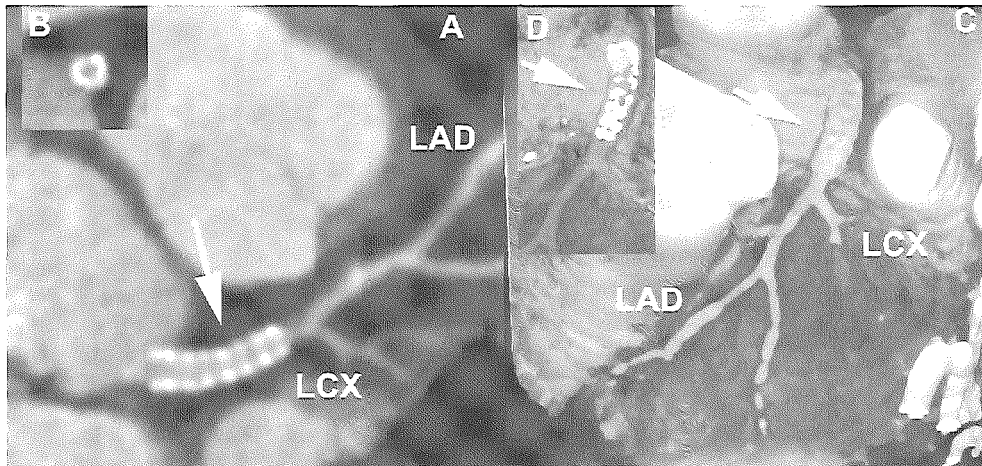


Figure 1. Multislice spiral CT coronary angiogram. The 2D curved multiplanar reconstruction (A) depicts the entire course of the left main and left anterior descending coronary artery (LAD). No neo intimal hyperplasia was noted within the struts of the stent (arrow). Cross section of the stent in the inset (B). The exterior shape of the stent (arrow) can be observed on the volume rendered representation (C) and can be highlighted by altering the settings (D).

(A full color version of this illustration can be found in the color section)

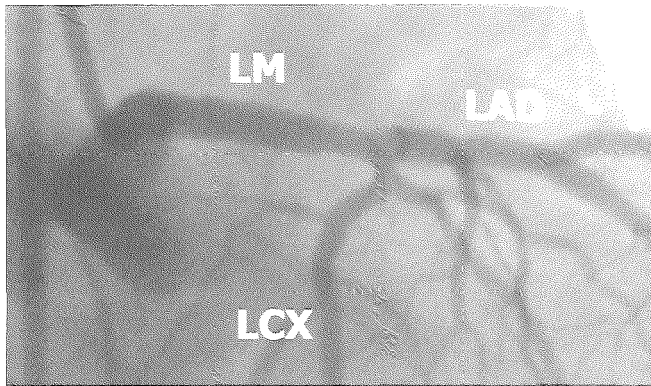


Figure 2. Conventional coronary angiogram. No re stenosis could be detected on the conventional angiogram. Left main (LM), left anterior descending (LAD) and left circumflex coronary artery (LCX).

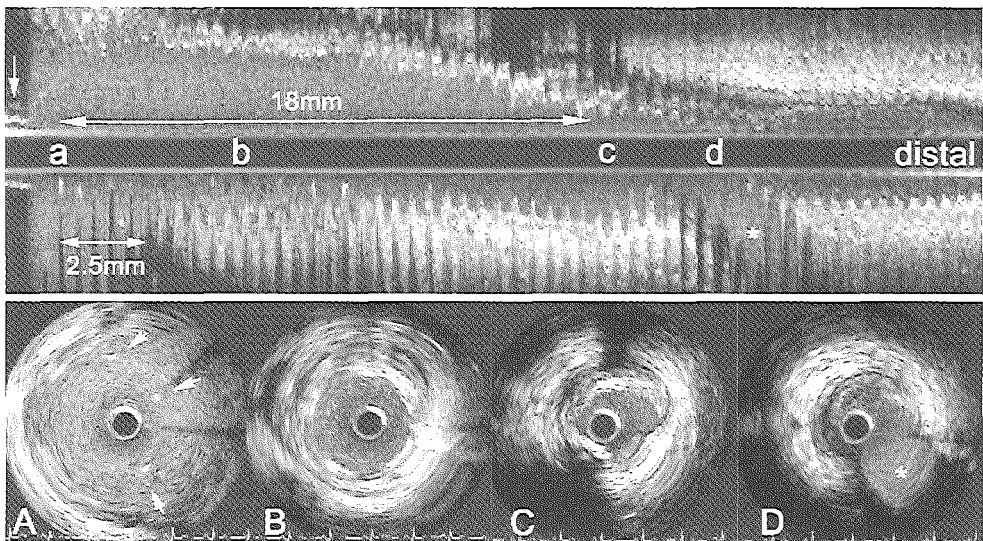


Figure 3. Intra coronary ultrasound (ICUS). Longitudinal reconstruction (top panel) of an ICUS pullback (speed was 0.5 mm/s) through the left main stem. Panels A,B,C and D show the ICUS cross sections, indicated in the longitudinal reconstruction by the corresponding characters a through d. The circumflex artery is indicated by * (in panel D and the longitudinal reconstruction). Panel C is located just distal from the stent and shows an eccentric mixed plaque with 30° superficial calcium at 7 o'clock and a spot of calcium at 12 o'clock. No hyperplasia was noted within the stent (B). Panel A is located outside the coronary artery showing stent struts (arrows) in the aorta. The longitudinal reconstruction shows the stent protruding 2.5mm (short double headed arrow) into the aorta. The arrow at the far left side of the longitudinal reconstruction indicates the 6F guiding catheter.

5.4

Four-Dimensional Cardiac Imaging With Multislice Computed Tomography

Koen Nieman
Peter MA van Ooijen
Benno J Rensing,
Matthijs Oudkerk
Pim J de Feyter

A 58 year old man was referred to our center for angiographic evaluation of unstable anginal complaints. Selective coronary angiography revealed 3 vessel disease.

Multislice CT angiography (Somatom plus 4 Volume Zoom, Siemens AG), a new noninvasive technique to image the heart and coronary arteries, was also performed (Figure). The entire heart was scanned within 1 single breath hold after injection of a contrast medium (iomeprol, 350 mg/mL, 144 mL at 4 mL/s). By use of retrograde ECG gating, a 3D volume consisting of thin slices can be reconstructed from the CT data during a preselected period (250 ms) within the RR interval of each cardiac cycle. 3D data sets were acquired during 20 different reconstruction intervals equally distributed throughout the cardiac cycle.

These 20 3D data sets, each representing a different cardiac phase, were further processed on a graphic workstation (Indigo 2, SGI) with 3D volume rendering software (Voxel View, Vital Images). By manual segmentation, the thoracic wall was removed from each volume. From these volumes, a large series of movie frames was recorded, like photographs, and ordered according to their phase. By running these frames at a speed corresponding to the original heart rate, we could create a 4D representation of the beating heart (Movie).

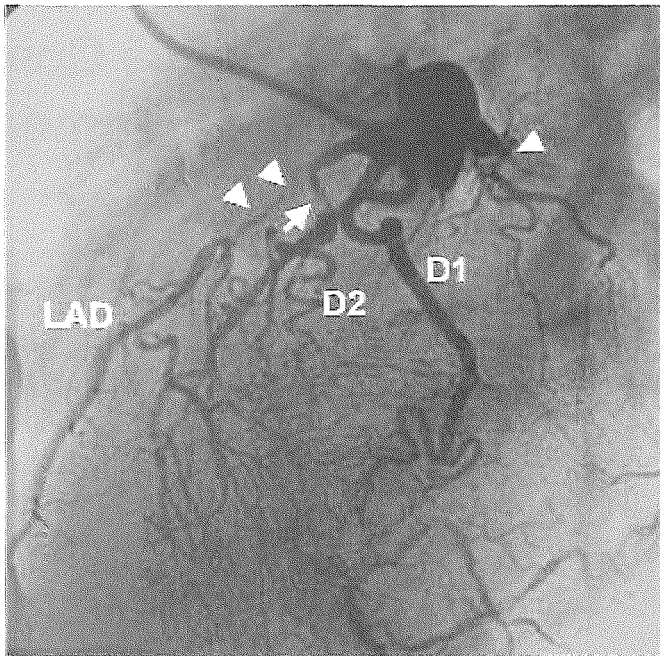


Figure 1. Selective coronary angiogram of left coronary artery (90° left anterior oblique view). Midsegment of left anterior descending coronary artery (LAD, arrowheads) and proximal circumflex artery are occluded and distal parts are filled by collateral vessels. Significant lesions can be observed in second diagonal branch (D2, arrow) as well.

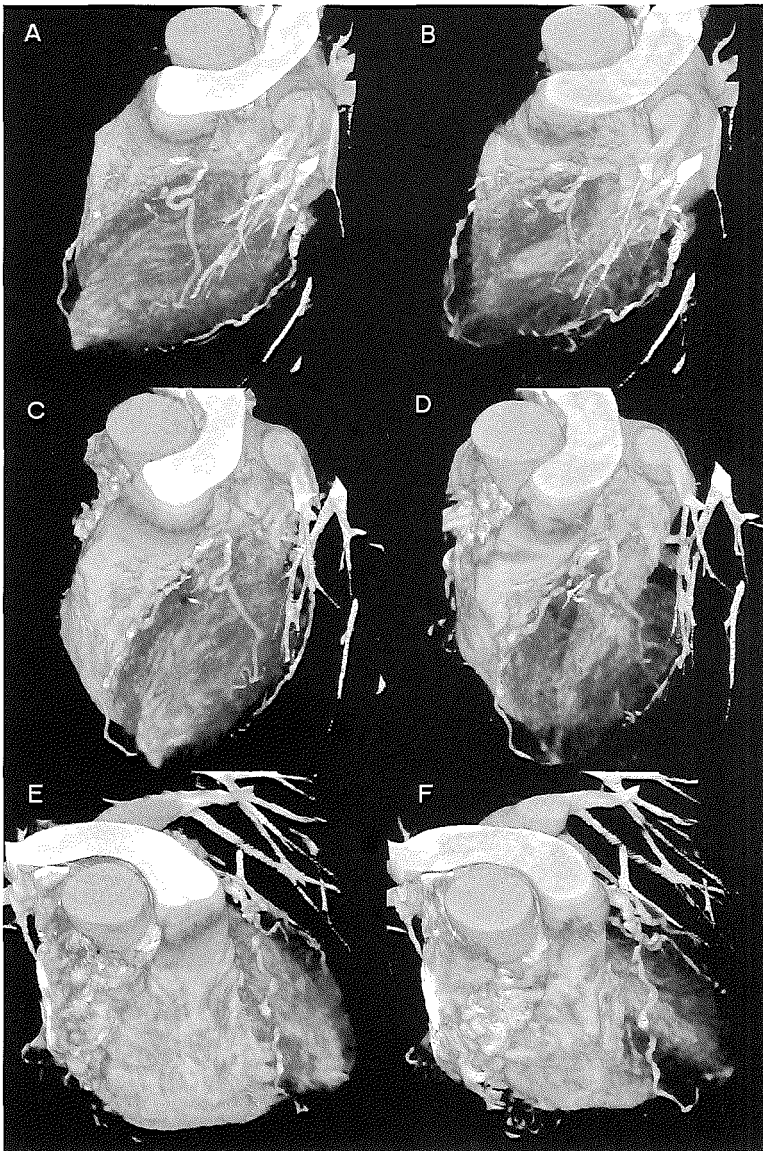


Figure 2. Still frames from an animated movie prepared by sequencing volume rendered CT angiograms at consecutive, temporarily overlapping cardiac phases, at a slowly changing view angle, creating the impression of a beating heart.

With a (shared) subscription to *Circulation*, the complete movie can be viewed at the following website: <http://www.circulationaha.org>

6.1

Reliable Noninvasive Coronary Angiography With Fast Submillimeter Multislice Spiral Computed Tomography

Koen Nieman
Filippo Cademartiri
Pedro A Lemos
Rolf Raaijmakers
Peter MT Pattynama
Pim J de Feyter

ABSTRACT

Background

Multislice spiral computed tomography (MSCT) is a promising technique for noninvasive coronary angiography, although clinical application has remained limited because of frequently incomplete interpretability, caused by motion artifacts and calcifications.

Methods and Results

In 59 patients (53 male, aged 58 ± 12 years) with suspected obstructive coronary artery disease, ECG gated MSCT angiography was performed with a 16 slice MSCT scanner (0.42 s rotation time, 12×0.75 mm detector collimation). Thirty four patients were given additional β blockers (average heart rate: 56 ± 6 min⁻¹). After contrast injection, all data were acquired during an approximately 20 s breath hold. The left main (LM), left anterior descending (LAD), left circumflex (LCX), and right coronary artery (RCA), including ≥ 2.0 mm side branches, were independently evaluated by two blinded observers and screened for $\geq 50\%$ stenoses. The consensus reading was compared with quantitative coronary angiography. MSCT was successful in 58 patients. Eighty six of the 231 evaluated branches were significantly diseased. Without exclusion of branches, the sensitivity, specificity and positive and negative predictive value to identify $\geq 50\%$ obstructed branches was 95% (82/86), 86% (125/145), 80% (82/102), and 97% (125/129), respectively. The overall accuracy for the LM, LAD, RCA, and LCX was 100%, 91%, 86%, and 81%, respectively. No obstructed LM, LAD, or RCA branches remained undetected. Classification of patients as having no, single, or multivessel disease was accurate in 78% (45/58) of patients and no patients with significant obstructions were incorrectly excluded.

Conclusions

Improvements in MSCT technology, combined with heart rate control, allow reliable noninvasive detection of obstructive coronary artery disease.

INTRODUCTION

During the past decade, considerable progress has been achieved in the field of noninvasive coronary imaging with MRI, electron beam computed tomography (EBCT), and, most recently, multislice spiral computed tomography (MSCT). With the use of 4 slice MSCT scanners, promising results have been published; however, cardiac motion and calcium deposits in the coronary artery wall rendered a substantial number of scans incompletely interpretable.^{1,3} Motion artifacts limit proper assessment, particularly at higher heart rates.⁴ Recently, a new generation of MSCT scanners, equipped with more and thinner detector rows and increased rotation speed, have been introduced. The purpose of the present study is to evaluate the diagnostic accuracy of noninvasive coronary angiography with the latest generation MSCT scanner, combined with effective heart rate control.

METHODS

Study Population

Fifty nine patients (53 male, aged 58 ± 12 years) who had suspected coronary obstructions and were scheduled for elective conventional angiography participated in the study. Criteria for exclusion included previous bypass graft surgery, irregular heart rate, allergy to iodine contrast media, and renal insufficiency (serum creatinine >120 mmol/L⁻¹). Significant coronary obstructions were absent in 8 patients. Single vessel disease was found in 20 patients, 2 vessel disease in 25 patients, 3 vessel disease in 4 patients, and 4 vessel disease in 1 patient. Eight patients previously underwent PTCA with stent implantation. The average interval between MSCT and conventional angiography was 21 ± 17 days. Thirty seven patients (64%) used β receptor blocking medication at the time of the examination. The study was approved by the ethics committee of the university medical center, and all participating patients gave informed consent.

Scan Protocol and Image Reconstruction

CT angiography was performed with the use of a 16 slice MSCT scanner with a 0.42 s rotation time (Sensation 16, Siemens). For cardiac protocols, the 12 inner detector rings are applied. Thirty four patients (58%), 22 of whom already used β blockers, had a prescan heart rate >65 min⁻¹, and were given a single oral dose of 100 mg metoprolol one hour before the examination in the absence of contraindications. A bolus of 120 to 140 mL iodixanol (320 mgI/ml⁻¹) was intravenously injected (4 to 5 mL/s⁻¹). As soon as the signal density level in the ascending aorta, which was monitored at a 1.25 s interval, reached a predefined threshold of 100 Hounsfield units, the patient was automatically instructed to maintain an inspiratory breath hold (20.5 ± 1.4 s), during which the CT data and ECG trace were acquired. Scan parameters: detector collimation 12×0.75 mm, table feed 6.7 mm/s⁻¹, tube voltage 120 kV, 400 or 450 mAs (depending on the patient size), and estimated radiation exposure between 8 and 9 mSv. After this feature became available, prospectively ECG controlled roentgen tube modulation was applied in patients ($n=15$) with a reliable ECG trace to decrease the roentgen output during systole and reduce the exposure by half at low heart rates.⁵ Synchronized to the recorded ECG, axial slices were reconstructed from the acquired MSCT data with the use of an algorithm that uses only the data from a half gantry rotation per slice, resulting in a temporal resolution of ≤ 210 ms.⁶ The continuous data acquisition allows slice reconstruction at different time positions within the cardiac cycle. Three image data sets were reconstructed during the mid to end diastolic phase, during which coronary artery displacement is relatively small, with reconstruction window positions starting at 350, 400, and 450 ms before the next R wave. If indicated, additional window positions were explored, although 400 and 450 ms generally provided nearly motion free results.

MSCT Image Interpretation

Two blinded reviewers independently evaluated the MSCT scans by assessment of the axial slices and with case dependent application of postprocessing tools, such as multiplanar reconstruction and thin slab maximum intensity projection. Vessel wall calcification was classified as either calcium spots (small isolated eccentric lesions) or severe calcification (large high density lesions, extending along the wall, causing partial volume and beam hardening artifacts). The image interpretability was classified as good, adequate, or poor. The 4 main coronary branches—left main (LM), left anterior descending (LAD), left circumflex (LCX), and right coronary artery (RCA), including side branches with a diameter of ≥ 2.0 mm—were screened for significant narrowing ($\geq 50\%$ diameter reduction) of the lumen. Cases of disagreement were settled by a joined consensus reading. Because of the known low interpretability of small coronary stents, the in stent lumen was not included in the analysis.

X-Ray Coronary Angiography

Conventional selective coronary angiography was performed with standard techniques and evaluated by a blinded reviewer with the use of quantitative coronary angiography (CAAS, Pie Medical), catheter-derived image calibration, and automated vessel contour detection, to determine the diameter of all coronary branches. The diameter stenosis, as a percentage of the reference diameter, was determined in two orthogonal directions and the average between the two determined the stenosis severity.

Statistical Analysis

The diagnostic accuracy of MSCT to detect significant stenoses in ≥ 2.0 mm diameter segments was evaluated regarding QCA as the standard of reference. All vessels, regardless of the image quality, were included. If a coronary branch contained more than one lesion, the most severe lesions in the most proximal branch determined the diagnostic accuracy of the assessment. Standard descriptive statistics were calculated for each observer and the precision of the overall parameters was expressed with a 95% confidence interval. Concordance between observers was calculated and expressed by the κ value.

RESULTS

The average heart rate was 56 ± 6 min⁻¹ (range 45 to 70 min⁻¹). One scan that was prematurely triggered by contrast medium detection in the superior vena cava was excluded from the study because of insufficient contrast enhancement. In the absence of a ≥ 2.0 mm RCA in a single patient, 231 vessels were available for evaluation. Calcified lesions were present in 61% of the branches, half of which limited to small calcified nodules (Figure 1).

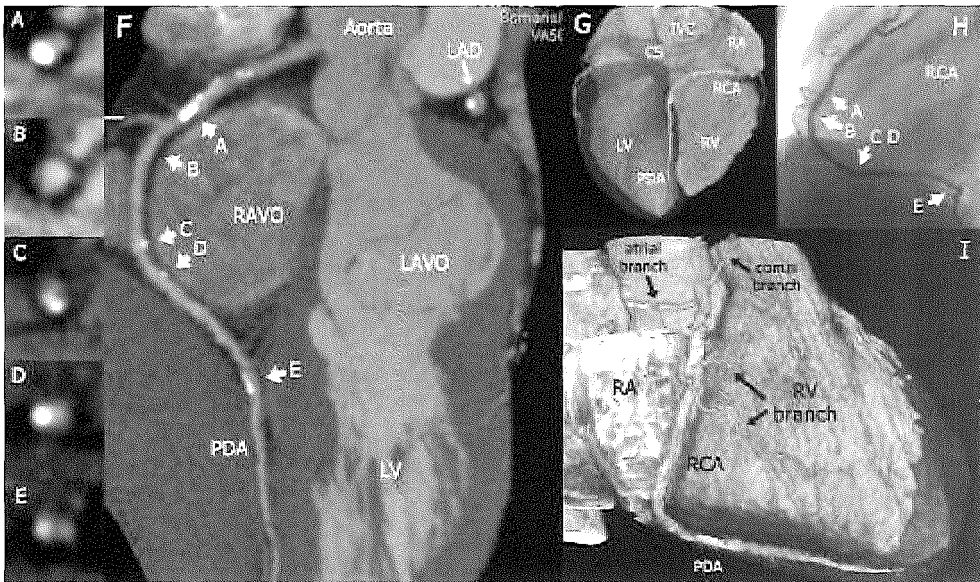


Figure 1. H, MSCT and conventional angiogram of an atherosclerotic RCA without significant stenoses. A and F, Blooming artifacts around the bright calcifications suggest stenosis. Cross sections A through E are indicated in panel F (curved MSCT reconstruction along the course of the RCA) and H. G, Three dimensional representations from an inferior and I, right oblique angle, show the PDA and side branches. RAVO/LAVO indicates right/left atrioventricular orifices; PDA, posterior descending; LV/RV, right/left ventricles; CS, coronary sinus; RA, right atrium; and IVC, inferior vena cava. (A full color version of this illustration can be found in the color section)

Table 1. Diagnostic accuracy to detect significantly stenosed coronary arteries*

	All Branches	RCA	LM	LAD	CX
≥50% stenosed branches	86	22	3	37	24
Well assessable	160 (69)	32 (56)	52 (90)	38 (66)	38 (66)
Adequately assessable	54 (23)	18 (32)	5 (9)	15 (26)	16 (28)
Poorly assessable	17 (7)	7 (12)	1 (2)	5 (9)	4 (7)
No detectable calcium	89 (39)	23 (40)	29 (50)	9 (16)	28 (48)
Small calcified nodules	74 (32)	14 (25)	19 (33)	26 (45)	15 (26)
Marked calcification	68 (29)	20 (35)	10 (17)	23 (40)	15 (26)
Sensitivity	82/86 (95, 89 98)	22/22 (100)	3/3 (100)	37/37 (100)	20/24 (83)
Specificity	125/145(86, 83 88)	27/35 (77)	55/55 (100)	16/21 (76)	27/34 (79)
Positive predictive value	82/102 (80, 75 83)	22/30 (73)	3/3(100)	37/42 (88)	20/27 (74)
Negative predictive value	125/129 (97, 93 99)	27/27 (100)	55/55 (100)	16/16 (100)	27/31 (87)

Values are n (% , 95% confidence interval). RCA, LM, LAD, and LCX indicate right, left main, left anterior descending, and left circumflex coronary artery, respectively.

* ≥50% lumen diameter reduction, in ≥2.0 mm diameter vessels, consensus reading.

All coronary branches included, the overall sensitivity and specificity to detect significantly stenosed branches was 95% (82/86) and 86% (125/145) (Figure 2). Of the vessels containing $\geq 70\%$ stenoses, 97% (62/64) were identified (Table 1). All undetected stenoses ($n=4$), 2 of which were moderate (51% and 55%), were located in the LCX and marginal branches. Twenty false positive assessments involved seven 40% to 49% lesions. Seven misinterpreted vessel segments contained extensive calcification, and 8 contained calcium spots. Concordance between both MSCT observers was reasonably good (κ value 0.69).

Contrast medium was detected within all 11 stents, and patency was confirmed by conventional angiography. One case of in stent restenosis (85%) in the distal LAD was not recognized by MSCT.

The predictive value of MSCT angiography to detect patients with no, single, or multivessel disease was 100% (7/7), 75% (12/16), and 74% (26/35), respectively (overall predictive value 78% [45/58]). Seven out of 8 patients without significant lesions were correctly identified. No incorrect exclusion of patients with significant lesions occurred.

DISCUSSION

Four slice MSCT scanners showed promising results but were not robust enough to consistently produce reliable coronary imaging because of insufficient spatial and temporal resolution.^{1,4} Generally, 20% to 30% of the proximal and middle coronary segments were noninterpretable because of insufficient image quality.^{1,3} The use of a scanner with thinner slices and faster rotation, combined with β blocking, improved the image quality and diagnostic accuracy of MSCT to detect significant disease in all ≥ 2.0 mm coronary segments. Advantages of the shorter scan time are a more comfortable breath hold (approximately 20 s), less venous contrast enhancement, and a lower contrast dose. The welltolerated examination can be performed within 15 minutes and requires no hospital admission. Currently, MSCT coronary angiography is not reliable in patients with arrhythmias, high heart rates, or severely calcified vessels. Disadvantages are the still considerable radiation dose and frequently required use of β blockers, which were well tolerated but require observation and a prolonged stay of the patient.

For alternative noninvasive coronary imaging modalities, such as EBCT and MRI, good diagnostic results were reported. However, assessment was usually limited to proximal and middle main branches, and $\leq 25\%$ of these branches were excluded because of insufficient image quality.^{7,8} Development of both techniques is ongoing, and although no direct comparisons have been performed, they seem at this moment outperformed by 12 slice MSCT with respect to stenosis detection. MSCT will not soon equal the versatility or quantitative accuracy of catheter based imaging techniques, but it does allow noninvasive detection and exclusion of coronary obstructions.

In what clinical setting CT coronary angiography is of most value for the early detection of coronary artery disease, or evaluation of chest pain, should be the focus of future studies.

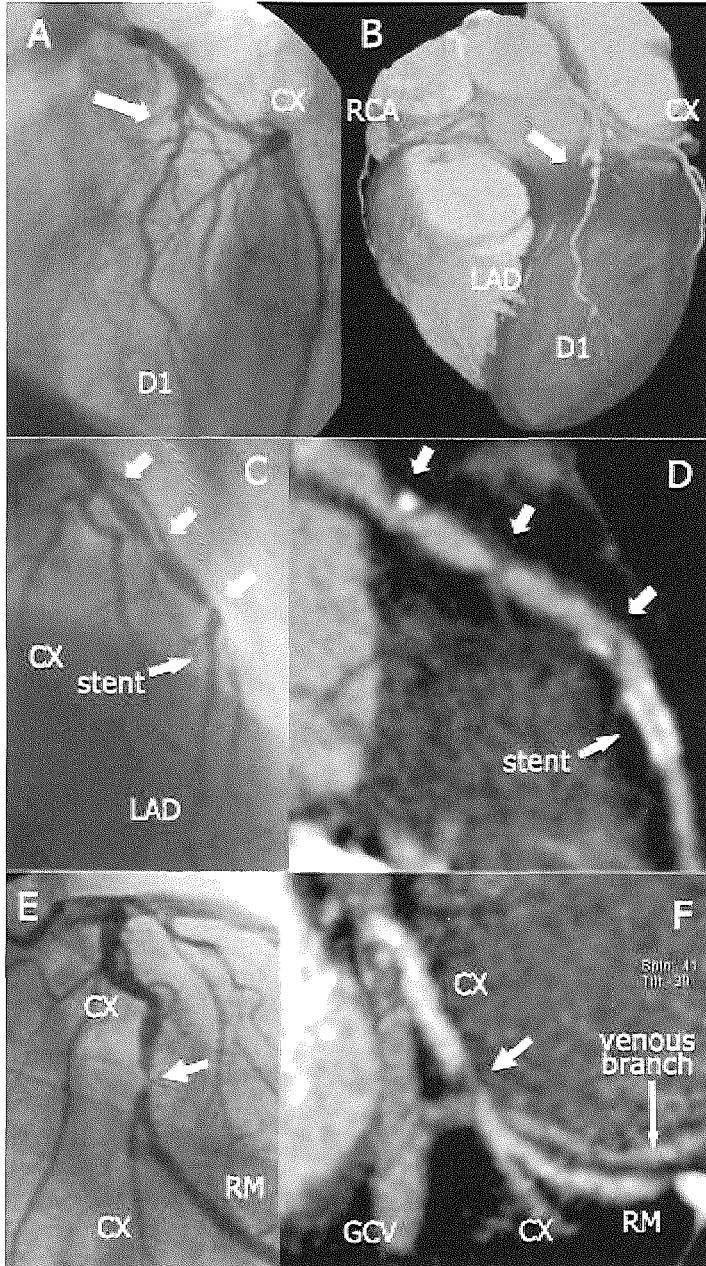


Figure 2. Three cases with corresponding conventional and MSCT angiograms. A and B, Occluded (arrow) LAD with distal collateral filling. C and D, Triple LAD lesions (arrows): <50%, 67%, 57%, and nonobstructed stent. E and F, High grade CX lesion (arrow). CX indicates circumflex; D1, diagonal branch; RM, marginal branch; and GCV, great cardiac vein.

REFERENCES

1. Achenbach S, Giesler T, Ropers D, et al. Detection of coronary artery stenoses by contrast enhanced, retrospectively electrocardiographicallygated, multislice spiral computed tomography. *Circulation*. 2001;103: 2535 2538.
2. Knez A, Becker CR, Leber A, et al. Usefulness of multislice spiral computed tomography angiography for determination of coronary artery stenoses. *Am J Cardiol*. 2001;88:1191 1194.
3. Nieman K, Rensing BJ, van Geuns RJ, et al. Usefulness of multislice computed tomography for detecting obstructive coronary artery disease. *Am J Cardiol*. 2002;89:913 918.
4. Nieman K, Rensing BJ, van Geuns RJM, et al. Non invasive coronary angiography with multislice spiral CT: the impact of heart rate. *Heart*. 2002;88:470 474.
5. Jakobs TF, Becker CR, Ohnesorge B. Multislice helical CT of the heart with retrospective ECG gating: reduction of radiation exposure by ECG controlled tube current modulation. *Eur Radiol*. 2002;12: 1081 1086.
6. Ohnesorge B, Flohr T, Becker C, et al. Technical aspects and applications of fast multislice cardiac CT. In: Reiser MF, Takahashi M, Modic M, Bruening R, eds. *Medical Radiology Diagnostic Imaging and Radiation Oncology*. Berlin, Germany: Springer; 2001:121 130.
7. Achenbach S, Moshage W, Ropers D, et al. Value of electron beam computed tomography for the noninvasive detection of high grade coronary artery stenoses and occlusions. *N Engl J Med*. 1998;339: 1964 1971.
8. Kim WY, Danias PG, Stuber M, et al. Coronary magnetic resonance angiography for the detection of coronary stenoses. *N Engl J Med*. 2001;345:1863 1869.

6.2

Computed Tomography Coronary Angiography

Pim J de Feyter
Koen Nieman
Thomas Flohr
Bernd Ohnesorge

Submitted for publication

ABSTRACT

Since the introduction in the early 1970s, computed tomography has been ever evolving, leading to non mechanical electron beam (EBCT) and multi slice spiral CT (MSCT) scanners, which have proven able to non invasively visualize the coronary arteries and assess the coronary lumen integrity. Either technique has inherent advantages and limitations but showed comparable diagnostic accuracy. However, recently introduced fast rotating 16 slice MSCT has become available and is currently considered the most reliable non invasive coronary imaging modality. Nevertheless, both MSCT and EBCT technology will probably be subject to continued technology improvements in the coming years. CT will not equal the quality and diagnostic versatility of conventional X ray angiography in the near future, but 16 slice MSCT angiography has emerged as a non invasive alternative in a subgroup of patients with a regular rhythm and low heart rate. Continuing innovation in CT technology to increase the spatial and temporal resolution is required in order to create a reliable non invasive alternative to diagnose coronary artery disease in larger, unselected patient groups.

INTRODUCTION

Invasive diagnostic coronary angiography is the gold standard for the identification of significant obstructive coronary disease. A variety of non invasive ischemia provoking tests are available to detect ischemia induced by coronary obstruction. Although these tests are routinely performed, they more than rarely result in false or inconclusive results, which causes the clinician to rely on diagnostic coronary angiography. A non invasive test that allows direct assessment of the coronary anatomy would be desirable. Earlier reports have shown that magnetic resonance imaging (MRI), electron beam computed tomography (EBCT) and (4 slice) multi slice computed tomography (MSCT) have the potential to image the lumen of the proximal and middle segments of the main epicardial coronary arteries, but the diagnostic accuracy was insufficient for substitution of conventional invasive coronary angiography.^{1,12}

Very recent advances of multi slice CT scanner technology have significantly improved the image quality, and have made it possible to more accurately define the coronary luminal integrity compared to the earlier generation multi slice scanners.^{13,14} The robustness and reliability of this newest MSCT scanner will boost its use into the diagnostic cardiological armamentarium.

We will outline the principle and relevant technical aspects of the latest MSCT technology in comparison to previous multi slice CT technology and EBCT to provide a better understanding of the characteristics, clinical value and remaining limitations of the technique, to improve interpretation of these new coronary images. The potential role of MSCT in clinical practice and in research will be explored.

Ideal requirements for high quality coronary imaging

To image the coronary arteries for the purpose of detection and quantification of stenosis, one requires a technique that is independent of patient characteristics and provides consistent high quality image data. This image data should represent a true 3 dimensional data set that can be acquired operator independent. To quantify and perhaps monitor progression of a coronary stenosis, the method needs the capability to differentiate 10% vessel lumen change in 3mm vessels. Therefore the spatial resolution in all three dimensions needs to be as high as 0.3mm, perhaps better in smaller branches. In addition to information about narrowing of the vessel lumen the method needs to visualize non obstructive atherosclerotic disease in the coronary vessel wall. High temporal resolution imaging is mandatory to eliminate artefacts or blurring due to cardiac motion. Although it is difficult to estimate at which temporal resolution, motion artifacts are largely eliminated, it is expected to be 100ms or less for imaging in the phases with limited cardiac motion at a normal heart rate ($< 100\text{min}^{-1}$), but 50ms or less for imaging of other phases with rapid cardiac motion.¹⁵ The scan time should be as short as possible. Acquisition of all data within a single and short breath hold time is mandatory in case of contrast enhanced CT techniques, in order to prevent repetitive contrast medium injections and to avoid motion artefacts due to breathing. Ideally, all data would be acquired within a single heart cycle or less and available for analysis immediately after acquisition. Analysis should be quick, user independent, quantitative and well presentable to referring clinicians. Finally the diagnostic procedure should be non invasive and harmless, i.e. require minimal or at best no radiation or intravenous contrast media. However, these are prerequisites that are not achievable by any non invasive technique currently in use, and should not be expected within the foreseeable future. The available angiographic techniques, both invasive and non invasive, have varying trade offs between scanner characteristics. The modality of choice therefore depends on the individual patient characteristics and specific clinical purpose of the examination.

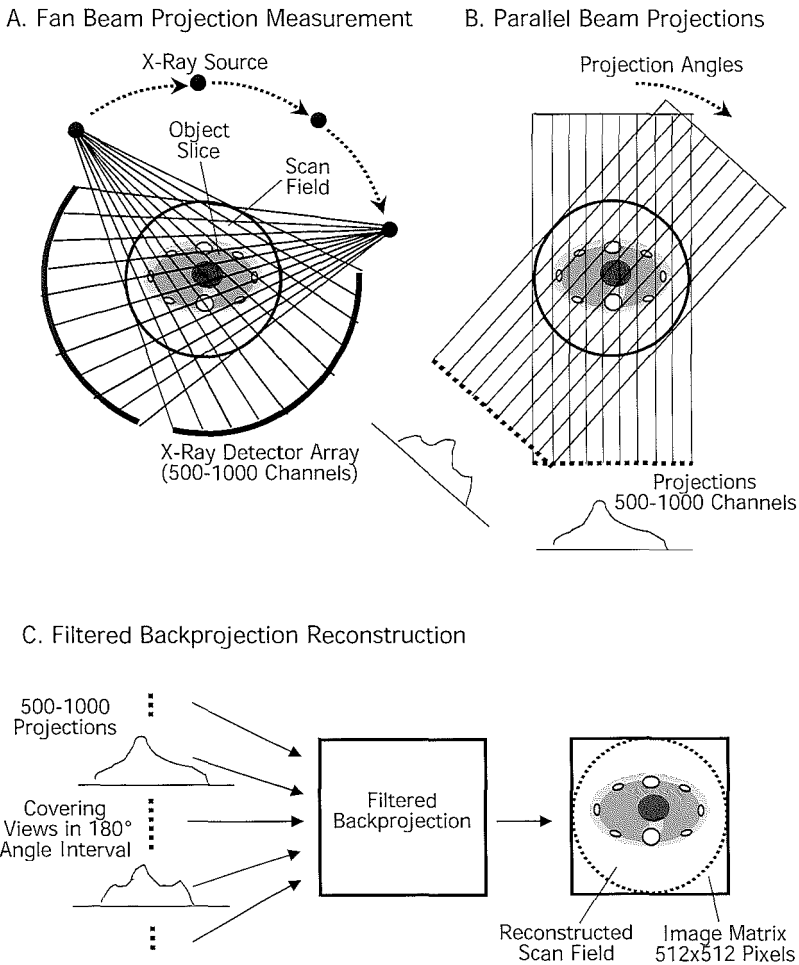


Figure 1. schematic diagram of CT data acquisition and image reconstruction

A) A fan shaped X ray beam passes through the cross section of the patient, located within the scan's field of view. The patient's morphology attenuates these X rays after which the residual rays are registered by a detector array on the opposite side. The electrical intensity signals from the detector are converted by analog digital converters (ADC) into digital intensity signal, which are transformed by computer into an attenuation projection profile. Each angular projection or attenuation profile consists of typically 500 1000 individual data points that belong to individual ray projections. A large number of attenuation profiles, from consecutive angular fan beam projections are generated and serve as basis for computation of the X ray attenuation distribution of the patient's cross sectional morphology that represents the image slice. B) For most reconstruction algorithms the measured fan beam projections are rearranged to parallel beam projections via 2 dimensional interpolation algorithms. To reconstruct a slice the minimally required amount of data are acquired during a half rotation of the X ray source and detector array, which consists of 500 1000 parallel beam projections. C) The final computation of the slice is performed via a so called backprojection of the filtered parallel beam projections.

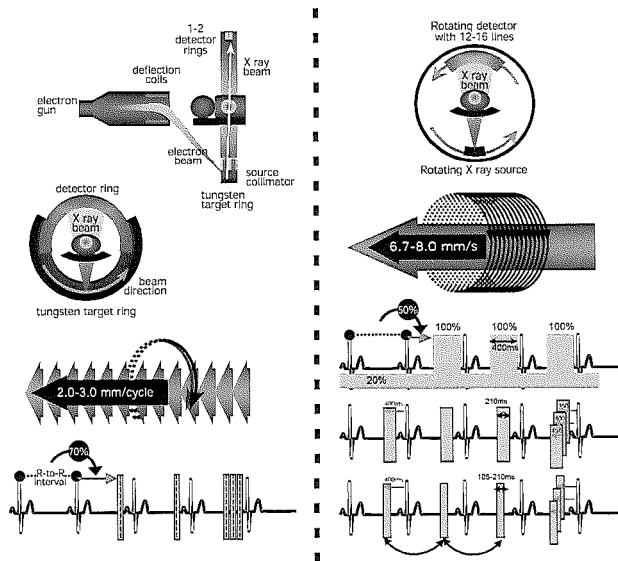


Figure 2. ECG synchronized EBCT and MSCT data acquisition and image reconstruction. Electron beam CT (A): an electron beam is generated by an electron gun and electromechanically guided along a static semi circular tungsten anode ring. After being hit by the electron beam an X ray fan beam is emitted from the tungsten target ring and passed through the patient. The attenuated X rays are registered by the static detector ring on the opposite side. Multiple fan beam projections are acquired during each 50ms sweep, and two consecutive sweep are required to reconstruct a cross sectional slice. The electron beam generation is triggered by the patient's ECG signal. Based on the previous heart cycles the generation of the electron beam is initiated during the predicted diastolic interval between 40% and 80% of the R R interval, to synchronize the acquisition to the motion of the heart. During every cardiac cycle one 1.5 or 3.0mm wide slice position is scanned, after which the table is moved to the next longitudinal position to wait for the next trigger. With a 3.0mm collimation protocol best longitudinal resolution can be achieved by acquisition of 1.0mm overlapping slices by the use of table increments smaller than the slice width (2.0mm). Until recently one image was acquired per heartbeat but recent technological advances allow for simultaneous acquisition of two 1.5 mm slices, or a number of images per heart cycle to facilitate retrospective selection of the image series with least motion artefacts. Multi slice spiral CT (B): Rotating around the patient are 12 16 parallel detector rows, with a submillimeter slice width each. While the patient continuously moves through the scanner, the tube current is altered according to the ECG. During systole the radiation output is lowered to 20%, while during diastole, triggered at the estimated 50% RR interval time point, the nominal exposure is used during a 400ms interval to acquire high quality images. This way the total dose can be reduced by 50%. Although unsuitable for coronary angiography, the systolic images can still be useful for functional evaluations of the left ventricle. From the acquired scan data, ECG synchronized cross sectional image series are reconstructed with an overlapping increment via spiral interpolation algorithms to improve the volumetric quality of the data set. Contrary to prospective triggering, retrospective ECG gating allows reconstruction timing related to the upcoming R wave or selective repositioning of reconstruction intervals during irregular R R intervals. By varying the position of the 210 ms reconstruction window within the 400 ms interval of nominal tube current, image datasets are retrospectively reconstructed during slightly different phases (at 350ms, 400ms and 450ms prior to the following R wave), and the most optimal result is selected for further analysis. The standard length of the reconstruction interval and temporal resolution at a 0.42s rotation time is 210ms. Depending on the heart rate the effective reconstruction interval can be between 105 and 210ms by using "segmented" reconstruction algorithms, that combine data from two consecutive heart beats.

Historical review and technical principles of cardiac CT

In 1979 G. Hounsfield and A.M. Cormack received the Nobel prize for their significant contributions to the development of computed axial tomography. Using computer reconstruction techniques, Hounsfield demonstrated that internal structures of an object could be reconstructed from the attenuation pattern of an X ray beam, which was passed through this object at different angles. In 1971 he constructed the first CT scanner that could image the brain.¹⁶ Cormack contributed with the development of fast signal processing algorithms that allowed for computer based CT image reconstruction based on the mathematical fundament published by Johann Radon in 1917.¹⁷ The first commercially available CT scanners were introduced in 1974 for brain and body imaging, and acquired only a single slice per rotation. The basic principles for acquisition of cross sectional image slices with CT are shown in figure 1.

In order to achieve very short image acquisition times to virtually freeze the cardiac motion, CT systems with fixed detector arrays and non mechanical movement of the x ray source have been developed. This so called Electron Beam CT (EBCT) technology (figure 2a) was first introduced in 1982.¹⁸ Initially ECG triggered EBCT was used for quantification of coronary calcium. The first study of contrast enhanced visualization of coronary arteries was reported in 1997 (figure 3).¹⁹

Introduced in 1990, spiral (or helical) scanning with continuous mechanical rotation of tube and detector array, continuous table feed, continuous X ray exposure and continuous data acquisition allowed for the generation of true volume image data without missed or double registration of anatomical details based on overlapping transaxial image slices.²⁰ For the first time, 3 dimensional CT angiographic evaluation of contrast enhanced vessels in different body regions was possible due to considerably improved longitudinal spatial resolution, faster scan speed and larger volume coverage. With acquisition of 1 2 slices per rotation, fastest rotation times of 0.75s and ECG synchronization these scanners did provide first results in the quantification of coronary calcification, but were still not fast enough to reliably image the coronary artery lumen.^{21,22} With the introduction of 4 slice spiral CT scanners in 1998, capable of simultaneous acquisition of four thin slices, combined with higher rotation speed and temporal resolution and scan time short enough to cover the entire heart within the duration of a long breath hold, imaging of the coronary arteries, including atherosclerotic plaque material, became possible.^{8 12} In 2002, technical progress has resulted in a generation of MSCT scanners that acquires up to 16 sub millimeter slices simultaneously (figure 2b), at a rotation time of 420ms, which has further advanced the quality and clinical implementation of non invasive coronary imaging (figure 4).^{13,23}

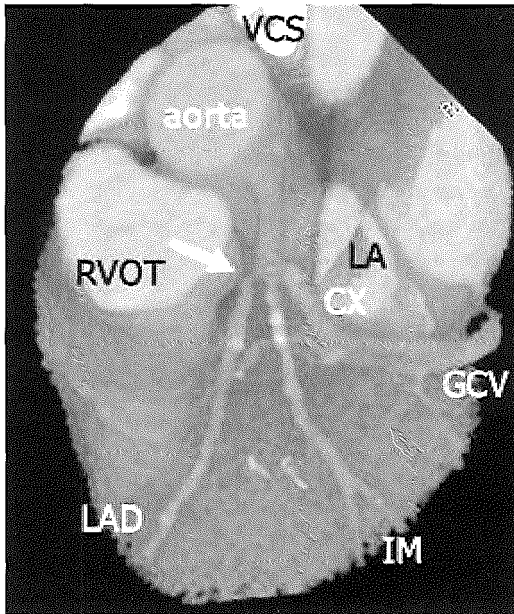


Figure 3. EBCT angiography. Volume rendered representation of an EBCT coronary angiogram showing a significant lesion (arrow) in the proximal left anterior descending coronary artery (LAD). Left circumflex (CX), intermediate coronary branch (IM) and great cardiac vein (GCV). Right ventricular outflow tract (RVOT), vena cava superior (VCS), left atrial appendage (LA).

Table 1. Modality characteristics and scan protocols

Modality	EBCT	4 slice spiral CT	16 slice spiral CT
Scan time (s)	30 40	30 40	15 20
Data acquisition	slice by slice	Continuous	Continuous
ECG synchronization	Prospective	Retrospective	Retrospective
HR optimisation	atropine (HR ↑)	β blocker (HR ↓)	β blocker (HR ↓)
Contrast agents (ml)	150	150	100
Detector collimation (mm)	1x1.5/3.0	4x1.0	12/16x0.75
In plane resolution (mm)	0.8x0.8	0.6x0.6	0.5x0.5
Slice increment (mm)	1.5/2.0	0.8	0.5
Temporal resolution (ms)	50 100	125 250	105 210

EBCT (C 300, GE/Imatron, San Francisco, CA), 4 MSCT (VolumeZoom, Siemens), 16 MSCT (Sensation 16, Siemens, Forchheim, Germany). Heart rate (HR).

EBCT image acquisition: ECG-triggered sequential scanning

A brief description of ECG synchronized EBCT coronary angiography is given in figure 2a. In summary, the EBCT scanner acquires consecutive images prospectively triggered by the patient's ECG. The current systems have a temporal resolution of 100ms, scan times per slice down to 50ms are under evaluation for upcoming systems but compromised signal to noise has to be taken into consideration. The latest generation EBCT scanners is capable of acquiring several images at different phases per cardiac cycle, allowing for retrospective selection of the best data set, at the price of a multiplied radiation dose. The most commonly used scan protocols and image characteristics of coronary artery imaging with EBCT are listed in table 1.

Multi-slice CT image acquisition: volumetric spiral scanning and ECG-gated image reconstruction

ECG gated cardiac CT requires overlapping spiral scanning protocols adapted to the heart rate in order to ensure complete phase consistent coverage and dedicated reconstruction algorithms to achieve high temporal resolution (figure 2b). So called "half scan" image reconstruction provides a temporal resolution equal to the duration of a half gantry rotation based on a data set acquired in a partial scan rotation (240 260°). A multi slice spiral interpolation between the projections of adjacent detector rows is used in order to compensate for table movement.²⁴ With a given rotation time the effective temporal resolution can be improved by using scan data from more than one heart cycle for reconstruction of an image, called segmented reconstruction.^{25,26} The partial scan data set for reconstruction of one image then consists of projections from multiple consecutive heart cycles. Depending on the interaction between rotation time and patient heart rate a temporal resolution between 25% and 50% of the rotation time can be achieved for two segmental reconstructions and less when more segments are included. Despite theoretically better temporal resolution, "segmented reconstruction" does not provide a consistent improvement of image quality as the algorithms are very sensitive to changing heart rates.

4 slice CT scanners, with an individual detector width of 1.0 mm, reconstructed slice width of 1.3mm and temporal resolution between 125 and 250ms, cover the entire heart during a 30 40s breath hold. With 8 slice CT scanners the breath hold time can be reduced to 20 25s without improvement of the spatial or temporal resolution. Recent 16 slice CT technology provides a thinner slice collimation between 0.5 and 0.75mm, reconstructed slice width of 0.75 1.0mm and improved in plane spatial resolution of 0.5x0.5mm.

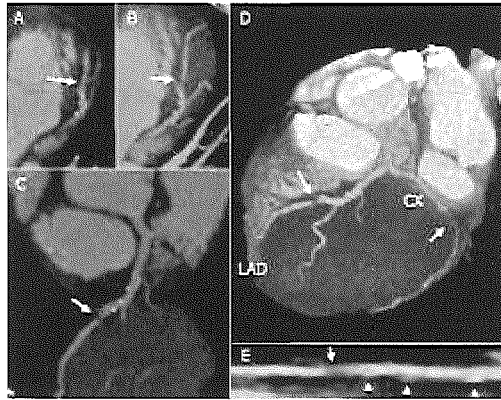


Figure 4. MSCT angiography and image processing techniques. Multiplanar reformation (MPR) involves the manoeuvring of cross sectional planes through the volumetric dataset, to display luminal variations (arrow) within the vessel of interest (A). Maximum intensity projection (MIP) of a thin slab (3.8 mm) positioned parallel to the vessel, resulting in selectively display of only the highest attenuation values within the considered volume, allows for assessment of longer vessel segments. Although more convenient than MPR, MIP is less suited for assessment of calcified or stented vessels, due to over projection of these high density structures on to the vessel lumen (B). By curving a cross sectional plane along a coronary artery, the entire course of the vessel unfolds within a single image (C). Rather than manual plotting a single curved plane, more convenient means to display the entire course of a vessel are available by automatic vessel tracking tools, which offer cross sectional views of a vessel from multiple rotational angles, and allow clear delineation of stenoses and atherosclerotic manifestations within the vessel wall (arrow heads) (E). Volume rendering techniques allow for attractive three dimensional display of the coronary artery obstructions and can be useful for the anatomic orientation of referring physicians (D). Three dimensional post processing techniques are generally not used for the initial assessment because the sensitivity of the coronary appearance to image display settings and superposition of the coronary lumen by stents, calcifications and contrast enhanced veins or atrial appendices. Image artefacts can be less recognizable and because volume rendered images contain little information with respect to the coronary vessel wall these techniques are applied conservatively for the evaluation of coronary atherosclerotic disease.

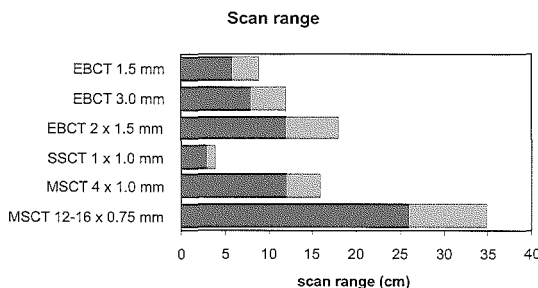


Figure 5. longitudinal scan range during a 40 second breath hold. Diagram showing the minimal and maximal coverage during a 40s scan at a heart rate between 60 (dark bar) and 90min⁻¹ (brighter bar). The scanners include the currently used EBCT at a collimation of 1.5 mm and 3.0mm with 1.0 mm overlap (C 300, GE Medical Systems, San Francisco, CA), the recently released EBCT scanner (e Speed, GE Medical

Systems) with a collimation of 2x1.5mm, 4 slice spiral CT (Somatom VolumeZoom, Siemens Medical Solutions, Forchheim, Germany), and 16 slice spiral CT (Somatom Sensation 16, Siemens Medical Solutions), in which case the dark bar and brighter extension indicate the coverage using the 12 slice and 16 slice scan protocol.

Rotation times below half a second and the extended number of slices, up to 16, result in a reduced scan time of less than 20s (figure 5). Further modality characteristics can be found in table 2.

PRACTICAL CONSIDERATIONS AND IMAGE QUALITY

Non invasive CT coronary imaging is a demanding application because high requirements for spatial resolution, low contrast detectability and temporal resolution have to be met at the same time. The small calibre coronary arteries have low X ray attenuation properties, and are in constant motion during cardiac contraction and respiration. The image quality depends on various patient and scanner parameters and usually improvement of one parameter has a negative effect on the other parameters, while some patient variables are immutable. Thus, optimisation of examination protocols is critical for best balance of imaging parameters and best examination results.

Data acquisition time and breath-hold duration

On average the cranio caudal size of the heart measures 10-12cm, but can be larger in patients with ischemic heart disease. EBCT and 4 slice MSCT can cover this range in 30-40s, which is a breath hold duration manageable by most patients, although shorter scan times are desirable. Because one slice is acquired per heart cycle, the duration of EBCT scans can be reduced by increasing the heart rate with an intravenous injection of atropine, but this occurs at the expense of a shorter, motion sparse diastolic interval. The same distance can be covered within 15-20s by 16 slice CT scanners (figure 5).

Spatial resolution and coronary artery size

X ray exposure, detector spacing, focal spot size, slice width and slice increment are the main determinants of in plane and longitudinal spatial resolution (figure 6). 4 slice MSCT provides an in plane spatial resolution of 0.6x0.6mm and a longitudinal resolution of 1.0mm whereas the in plane spatial resolution of EBCT equals 0.8x0.8 mm and the longitudinal resolution is approximately 2.5mm based on 3.0mm slices and 2.0mm slice increment. 1.5mm thin slices can also be used for EBCT but compromised volume coverage and signal to noise has to be taken into consideration. Both scanner technologies only allow assessment of the larger proximal and mid segments of the coronary tree. Using submillimeter slices and an in plane spatial resolution of 0.5x0.5mm 16 slice MSCT scanners allow assessment of almost the entire coronary tree including the larger side branches (figure 7).

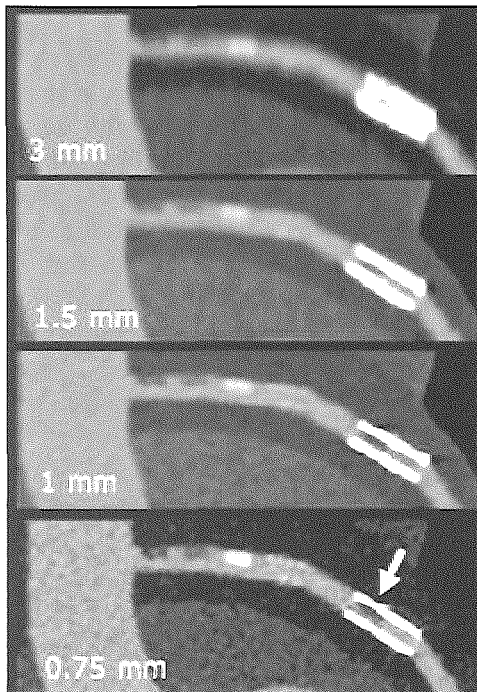


Figure 6. Phantom model using varying detector widths

A static contrast enhanced (250HU) coronary artery phantom with three consecutive plaques containing material resembling lipid (30HU), fibrous (80HU) and calcified tissue (500HU), and a stent partially obstructed by lipid like plaque material (arrow), were scanned and reconstructed using 3.0mm, 1.5mm, 1.0mm and 0.75mm slices. The longitudinal cross sections show that thinner slices allow for improved differentiation of the various plaque components.

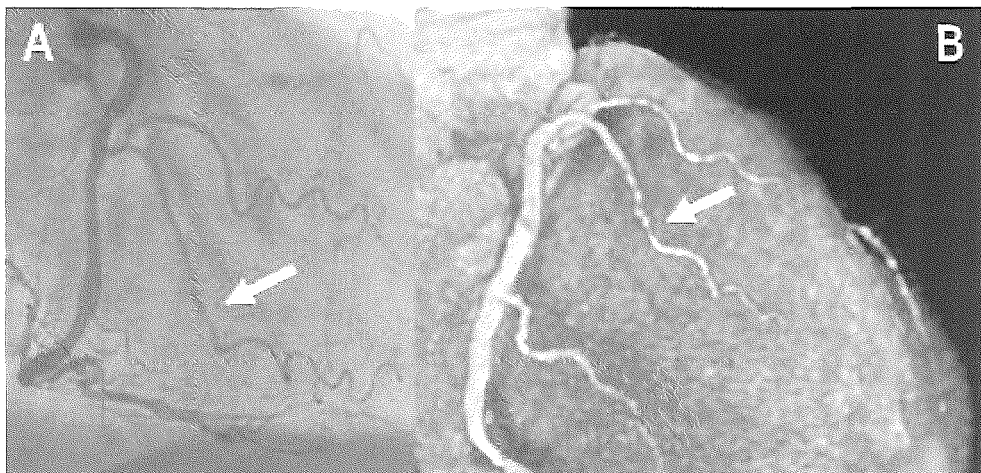


Figure 7. High resolution MSCT coronary imaging. MSCT coronary angiogram and corresponding conventional coronary angiogram showing subtle variation (arrow) of the lumen diameter (<2.0mm) of the small right ventricular branches of the right coronary artery.

Temporal resolution and cardiac motion

The duration of the diastolic, relative motion sparse period in the cardiac cycle is directly related to the heart rate. Because CT requires a defined period of time per heart cycle to acquire its data, the heart rate plays a significant role in image quality with respect to motion artefacts. The temporal resolution of one slice is 100ms for EBCT scan times per slice down to 50ms are under evaluation for latest generation scanners. 16 slice CT requires 210ms for heart rates below 70min^{-1} , and between 105 and 210ms for heart rates above 70min^{-1} , based on heart rate adaptive reconstruction algorithms.²³ However, it has been shown that MSCT coronary imaging provides best diagnostic accuracy and reliability of results in patients with spontaneous or drug induced slow heart rates of less than 65min^{-1} , because of the prolongation of the diastolic, motion free period.^{27 29} At higher heart rates adequate image quality can also be achieved but is less consistent. The temporal resolution of MSCT scanners remains the most limiting factor and future developments to overcome this limitation will be discussed (in the section future developments).

Image reliability and irregular heart rhythm

The reliability of CT in patients with arrhythmias is limited. Using MSCT misinterpretations of the ECG signal can be corrected by retrospective editing of the ECG trace. Persistent irregular heart rates, such as in patients with atrial fibrillation, result in varying filling conditions between consecutive heart cycles and reconstruction of slices at different cardiac phases. The consequent inter slice discontinuity, which reduces the interpretability by suggesting non existent coronary interruptions, may result in the false appearance of a coronary obstruction.

High-density structures and image artifacts

Presence of severe calcification represent a limitation of CT coronary imaging because beam hardening and partial volume effects can completely obscure the coronary lumen and do not allow for assessment of the integrity of the coronary lumen. Related to similar effects, metal objects such as stents, surgical clips and sternal wires can also obscure the evaluation of underlying structures. Use of the thinnest possible slice width reduces partial volume artifacts and improves assessability of calcified coronary segments. Additionally, dedicated filtering could be beneficial to the imaging of calcified vessels.

Contrast enhancement and tissue discrimination

The differences in X ray attenuation between non enhanced blood, the vessel wall and epicardial fat is insufficient to distinguish them by CT. Therefore

injection of an iodine containing contrast medium is used to increase the CT value of the coronary lumen to make it distinguishable from the surrounding tissues. An intravenous injection of 100-120ml of contrast at a rate of 3-4ml per second raises the CT density of the blood in the coronary arteries from 50 up to 250HU for the duration of the scan.

Radiation dose and image quality

The X ray dose determines the signal intensity per voxel and thus the image quality. The signal to noise ratio is decreased in large patients. Also thinner slices require a higher radiation dose to maintain good contrast to noise. Increasing the dose improves image quality but is obviously limited by patient safety considerations. Despite a thin slice width the contrast to noise ratio of MSCT is high, which is crucial to the discrimination of different non enhanced tissues. The use of radiation also limits repeated CT investigation and technical improvements are required to reduce the radiation exposure. Dose estimates for CT are summarized in table 1.

Image evaluation techniques

With the advent of multi slice CT technology the number of image slices that are generated per study has substantially increased and thus three dimensional postprocessing methods have gained importance (figure 4). A CT coronary angiogram consists of a stack of slices, varying between 80 for EBCT and 300 for MSCT, that can be processed as a three dimensional volume for which multiple techniques are available. Contrary to selective X ray angiography, also the cardiac cavities and coronary veins are opacified, which is one reason why projectional display similar to conventional angiography is not readily available. Evaluation of the extensive number of individual source images is time consuming, and particularly difficult when the vessel runs perpendicular to these axial slices. The use of thin slab maximum intensity projections is convenient and allows for quick assessment of the data set. However, in the presence of high density structures such as stents or calcium, or to evaluate the vessel wall, multiplanar reconstructions are better suited (figure 4).

CLINICAL RESULTS: IMAGE QUALITY AND DIAGNOSTIC ACCURACY

The imaging characteristics and scan protocol of currently available CT scanners are listed in table 1. Typically the evaluation of the coronary arteries with 4 slice MSCT, EBCT and other non invasive modalities has been limited to the proximal and middle segments of the major coronary branches.

Distal segments and side branches were excluded because the small size and limited contrast enhancement caused insufficient image quality and precluded evaluation. Of the proximal and middle segments only 70% to 80% of all available segments could be interpreted, which significantly limits the clinical value of the techniques. The reason for non assessability is often multi factorial and includes calcifications, cardiac or respiratory motion, and adjacent contrast filled structures blending with the coronary artery segments. When the image quality is sufficient (in 70% of the segments), the sensitivity to detect stenotic disease ranges between 75% and 90%, the specificity between 85% and 90% (table 2).

Initial studies showed little difference between the diagnostic accuracy of EBCT and 4 slice MSCT scanners. EBCT appears more robust at higher heart rates, while MSCT could better assess smaller segments because of its high image resolution and low image noise. Some studies showed significantly better results for 4 slice MSCT in patients with moderate heart rates.^{28,29} The 16 slice spiral CT scanners provide a major improvement in the image quality, and robustness of coronary imaging. The assessability of the entire coronary tree has significantly increased to more than 90% of all branches, including larger side branches and distal vessel segments (figure 7). The scan time and thus the required breathhold duration have been reduced to approximately 20 seconds, which can be performed by most patients. The submillimeter, and near isotropic voxel size allow for oblique and multiplanar reconstructions to display longer stretches of vessels, and facilitate the data analysis with improved vessel sharpness. In the study by Nieman et al, a sensitivity to identify a significant stenosed branches was reported as 95%, with a specificity of 86%, without exclusion of any segments due to suboptimal image quality.¹³ Ropers et al, excluded 12% of the segments but found a sensitivity of 92% and higher specificity of 93%. The consistently high image quality allows for reliable application of CT coronary angiography in clinical practice, although limitations such as irregular or high and non controllable heart rate, and extensively calcified vessels remain.

Is invasive conventional coronary angiography redundant?

At this moment conventional coronary angiography is still the gold standard for imaging of coronary obstruction, but non invasive 16 slice MSCT coronary angiography has now reached a sufficient level of reliability in defined subgroups of patients to be an alternative to invasive diagnostic angiography.

Table 2. Diagnostic performance to detect >50% stenoses

Study	Modality	N	Excluded (%)	Sensitivity (%)	Specificity (%)
Nakanishi, et al	EBCT	37	NR	74	91
Reddy, et al	EBCT	23	10	88	79
Schermund, et al	EBCT	28	12	83	91
Rensing, et al	EBCT	37	19	77	94
Achenbach, et al	EBCT	125	25	92*	94*
Budoff, et al	EBCT	52	10	78	91
Nieman, et al	4 MSCT	31	27	81	97
Achenbach, et al	4 MSCT	64	32	85	84
Knez, et al	4 MSCT	44	6	78	98
Vogl, et al	4 MSCT	38	19	75	91
Kopp, et al	4 MSCT	102	15	90/95†	95/96†
Giesler, et al ‡	4 MSCT	100	29	91	89
Nieman, et al ‡	4 MSCT	78	32	84	95
Nieman, et al	16 MSCT	58	0	95	86
Ropers, et al	16 MSCT	77	12	92	93

NR, not reported, *(70% stenoses, †Partial overlap with previous studies by the same groups

‡Without consensus reading

This well defined subgroup consists of patients with chest pain, refractory to treatment, who are in sinus rhythm and have a spontaneous or pharmacologically induced (beta blockers or verapamil) heart rate below 65min^{-1} in the absence of extensive coronary calcification. Identification of significant obstruction(s) with this newest generation 16 slice MSCT scanner would allow to select and refer these patients for percutaneous catheter based coronary intervention. Percutaneous coronary treatment, requiring on line pre treatment coronary angiography, would confirm the non invasive diagnosis and would act as a "safety net" in case of misdiagnosis.

To overcome the remaining limitation of CT coronary angiography and to thus expand the group of patients that can be routinely examined with this technique, further improvements of technology are needed that approach the ideal imaging requirements of 0.3mm spatial resolution and less than 100ms temporal resolution per slice at the same time.

CORONARY WALL IMAGING

Initially the major application of cardiac CT scanning was quantification of coronary calcium. The presence of calcium is a specific marker of coronary atherosclerosis, but has only a limited predictive value for the presence of significant obstructive coronary disease.³⁰ Calcium is a predictor of adverse coronary events but whether this is additional to the conventional risk factors remains unclear. CT allows identification of non obstructive coronary plaques and characterization of coronary plaque components. Plaques components such as fat, fibrous tissue or calcium impart differences in X ray attenuation, resulting in differences in CT density values and thus allowing differentiation in a "soft" plaque (fat, thrombus, necrotic material) a "hard" plaque (fibrous tissue) and calcific plaque (figure 8).³¹ Detection and evaluation of pre clinical and clinical atherosclerotic plaque burden in different development stages may become an important applications of CT coronary angiography. Further studies are needed to establish the reliability and reproducibility of the technique. Intriguing is the possibility that CT scanning can be used as an initial non invasive screening technique in high risk individuals to identify a soft coronary plaque. In these individuals additional intracoronary techniques (palpography, thermography, optical coherence tomography) may then establish the "vulnerability" of the plaque.

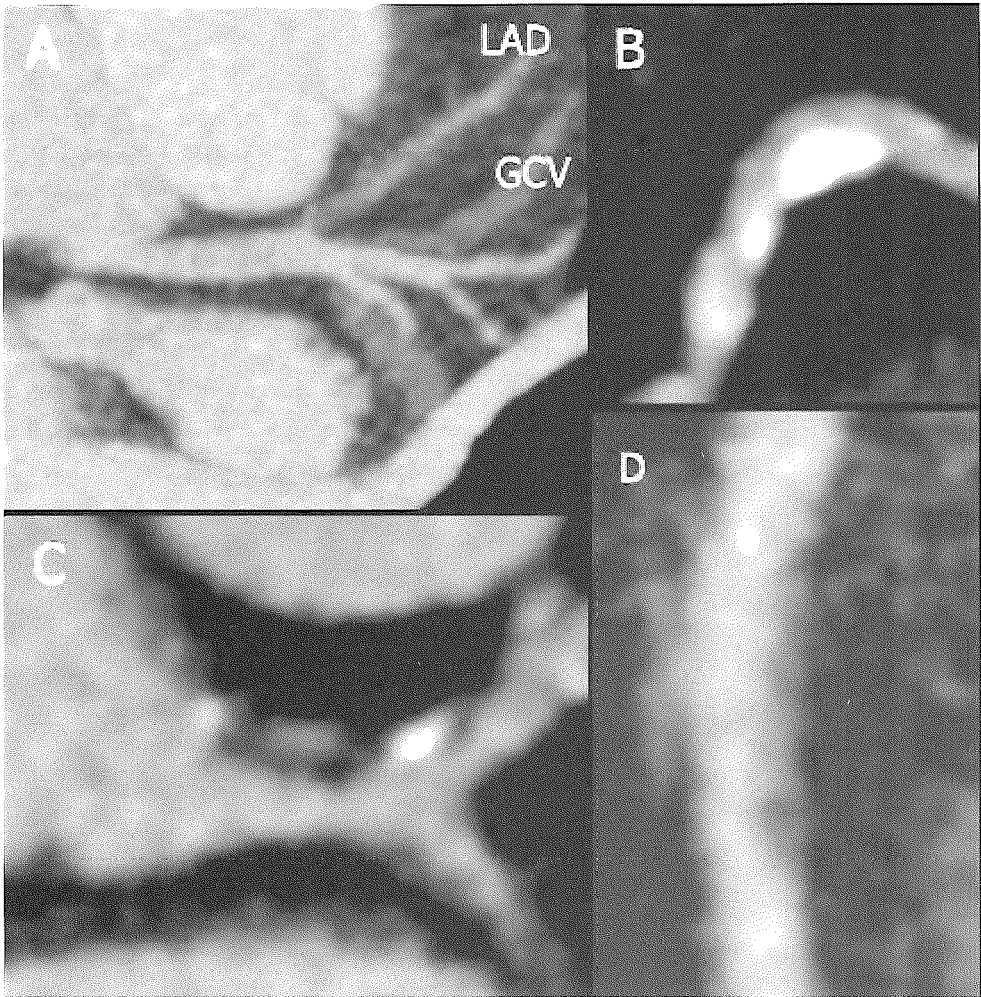


Figure 8. MSCT plaque imaging.

Different manifestations of coronary artery disease including a calcified plaque (A), a non calcified plaque (B), a thrombotic occlusion (C), and a mixed plaque with calcified components and non calcified components of varying density (D).

FUTURE DEVELOPMENTS

Technology Perspective of EBCT

The very short acquisition times of EBCT down to 50ms combined with prospectively ECG triggered scanning enable motion free imaging of the coronary arteries for patients with moderate and higher heart rates and stable sinus rhythm. However, the restrictions in spatial resolution and contrast to noise ratio as well as rather long breath hold times limit the ability of EBCT coronary angiography today to visualize all main segments of the coronary artery tree and non calcified atherosclerotic plaques.

New EBCT detectors are under evaluation that allow for simultaneous acquisition of two 1.5mm slices and increased in plane spatial resolution that is provided by finer structuring of the elements of the fixed detector ring. With these detectors the heart can be scanned with 1.5mm slices in a 30-40s breath hold. Further increased spatial resolution in the longitudinal axis and more comfortable breath hold durations of ≤ 20 s can be achieved if EBCT systems with multiple stationary detector rings would become available that provides simultaneous ECG synchronized acquisition of more than ten slices with less than 1mm collimation per slice. Such EBCT based multi slice detector concepts would require fundamental alterations in the scanner hardware and substantial upgrade of the power supply, as well as new cone beam reconstruction algorithms. Further improvement of EBCT coronary imaging is possible but requires high technological development efforts.

Future Development Potential of MSCT

The rather long temporal resolution of current MSCT should be decreased to provide motion free and robust coronary imaging. Increased temporal resolution can be provided by segmented reconstruction techniques using 2 or more segments from consecutive heart cycles for reconstruction (figure 2b). For 0.42s rotation time a temporal resolution of 105ms can be achieved using 2 segments.^{24,32} Further increased rotation speed is the most favorable approach to increase temporal resolution. For example 0.3s rotation time, that produces 150ms temporal resolution, or shorter by using multi segment reconstruction algorithms, may be able to provide motion free data in patients with low and moderate heart rate (approximately up to 80min^{-1}), thereby reducing the number of patients that require heart rate controlling medication. Obviously, significant development efforts will be needed to handle the increase of mechanical forces and the increased data transmission rates. Rotation times of less than 0.2s that would be needed to provide temporal resolution of less than 100ms, independent of heart rate, appear to be beyond today's mechanical limits.

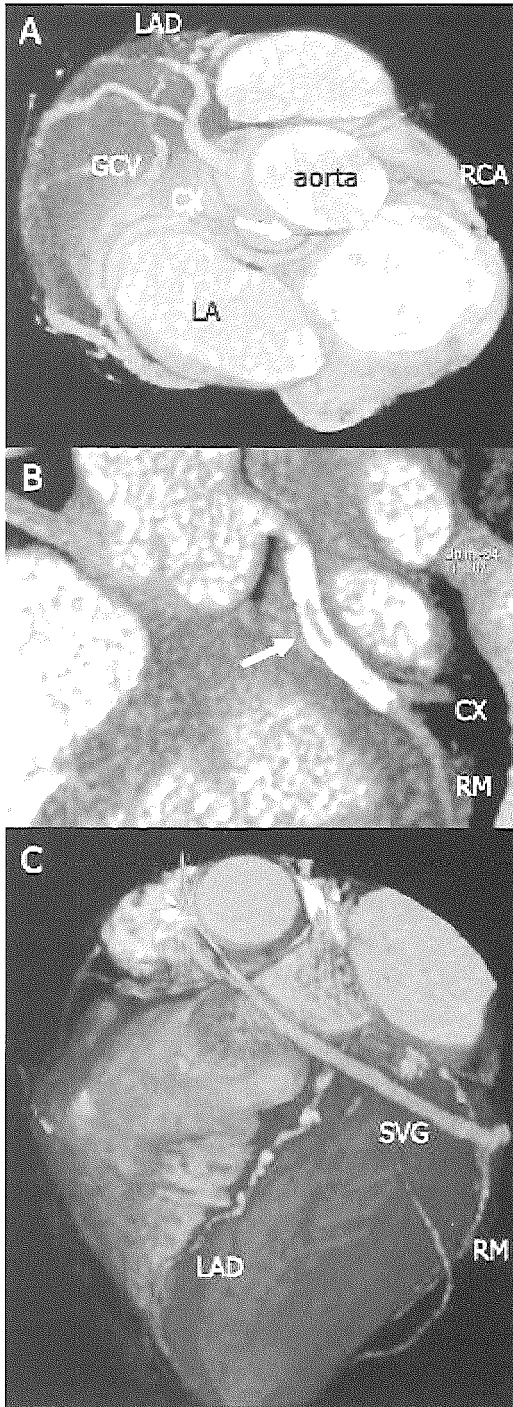


Figure 9. Miscellaneous coronary imaging. Anomalous left circumflex coronary artery originating from the right coronary artery and passing between the aorta and left atrium to the left atrio ventricular groove (A). A volume rendered angiogram, clipped through an occluded stent (arrow) in the proximal left circumflex branch (B). Angiographic imaging of a venous bypass graft from the aorta to a posteriolateral branch and beyond (C).

Concepts with multiple tubes and detectors have been described already in 1975. Theoretically, such approaches would allow for temporal resolution better than 100ms with mechanical CT if the substantial system design challenges can be overcome. Thinner slices are technically feasible but require a higher radiation dose to maintain a high contrast to noise and more detector rows to maintain a short scan time (<20s). As a complement to further increased spatial resolution advanced beam hardening and metal artefact reduction algorithms can be developed that improve imaging of heavily calcified and stented coronary vessels, which to date are restricted to cerebral and bone imaging.

The ultimate CT scanner should cover the entire coronary anatomy in single heart beat without movement of the table. This can be achieved with area detectors that cover 120mm scan range while maintaining a slice thickness of <0.5mm (figure 10). Area detector technology and related new cone beam reconstruction techniques are in research, that can provide in plane and through plane spatial resolution as low as 0.2mm. With these CT scanners imaging of high resolution morphology as well as dynamic and functional information via repeated scanning of the same scan range may be possible. The application potential of such technology is being evaluated with first experimental systems using phantom models and post mortem hearts. Initial experience shows that today's flat panel detector technology is yet limited in low contrast resolution and the high radiation dose is unacceptable for use in human subjects which is needed to provide adequate signal to noise ratio even for high contrast studies. Due to the intrinsic slow decay times of flat panel detectors available today only slow rotation times (20s are possible (figure 10) at the present time.

Latest multi slice CT scanners also allow combining 16 slice CT with PET cameras. These systems may allow for a clinical combination of CT coronary angiography and cardiac PET scans in a single examination and subsequent fusion of the information on coronary morphology and myocardial function and metabolism. The clinical potential of these scanners is currently under evaluation and first study data can be expected in the near future.

Quantitative CT coronary angiography

Quantitative measurement tools will be needed for CT coronary angiography to facilitate evaluation of three dimensional cardiac and coronary image data that are based on a large amounts of trans axial slices. Semi or fully automated segmentation of cardiac anatomy and coronary arteries will support the quantitative assessment of vessel diameters and stenosis severity, although this can only be meaningful if the spatial resolution is adequate to make quantitative assessments in the small coronary vessels.

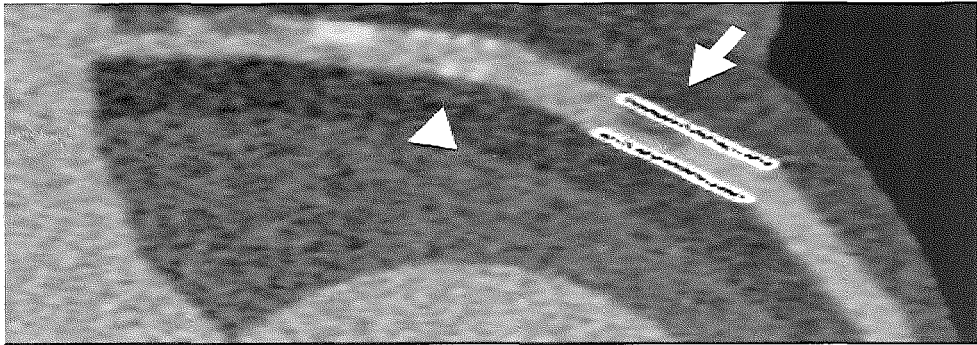


Figure 10. Phantom model by flat panel CT. Phantom model described in figure 6 scanned by a prototype flat panel CT. The images are acquired with a 20s rotation time and results in a high spatial resolution (0.2 mm) but low contrast resolution. The in stent stenosis (arrow), as well as the small calcium speckles (arrow head) are well distinguished.

Table 3. CT coronary angiography: future applications

Risk stratification of asymptomatic individuals to develop coronary artery disease:

Calcium score

Atherosclerosis imaging

Early detection / exclusion of coronary obstructions:

Atypical chest pain

Prior to non cardiac surgery

High risk asymptomatic patients

Work up of chest pain:

Detection / confirmation of obstructive disease in an emergency or out patient setting

Visualization / quantification of obstructive CAD and planning of interventions

Follow up:

Percutaneous or surgical revascularisation

Acute coronary syndromes: progression

Progression of coronary atherosclerosis: plaque content or stenosis

Monitoring (pharmacological) interventions

Miscellaneous:

Coronary Anomalies

Myocardial perfusion

Left/right ventricular function

CT coronary imaging: future applications

Obviously, the assessibility of a non invasive, patient friendly, repeatable coronary imaging technique would open many new avenues of research that would significantly increase our knowledge of preclinical and clinical phases of coronary atherosclerosis (Table 3). Non invasive coronary imaging in the preclinical phase may result in an earlier detection of the disease and earlier treatment, potentially preventing progression to fatal or non fatal myocardial infarction. Additional application of CT imaging would include the assessment of coronary anomalies, arterial and venous bypass grafts and intra coronary stents. (figure 9).

CONCLUSION

It is remarkable that an X ray based diagnostic imaging technique which was invented more than 100 years ago has continuously evolved over time, and there are no reasons to doubt that further improvements will follow. CT coronary angiography is rapidly on its way to become a non invasive alternative to conventional catheter based coronary angiography. Today the reliability of the technique is insufficient to replace conventional coronary angiography in all patients. However CT coronary angiography may be an adequate alternative with practical benefits, in a well defined subgroup of patients who have a regular heart rhythm with a low heart rate. Additionally, CT provides information regarding the morphologic character of coronary obstruction with intriguing but currently unexplored potential. Continuing innovation in CT technology to increase the spatial and temporal resolution is required to diagnose coronary artery disease in larger, unselected patient groups.

REFERENCES

1. Wielopolski PA, van Geuns RJ, de Feyter PJ, et al. Coronary arteries. *Eur Radiol.* 2000;10:12 35.
2. Nakanishi T, Ito K, Imazu M, et al. Evaluation of coronary artery stenoses using electron beam CT and multiplanar reformation. *J Comput Assist Tomogr.* 1997;21:121 117.
3. Reddy G, Chernoff DM, Adams JR, et al. Coronary artery stenoses: assessment with contrast enhanced electron beam CT and axial reconstructions. *Radiology* 1998;208:167 172.
4. Schmermund A, Rensing BJ, Sheedy PF, et al. Intravenous electron beam computed tomographic coronary angiography for segmental analysis of coronary artery stenoses. *J Am Coll Cardiol.* 1998;31:1547 1554.

5. Rensing BJ, Bongaerts A, van Geuns RJ, et al. Intravenous coronary angiography by electron beam computed tomography: a clinical evaluation. *Circulation* 1998;98:2509 2512.
6. Achenbach S, Moshage W, Ropers D, et al. Value of electron beam computed tomography for the noninvasive detection of high grade coronary artery stenoses and occlusions. *N Engl J Med.* 1998;339:1964 1971.
7. Budoff MJ, Oudiz RJ, Zalace CP, et al. Intravenous three dimensional coronary angiography using contrast enhanced electron beam computed tomography. *Am J Cardiol.* 1999;83:840 845.
8. Nieman K, Oudkerk M, Rensing BJ, et al., Coronary angiography with multi slice computed tomography. *Lancet* 2001;357:599 603.
9. Achenbach S, Giesler T, Ropers D, et al. Detection of coronary artery stenoses by contrast enhanced, retrospectively electrocardiographically gated, multislice spiral computed tomography. *Circulation* 2001;103:2535 2538.
10. Knez A, Becker CR, Leber A, et al. Usefulness of multislice spiral computed tomography angiography for determination of coronary artery stenoses. *Am J Cardiol.* 2001;88:1191 1194.
11. Vogl TJ, Abolmaali ND, Diebold T, et al. Techniques for the detection of coronary atherosclerosis: multi detector row CT coronary angiography. *Radiology* 2002;223:212 220.
12. Kopp AF, Schroeder S, Kuettner A, et al. Non invasive coronary angiography with high resolution multidetector row computed tomography: results in 102 patients. *Eur Heart J.* 2002;23:1714 1725.
13. Nieman K, Cademartiri F, Lemos PA, et al. Reliable Noninvasive Coronary Angiography with Fast Submillimeter Multislice Spiral Computed Tomography. *Circulation* 2002;106:2051 2054.
14. Ropers D, Baum U, Pohle K, et al. Detection of coronary artery stenoses with thin slice multi detector row spiral computed tomography and multiplanar reconstruction. *Circulation* 2003 (in press).
15. Wang Y, Watts R, Mitchell I, et al. Coronary MR angiography: selection of acquisition window of minimal cardiac motion with electrocardiography triggered navigator cardiac motion prescanning initial results. *Radiology* 2001;218:580 585.
16. Hounsfield GN. Computerized transverse axial scanning tomography: Part I, description of the system", *Br J Radiol* 1973;46:1016 1022.
17. Radon J, Uber die bestimmung von funktionen durch ihre integral werte langs gewisser mannigfaltigkeiten. *Ber. Von Sachs. Akademische Wissenschaft* 1917; 69:262 277.
18. Boyd DP, Lipton MJ. Cardiac Computed Tomography. *Proceedings of the IEEE* 1982;71:298 307.
19. Moshage WE, Achenbach S, Seese B, et al. Coronary Artery Stenosis: Three dimensional Imaging with Electrocardiographically Triggered Contrast enhanced Electron beam CT. *Radiology* 1995;96:707 714.
20. Kalender W, Seissler W, Klotz E, et al. Spiral Volumetric CT with Single Breath Hold Technique, Continuous Transport and Continuous Scanner Rotation. *Radiology* 1990;176:181 183.

Computed Tomography Coronary Angiography

21. Becker CR, Jakobs TF, Aydemir S, et al. Helical and Single Slice Conventional CT Versus Electron Beam CT for the Quantification of Coronary Artery Calcification. *Am J Roentgenol* 2000;174:543 547.
22. Carr JJ, Crouse JR, Goff DC Jr, et al. Evaluation of Subsecond Gated Helical CT for Quantification of Coronary Artery Calcium and Comparison with Electron Beam CT. *Am J Roentgenol* 2000;174:915 921.
23. Flohr T, Stierstorfer K, Bruder H, et al. New Technical Developments in Multislice CT, Part 2: Sub Millimeter 16 Slice Scanning and Increased Gantry Rotation Speed for Cardiac Imaging. *RöFo, Fortschr Röntgenstr* 2002;174:1022 1027.
24. Kachelriess M, Ulzheimer S, Kalender WA. ECG Correlated Image Reconstruction from Subsecond Multi Row Spiral CT Scans of the Heart. *Med Phys* 2000;27:1881 1902.
25. Ohnesorge B, Flohr T, Becker CR et al. Cardiac imaging by means of electrocardiographically gated multisection spiral CT: initial experience. *Radiology* 217:564 571.
26. Flohr T, Ohnesorge B. Heart Rate Adaptive Optimization of Spatial and Temporal Resolution for ECG Gated Multi Slice Spiral CT of the Heart. *J Comp Assist T* 2001;25:907 923.
27. Hong C, Becker,CR, Huber A, et al. ECG Gated Reconstructed Multi Detector Row CT Coronary Angiography: Effect of Varying Trigger Delay on Image Quality. *Radiology* 2002;220:712 717.
28. Nieman K, Rensing BJ, van Geuns RJ, et al. Non invasive coronary angiography with multislice spiral computed tomography: impact of heart rate. *Heart*. 2002;88:470 474.
29. Giesler T, Baum U, Ropers D, et al. Noninvasive visualization of coronary arteries using contrast enhanced multidetector CT: influence of heart rate on image quality and stenosis detection. *Am J Roentgenol*. 2002;179:911 916.
30. O'Rourke RA, Brundage BH, Froelicher VF, et al. American College of Cardiology/American Heart Association Expert Consensus Document on Electron Beam Computed Tomography for the Diagnosis and Prognosis of Coronary Artery Disease: Committee Members. *Circulation* 2001;102:126 140.
31. Schroeder S, Kopp AF, Baumbach A, Meisner C, Kuettner A, Georg C, Ohnesorge B, Herdeg C, Claussen CD, Karsch KR. Noninvasive Detection and Evaluation of Atherosclerotic Coronary Plaques With Multislice Computed Tomography. *J Am Coll Cardiol* 2001;37:1430 1435.
32. Boese JM, Bahner ML, Albers J, et al.[Optimizing temporal resolution in CT with retrospective ECG gating]. *Radiologe*. 2000;40:123 129.

7

Summary and Conclusions Samenvatting en Conclusies

CORONARY SPIRAL CT

NON-INVASIVE CORONARY ARTERY IMAGING WITH MAGNETIC RESONANCE IMAGING AND ELECTRON BEAM COMPUTED TOMOGRAPHY

In the 1990s magnetic resonance imaging and electron beam computed tomography have been used for the non invasive imaging of the coronary arteries. The imaging characteristics of both modalities and the diagnostic accuracy to detect obstructive disease in the coronary arteries are reviewed in chapter 2. Despite impressive initial results, at the current stage of technological development both techniques lack the robustness for consistent image quality and reliable detection of coronary artery disease.

CARDIAC AND CORONARY ARTERY IMAGING WITH MULTISLICE SPIRAL COMPUTED TOMOGRAPHY

With the introduction of multislice computed tomography scanners, of which the most recent generation is equipped with 16 detectors rings with a sub millimetre detector width, and a temporal resolution approaching 200 ms (or up to 100 ms when using bisegmental reconstruction algorithms), high resolution images of the heart and the coronary arteries can be obtained. After intravenous injection of an iodine containing contrast medium the entire heart can be scanned in a 35 40 s breath hold. After retrospective ECG gated image reconstruction, the result of the MSCT scan is a large stack of slices, or a three dimensional data set of the contrast enhanced heart at a specific phase within the cardiac cycle. The tomographic and volumetric imaging of the heart and particularly the coronary arteries offers a new perspective to most cardiologists as well as radiologists, which differs significantly from conventional angiography, which produces a series of two dimensional projections of a selectively enhanced coronary artery. In CT all blood containing cavities are contrast enhanced, including the cardiac cavities and cardiac veins, which on one hand hinders assessment by partial superposition of contrast enhanced structures over the coronary arteries, but also provides a new three dimensional view of the heart. This volumetric representation of the coronary arteries and other cardiac structures is described in chapter 3.1.

DETECTION AND VISUALIZATION OF CORONARY ARTERY STENOSIS

Contrast enhanced ECG gated multislice spiral CT has shown able to image the coronary arteries and coronary artery bypass grafts. The initial results in a small group of patients, using advanced post processing, including rotating volume rendered reconstructions, in comparison to conventional coronary angiography

are presented in chapter 3.2. A larger study in 53 symptomatic patients without a previous history of coronary stenting or bypass surgery the method showed a good diagnostic performance. In assessable coronary segments MSCT was capable of detecting significant coronary obstruction with a sensitivity of 82% and specificity of 93%. However, 30% of the vessels were regarded as non assessable due to motion artifacts and extensive presence of calcified atherosclerotic disease. Had the lesions in the non assessable been included in the study as false negative results, the sensitivity would have decreased to 61%, only (chapter 3.3). Partially due to the decreasing vessel diameter, the mid segments of the right coronary artery and left circumflex were less assessable, which can be explained by the extended motion radius of these segments compared to the most proximal segments. Particularly the right coronary artery is vulnerable to motion artifacts because of its large motion radius and shorter motion free interval. Due to the presence of extensive calcified atherosclerotic degeneration of the coronary artery wall the assessment of the vessels can be impaired. Other limiting factors, particularly using the 4 slice system, include the long data acquisition time of 40s, which is difficult to perform for a substantial number of patients, requires a long contrast enhancement plateau (i.e. high contrast dose), and result in assessment limiting enhancement of the venous system. Additionally, cardiac arrhythmias result in varying end diastolic volumes that despite accurate gating result in incomplete inter slice continuity. At a given duration of the image reconstruction window, which determines the temporal resolution of the scanner, motion artefacts occur with increased frequency when the R to R interval, and more explicitly the relatively motion sparse diastolic phase, becomes shorter. Comparing patients with different heart rates, the number of non assessable segments was significantly lower in patients with a low heart rate. Consequently, the overall assessability, which includes missed lesions in non assessable segments, was better in these patients compared to those with a higher heart rate (chapter 3.4). Additionally, after suspending respiration for approximately 20 seconds, the heart rate progressively increases during the remain of the breath hold. Our experiences, and those of other institutes, are summarised and discussed in chapter 3.5.

IMAGING OF THE CORONARY ARTERY WALL

Besides imaging of the coronary lumen ECG synchronized CT can be applied for imaging atherosclerotic degeneration of the coronary vessel wall. Electron beam CT, as well as multislice spiral CT are being used for imaging of calcified deposits in the coronary arteries. The methodology and use of coronary calcium quantification, particularly within the setting of the emergency ward, has been reviewed in chapter 4.2. In addition to the calcified plaque components, the high spatial resolution and contrast to noise of multislice spiral CT allow for visualization of the non calcified plaque components. In larger, and less mobile vessels, such as the carotid arteries, the potential for plaque imaging, using CT

and MRI, has been described in several studies (chapter 4.1). Using the latest generation CT scanner with sub millimetre detector row width, the plaque imaging potential of MSCT has been compared with the current standard of in vivo coronary wall imaging: intra coronary ultrasound (chapter 4.3). While the qualitative and morphologic resemblance of the CT and ICUS acquisitions can be impressive, differentiation of non calcified plaque material by MSCT for the moment remains difficult and dependent on the scanning conditions. The role of CT, as well as MR coronary plaque imaging remains yet undetermined and warrants further exploration.

CARDIAC IMAGING AFTER CORONARY REVASCULARIZATION

Additionally to the coronary arteries MSCT could have a role in the non invasive evaluation of coronary artery bypass grafts. In chapter 5.1 ECG gated CT angiography was compared with conventional coronary angiography in a small group of symptomatic patients who previously underwent coronary artery bypass surgery. The high sensitivity of CT and MRI to detect occlusion of the proximal bypass grafts has been described previously. Contrary to these studies MSCT was used to detect occlusions as well as stenoses in both the proximal segments and the sequential graft segments. While particularly the venous grafts, and to a certain extent the arterial grafts were well visualized, allowing detection of both occlusions and stenoses, the often diffusely degenerated coronary arteries were significantly more difficult to assess. Considering the fact that recurrent angina can be caused both by graft stenosis or progressive coronary artery disease, the usefulness of non invasive techniques, including both MRI and MSCT, in the clinical assessment of symptomatic post surgical patients is at this stage limited, unless the grafts alone are the substance of interest. Due to the highly attenuating metal, implanted stents are easily recognized on CT images. However, the strong attenuation causes blooming artefacts ranging beyond the boundaries of the actual stent structure, which limits the assessment of the in stent lumen in small coronary stents. Some relief is offered by the higher spatial resolution of the most recent spiral CT scanners (chapter 5.2). In the case report in chapter 5.3 imaging of coronary stents is illustrated by advanced post processing techniques, such as virtual endoscopic fly through. Although virtual endoscopy is used for detection of intestinal disease, this technique is of limited value in the assessment of coronary arteries, considering the small size of these vessels and the three dimensional spatial resolution of MSCT (chapter 5.4 and 5.5).

The continuous data acquisition and retrospective ECG gated image reconstruction allow for the reconstruction of the heart at any phase within the cardiac cycle, offering potential for high resolution 3D ventricular function assessment by spiral CT, by using, or recycling, the data that was originally acquired for the initial evaluation of the coronary arteries. This is illustrated by an animated four dimensional reconstruction of a rotating and contracting heart (chapter 5.5).

CORONARY IMAGING WITH THE MOST RECENT MSCT TECHNOLOGY

With the experience from the 4 slice studies, a study comparing 16 slice computed tomography with conventional coronary angiography was performed with the implementation of heart rate control by oral administration of β -receptor blocking medication in all patients with a heart rate of over 65 beats per minute to reduce the occurrence of motion artefacts. This combination of improved scanner technology and heart rate control improved the diagnostic accuracy of CT angiography substantially. Without exclusion of less assessable coronary arteries, 95% of the coronary arteries with significant stenosis were detected. The high sensitivity came at the expense of a slightly lower specificity of 86%. In 78% of the 58 patients a correct diagnosis in the terms of none, single or multi vessel disease could be made, and no patients with lesions were incorrectly assessed as normal (Chapter 6.1). The higher spatial resolution allows assessment of smaller branches and better discrimination of the calcified deposits from the arterial lumen. The faster rotation speed reduces the occurrence of motion artefacts, and combined with the extended number of detector rings the entire heart can be scanned in 20s, which makes the breath hold easier to perform without the previously mentioned increase in heart rate, and requires a lower total contrast medium dose.

An early review of the newest CT technology, including recent advancements in electron beam CT can be found in chapter 6.2. After the validation of the technical potential of coronary angiography with spiral CT, the time has come to determine the place of non invasive coronary angiography in clinical practise. Apart from being a milder alternative to invasive coronary angiography, CT coronary angiography could be introduced earlier in the diagnostic work up of chronic and acute chest pain syndromes, as well as follow up after revascularization. The clinical applications would benefit from further technical improvement of CT technology, of which a brief outlook is supplied in the final chapter.

CORONAIRE SPIRAAL CT

NIET-INVASIEVE AFBEELDING VAN DE CORONAIRE ARTERIËN MET MAGNETISCHE RESONANTIE TOMOGRAFIE EN ELEKTRONENBUNDEL COMPUTERTOMOGRAFIE

In de negentiger jaren zijn magnetische resonantie tomografie en elektronenbundel computertomografie gebruikt voor de afbeelding van de coronaire arteriën (kransslagaderen). De eigenschappen van beide modaliteiten, alsmede de diagnostische nauwkeurigheid om vernauwende afwijkingen aan de coronaire arteriën te detecteren, worden, besproken in hoofdstuk 2. Ondanks indrukwekkende initiële resultaten lijkt bij de huidige staat van de technische ontwikkeling, geen van beide technieken in staat om op consistente en betrouwbare wijze coronaire vernauwingen te detecteren.

AFBEELDING VAN HET HART EN DE CORONAIRE ARTERIËN MET MULTIDETECTOR SPIRAAL COMPUTERTOMOGRAFIE

Met de introductie van multidetector spiraal computertomografie (MSCT), waarvan de meest recente generatie is uitgerust met 16 submillimeter detectorrijen en een temporele resolutie (sluiterijd) die de 200 milliseconden nadert, kunnen beelden met een hoge spatiele resolutie (beeld oplossend vermogen) van het hart en de coronaire arteriën worden verkregen. Na intraveneuze toediening van een jodium houdend contrastmiddel wordt gedurende een enkelvoudige ademhalingspauze het gehele hart gescand. Na retrospectieve ECG geleide beeldreconstructie resulteert dit in een stapel tomogrammen, of een driedimensionale dataset van het contrast versterkte hart tijdens een bepaald moment in de hartcyclus. Deze tomografische of volumetrische afbeelding van het hart biedt een perspectief dat nieuw is voor de meeste cardiologen, alsmede radiologen, en die substantieel verschilt van de gebruikelijke coronaire angiografie welke resulteert in tweedimensionale projecties van de selectief contrastgevulde coronaire vaten. In het geval van MSCT worden alle bloed bevattende holten binnen het hart gevuld met contrast, wat aan de ene kant hinderlijk is vanwege overlappende structuren, maar tevens een volledig driedimensionaal beeld geeft van het gehele hart. Deze ruimtelijke representatie van de coronaire arteriën en overige hartstructuren wordt beschreven in hoofdstuk 3.1.

DETECTIE EN VISUALISATIE VAN CORONAIRE VERNAUWINGEN

Contrast versterkte ECG geleide multidetector spiraal CT heeft laten zien in staat te zijn de coronaire arteriën en chirurgische coronaire omleidingen af te beelden. De eerste resultaten in een kleine populatie vergeleken met conventionele coronaire angiografie zijn beschreven in hoofdstuk 3.2, waarbij gebruik gemaakt werd van geavanceerde beeldbewerkingsmethoden zoals roterende volumetrische reconstructies van het hart. In een grotere groep van 53 symptomatische individuen zonder voorgeschiedenis van coronaire chirurgie of percutane interventie met stents, werden motiverende diagnostische resultaten gezien. MSCT bleek in staat met een sensitiviteit van 82% and specificiteit van 93%, vernauwingen in de coronaire arteriën te kunnen detecteren. Echter, op voorhand moest 30% van de vaatsegmenten wegens onvoldoende beeldkwaliteit worden uitgesloten. Wanneer deze onbeoordeelbare vaten waren geïnccludeerd, en de afwijkingen in deze vaten als niet gedetecteerd waren beschouwd, zou de sensitiviteit gedaald zijn tot 61% (hoofdstuk 3.3). Deels vanwege de geringere diameter bleken de middensegmenten van de rechter coronaire arterie en de ramus circumflexus minder beoordeelbaar, wat verklaard kan worden door de meer uitgesproken beweging van deze segmenten gedurende de hartcyclus, in vergelijking tot de proximale segmenten. Met name de rechter coronaire arterie is gevoelig voor bewegingsartifecten door de omvangrijke beweging en kortdurende bewegingsvrije fase. De aanwezigheid van uitgebreide atherosclerotische degeneratie van de arterievaatwand is beoordelings beperkend. Andere limiterende factoren, met name voor 4 detector MSCT, zijn de lange scanduur en ademhalingspauze van 40 seconden, die moeilijk vol te houden is voor een deel van de patiënten en een langdurig contrastinjectie vereist, en daardoor een beoordelingshinderende contrastvulling van de coronaire venen veroorzaakt. Verder leidt een onregelmatige hartritme tot acquisitie van data tijdens variërende enddiastolische vullings toestanden van hart, wat resulteert in een discontinuïteit tussen de tomogrammen. Bij een gegeven scan/reconstructieduur per hartcyclus zullen bewegingsartifecten vaker en in ernstiger mate voorkomen wanneer de duur van de hartcyclus wordt verkort. Scans van patiënten met een lage hartfrequentie bleken significant beter beoordeelbaar dan bij een hoge hartfrequentie. Daardoor is de algehele sensitiviteit voor de detectie van vernauwingen beter bij een lage hartfrequentie (hoofdstuk 3.4). De hartfrequentie gedurende het vasthouden van de adem tijdens de scan blijkt na ongeveer 20 seconden progressief toe te nemen. Onze ervaringen, alsmede die van andere instituten, zijn samengevat in een uitgebreide bespreking (hoofdstuk 3.5).

AFBEELDING VAN DE CORONAIRE VAATWAND

Naast afbeelding van het coronaire lumen kan ECG gesynchroniseerde MSCT tevens toegepast worden voor de afbeelding van de atherosclerotische vaatwand zelf. Zowel elektronenbundel tomografie (EBCT) als MSCT worden gebruikt voor de afbeelding van verkalkingen in de vaten rond het hart. De methodologie en het gebruik van coronaire calcium kwantificatie, met name in de context van het acute coronaire syndroom, worden besproken in hoofdstuk 4.1.

Behalve de verkalkte plaque componenten is, dankzij de hoge spatiele resolutie en de hoge contrast beeldruis verhouding, MSCT tevens in staat het niet verkalkte plaque materiaal af te beelden. In grotere vaten zoals de halsvaten is de potentiële waarde van plaque visualisatie reeds beschreven in een aantal studies. Alhoewel de kwalitatieve vergelijking tussen intravasculaire echografie en MSCT soms verbluffend is, blijft de differentiatie van niet verkalkt atherosclerotisch materiaal moeilijk en is de beoordeelbaarheid sterk afhankelijk van de beeldkwaliteit. De waarde van coronaire plaque visualisatie met CT en/of magnetische resonantie tomografie blijft vooralsnog onduidelijk en behoeft verder onderzoek (hoofdstuk 4.2).

CARDIALE AFBEELDING NA CORONAIRE REVASCULARISATIE

Naast de afbeelding van de coronaire arteriën zou MSCT een rol kunnen hebben bij de niet invasieve evaluatie van chirurgische coronaire omleidingen. In hoofdstuk 5.1 wordt ECG geleide CT angiografie vergeleken met conventionele angiografie in een kleine groep symptomatische patiënten die omleidingschirurgie hebben ondergaan. De hoge sensitiviteit voor de detectie van volledige afsluitingen van de proximale omleidingsegmenten werd reeds eerder beschreven voor zowel magnetische resonantie als computertomografie. In tegenstelling tot deze eerdere studies werd MSCT gebruikt om zowel proximale als meer distale afsluitingen alsmede onvolledige vernauwingen af te beelden, in opeenvolgende omleidingsegmenten. Terwijl met name de veneuze omleidingen, en in mindere mate de arteriële omleidingen goed werden afgebeeld, bleken de ernstig verkalkte coronaire vaten van deze postchirurgische patiënten minder goed beoordeelbaar. Omdat heroptredende angineuze klachten zowel door vernauwingen in de omleidingen als in de oorspronkelijke vaten kunnen worden veroorzaakt, is niet invasieve angiografische diagnostiek vooralsnog van beperkte waarde in deze patiëntengroep, tenzij men enkel in de omleidingen geïnteresseerd is.

Coronaire stents worden wegens het sterk röntgenstralenverzwakkend karakter van het gebruikte metaal eenvoudig herkend met CT. Echter, deze röntgenstralenverzwakkende werking veroorzaakt tevens artefacten die strekken tot buiten de grenzen van het materiaal, en beperken hiermee de beoordeelbaarheid van het lumen binnen de kleine coronaire stents. De hogere spatiele resolutie van de meest recente generatie scanners biedt enige verbetering (hoofdstuk 5.2). In een casus beschreven in hoofdstuk 5.3 wordt de afbeelding van coronaire stents

geïllustreerd door geavanceerde beeldbewerking in de vorm van virtuele endoscopie, waarmee een blik van binnen de stent wordt gegund. Alhoewel virtuele endoscopie toegepast wordt voor de diagnostiek van darmafwijkingen, is de waarde van deze techniek van beperkte waarde voor de beoordeling van de coronaire vaten, gezien de spatiele resolutie van de scanner ten opzichte van de geringe omvang van de coronaire arteriën.

Dankzij de continue data acquisitie en retrospectieve ECG geleide reconstructie is het mogelijk het hart gedurende elke fase af te beelden. Door de spiraal data, die in eerste instantie verzameld werd ter beoordeling van de coronaire arteriën te hergebruiken, kan een driedimensionale evaluatie van de linker ventrikel worden uitgevoerd. Dit wordt geïllustreerd door een geanimeerde vierdimensionale reconstructie van een roterend en contraherend hart (hoofdstuk 5.4).

CORONAIRE AFBEELDING MET DE MEEST RECENTE MSCT TECHNOLOGIE

Met ervaring van de 4 slice MSCT scanners werd 16 slice MSCT, in combinatie met β receptor blokkers in patiënten met een hartfrequentie van meer dan 65 slagen per minuut ter voorkoming van bewegingsartifecten, vergeleken met conventionele coronaire angiografie. Deze combinatie van verbeterde scanner technologie en hartfrequentiebeperking geeft een sterke verbetering van de nauwkeurigheid van MSCT angiografie. Zonder exclusie van minder beoordeelbare vaten werd 95% van de vernauwde coronaire arteriën gedetecteerd. Deze hoge sensitiviteit ging ten koste van de een minder hoge specificiteit van 86%. In 78% van de gevallen konden patiënten juist geclassificeerd worden als hebbende meervoudig vaatlijden, enkelvoudig vaatlijden of geen vernauwend vaatlijden. Verder werd geen van de patiënten met vernauwingen onterecht beoordeeld als normaal (hoofdstuk 6.1). Een verbeterd onderscheid tussen verkalkingen en het contrast houdend lumen, alsmede een verbeterde afbeelding van de kleinere aftakkingen is mogelijk door de hogere spatiele resolutie van de nieuwe scanners. De snellere rotatiesnelheid vermindert het optreden van bewegingsartifecten en in combinatie met het uitgebreide aantal detectorringen kan de scan worden gemaakt in 20 seconden. Als gevolg van deze korte scantijd is de ademhalingspauze korter, treedt er minder hartfrequentieversnelling op en kan de totale contrastdosis worden verlaagd.

Deze meest recente spiraal CT technologie, inclusief de recente ontwikkelingen binnen de elektronenbundel computertomografie, worden besproken in hoofdstuk 6.2. Na de validatie van de technische mogelijkheden van coronaire angiografie met spiraal CT is het moment aangebroken om de plaats van niet invasieve coronaire angiografie in de klinische praktijk te bepalen. Behalve als milder alternatief voor conventionele angiografie zou spiraal CT angiografie eerder ingezet kunnen worden in de behandeling van chronische en acute coronaire hartziekten. De klinische toepassingen zouden baat hebben bij verdere verbetering van de CT technologie, waarvan een beperkte vooruitblik is gegeven in het laatste hoofdstuk.

Dit proefschrift is het resultaat van onderzoek ontstaan uit een samenwerking tussen de afdelingen cardiologie en radiologie, en in praktische zin uitgevoerd op twee verschillende locaties zijnde de Daniel den Hoed Kliniek en het Dijkzigt Ziekenhuis, onderdelen van het Erasmus Medisch Centrum in Rotterdam. Vandaar dat er velen zijn die ik wil bedanken voor hun bijdrage aan de totstandkoming van dit proefschrift.

Allereerst wil ik professor Roelandt en professor Krestin, als respectievelijke hoofden van de afdelingen cardiologie en radiologie danken voor het creëren van het samenwerkingsverband dat als basis diende voor onder andere dit proefschrift. Voor het beoordelen van dit proefschrift wil ik de leden van de promotiecommissie, professor Krestin, professor Serruys, professor Simoons, professor van Rossum, professor van der Steen en professor van der Wall bedanken.

Heel veel heb ik te danken aan mijn promotor Pim de Feijter. Beste Pim, je hebt de voorwaarden gecreëerd en zorg gedragen van de begeleiding bij dit onderzoek, en alles wat daarbij komt kijken. Essentieel was jouw overzicht van het grote geheel, en de manier waarop je non invasieve coronaire imaging in een klinische context plaatste, terwijl ik stoeide met voxels, pitches en reconstructie incrementen. Zowel professioneel als op het persoonlijk vlak kijk ik met veel genoegen terug op de afgelopen jaren. Yvonne, jouw bemoedigende woorden, evenals je gezelschap tijdens de enerverende septemberdagen in Washington, heb ik erg gewaardeerd.

Voor mij begon dit onderzoek op de radiologieafdeling van de Daniel den Hoed Kliniek. Hier heb ik de eerste kneepjes van de cardiovasculaire radiologie geleerd en ben daarom veel dank verschuldigd aan alle laboranten en radiologen, die altijd bereid om buiten de gebruikelijke uren om nog "een hart" te doen. Arie Munne, bedankt voor de waardevolle en amusante samenwerking. Peter van Ooijen, jou ben ik veel dank verschuldigd. In een wereld waar een beeld meer dan duizend woorden kan zeggen was jouw hulp en instructie op het gebied van de geavanceerde beeldbewerking onontbeerlijk. Als instant computer helpdesk heb je me onnoembare keren gered wanneer ik weer in een PACS, FTP of intranet web vastzat. Ook als kamergenoot in ons waarschijnlijk arbeidswettechnisch onacceptabele kelderonderkomen heb ik zeer gewaardeerd. Benno Rensing, jij hebt me aanvankelijk benaderd voor dit onderzoek, en behalve voor dat, heb ik je steun en hulp erg gewaardeerd. Robert Jan van Geuns, als mijn voorganger heb jij de werkomgeving gecreëerd, en me daarin geïntroduceerd zodat ik na jou een vlotte start kon maken. Als de andere laatste overblijver in de Daniel heb ik dankzij Piotr Wielopolski regelmatig kunnen genieten van een broodnodige siësta in de MRI scanner, en weet ik iets meer over cardiale MRI, en over irreversibele beeldcompressie en de flexibiliteit van flowdiagrammen. Professor Oudkerk, beste Matthijs, dankzij jou waren de organisatorische en materiele voorwaarden aanwezig voor een voorspoedige start van dit onderzoek. Hiervoor, en voor je begeleiding tijdens de beginperiode in de Daniel, ben ik je zeer erkentelijk.

In het najaar van 2001 werd dit project verder voortgezet ten noorden van de Maas, in een nieuwe omgeving met nieuwe apparatuur en veel nieuwe collega's.

Vanaf het moment dat ons project doorstartte in het Dijkzigtziekenhuis, heb ik intensief en met bijzonder veel plezier samengewerkt met mijn scanmaatjes Filippo Cademartiri en Rolf Raaijmakers. Dankzij jullie inzet wisten we het beste uit de apparatuur te halen en in korte tijd de eerste resultaten met de 16 slice technologie te publiceren, en tegelijkertijd ad hoc geplande excursies voor buitenlandse gasten te verzorgen. Ook de inzet en enthousiasme van Pedro Lemos was onmisbaar in het geheel. Pedro, muito obrigado voor de enorme hoeveelheden invasief materiaal dat je in recordtijd verwerkte, en voor de essentiële briefing voor mijn vakantie naar Brasil.

Peter Pattynama bedankt voor je nuttige radiologisch perspectief bij de uitvoering van het onderzoek, en het beoordelen van de omleidingen. Henri Vrooman bedankt voor je hulp bij het invoeren van mijn data in de VoxelView. Ook de laboranten andere medewerkers op de afdeling Radiologie wil ik bedanken voor hun hulp.

Professor Serruys, beste Patrick, jouw talent om mensen van eenzelfde geest en ambitie bij elkaar te krijgen, en de vooruitgang op het gebied van de non invasieve diagnostiek een podium te geven waren van onmisbare waarde. Voor deze boeiende en leerzame periode ben ik jou en de medewerkers van het interventie lab erg dankbaar., Titia, bedankt voor alle hulp bij het verzamelen, kopiëren, van de invasieve gegevens en dergelijke, en Jan, Paula, bedankt voor jullie hulp bij het uitdraaien van de glossies.

Tijdens mijn onderzoeksperiode heb ik onder verschillende omstandigheden met veel plezier samengewerkt, of prettig gesocialiseerd met Aad van der Lugt, bedankt voor jouw inbreng wat betreft de wat omvangrijkere plaques, Edward Leter, voor het immobiliseren van de patiënten met jouw opblaasbaar bubbeltjes matras, Jurgen Ligthart, voor je praktische hulp op het cath lab en introductie in de wereld van de intravasculaire echografie.

Exploring the performance of state of the art, though work in progress scanning equipment requires intensive co operation with those who developed it. Many thanks to Bernd Ohnesorge, Thomas Flohr, Loke Gie Haw, Stefan Schaller, Christoph Pankin, Eberhard Norman, and the many others at the Siemens Medical Solutions HQ and R&D site in Forchheim.

Zonder de enorme inzet en enthousiasme van Andries Zwamborn was het nooit gelukt dit proefschrift op tijd en in deze staat aan u te presenteren. Daarnaast, Andries, ben ik je uiteraard ook erg dankbaar voor het maken van al die prachtige posters.

Voor hun secretariële ondersteuning en gezelligheid wil ik Denise Ferdinandus, Marijke den Heijer bedanken. Eric Boersma bedankt voor je last minute statistisch advies.

Beste Pa, lieve Mams, bedankt voor alles wat jullie me hebben geboden, en alles waar jullie me vrij in hebben gelaten.

Lieve Nanae, jouw steun, begrip en geduld geven ons de kans om een nog grotere uitdaging aan te gaan. Shiawase.

1. De Feijter PJ, Nieman K, van Ooijen PMA, Oudkerk M. Non invasive coronary artery imaging with electron beam computed tomography and magnetic resonance imaging. **Heart** 2000; 84: 442 448.
2. Nieman K, Oudkerk M, Rensing BJ, van Ooijen PMA, Munne A, van Geuns RJM, de Feijter PJ. Coronary angiography with multi slice computed tomography. **The Lancet** 2001; 357: 599 603.
3. Nieman K, van Ooijen PMA, Rensing BJ, Oudkerk M, de Feijter PJ. Four dimensional cardiac imaging with multi slice computed tomography (Images in cardiovascular medicine). **Circulation** 2001; 103: e62.
4. Nieman K, Munne A, Rensing BJ, de Feijter PJ. Non invasive coronary angiography with multi slice computed tomography, a case report. **Thoraxcentre Journal** 2001; 13: 2 3.
5. Sianos G, Vourvouri E, Nieman K, Ligthart JMR, Thuri A, de Feyter PJ, Serruys PW, Roelandt JRTC. Aneurysm of the abdominal aorta (Images in cardiovascular medicine). **Circulation** 2001; 104: e10 e11.
6. Leter E, Levendag P, Nieman K, Slager C, Carlier S, Serruys PW, Nowak P. Comparison of different methods to define a target volume for external beam radiation therapy of restenotic coronary arteries. **Cardiovascular Radiation Medicine** 2001; 2: 208 212.
7. De Feyter PJ, Nieman K. New coronary imaging techniques: what to expect? **Heart** 2002; 87: 195 197.
8. Leter EM, Nowak PJ, Nieman K, de Feyter PJ, Carlier SG, Munne A, Serruys PW, Levendag PC. Definition of a moving gross target volume for stereotactic radiation therapy of stented coronary arteries. **International Journal of Radiation Oncology Biol. Phys.** 2002; 52: 560 565.
9. Al Hashimi H, Nieman K, ten Cate FJ, Drunen DV, Simoons ML. Imaging of a non coronary sinus of Valvaslva aneurysm with transthoracic echocardiography and multi slice computed tomography. **Netherlands Heart Journal** 2002; 10: 203 206.
10. Nieman K, Rensing BJ, Munne A, van Geuns RJM, Pattynama PMT, de Feyter PJ. Three dimensional coronary anatomy in contrast enhanced multislice computed tomography. **Preventive Cardiology** 2002; 5: 79 83.
11. Nieman K, van Geuns RJM, Wielopolski P, Pattynama PMT, de Feyter PJ. Noninvasive Coronary imaging in the new millennium: a comparison of computed tomography and magnetic resonance techniques. **Reviews in Cardiovascular Medicine** 2002; 3: 77 84.
12. Nieman K, Rensing BJ, van Geuns RJ, Munne A, Ligthart JM, Pattynama PM, Krestin GP, Serruys PW, de Feyter PJ. Usefulness of multislice computed tomography for detecting obstructive coronary artery disease. **American Journal of Cardiology** 2002; 89: 913 918.

List of publications

13. Nieman K, Ligthart JM, Serruys PW, de Feyter PJ. Left main rapamycin coated stent: invasive versus noninvasive angiographic follow up (Images in cardiovascular medicine). **Circulation** 2002; 105: e130 131.
14. Nieman K, Cademartiri F, Lemos PA, Raaijmakers R, Pattynama PMT, de Feyter PJ. Reliable noninvasive coronary angiography with fast submillimeter multislice spiral computed tomography. **Circulation** 2002; 106: 2051 2054.
15. Nieman K, Rensing BJ, van Geuns RJM, Vos J, Pattynama PMT, Krestin GP, Serruys PW, de Feyter PJ. Non invasive coronary angiography with multislice spiral computed tomography: impact of heart rate. **Heart** 2002; 88: 470 474.
16. van Ooijen PMA, Nieman K, de Feyter PJ, Oudkerk M. Noninvasive coronary angioscopy using electron beam computed tomography and multidetector computed tomography. **American Journal of Cardiology** 2002; 90: 998 1002.
17. Leter EM, Nowak PJ, Nieman K, Marijnissen JP, Carlier SG, de Pan C, Serruys PW, Levendag PC. Dosimetric comparison between high precision external beam radiotherapy and endovascular brachytherapy for coronary artery in stent restenosis. **International Journal of Radiation Oncology Biol. Phys.** 2002; 54: 1252 1258.
18. Nieman K, Roos Hesselink J, de Feijter PJ. Non invasive coronary angiographic assessment after corrected tetralogy of Fallot. **Heart** 2003 (in press).
19. Nieman K, van der Lugt A, Pattynama PMT, de Feyter PJ, Non invasive visualization of atherosclerotic plaques with electron beam and multi slice spiral computed tomography. **J of Intervention Cardiology** 2003 (in press).
20. Nieman, K, Cademartiri F, Raaijmakers, R, Pattynama PMT, de Feijter PJ. Non invasive angiographical evaluation of coronary stents with multislice spiral computed tomography. **Herz** 2003 (in press).
21. Arampatzis CA, Ligthart JMR, Schaar JA, Nieman K, Serruys PW, de Feijter PJ. Detection of a vulnerable plaque: a treatment dilemma. **Circulation** 2003 (in press).
22. Ohnesorge B, Nieman K. State of the art in non invasive cardiac imaging with multislice CT technology. **Hospital Management International** 2003 (in press).
23. Nieman, K Pattynama, PMT, Rensing, BJ, van Geuns, RJM, de Feyter, PJ. CT angiographic evaluation of post CABG patients: assessment of grafts and coronary arteries. **Radiology** 2003 (under review).
24. Cademartiri F, Nieman K, Raaijmakers RHJM, de Feyter PJ, Flohr T, Alfieri O, Krestin GP. Non invasive demonstration of coronary artery anomaly performed using 16 slice multidetector spiral computed tomography. **Italian Heart Journal** 2003 (in press).
25. Cademartiri F, Nieman K, Mollet N. An unusual case of chest murmur demonstrated with three dimensional volume rendering with 16 row multislice spiral CT. **Heart** 2003 (in press).

BOOK CHAPTERS

1. De Feijter PJ, Nieman K. Computed tomography for acute coronary syndromes.
In: Theroux A (Ed.). *Acute Coronary Syndrome, a Companion to Braunwald's Heart Disease*, WB Saunders, New York, USA. 2003 (in press).
2. Nieman K. Non invasive multi slice spiral computed tomography.
In: Shah PK, Falk E, de Feyter PJ. *Atlas Colour Handbook of Ischaemic Heart Disease* (in press).
3. Nieman, K, Cademartiri F. Angiography for the detection of coronary artery stenosis.
In: Schoepf UJ (Ed.). *CT of the Heart: Principles and Methods*, Humana Press, USA (in press).
4. Cademartiri F and Nieman K. Contrast material injection techniques in CT angiography of the coronary arteries.
In: Schoepf UJ (Ed.). *CT of the Heart: Principles and Methods*, Humana Press, USA (in press).

List of publications

Koen Nieman was born on the 18th of June, 1973 in Tilburg, the Netherlands. He attended secondary education at the Rodenborch College in 's Hertogenbosch (VWO) and graduated in 1991.

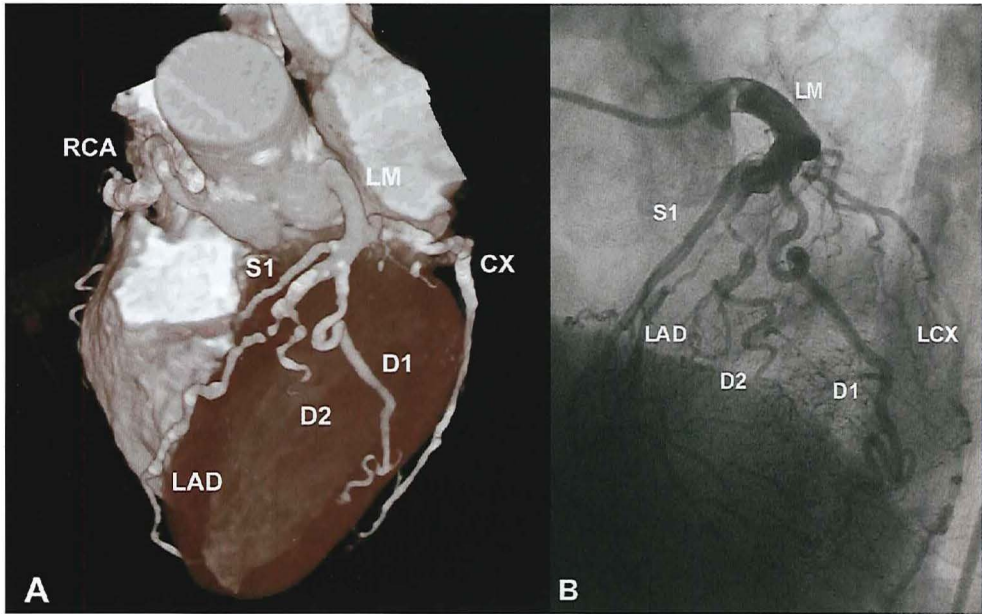
Subsequently, he studied Medicine at the University of Nijmegen. Part of his clinical training took place at the departments of internal medicine of the King Edward VIII Hospital and department of cardiology of the Wentworth Hospital in Durban (University of Natal), South Africa, the department of general practice at the University of Nottingham, United Kingdom, and the Mafeteng Governmental Hospital in Lesotho (developing country medicine). After graduating in 1998 he worked for a brief period as a house officer at the emergency ward of the St Joseph Hospital in Veghel. That same year the author participated in the Japan Prizewinners Programme, organized by the Dutch Ministry of Education, and performed internships at the department of (medical) engineering of the Akita University, and at the medical engineering laboratory of the medical systems division of the Toshiba Corporation in Otawara, Japan. After returning to the Netherlands, he worked as a house officer at the department of Cardiology at the Zuiderziekenhuis in Rotterdam.

From January 1st, 2000 he was employed as a research fellow at the Thoraxcenter in Rotterdam and started his scientific work in co operation with the departments of cardiology and radiology of the Erasmus Medical Center Rotterdam, which resulted in this thesis.

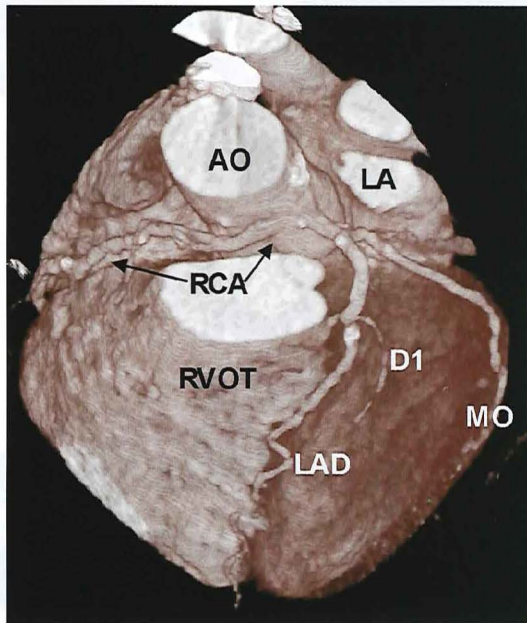
October 2002 he started his training as a cardiologist at the Thoraxcenter (Prof. dr. JRTC Roelandt and Prof. dr. ML Simoons), which includes a two years residency at the department of internal medicine of the Havenziekenhuis in Rotterdam.

Color Section

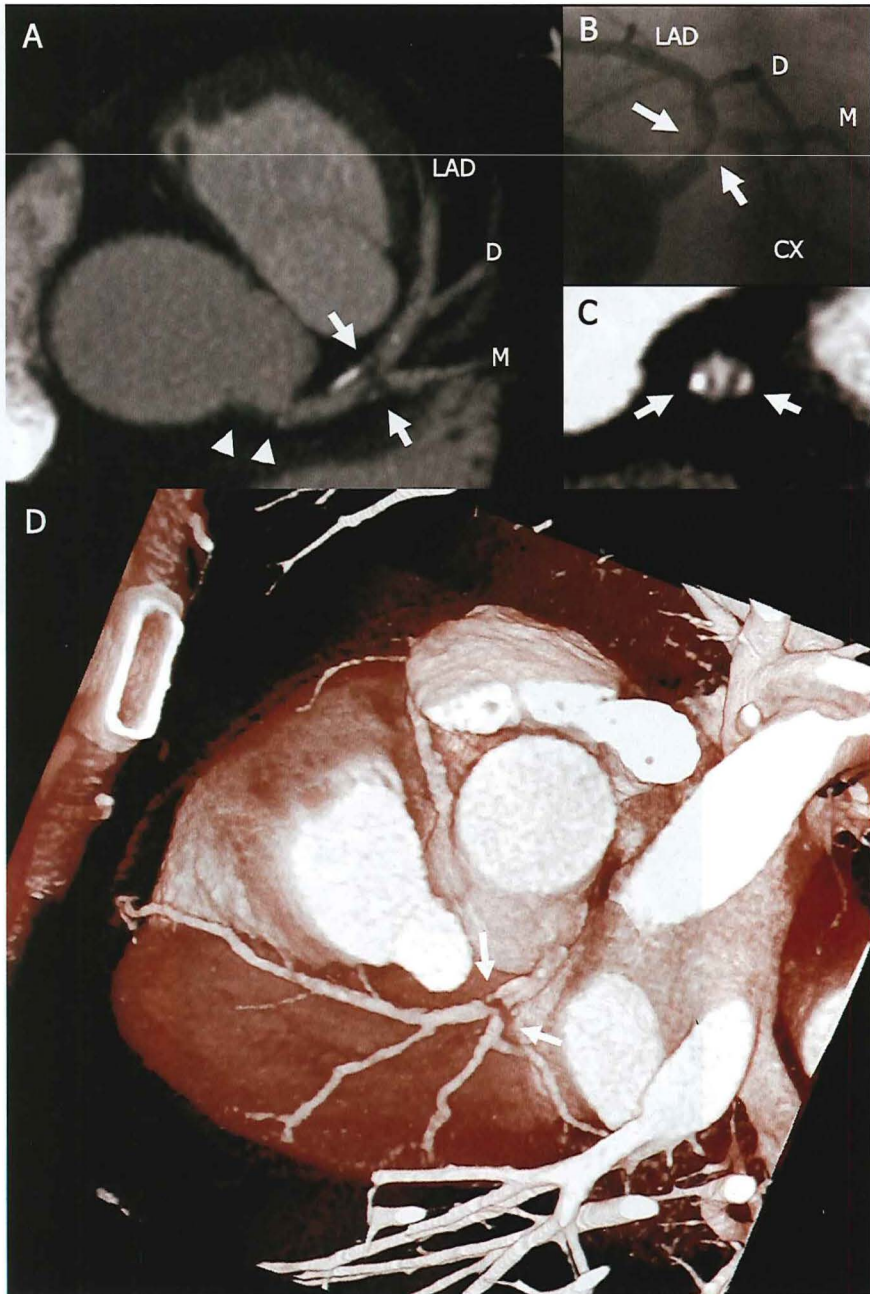
Color Section



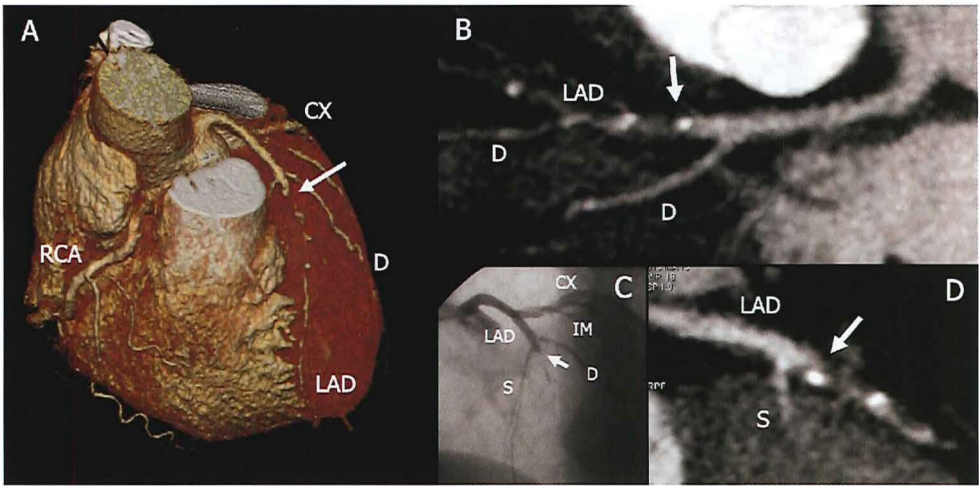
Chapter 3.2 Figure 1. MSCT and conventional angiography: obstructive disease.



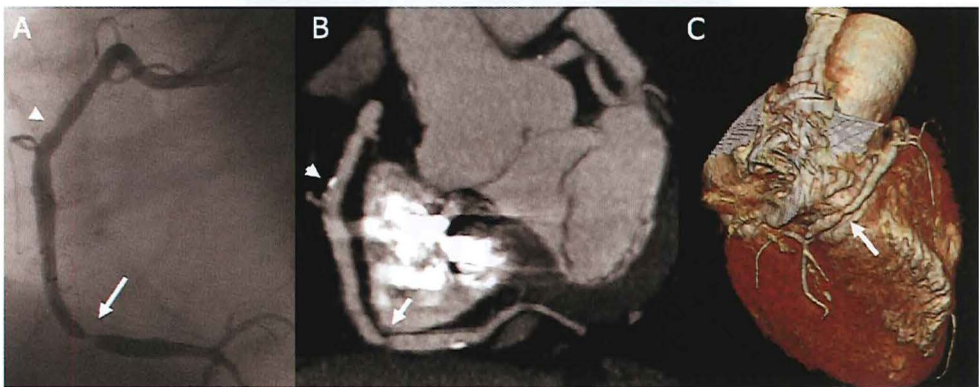
Chapter 3.2 Figure 4. Coronary anomaly by MSCT.



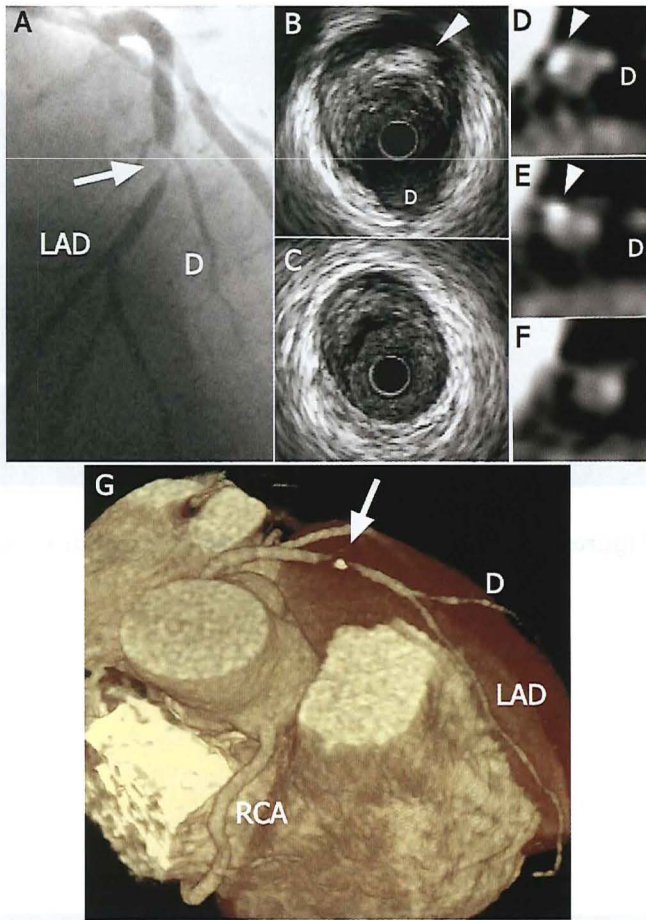
Chapter 3.5 Figure 3. Left main disease by MSCT.



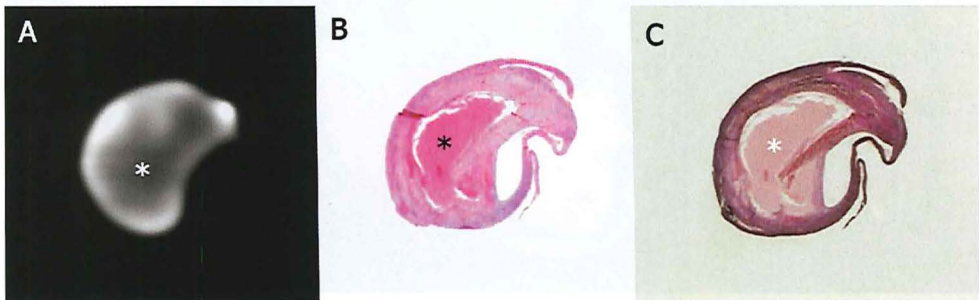
Chapter 3.5 Figure 6. Occlusion of the left anterior descending coronary artery.



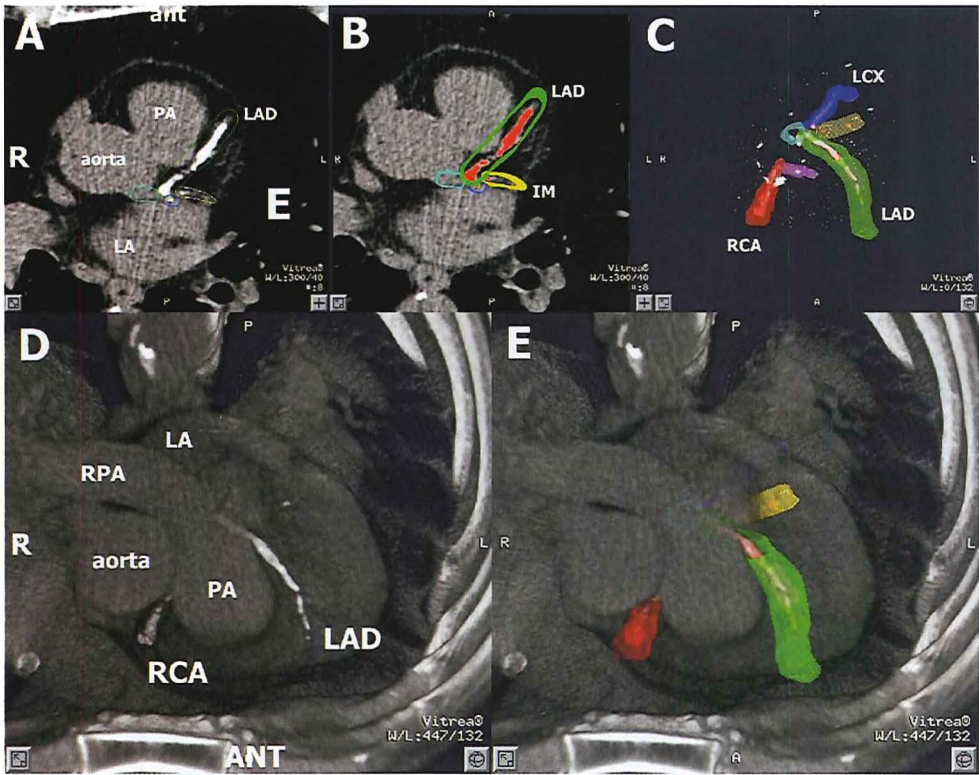
Chapter 3.5 Figure 8. Stenosis of the right coronary artery.



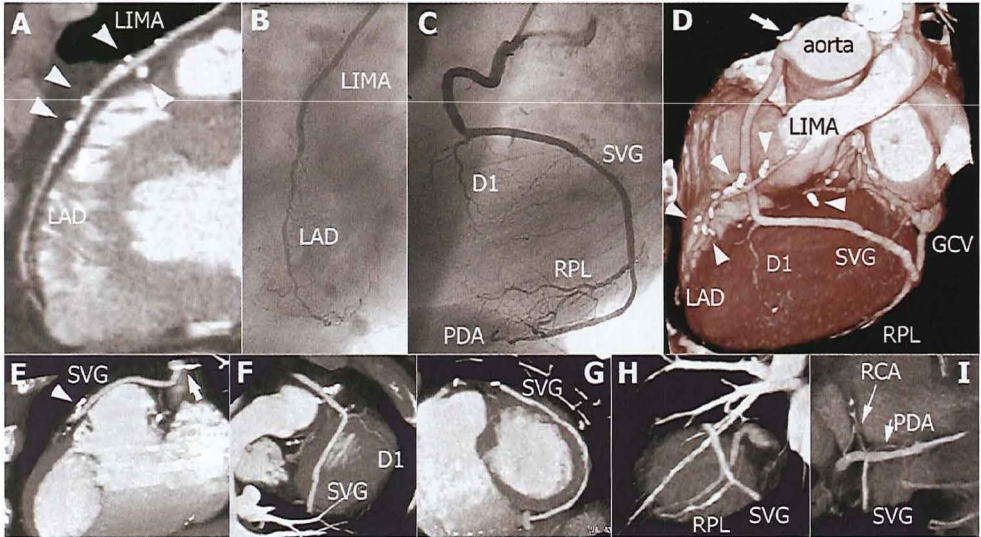
Chapter 4.1 Figure 1. Intracoronary ultrasound, conventional and MSCT angiography.



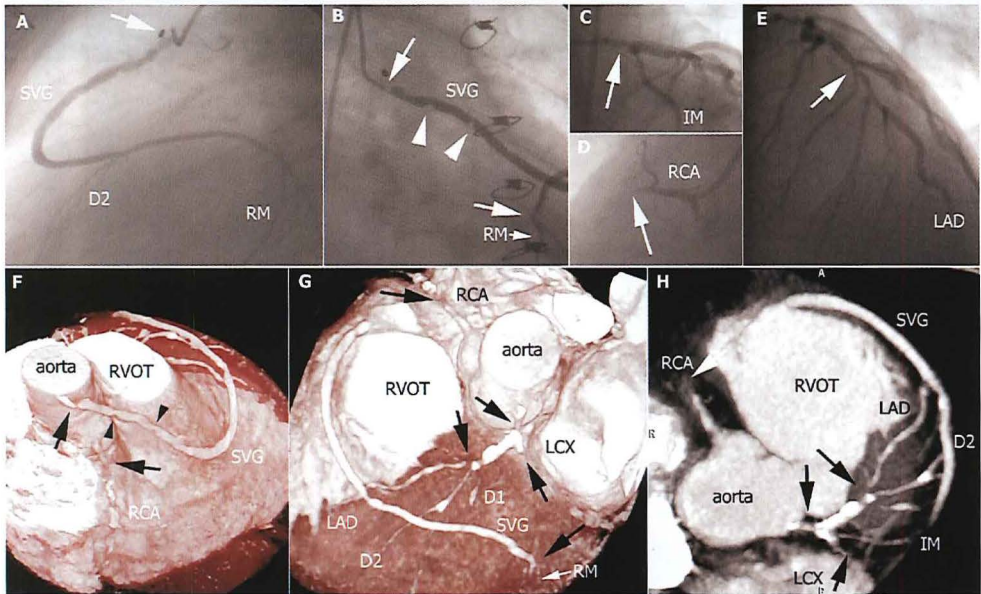
Chapter 4.1 Figure 3. MSCT and histology specimen of a carotid plaque.



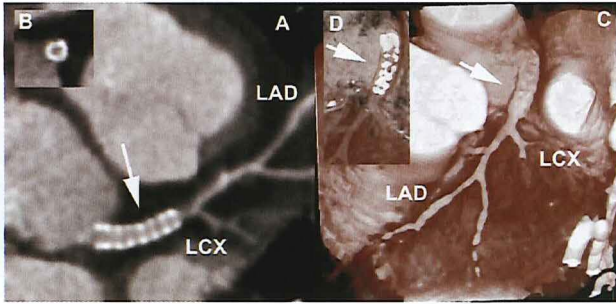
Chapter 4.2 Figure 4. Coronary calcium quantification.



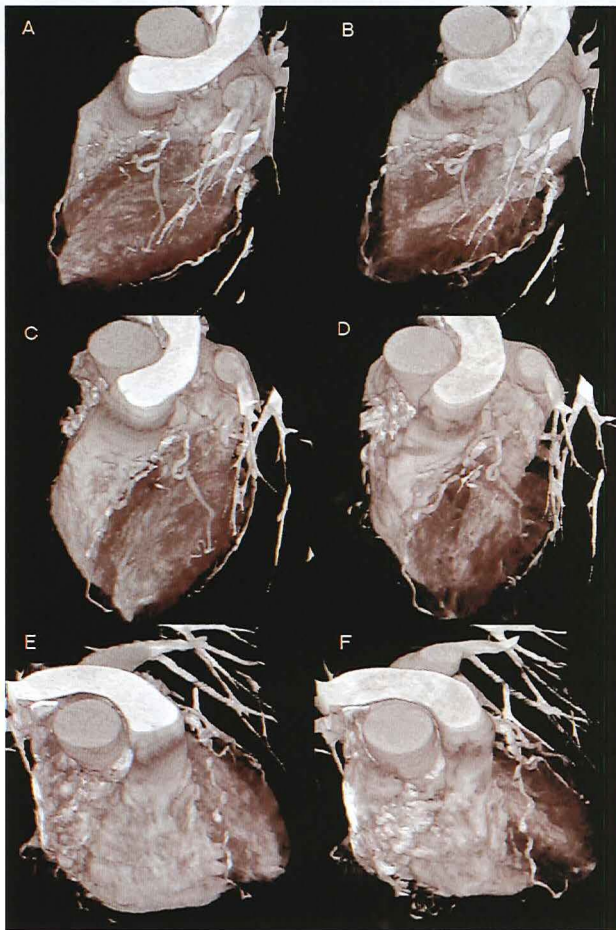
Chapter 5.1 Figure 1. Normal coronary artery bypass grafts by MSCT.



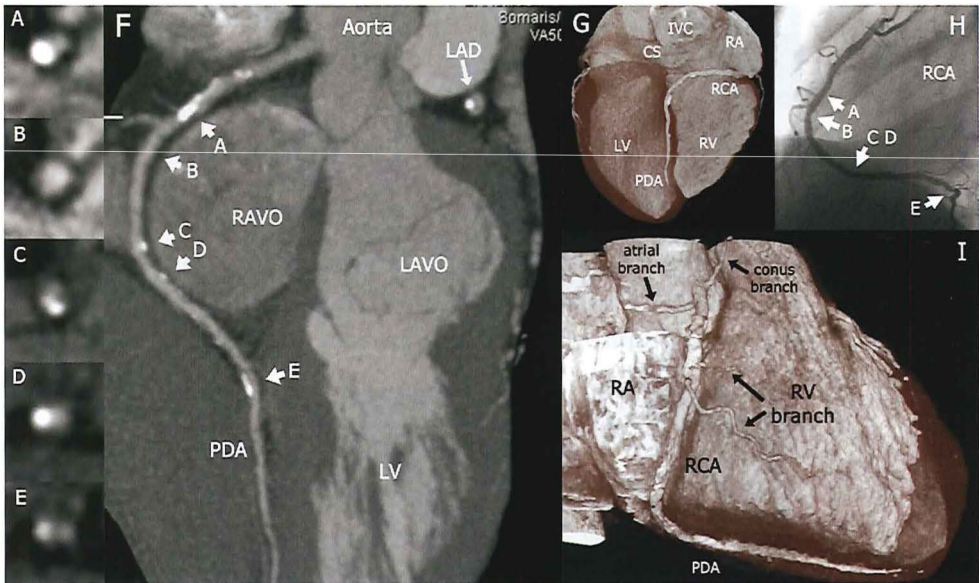
Chapter 5.1 Figure 3. Graft and coronary artery disease by MSCT.



Chapter 5.3 Figure 1. Left main coronary artery stent.



Chapter 5.4 Figure 2. four-dimensional cardiac CT.



Chapter 6.1 Figure 1. Non-obstructive disease of the right coronary artery.